Characterisation of the localisation and function of the mammalian transient receptor potential channel seven

Ralphs, Katherine L.

Award date:
2005

Awarding institution:
University of Bath

Characterisation of the Localisation and Function of the Mammalian Transient Receptor Potential Channel Seven

Submitted by

Katherine L. Ralphs

For the degree of PhD

Of the University of Bath

2005

ProQuest LLC
789 East Eisenhower Parkway
P.O. Box 1346
Ann Arbor, MI 48106-1346

Abstract

The transient receptor potential (TRP) superfamily is a large family of putative calcium entry channels. TRPC (where C is classical or canonical) is a subfamily of TRP and is made of seven members (TRPC1-7) that can be divided into two functional groups; receptor-activated calcium channels and store-operated calcium channels, however these groupings are somewhat controversial. TRPC7 is the latest member of the TRPC subfamily and is known to be alternatively spliced in both mouse and human. However, in comparison to other members of the TRPC subfamily there is relatively little information on functional characteristics, tissue distribution and cellular localisation of TRPC7.

As a result of this study, an anti-hTRPC7 antibody was produced, it has been characterised by performing immunocytochemistry and Western blotting on an over-expression system of hTRPC7. The anti-hTRPC7 antibody was used to elucidate the sub-cellular localisation of over-expressed hTRPC7 and one of its splice variants, hTRPC7A, there appeared to be no difference in localisation however, experiments have revealed that there may be a functional difference between them. Using the anti-hTRPC7 antibody endogenous expression of the protein was detected in pancreatic and cardiac cells, where it was associated with focal adhesion proteins. Also using the anti-hTRPC7 antibody, endogenous expression was detected in 3T3-L1 adipocytes and pituitary cells where it was associated with the Golgi and expression increased during differentiation of 3T3-L1 fibroblasts to 3T3-L1 adipocytes. Primary neurones were also tested for the expression of TRPC7 however, it was not detected in these cell types.

Publications Resulting From This Work:

Poster Presentations:

British Society for Cell Biology, Annual Spring Meeting, 31st March 2004 – 3rd April 2004, University of Kent Canterbury.

Title:
Expression of TRPC7 in pancreatic ductal cells: an association with focal adhesion complexes?
Authors:
Katherine L. Ralphs, Patty Chen, David Tosh and Adrian Wolstenholme

BioScience2004, 17th – 21st August 2004, SECC, Glasgow.

Title:
The expression of TRPC7 in pancreatic cells and 3T3-L1 adipocytes
Authors:
Katherine L. Ralphs, Patty Chen, David Tosh and Adrian Wolstenholme

Acknowledgements

First I would like to thank my supervisor Adrian Wolstenholme for all his help and encouragement throughout my PhD, his enthusiasm for the project is one of the reasons why this has been such a great project to work on. Thank you to Dr Adrian Rogers for his much appreciated help and input on the functional studies the cultured embryonic cardiomyocytes, cortex and spinal cord and for being jolly good company in the lab! Thanks to Prof. Geoff Holman and lab 1.37, particularly Dr Scott Lawrence for the adult cardiomyocytes and for being a mine of technical help and ideas, Dr Francoise Kourmanov and Judith Richardson for the 3T3-L1 cell line and all their help and advice. Thanks also to Dr David Tosh for the cultured embryonic pancreatic tissue the primary human pancreatic cultures, also for his valuable and enthusiastic input during discussions, it pushed the project forward in unexpected directions. I would next like to thank Dr Barbara Reaves for her help and expertise in many aspects of this project. Thanks to Patty Chen for the Northern blot she carried out on hTRPC7 and the hTRPC7A construct. Thanks to Dr Herve Aptel who has been a good source of information and help for the functional studies. Thanks to Dr Isobel Franklin for the hTRPC7 constructs. Thanks also to Prof. Sue Wonnacott, Dr Momna Hejmadi and lab 0.43 for another perspective on TRPC7 and their input during lab meetings. I would also like to thank the University of Bath for funding this project.

Thanks to all the lovely friends I have made during my three years at Bath, most of all the folks of lab 0.47 and the write-up room for making me feel so welcome and being such a great laugh, never a dull (or quiet) day...! Virginia Portillo, Sabina Alam, Patty Chen, Darran Yates, Adrian Rogers, Sandra Barns, Claire Mahoney, Tom Walsh, Momna Hejmadi, Al Monk, Sam Boundy, Jon Thomas, Nathalie Aptel, Adrian Lifshitz, Federico Dajas, Verna Lavender, Francoise Kourmanov and Judith Richardson. Thanks so much to all of you, for being kind, helpful and a good laugh.

I would like to thank my friends and family at home in Kenilworth, above all my Mum, Dad, sister Natalie and cat Tig, I guess there is something to be said for having pushy parents!! Your love and support throughout my PhD (and my whole life!) has meant so much and 'thank you' does not seem enough. Thanks so much to the rest of my family for always being there. Of my friends from home I would very much like to thank Jo and Nigel Jakeman and Alison Evans for their invaluable support. I would also like to thank Sue Lawrence and the rest of the family in W-S-M for being so welcoming and supportive.

Last, but definitely not least I want to thank Scott Lawrence (again), I have so much to thank you for; your guidance, encouragement, support and love has meant the world to me.

This thesis is dedicated to the memory of

George Ralphs

Abbreviations

ABC	Avidin biotin complex
ACh	Acetylcholine
AChR	Acetylcholine receptor
ADH	Anti-diuretic hormone
ADP	Adenosine diphosphate
Amp^r	Ampicillin resistant
AMV RT	Avian myeloblastosis virus reverse transcriptase
APS	Ammonium persulphate
ATP	Adenosine triphosphate
BDM	2,3-butanedione monoxime
BME	Basal medium Eagle
bp	Base pairs
BSA	Bovine serum albumin
°C	Degrees Centigrade
$C_6H_5Na_3O_7$	Sodium citrate
Ca^{2+}	Calcium
Ca^{2+}ATPase	Ca^{2+}adenosine triphosphatase
$CaCl_2$	Calcium chloride
cADP	Cyclic ADP
CaM	Calmodulin
cAMP	Cyclic adenosine monophosphate
CaMK	Ca^{2+}/CaM-dependent kinase
CCE	Capacitative Ca^{2+} entry
cDNA	Complementary DNA
CH_3COOH	Acetic acid
CH_3COOK	Potassium acetate
CH_3COONa	Sodium acetate
CHO	Chinese hamster ovary
CICR	Ca^{2+}-induced Ca^{2+} release
CIF	Ca^{2+} influx factor
CIRB	CaM $InsP_3R$ binding domain
cKRH	Cardiomyocytes Krebs-Ringers HEPES
cm	Centimeters
CMV	Cytomegalo virus
CNBr	Cyanogen bromide
CNS	Central nervous system
CPA	Cyclopiazonic acid
CO_2	Carbon dioxide
cRNA	Complementary ribonucleic acid
CTP	Cytidine triphosphate
DAB	3, 3'-diaminobenzidine
DAG	Diacylglycerol
DEPC	Diethylpyrocarbonate
ddH_2O	Double distilled water
DIC	Differential interference contrast
DMEM	Dulbecco's modified Eagle's medium
DMSO	Dimethyl sulphoxide
DNA	Deoxyribonucleic acid

DNAse	Deoxyribonuclease
DOC	Deoxycholic acid
DOG	1,2-dioctanoyl-*sn*-glycerol
DTT	Dithiothreitol
ECM	Extracellular matrix
ECMV	Encephalomyocaritis virus
EDTA	Diaminoethane-tetra-acetic acid disodium salt
EGFP	Enhanced green fluorescent protein
EGTA	Ethylene glycol-bis (2-aminoethylether)-N, N, N', N' tetra acetic
EFA	Essential fatty acid
ELISA	Enzyme linked immunosorbent assay
ER	Endoplasmic reticulum
ERG	Electroretinogram
EtBr	Ethidium bromide
FAF-BSA	Fatty acid free BSA
FAK	Focal adhesion kinase
FBS	Foetal bovine serum
FCS	Foetal calf serum
FCA	Freund's complete adjuvant
FIA	Freund's incomplete adjuvant
FITC	Fluorescein isothiocyanate
FKBP	FK506 binding protein
FRET	Fluorescence resonance energy transfer
Fura 2-AM	Fura 2-Acetomethyl ester
g	grams
GABA	γ-aminobutyric acid
GEE	Glycine ethyl ester
GFAP	Glial fibrillary acidic protein
GFP	Green fluorescent protein
GH	Growth hormone
Gln	Glutamine
GLUT	Glucose transporter
Gly	Glycine
GPCR	G-protein coupled receptor
GTP	Guanosine triphosphate
H^+	Hydrogen
H_2O	Water
H_2O_2	Hydrogen peroxide
H_2SO_4	Sulphuric acid
H_3BO_3	Boric acid
HAT	Hypoxanthine, Aminopterin and Thymidine
HCF	Hybridoma cloning factor
HCl	Hydrochloric acid
HEK293	Human embryonic kidney 293
hINADL	Human INAD like
HPSF	High purity salt free
HT	Hypoxanthine, Thymidine
hTRPC	Canonical or classical human transient receptor potential
I_{ARC}	Arachidonate regulated channel
IBMX	Isobutylmethylxanthine
I_{CRAC}	Ca^{2+} release activated current

IgG	Immunoglobulin G
IgG (H and L)	Immunoglobulin G heavy and light chains
INAD	Inactivation no afterpotential D
$InsP_3$	Inositol 1,4,5-trisphosphate
$InsP_3R$	Inositol 1,4,5-trisphosphate receptors
IP	Immunoprecipitation
iPLA2	Ca^{2+} independent phospholipase A2
IRES	Internal ribosome entry site
K^+	Potassium
Kan^r	Kanamycin resistant
kb	Kilo bases
KCl	Potassium chloride
kD	Kilo Daltons
KH_2PO_4	Potassium dihydrogen orthophosphate
KLH	Keyhole limpet haemocyanin
KOH	Potassium hydroxide
La^{3+}	Lanthanum
LB	Luria Bertani
M	Moles
MALT	Mucosa associated lymphoid tissue
MAP	Microtubule associated protein
MCS	Multiple cloning site
MEMFA	MOPS, EGTA, $MgSO_4$, Formalin
μg	Micrograms
mg	Miligrams
mGluR	Metabotrophic glutamate receptor
$MgSO_4$	Magnesium sulphate
min	Minute
μl	Microlitre
ml	Millilitre
Mlsn	*Melastatin*
μm	Micrometer
mm	Millimeter
μM	Micromole
mM	Millimole
$MnCl_2$	Manganese chloride
MOPS	3-[N-morpholino]propanesulphonic acid
mRNA	Messenger RNA
μs	Microsecond
mTRPC	Canonical or classical mouse transient receptor potential
NA	Not applicable
Na^+	Sodium
$Na_2B_4O_7$	Sodium tetraborate
NaCl	Sodium chloride
Na_2CO_3	Sodium carbonate
$NaHCO_3$	Sodium hydrogen carbonate
Na_2HPO_4	Disodium hydrogen orthophosphate
nACh	Nicotinic acetylcholine
NaN_3	Sodium azide
NCS	Newborn calf serum
NCX	Na^+/Ca^{2+} exchangers

NHERF	Na^+/H^+ exchange regulatory factor
NFATc	Nuclear factor of activated T-cells
ng	Nanograms
nM	Nanomoles
NMDA	*N*-Methyl-D-Aspartate
NMDAR	*N*-Methyl-D-Aspartate receptor
NMS	Non-immune mouse serum
NP	No product
NT	Neurotransmitter
NTR	Neurotransmitter receptors
OAG	1-oleoyl-2-acetyl-sn-glycerol
OD	Optical density
PBS	Phosphate buffered saline
PBST	PBS with Tween-20
PBSTM	PBS with Tween-20 and Marvel
PDZ	PSD-95, Dlg A, ZO-1
PEG	Polyethylene glycol
PFA	Paraformaldehyde
PIP_2	Phosphatidylinositol 4,5-bisphosphate
PMCA	Plasma membrane Ca^{2+} ATPase
PMSF	(4-bromo) Phenylmethyl sulphonylfluoride
PKC	Protein kinase C
PKD	Polycystic kidney disease
PKG	Protein kinase G
PLC	Phospholipase C
PLIK	Phospholipase C interacting kinase
PLL	Poly-L-lysine
PRL	Prolactin
Pro	Proline
P/S	Penicillin/streptomycin
PSS	Physiological saline solution
PUFA	Polyunsaturated fatty acid
RACC	Receptor activated Ca^{2+} channel
RbCl	Rubidium chloride
RGS	Regulators of G-protein signalling
RNA	Ribonucleic acid
RNAi	RNA interference
ROC	Receptor operated channel
rpm	Revolutions per minute
RT-PCR	Reverse transcriptase polymerase chain reaction
RyR	Ryanodine receptor
S-1-P	Sphingosine-1-phosphate
SA	Sino atrial
SCaMPER	Sphingolipid Ca^{2+} release mediating protein of endoplasmic reticulum
SDS	Sodium dodecyl sulphate
SDS-PAGE	SDS polyacrylamide gel electrophoresis
SERCA	Sarco-endoplasmic reticulum Ca^{2+} ATPase
siRNA	Small interfering RNA
SMC	Submicrovillar cisternae
SMOC	Second messenger operated channel
SOC	Store operated channel

SOCE	Store operated Ca^{2+} entry
SPC	Sphingosylphosphorylcholine
SR	Sarcoplasmic Reticulum
T-tubules	Transverse tubules
TBE	Tris borate EDTA
TEMED	N, N, N, N'- Tetramethyl ethylenediamine
Tfl	*Thermus flavus*
TG	Thapsigargin
TGN	Trans Golgi network
TK	Tyrosine kinase
TMB	Tetramethyl benzidene
TMD	Transmembrane domain
TRH	Thyrotropin releasing hormone
Tris	Tris (hydroxymethyl) methylamine
TRP	Transient receptor potential
TRPγ	Transient receptor potential gamma
TRPA	ANKTM1 transient receptor potential
TRPC	Canonical or classical transient receptor potential
TRPL	Transient receptor potential-like
TRPM	Melastatin transient receptor potential
TRPML	Mucolipidin transient receptor potential
TRPP	Polycystin transient receptor potential
TRPV	Vanilloid transient receptor potential
TTP	Thymidine triphosphate
UV	Ultraviolet
VGCC	Voltage gated Ca^{2+} Channels
VNO	Vomeronasal organ
VOCC	Voltage operated Ca^{2+} Channels
v/v	Volume for volume
WB	Western blot
WT	Wild type
w/v	Weight for volume
x g	gravitational force

Symbols for amino acids:

A	Ala	Alanine
B	Asx	Asparagine or Aspartic Acid
C	Cys	Cysteine
D	Asp	Aspartic Acid
E	Glu	Glutamic Acid
F	Phe	Phenylalanine
G	Gly	Glycine
H	His	Histidine
I	Ile	Isoleucine
K	Lys	Lysine
L	Leu	Leucine
M	Met	Methionine
N	Asn	Asparagine
P	Pro	Proline
Q	Gln	Glutamine

R	Arg	Arginine
S	Ser	Serine
T	Thr	Threonine
V	Val	Valine
W	Trp	Tryptophan
Y	Tyr	Tyrosine
Z	Glx	Glutamine or Glutamic Acid

Contents

Chapter 1
Introduction

1.1 - Introduction

Transient receptor potential (TRP) channels have been studied since their original identification in *Drosophila* (Pak et al., 1970). Since the identification of the archetypal TRP an abundance of vertebrate TRP channels have been identified and categorised into many subfamilies (discussed in sections 1.3 and 1.4). One aspect of TRP channels has remained constant across all subfamilies of TRP; they are putative calcium ion (Ca^{2+}) influx channels. Relatively recently the final member of the TRPC subfamily (where C is classical or canonical), TRPC7, had been identified in mouse (Okada et al., 1999) and later in human by our laboratory and another independent group (Murphy Unpublished Data; (Riccio et al., 2002a) Accession Numbers: AJ272034 and AC063980 respectively). Despite TRPC7 being a putative Ca^{2+} influx channel relatively little else is known about it, as with many other members of the TRP superfamily the question of its functional mechanism of activation has yet to be answered. In this chapter I shall introduce Ca^{2+} as an important ion for cell and tissue systems and review the current literature implicating the TRP superfamily in Ca^{2+} signalling roles.

1.2 - Calcium Signalling

1.2.1 - The Importance of Calcium

Calcium (Ca^{2+}) is an extremely important ion; it acts as an intracellular messenger relaying information within cells to regulate their activity. Ca^{2+} triggers life at fertilisation and Ca^{2+} also controls the development, differentiation and proliferation of cells and is also involved in the pathways mediating cell death, apoptosis and necrosis (Berridge et al., 1998; Berridge et al., 2000). The normal resting level of intracellular Ca^{2+} is approximately 100nM and extracellular concentration of Ca^{2+} is 2mM (Bootman et al., 2001; Clapham, 1995). Ca^{2+} must be maintained at low levels in cells as it can precipitate phosphate, very high levels of intracellular calcium can also lead to cell necrosis through the activity of Ca^{2+} sensitive protein digesting enzymes, such as the protease calpain (Clapham, 1995). Many cellular proteins have been adapted to bind and

buffer Ca^{2+} (Clapham, 1995). Calcium is a highly versatile intracellular signal, for example, where it takes hours to drive events such as gene transcription; it can take microseconds to trigger exocytosis (Berridge et al., 2000).

1.2.2 - Spatial Calcium Signalling

The action of Ca^{2+} is local, when activated, both Ca^{2+} entry and release channels introduce Ca^{2+} into the cytoplasm, however these channels have only brief opening times and introduce small plumes of Ca^{2+} around the mouth of the channel before diffusing into the cytoplasm (Berridge et al., 2000; Clapham, 1995). The rate of diffusion is slow and it is estimated that Ca^{2+} migrates no further that 0.1-0.5μm in about 50μs before encountering a binding protein (Berridge et al., 2000; Clapham, 1995). These small plumes provides local and highly specific control of many physiological functions but are also used as the basic building blocks of complex global Ca^{2+} signals such as oscillations and waves (Berridge et al., 2000). Cells do not have a uniform Ca^{2+} concentration and cellular buffers and channels are non-uniformly distributed (Clapham, 1995). An important aspect of intracellular calcium signalling is ion channel clustering, for example it has been shown that channel and receptor proteins are often not uniformly distributed around the PM but instead are grouped together (Shuai and Jung, 2003; Damjanovich et al,1999). The theory is that an optimal clustered distribution of Ca^{2+} channels enhances the cells capability to create a large Ca^{2+} response to a weak stimulation (Shuai and Jung, 2003).

1.2.3 - Intracellular Calcium Stores

Calcium signalling makes use of the Ca^{2+} from the extracellular space and intracellular stores; primarily the endoplasmic reticulum (ER; or sarcoplacmic reticulum in muscle; SR) but also, to an extent, the mitochondria and Golgi apparatus also play a role in Ca^{2+} signalling. Many processes regulate intracellular calcium concentration, these processes can be divided in to calcium 'on' and 'off' mechanisms depending on whether they serve to increase or decrease cytosolic Ca^{2+} concentration. (Berridge et al., 2000; Bootman et al., 2001). Calcium 'on' mechanisms involves a diverse set of channels located at the plasma membrane (PM); they regulate the influx of calcium from the extracellular space

and channels on the ER/SR. Another diverse set of mechanisms are responsible for the 'off' mechanism, to remove intracellular calcium and sequester it in intracellular Ca^{2+} stores, these include Ca^{2+}-adenosine triphosphatases (Ca^{2+}ATPases) on the PM and ER/SR and ion exchangers, for example the Na^{+}/Ca^{2+} exchanger (NCX). (Bootman et al., 2001).

1.2.3.1 - Endoplasmic Reticulum

The ER is a multifunctional signalling organelle; one of its primary functions is as a source and store of Ca^{2+}. The ER is a highly dynamic organelle, it undergoes constant fusion and budding as part of the complex trafficking events that occurs within cells, and so the stores of Ca^{2+} are not static entities, but are heterogeneous, widely distributed and constantly changing (Gill et al., 1996). The ER is divided in to rough ER, smooth ER and nuclear membrane. The rough ER is so named because it is associated with ribosomes, it is actively and primarily involved in protein synthesis however, it may also play a role in Ca^{2+} signalling. The smooth ER is mainly responsible for Ca^{2+} signalling, in muscle cells the SR is highly arranged to line up with the transverse tubules (t-tubules), invaginations of the PM and appear as striations, the highly regular organisation ensures that the SR can release Ca^{2+} synchronously in order to create the rapid global signals necessary to contract the large muscle cells (Berridge, 2002). The ER/SR is capable of both signal reception and signal transmission. Input signals include intracellular messengers such as inositol 1,4,5-trisphosphate ($InsP_3$), sphingosine-1-phosphate (S-1-P) and Ca^{2+} itself, in response, the ER can generate a number of output signals including Ca^{2+} (Berridge, 2002). The fact that Ca^{2+} can act as both an input and output signal highlights the role of the ER as an excitable system capable of spreading Ca^{2+} signals throughout the cell using a regenerative process of Ca^{2+}-induced Ca^{2+} release (CICR), this process is of high importance in Ca^{2+} signalling (Berridge, 2002).

The ER contains $InsP_3$ Receptor ($InsP_3R$) and Ryanodine Receptors (RyRs); they are responsible for releasing Ca^{2+} in response to the input signals (Figure 1). However, in addition to the receptors there is also a leak pathway in the ER. Both the regulated release

and the leak of Ca^{2+} are counteracted by the SR/ER Ca^{2+} ATPase (SERCA) pump that functions to maintain an internal store of Ca^{2+} by pumping Ca^{2+} into the ER/SR (Berridge, 2002).

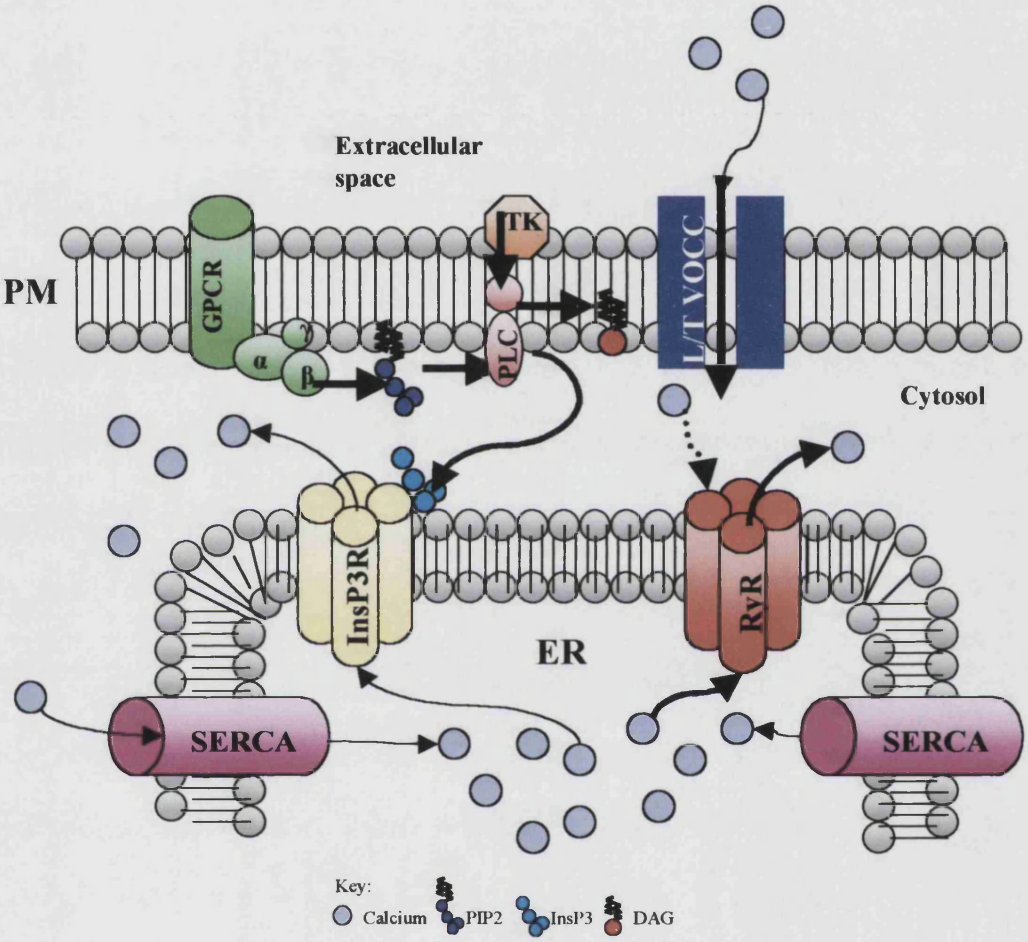

Figure 1.1: A schematic diagram of the main Ca^{2+} channels in the ER and their association with membrane proteins. GPCR G-protein coupled receptor; $InsP_3$ inositol 1,4,5-trisphosphate, PIP_2 phosphatidylinositol 4,5-bisphosphate, DAG diacyl glycerol L/T VOCC L/T type voltage operated calcium channel; PM plasma membrane; $InsP_3R$ $InsP_3$ Receptor; RyR Ryanodine Receptor; ER endoplasmic reticulum; SERCA SR/ER Ca^{2+} ATPase.

1.2.3.2 - Mitochondria

The mitochondria play an important role in regulating cytosolic Ca^{2+} levels. The function of the ER is intimately connected with the mitochondria. Mitochondria and the ER form a highly dynamic interconnected network where they cooperate to generate Ca^{2+} signals, the mitochondria makes tight, synaptic like contacts with the ER. The mitochondria play an important role in shaping the calcium signal from the ER and they assist with recovery by rapidly sequestering Ca^{2+} before returning it to the ER (Berridge, 2002; Rutter and Rizzuto, 2000). Mitochondria can also reduce cytosolic calcium transients and diminish cellular responses by use of a high capacity rapid calcium uniporter (Bootman et al., 2001; Montero et al., 2000; Rutter and Rizzuto, 2000).

1.2.3.3 - Golgi Apparatus

It is only recently that the Golgi apparatus has been accepted as a store for Ca^{2+}, and because of its defined intracellular localisation it has been hypothesised to be involved in generating highly localised Ca^{2+} gradients (Rizzuto, 2001). Functional and biochemical data support the theory that the Golgi has a capacity in Ca^{2+} storage; for example direct measurement of Ca^{2+} fluxes with targeted aquorin and the localisation of the $InsP_3R$ and some calcium binding proteins (Lin et al., 1999; Pinton et al., 1998; Scherer et al., 1996).

1.2.4 - Store Calcium Release

There are several types of messenger-activated channels that mediate the release of Ca^{2+} from intracellular stores in to the cytoplasm. In non-excitable cells the initial signal for store release of Ca^{2+} is activated by the coupling of a ligand such as hormones, growth factors and neurotransmitters on to a G-protein coupled receptor or a tyrosine kinase linked receptor (RTK) on the PM (Figure 1.2; (Berridge, 1993; Putney, Jr. and Bird, 1993a). In both cases the signal results in the generation of $InsP_3$, the key activator of Ca^{2+} release (Figure 1.2; (Berridge, 1993; Putney, Jr. and Bird, 1993a). G-protein coupled receptors (GPCR) undergo conformational changes upon binding of the ligand, this

activates, via the guanosine triphosphate (GTP) binding protein, phospholipase C-β1 (PLC-β1). The activation of PLC-β1 causes the hydrolysis of the lipid precursor, phosphatidylinositol 4,5-bisphosphate (PIP_2) to produce $InsP_3$ and diacylglycerol (DAG) (Berridge et al., 2000). The TK receptors undergo ligand-mediated dimerisation, allowing the kinase domains to phosphorylate each other on specific tyrosines. It is the phosphotyrosines that provide the docking site for PLC-γ1; this is then translocated from the cytosol to the PM where it cleaves PIP_2 to produce $InsP_3$ and DAG (Berridge et al., 2000). $InsP_3$ is a highly mobile but short-lived messenger that diffuses in to the interior of the cell where, on the ER/SR it encounters the tetrameric $InsP_3R$. The binding of $InsP_3$ to $InsP_3R$ leads to a conformational change of the receptor allowing the integral channel to be opened and the exit of Ca^{2+} into the cytosol from the ER/SR, the Ca^{2+} then goes on to be involved in specific cellular processes. The $InsP_3R$ require $InsP_3$ to open, however Ca^{2+} regulates their activation at their cytosolic surface. For example, during modest increases of Ca^{2+}, $InsP_3$ opening is enhanced, however where there are high levels of Ca^{2+} their opening is inhibited (Putney, Jr. and Bird, 1993b; Venkatachalam et al., 2002). $InsP_3$ mediated signal pathways can increase cellular concentrations of Ca^{2+} from 100nM to approximately 1000nM, depending on cell type (Bootman et al., 2001; Clapham, 1995).

RyR are tetrameric proteins predominantly found on the ER/SR of excitable cells for example neurons and muscle cells. RyRs are gated by electromechanical coupling to the PM voltage operated Ca^{2+} channels (VOCC; for example the dihydropyridine receptor in skeletal muscle), cyclic adenosine diphosphate (cADP) ribose and Ca^{2+} itself. They are very similar to the $InsP_3R$, structurally and functionally however, they have twice the conductance of $InsP_3R$ (Clapham, 1995).

Another Ca^{2+} release channel is sphingolipid Ca^{2+} release mediating protein of endoplasmic reticulum (SCaMPER), it is activated by sphingosylphosphorylcholine (SPC) and S-1-P and it is expressed in a number of different cell types. This is largely uncharacterised, and is much smaller and bears no resemblance to $InsP_3R$ and RyR (Bootman et al., 2001).

1.2.5 - Extracellular Calcium Entry

There are many different types of calcium entry channels on the PM, usually they are grouped together according to their mechanism of action, they are, voltage operated Ca^{2+} channels (VOCC), receptor operated channels (ROC), store operated channels (SOC) and second messenger operated channels (SMOC).

1.2.5.1 - Voltage Operated Calcium Channels (VOCC)

VOCC also referred to as voltage gated Ca^{2+} channels (VGCC), they are found in excitable cells and generate the rapid Ca^{2+} fluxes that control cellular processes such as muscle contraction or exocytosis at synaptic endings (Berridge et al., 2000). Most mammalian VOCCs are comprised of five protein subunits ($\alpha 1$, $\alpha 2$, β, γ, δ), the $\alpha 1$ subunit is the Ca^{2+} channel and the other subunits regulate channel gating (Catterall, 2000). As with many Ca^{2+} release and entry channels multiple isoforms of the subunits have been found and different types of VOCCs are expressed in a tissue specific manner (Bootman et al., 2001). VOCCs are activated by depolarisation of the PM, the influx of Ca^{2+} ions following membrane depolarisation leads to the release of synaptic vesicles, this process occurs within microseconds (Berridge et al., 2000). Electrophysiological studies have revealed different Ca^{2+} currents flow through these channels and as such these have been designated; L-, N-, P-, Q-, R- and T-type VOCCs (Catterall, 2000).

1.2.5.2 - Receptor Operated Channels

Also known as ligand-gated channels, a ROC opens in response to the binding of a ligand and allows the entry of extracellular ions. An example of a ROC is the *N*-Methyl-D-Aspartate Receptor (NMDAR); this opens in response to the binding of glutamate on the extracellular domain (Berridge et al., 2000). There is a wide variety of ROCs who are structurally and functionally diverse and they are activated by a wide range of agonists, for example adenosine triphosphate (ATP), Serotonin (5-HT), glutamate and acetylcholine (Bootman et al., 2001).

1.2.5.3 - Store Operated Channels (SOC)

There is much controversy surrounding this mechanism of extracellular Ca^{2+} entry and in the past it has often been called many things; capacitative calcium entry (CCE) channels (Putney, Jr., 1986), store operated Ca^{2+} entry (SOCE) channel and the term associated with it, describing the current through the channel was calcium release activated current (I_{CRAC}) coined by Hoth and Penner (1992). A consensus appears to have been met and the Ca^{2+} entry channels in question are now commonly known as store operated channels (SOC). In 1981 Casteels and Droogmans demonstrated that in vascular smooth muscle cells the depletion of agonist sensitive intracellular Ca^{2+} stores increased the rate of Ca^{2+} uptake from outside of the cell (Casteels and Droogmans, 1981). From this initial observation a model was developed and Putney first introduced the idea of CCE in 1986.

The cytosolic Ca^{2+} signals generated involved two closely linked components; rapid, transient release of Ca^{2+} stored in the ER followed by a slowly developing entry of extracellular Ca^{2+} (Berridge et al., 1998; Clapham, 1995; Ma et al., 2001; Parekh and Penner, 1997; Putney, Jr. and Bird, 1993b; Putney, Jr. and McKay, 1999; Putney, Jr. and Ribeiro, 2000). The initial signal for store release of Ca^{2+} is mediated by the action of $InsP_3$ on the $InsP_3R$ and is described above in section 1.2.4. The resulting depletion of Ca^{2+} triggers the slow activation of the SOCs, this phase of the Ca^{2+} signal serves to mediate longer term cytosolic Ca^{2+} elevations and replenishes intracellular Ca^{2+} stores (Figure 1.2) (Parekh and Penner, 1997; Putney, Jr. and Bird, 1993b; Venkatachalam et al., 2002).

1.2.5.3.1 - SOC Mechanism of Action

Likely hypotheses for mechanisms regulating entry of Ca^{2+} after store depletion are the conformational coupling, exocytosis and the chemical coupling mechanisms (Clapham, 1993; Gill et al., 1996; Irvine, 1990; Randriamampita and Tsien, 1993; Smani et al., 2004). The original model for the mechanism of activation of SOCs was the conformational coupling of the $InsP_3$ receptor on the ER membrane to the SOC on the PM (Gill et al., 1996; Irvine, 1990). The exocytosis model involves the fusion of vesicles containing SOCs linked with $InsP_3Rs$ on the ER, with the PM (Fasolato et al., 1993). This

mechanism is similar to the conformational coupling model and there has been considerable evidence to support the exocytosis model (Yao et al., 1999). The chemical coupling model involves the release of a diffusible SOC activating messenger called calcium influx factor (CIF) from the ER indicating to the SOC the depletion of Ca^{2+} stores (Clapham, 1993; Clapham and Neer, 1993; Randriamampita and Tsien, 1993; Smani et al., 2004). However, the mechanism for coupling ER Ca^{2+} store depletion with Ca^{2+} entry is a thus far unresolved question and despite the numerous hypotheses (Barritt, 1998; Berven et al., 1994; Bird and Putney, Jr., 1993; Bode and Netter, 1996; Casteels and Droogmans, 1981; Putney, Jr., 1986; Putney, Jr., 1997; Somasundaram et al., 1995; Venkatachalam et al., 2002) not one has been shown conclusively to be the case.

1.2.5.3.2 - Are SOCs TRPs?

Many groups believe they have found SOCs in many different cell types; from smooth muscle cells (Albert and Large, 2003; Lin et al., 2004) to endothelial cells (Cioffi et al., 2003; Norwood et al., 2000). It has widely been proposed that the molecular candidates for SOCs are a family of non-selective cation channels, transient receptor potential channels (TRPs), it was first proposed when a group lead by Schilling expressed D*rosophila* TRP and a similar protein, TRP-like (TRPL) in Sf9 insect cells, they found that the expression of TRP gave a depletion activated inward current of Ca^{2+} (Hu et al., 1994; Putney, Jr. and McKay, 1999; Vaca et al., 1994). Since this discovery many of the mammalian TRPs have been proposed to be SOCs, however this, as well as the original TRP observation, remains controversial (Putney, Jr. and McKay, 1999). Bernd Nilius and others are more sceptical about SOCs and the role TRPs have to play, as there is no consensus in the field on what is required to define a SOC. Many believe that three criteria must be reached before a candidate protein can be recognised as a SOC; it must be activated by various forms of store depletion, there must be a close correlation between current activation/ deactivation and changes in the Ca^{2+} content of the store, and finally the phenomenon must disappear when the candidate protein or gene is eliminated in a transgenic model, a controlled antisense or by ribonucleic acid interference (RNAi). Importantly these criteria have not yet been met for any identified model (Nilius, 2004).

1.2.5.4 - Second Messenger Operated Channels (SMOC)

SMOC are also known as receptor activated Ca^{2+} channels (RACC) and RACC is defined by Barritt (1999) as any PM Ca^{2+} channel, other than a VOCC, which is opened as a result of the binding of an agonist to its receptor, where the receptor protein is separate from the channel protein and for which the mechanism of channel opening does not involve depolarisation of the PM (Barritt, 1999). By this definition SOCs are a subgroup of RACC, however this section will concentrate on the other subgroup; SMOC. Second messenger-operated channels are triggered by the same initial signals that trigger SOCs, however instead of $InsP_3$ leading to the SOC pathway, Ca^{2+} channels are activated by intracellular lipid messengers such as DAG (Figure 1.2) and polyunsaturated fatty acids (PUFAs) such as arachidonic, linoleic and linolenic acids (three essential fatty acids; EFA) (Ambudkar, 2004; Bootman et al., 2001; Chyb et al., 1999; Hofmann et al., 1999; Mignen and Shuttleworth, 2000). Each of the three EFAs has been shown to induce recovery of Ca^{2+} stores and re-entry of Ca^{2+} into cells for the cell growth cycle of quiescent cells (Gill et al., 1996). These unknown Ca^{2+} channels activate substantial Ca^{2+} influx in the absence of Ca^{2+} store release (Ambudkar, 2004; Bootman et al., 2001; Chyb et al., 1999; Hofmann et al., 1999; Mignen and Shuttleworth, 2000). The TRP family of non-selective cation channels has again been suggested as a molecular candidate for SMOC however, this has not yet been definitively proven (Hofmann et al., 1999; Minke and Cook, 2002; Montell, 2001).

Figure 1.2 (following page): Schematic diagrams two proposed mechanisms of Ca^{2+} influx, **a** shows the proposed SOC Ca^{2+} signal cascade and **b** shows the proposed SMOC Ca^{2+} signalling cascade (Not to scale). PM Plasma membrane; GPCR G-protein coupled receptor; TK Tyrosine kinase; PLC Phospholipase C; SOC/TRP Store operated/ Transient receptor potential channel (see section 1.3.5.3.2), SMOC/TRP Second messenger operated/ Transient receptor potential channel; ER Endoplasmic reticulum; SERCA SR/ER Ca^{2+} ATPase; $InsP_3R$ $InsP_3$ Receptor; ? Unknown mechanism of action. (Not to scale; (Berridge, 1993; Berridge et al., 2000; Putney, Jr. and Bird, 1993b).

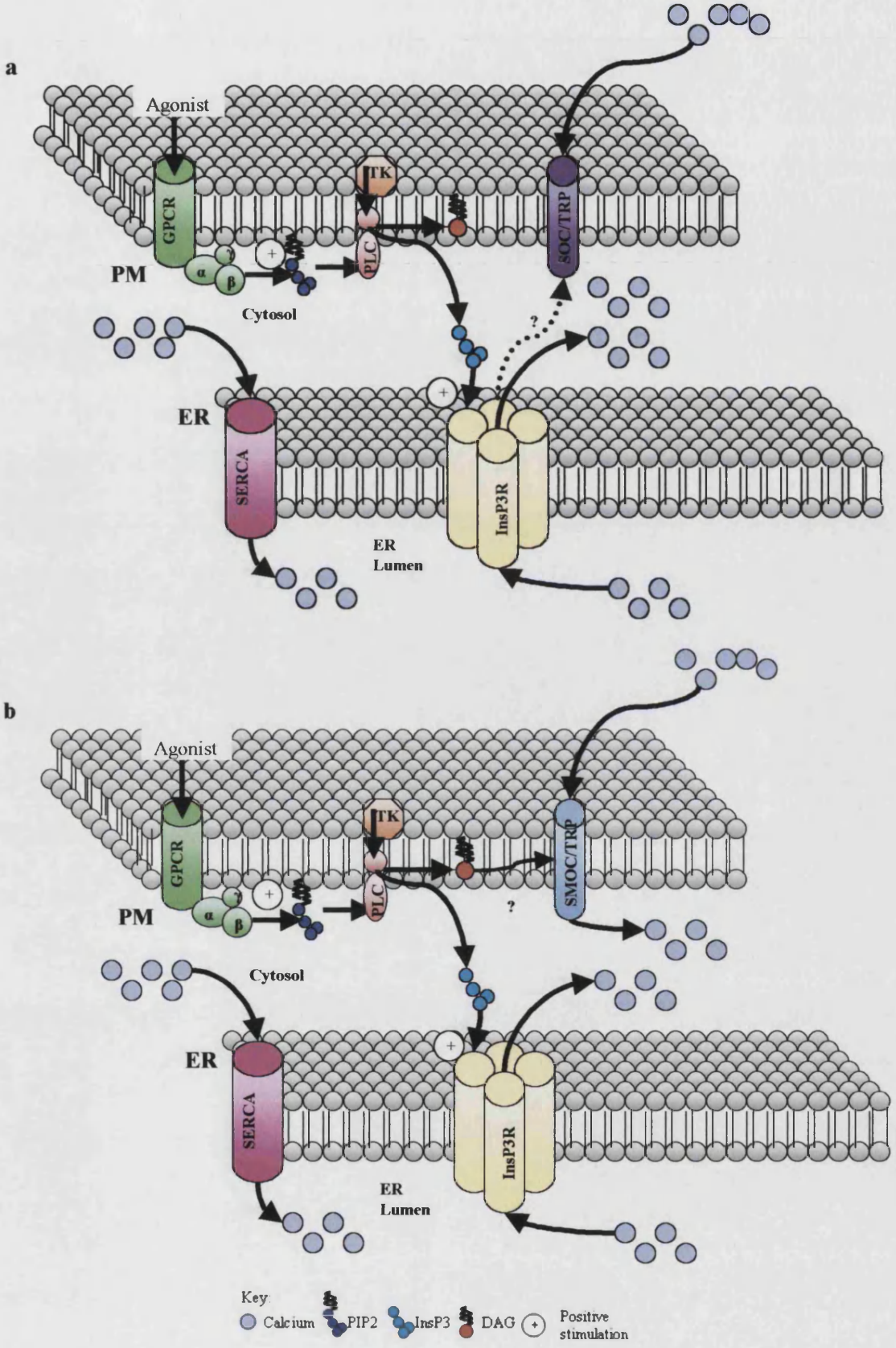
a
Agonist
GPCR
TK
PLC
SOC/TRP
PM
α
β
Cytosol
?
ER
SERCA
InsP3R
ER
Lumen
b
Agonist
GPCR
TK
PLC
SMOC/TRP
PM
α
β
?
Cytosol
ER
SERCA
InsP3R
ER
Lumen
Key:
Calcium
PIP2
InsP3
DAG
Positive
stimulation

1.3 - Transient Receptor Potential (TRP) Protein

1.3.1 - TRP

The original TRP protein was first identified in *Drosophila* after a series of experiments identified a defective light response in the retina of the *Drosophila* (Cosens and Manning, 1969). The mutant *Drosophila* used by Cosens and Manning was dubbed transient receptor potential or '*trp*' (Pak et al., 1970) because the receptor potential declines to baseline during prolonged illumination (Hardie and Minke, 1993). The sensitivity of the response recovers after about one minute in the dark (Hardie and Minke, 1993). In 1989 the *trp* gene was cloned (Montell and Rubin, 1989; Wong et al., 1989) and it was found that the *trp* mutant *Drosophila* was a 'null' mutant, as no gene product (protein) was produced (Hardie and Minke, 1993). A hypothesis was formulated proposing the *trp* gene to encode a channel that was part of a two channel system, the correlation between *trp* and the exhaustion of cellular Ca^{2+} provided the basis of a series of experiments that showed the *trp* gene product, TRP to be a Ca^{2+} influx channel (Hardie and Minke, 1993; Minke and Cook, 2002). It was found that upon application of La^{3+} (a known Ca^{2+} channel blocker), WT flies from several species mimicked the behaviour of the *trp* mutant and application of La^{3+} to the mutant had virtually no effect (Hardie and Minke, 1992; Hochstrate, 1989; Suss-Toby et al., 1991). Therefore, under the assumption that Ca^{2+} is required for sustained excitation, it was suggested that a TRP mediated mechanism is responsible for replenishing cellular Ca^{2+} fast enough during strong illumination and therefore TRP is a Ca^{2+} channel or transporter (Hardie and Minke, 1993; Minke and Cook, 2002). Compelling evidence supported the hypothesis that TRP is a PM Ca^{2+} channel by reasoned argument drawing on evidence from structural analysis (the TRP structure appeared to be homologous to one subunit of a voltage gated channel) and functional data, much of it involving the Ca^{2+} channel blocker La^{3+} (Hardie and Minke, 1992).

1.3.2 - Molecular Identification of TRP

When the *trp* gene was cloned and sequenced it was found to encode a 1275 amino acid protein with multiple (most likely six; Figure 1.3) membrane spanning regions (Montell and Rubin, 1989; Wong et al., 1989). The predicted structure was highly reminiscent of the superfamily of voltage and second messenger gated ion channels (Jan and Jan, 1992; Phillips et al., 1992). However, the amino acid sequence suggested that, if TRP is a channel, it is not voltage gated because the fourth putative transmembrane segment lacks the positively charged residues needed to form a voltage sensor in voltage gated ion channels (Stuhmer et al., 1989). Voltage gated channel subunits consist of four homologous domains, each with six transmembrane helices (S1-6) however, the TRP sequence includes only one such domain, it therefore seems probable that like the voltage gated K^+ channels, TRP proteins are subunits of a tetrameic structure (Hardie and Minke, 1993). It does remain unclear whether the channels are assembled as homomers or are heteromeric assembling with other proteins (Hardie and Minke, 1993).

In the intracellular N-terminal region of the 1275 amino acid TRP protein there are four ankyrin repeats (Figure 1.3; (Phillips et al., 1992). Ankyrin repeats are 33 amino acid residue motifs that mediate specific protein-protein interactions with a diverse repertoire of macromolecular targets (Sedgwick and Smerdon, 1999). Ankyrin provides, among other things, a mechanism for linking membrane proteins to the cytoskeleton, and plays a role in subunit interactions of proteins with two or more subunits (Michaely and Bennett, 1993). If TRP is a subunit of a tetrameric channel the ankyrin repeat may play a role in the interactions of the subunits or localisation of the channel (Minke and Cook, 2002). Shortly before the membrane spanning region is a segment of hydrophobicity, this is called hydrophobic domain 1 or the coiled coil domain (Figure 1.3; (Minke and Cook, 2002). The coiled coil is a ubiquitous protein motif that is commonly used to control oligomerisation and may contribute to the homo- or heteromerisation of the protein (Vazquez et al., 2004).

Close to the membrane spanning region in the C-terminal region is an area termed the TRP box (Figure 1.3), this is a region of six amino acids (EWKFAR) that only increased

in significance after the identification of other TRPs (Montell, 2001). The TRP box is a highly conserved region across species and TRP subfamilies (Montell, 2001). TRP also contains a putative Calmodulin (CaM) binding domain in the C-terminal region (residues 628-977; Figure 1.3) (Phillips et al., 1992). Further reports have suggested that TRP binds to CaM in a Ca^{2+} dependent manner (Chevesich et al., 1997). The function of CaM in Drosophila phototransduction appears to be diverse but is not yet clear (Minke and Cook, 2002). Close to the putative CaM binding domain on the C-terminus there is a PEST sequence (Figure 1.3), this is a signal for protein degradation by the Ca^{2+} dependent protease calpain, this is a typical sequence for CaM binding proteins (Li and Montell, 2000; Minke and Cook, 2002). Due to this, it was expected that TRP would show a fast turnover rate, however research has revealed a relatively slow turn over rate of only 25% in eight days (Li and Montell, 2000; Minke and Cook, 2002).

There are other structural features of TRP (Figure 1.3); in the C-terminal region there is a proline rich sequence in which the dipeptide KP (Lys-Pro) is repeated 27 times (Minke and Cook, 2002). Near the end of the C-terminus a sequence of amino acids is repeated in tandem nine times; D K D K K P G/A D (Asp-Lys-Asp-Lys-Lys-Pro-Gly/Ala-Asp) this is known as the 8 x 9 region and may be important for protein-protein interactions (Minke and Cook, 2002). At the end of the C-terminal region there is a binding domain for the PDZ scaffold, the protein 'inactivation no after-potential' D (INAD) (Shieh and Zhu, 1996; Tsunoda et al., 1997; Xu et al., 1998). PDZ domains are common structures in a wide variety of proteins and are known to be involved in signal transduction pathways, the name PDZ is derived from the names of three proteins containing PDZ domains; PSD-95, the *Drosophila* disc-large tumour suppressor protein DlgA and the tight junction protein ZO-1 (Saras and Heldin, 1996).

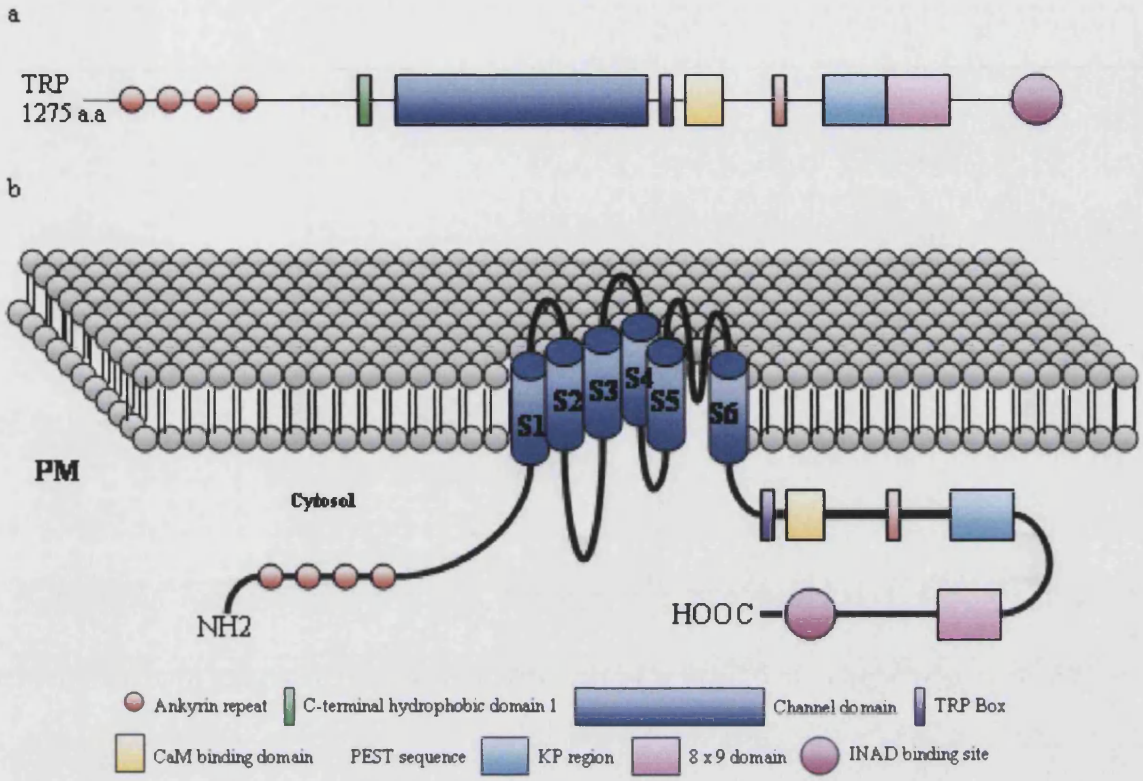

Figure 1.3: Schematic diagrams of TRP; **a** shows location of domains of putative motifs along the 1275 amino acid (a.a) protein, **b** shows a schematic diagram of the expected conformation TRP in a lipid bilayer membrane. S1-6 are the channel domain. (Diagrams not to scale). Adapted from Minke and Cook 2002.

1.3.3 - Discoveries of TRPL and TRPγ

After identification of TRP two other related *Drosophila* proteins were identified; TRP-like (TRPL) and TRP-gamma (TRPγ) (Figure 1.4;(Phillips et al., 1992; Xu et al., 2000). TRPL and TRPγ are 1124 and 1128 amino acids respectively and have 39% and 54% identities respectively to TRP, however they share the most identity in the putative transmembrane regions (Minke and Cook, 2002). TRPL and TRPγ do not contain the PEST region, 8 x 9 region, KP repeat region or an INAD binding domain (Minke and Cook, 2002).

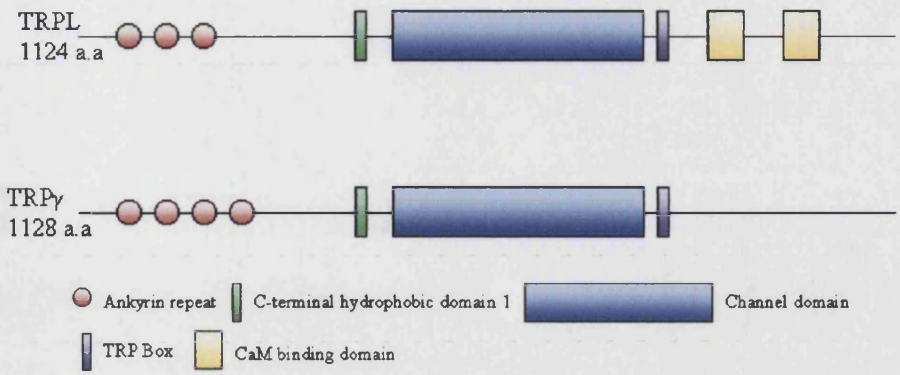

Figure 1.4: Schematic diagrams of TRPL and TRPγ. (Not to scale). Adapted from Minke and Cook 2002.

1.3.4 - TRP Mechanism of Action

TRP is an ion channel with particular significance for Ca^{2+} entry and has been put forward as a candidate for SOC and SMOC (Hofmann et al., 1999; Hu et al., 1994; Minke and Cook, 2002; Montell, 2001; Putney, Jr. and McKay, 1999; Vaca et al., 1994). Conflicting reports have resulted from work carried out to determine whether TRPs are SOCs or SMOCs, several groups have come to the conclusion that TRP is a SOC (Hardie and Minke, 1993; Vaca et al., 1994) whereas another group found that the channel may in fact be a SMOC, regulated by DAG (Chyb et al., 1999).

Functional analysis of TRPL and TRPγ showed them to be channel proteins permeable to Ca^{2+} (Hu et al., 1994; Xu et al., 2000). Both TRPL and TRPγ were shown to be constitutively active under basal conditions and it was shown that TRPL was unlikely to be a SOC as it was insensitive to release of Ca^{2+} from internal stores by thapsigargin (TG) and it has been suggested that TRPL is a SMOC regulated by PUFAs, DAG or PIP_2 (Chyb et al., 1999; Estacion et al., 2001; Vaca et al., 1994).

The jury may still be out as to whether TRP, TRPL and TRPγ are SOCs or SMOCs however, the general view now seems to be that they are SMOCs possibly activated by DAG. The difficulty appears to be that, when expressed *in vitro*, they can behave as SOCs, but *in vivo* they behave as SMOCs (Hardie, 2003).

1.3.5 - Associated Proteins

There are some indications that proteins containing one or more PDZ domain may be required for proper compartmentalisation of ion channels, proteins with multiple PDZ domains may link multiple signalling proteins together in one complex (Chevesich et al., 1997). PDZ motifs occur in a large variety of proteins and bind to diverse proteins, such as signalling, cell adhesion and cytoskeletal proteins (Li and Montell, 2000). Since the molecular identification of TRP and TRPL it has been found that the proteins function as part of a supramolecular signalling complex involved in *Drosophila* phototransduction, this signalling complex is now known as the signalplex (Montell, 1999). It appears that TRP and the protein INAD play a pivotal role in the signalplex (Li and Montell, 2000). INAD is made primarily of five 90 amino acid protein PDZ domains (Shieh and Niemeyer, 1995). It is known that TRP has an INAD binding motif on its C-terminal region however TRPL does not, TRPL was however found to co-immunoprecipitate with INAD through its heteromeric association with TRP (Xu et al., 1997; Xu et al., 1998). In a yeast two hybrid screen a FK-binding protein (FKBP) called FKBP59 was identified as an INAD binding partner in *Drosophila* and it was found to bind tightly to TRPL, altering channel regulation when heterologously expressed in Sf9 cells (Goel et al., 2001). FKBPs are immunophillins named for their ability to bind the immunosuppressant drug FK506, immunophillins are peptidyl-prolyl *cis-trans* isomerases that recognise specific XP dipeptides in their target proteins (Sinkins et al., 2004) for example FKBP12 binds to a leucyl-prolyl (LP) dipeptide in the $InsP_3R$ or valyl-prolyl (VP) in the RyR (Gaburjakova et al., 2001; Marks, 1996).

1.4 - The TRP Superfamily

With the discovery of TRP homologues in *Calliphora* and *Loglio* (squid) came the hypothesis that TRP homologues may be present in many species, even vertebrates (Huber et al., 1996; Minke and Cook, 2002; Monk et al., 1996). It was found that *Calliphora* and *Loglio* had a 77% and 46% sequence identity respectively with *Drosophila* TRP, the highest sequence similarities was through the membrane spanning regions, though they also both have CaM binding domains on the C-terminus and ankyrin repeats on the N-terminus however, *Calliphora* had a much shorter KP repeat region (Huber et al., 1996; Monk et al., 1996).

By performing genome database searches 13 members of a TRP 'superfamily' were identified in *Caenorhabditis elegans* and it was possible to subdivide these into three subfamilies, initially named short-, long- and osm-TRP (Harteneck et al., 2000). The short TRPs had the highest sequence identity to TRP and TRPL, the long TRPs, at that time less well characterised, had a higher identity to the short TRPs than to the osm TRPs, named after the founding member osm-9, which were the most well characterised group and are implicated in chemo-, mechano- and osmoregulation (Harteneck et al., 2000). As the field developed, mammalian homologues of the TRP superfamily were found in human, rat, mouse and bovine tissue, and the subfamilies have since been renamed, in an effort to standardise and avoid confusion, the mammalian superfamily has also grown to include three more sub families. The short TRP subfamily became the TRPCs, where C is classical or canonical to reflect the high homology with the archetypal *Drosophila* TRP, there are seven members all identified between 1995 and 1999 (Minke and Cook, 2002). The long TRP subfamily was renamed TRPM after the founding member, melastatin (*mlsn*) (Birnbaumer et al., 2003). The osmTRP subfamily have been renamed TRPV after the mammalian founding member, the vanilloid receptor (Birnbaumer et al., 2003). Four more novel and largely uncharacterised members of the TRP superfamily have been identified; Polycystic TRP (TRPP), Mucolipidin TRP (TRPML), ANKTM TRP (TRPA) and NompC TRP (TRPN). The relationship between the subfamilies is summarised in the phylogenetic tree below (Figure 1.5). The first

human TRP to be identified, TRPC1 was discovered by two separate groups (Wes et al., 1995; Zhu et al., 1995), however the first detailed localisation study of a mammalian TRP was carried out in rat, the protein was called TRP-R (Funayama et al., 1996). They found the protein to have a 51.8% and 44% amino acid identity to TRP and TRPC1 respectively, it was found to be present in the brain from prenatal stages (Funayama et al., 1996) TRP-R has since been found to be a splice variant of TRPC4 (Garcia and Schilling, 1997). The TRPC subfamily will be discussed in greater detail in a later section.

Although much of the research carried out on the TRP superfamily has centred on the premise that they are Ca^{2+} entry channels it is also known that most also have significant non-selective permeability to K^+ and Na^+ (Beech et al., 2004; Sinkins et al., 1998). However, for the purposes of this work the permeability of TRP channels for K^+ and Na^+ will not be discussed in detail.

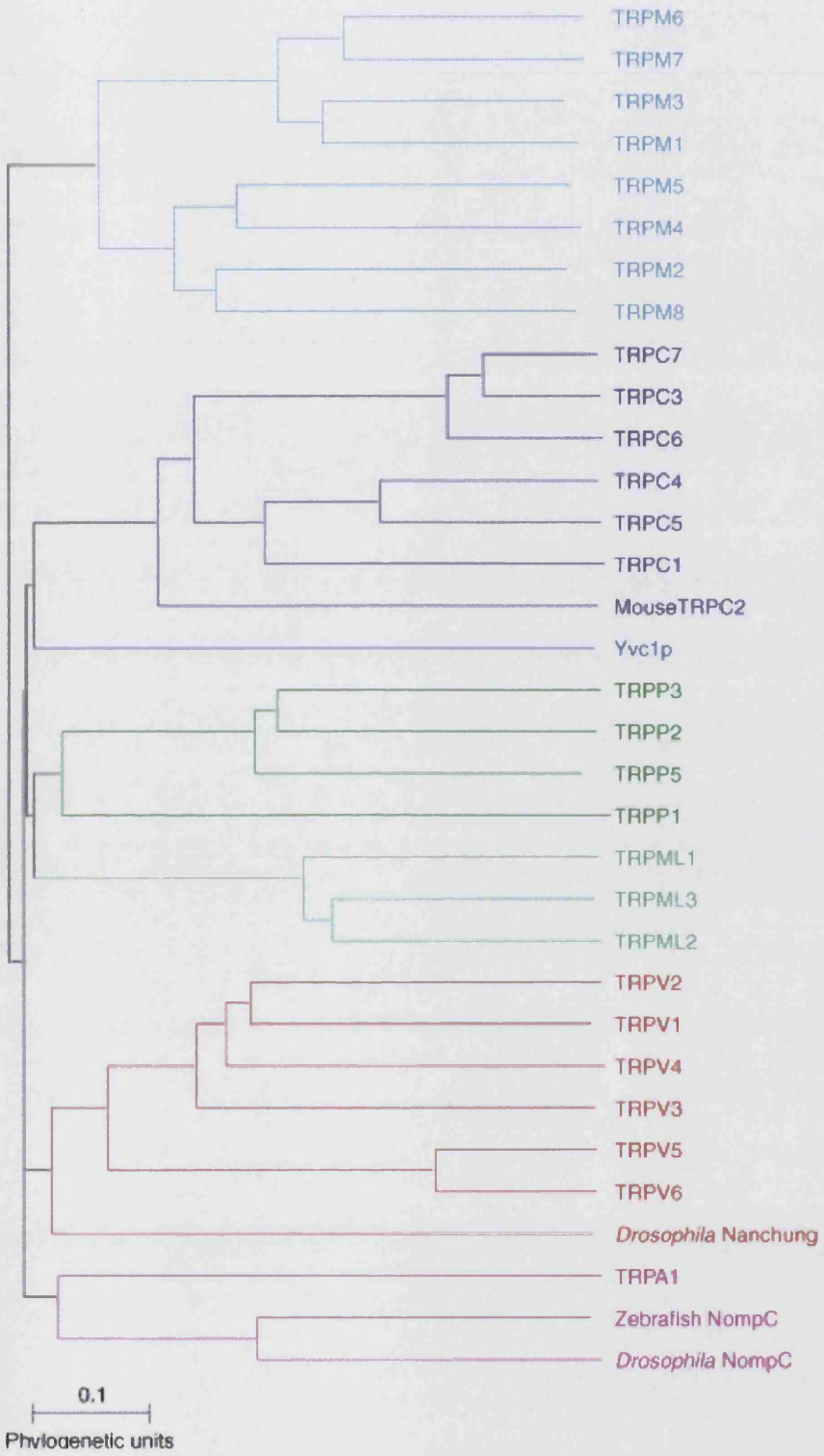

Figure 1.5: A phylogeny tree showing the relationships between all human TRPs except where the species is identified, the different colours represent the different subfamilies. 0.1 represents approximately 10% difference. (Moran *et al* 2004).

1.4.1 - Melastatin TRPs (TRPM)

The mammalian TRPM subfamily, was named after its founding member, the melastatin receptor; this subfamily has eight members, TRPM1-8 has a variety of functions and structural motifs but all have been implicated in Ca^{2+} permeability to varying degrees (Birnbaumer et al., 2003). However, TRPM 4 and 5 are selective for monovalent cations ie, Na^{+} (Hofmann et al., 1999). TRPMs range from 1104 to 2022 amino acids in length and are approximately 20% identical to *Drosophila* TRP (Figure 1.6; (Birnbaumer et al., 2003; Montell, 2001). This subfamily shares a degree of homology in the C-teminus where the TRP box is present. There are some differences between the TRP box of the TRPM subfamily and the archetypal TRP and TRPC subfamily; the TRPM consensus is [VIYFL]WK[FAY][QN]R (Birnbaumer et al., 2003; Montell, 2001). TRPM2 (Figure 1.6) has a long C-terminus, which carries a Nudix domain and an atypical α-kinase domain (Birnbaumer et al., 2003; Clapham, 2003). Nudix domains are found in a diverse family of enzymes that catalyse the hydrolysis of nucleoside diphosphate derivatives (Perraud et al., 2001). The TRPMs have been implicated in the signalling pathways that produce sweet, bitter and umami (amino acid) taste sensations and cold sensations (Clapham, 2003; McKemy et al., 2002; Zhang et al., 2003).

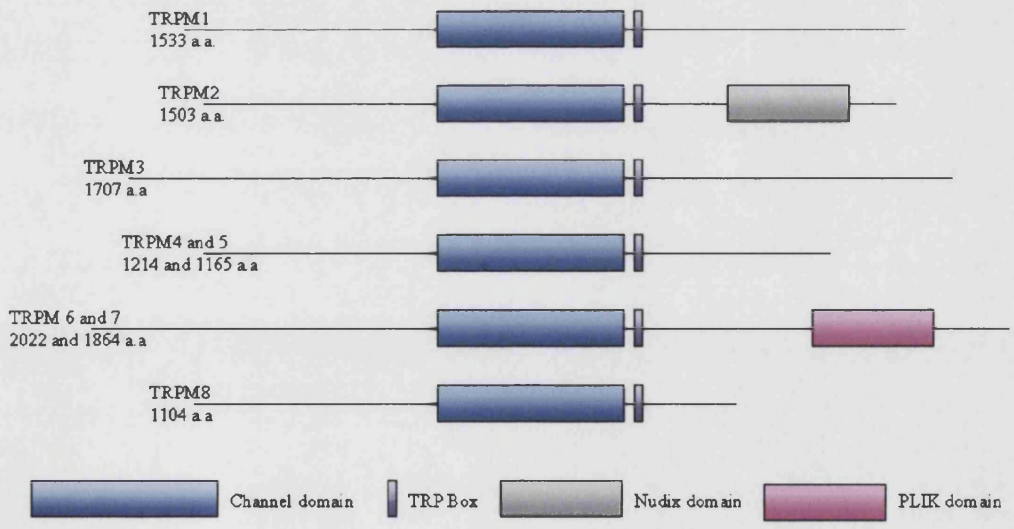

Figure 1.6: Schematic diagrams of the members of the TRPM subfamily. (Not to scale). Adapted from Birnbaumer *et al* 2003.

1.4.2 - Vanilloid TRPs (TRPV)

TRPVs are non-selective cation channels implicated in Ca^{2+} entry (Birnbaumer et al., 2003; Caterina et al., 1997). TRPVs, of which there are six members (TRPV1-6), were named after their founding member, the vanilloid receptor. All have a C-terminal TRP box, which shares a varied homology to other TRP subfamilies, the consensus is [IL]W[KR][LA]Q[RWVI], the highest homology to other TRP subfamilies is in the membrane spanning regions (Figure 1.7; (Birnbaumer et al., 2003). The TRPV subfamily is more similar in length to the TRPC subfamily, marginally shorter than the TRPMs, ranging form 729 to 871 amino acids (Birnbaumer et al., 2003). TRPV 5 and 6 are Ca^{2+} selective over Na^{+} unlike much of the TRP superfamily, which are non-selective for cations (Hofmann et al., 1999). The TRPV subfamily has been implicated in nociception, heat sensation and osmo-regulation (Caterina et al., 1997; Chuang et al., 2001; Guler et al., 2002; Jordt and Julius, 2002; Montell, 2001; Peier et al., 2002; Smith et al., 2002; Xu et al., 2002).

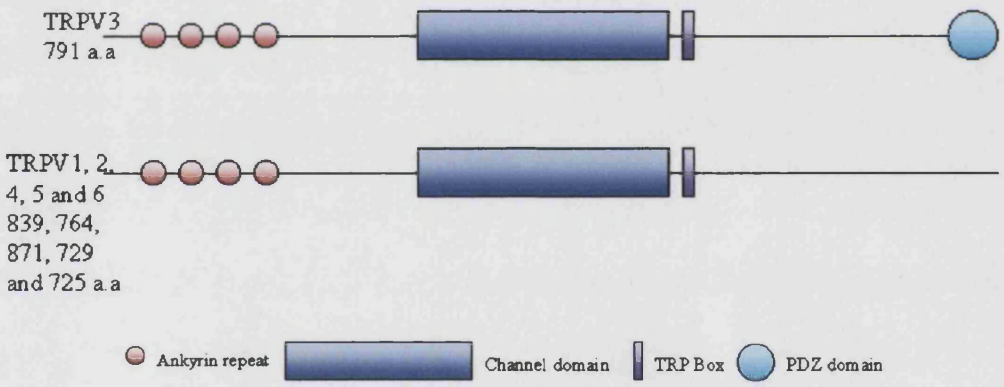

Figure 1.7: Schematic diagram of members of the TRPV subfamily. (Not to scale). Adapted from Birnbaumer *et al* 2003.

1.4.3 - Polycystic TRP (TRPP)

TRPP sub family is a relatively new member of the TRP superfamily and is named after polycystic kidney diseases 1 and 2 (PKD 1 and 2), it was the sequence analysis of PKD2 that revealed it to be a distant relative of TRP channels (Birnbaumer et al., 2003). There are now five members of the subfamily, (TRPP1-5) and they range in size from 609 to 4303 amino acids, they do not have ankyrin repeats on their N-termini or a TRP box on

their C-termini. However they have a wide range of protein interaction motifs on their C-termini (Birnbaumer et al., 2003; Clapham, 2003).

1.4.4 - Mucolipidin TRP (TRPML)

A small novel TRP subfamily, the TRPML are currently not well characterised. They were first identified in *C. elegans* (Hersh et al., 2002) and more recently found in humans (Bargal et al., 2000; Bassi et al., 2000; Sun et al., 2000). Currently there are three members of this family(TRPML1-3) and they are short in length compared to the other TRP channels, from approximately 550 to 580 amino acids in length, they have the highest degree of identity with the other TRP subfamilies throughout the membrane spanning region (Clapham, 2003; Montell, 2001). It is hypothesised that TRPMLs are localised to intracellular vesicles, as mutations in TRPML1 are associated with mucolipidosis type IV, a neurodegenerative lysosomal storage disorder (Sun et al., 2000).

1.4.5 - ANKTM TRP (TRPA)

TRPA1 or ANKTM1 is currently the only member of this subfamily, it is a Ca^{2+} permeable non-selective cation channel and is homologous to the gene painless in Drosophila, which is known to be required in nociception (Clapham, 2003; Tracey, Jr. et al., 2003). TRPA1 is distinguished by 14 ankyrin repeats on its N-terminus and is activated by cold temperatures of less than 15°C (Clapham, 2003). Recently TRPA1 has been linked to being a component of or being a mechanosensitive channels in vertebrate hair cells (Corey et al., 2004).

1.4.6 - NompC TRP (TRPN)

This subfamily of TRP has not as yet been identified in vertebrates, it has been described in *Drosophila* mechanosensory organs and *C. elegans* mechanosensory neurons (Walker et al., 2000). Similar to TRPA, TRPN has 29 ankyrin repeats on the N-terminal region, this leads to an overall length of approximately 1600 amino acids (Littleton and

Ganetzky, 2000; Walker et al., 2000). TRPN has an approximately 20% identity with TRP over the transmembrane domain (TMD) (Montell, 2001).

1.5 - Classical/Canonical TRPs (TRPC)

This subfamily of TRP is named classical or canonical, as it appears to be highly analogous to the archetypal *Drosophila* TRP in terms of structure. There are seven members of the mammalian TRPC subfamily (TRPC1–7). The TRPC sub family can be further divided into four groups based upon sequence homology and, to an extent, the currently known function of the proteins; TRPC1, TRPC2, TRPCs 3, 6 and 7 and TRPCs 4 and 5. Often TRPC1 is placed in the group with TRPCs 4 and 5, however, due to the sheer volume of data on TRPC1 compared to TRPCs 4 and 5, it shall, for the time being, be in a separate group. TRPC2 will be discussed separately because of the interesting differences between it and the other members of the TRPC subfamily.

1.5.1 - Structure of TRPCs

All the TRPCs, with the exception of TRPC7, were identified in a relatively short space of time by database searches. TRPC1 was discovered in 1995 by two separate laboratories; both groups identified the first mammalian homologue to *Drosophila* family of TRPs through searching databases. Zhu et al used the Genbank human kidney complementary DNA (cDNA) library and cloned it from HEK293 cells (Zhu et al., 1995). Wes et al used human genomic and foetal brain cDNA libraries (Wes et al., 1995). Results between the two groups were consistent and in addition Wes et al identified two other human TRPC proteins, designated hTRPCs 2 and 3 (Wes et al., 1995). It was thought that *htrpc2* was a pseudogene due to the presence of a stop codon corresponding to amino acid residue 690 (Wes et al., 1995), however a full-length version of *trpc2* was later discovered in mouse (Zhu et al., 1995). The murine sequences of the first three human *trpc*s were obtained alongside those of *trpc*s 5 and 6 (Zhu et al., 1995), *trpc4* was identified previously (Petersen et al., 1995). *trpc7* was identified in 1999 in mouse by Okada et al and more recently in human by Murphy et al and Riccio et al (Okada et al., 1999; Riccio et al., 2002a) C Murphy Unpublished data). All TRPCs share similar homologies to *Drosophila* TRP (Table 1.1) and to each other.

TRPC	Species	Number of Amino Acids	% Identity to TRP
TRPC1	Human	793	40%
	Mouse	809	40%
TRPC2	Mouse	1172	25-30%
TRPC3	Human	848	34%
	Mouse	836	34%
TRPC4	Human	977	41%
	Mouse	974	41%
TRPC5	Human	973	36%
	Mouse	975	36%
TRPC6	Human	931	37%
	Mouse	930	37%
TRPC7	Human	862	33%
	Mouse	862	33%

Table 1.1: showing each of the TRPCs and their approximate identities to *Drosophila* TRP (Birnbaumer *et al* 2003; Minke and Cook 2002).

The sequences of the TRPCs are largely similar to Drosophila TRP (Figures 1.5 and 1.6); three or four ankyrin repeats at the N-terminus and a hydrophobic coiled coil domain shortly before the channel region (Figures 1.8 and 1.9; (Birnbaumer et al., 2003). TRPC2 has a putative CaM-binding domain on the N-terminus before the ankyrin repeats (Birnbaumer et al., 2003). The channel region is highly homologous among all the TRP superfamily and consists of six membrane spanning domains (S1-6) and a putative pore region between S5 and S6 (Minke and Cook, 2002). After the TMD there is the TRP box followed by a proline rich region (not as extensive as the TRP proline rich region of 27 repeats of KP described in section 1.3.2; (Birnbaumer et al., 2003). There is also an $InsP_3R$ binding site and a CaM binding site (two in TRPCs 4 and 5) on the C-terminal tail (Birnbaumer et al., 2003). Here the similarity with TRP ends; the TRPCs are generally shorter proteins and therefore do not carry the other motifs associated with TRP, however there is a putative PDZ binding domain on the C-terminus of TRPCs 4 and 5 (Clapham, 2003).

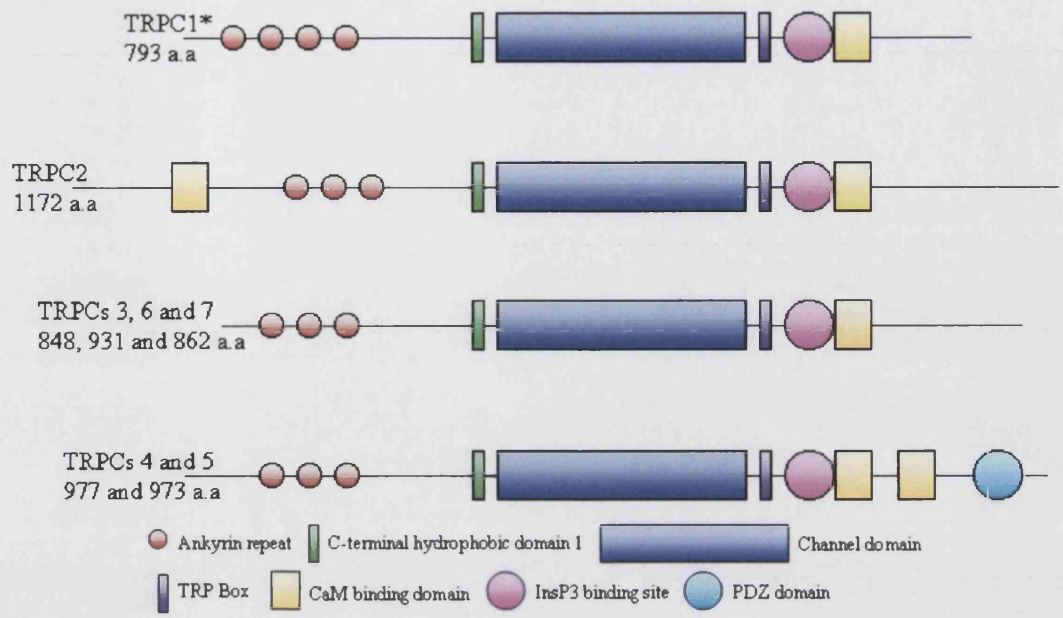

Figure 1.8: Schematic diagrams (not to scale) of all members of the TRPC subfamily in their individual subgroups. (* = some of the TRPC1 splice variants have 3 ankyrin repeats) (Birnbaumer *et al* 2003)

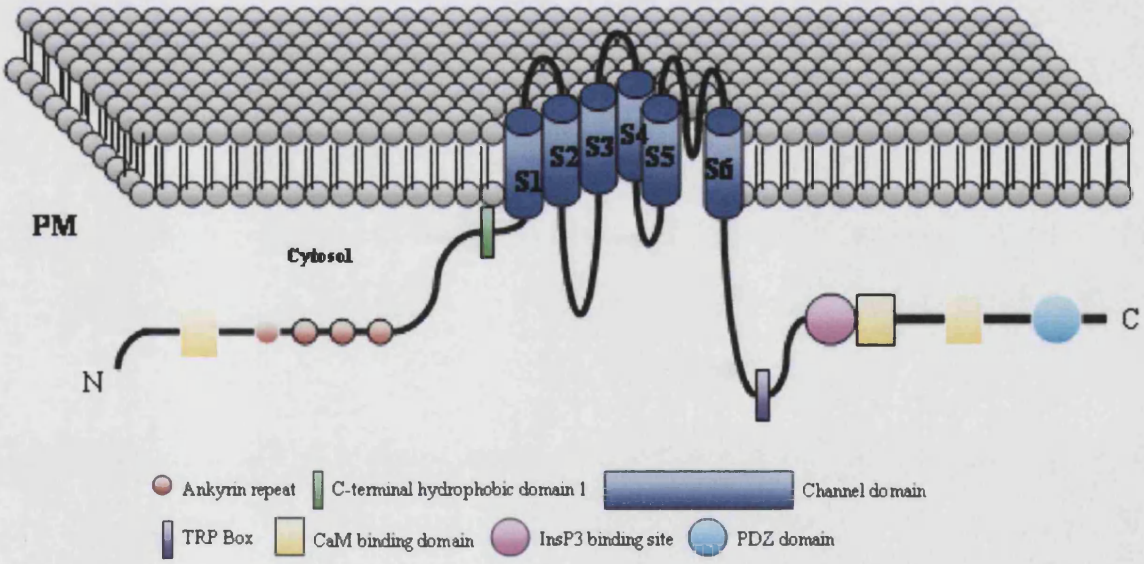

Figure 1.9: A schematic diagram (not to scale) of the expected conformation of a TRPC in the lipid bilayer membrane. (CaM binding domain, ankyrin repeat and PDZ domain without black outline are unique to specific TRPCs, see Figure 1.8 above).

Many of the TRPCs have a number of different isoforms as a result of alternative splicing summarised in Table 1.2 below:

TRPC	Number of Isoforms	Amino Acid Lengths	References
TRPC1	4 (Mouse: FL (α), β, γ, δ)	TRPC1α = 793, TRPC1β = 759	(Zhu et al., 1995) (Sakura and Ashcroft, 1997)
TRPC2	4 (Mouse: FL (A), B, α, β, sm)	TRPC2A = 1172, TRPC2B = 1072 TRPC2α = 866 TRPC2β = 890	(Wes et al., 1995) (Yildirim et al., 2003) (Hofmann et al., 2000) (Vannier et al., 1999) (Chu et al., 2005)
TRPC3	2 (Human: FL, 3a)	hTRPC3 = 848 hTRPC3a = 921	(Wes et al., 1995) (Yildirim et al., 2005)
TRPC4	2 (Human: FL, β)	TRPC4 = 977, TRPC4β = 894	(Zhu et al., 1996) (Mery et al., 2001)
TRPC5	1 (Human: FL only)	TRPC5 = 973	(Zhu et al., 1996)
TRPC6	3 (rat: FL (A) B, C)	rTRPC6A = 930 rTRPC6B = 876 rTRPC6C = 808	(Zhang and Saffen, 2001)
TRPC7	5 (Human: FL, A, B, C, γ)	TRPC7 = 862 TRPC7A = 802 TRPC7B = 808 TRPC7C = 260 TRPC7γ = 748	(Okada et al., 1999) Adrian Wolstenholme Unpublished data Xu and Beech GenBank

Table 1.2: splice forms for all of the TRPC subfamily, TRPC2* =β hypothesised to be a third splice form.

1.5.2 - The Functional Mechanisms of Action of the TRPCs

Since *Drosophila* TRP is now generally thought of as being receptor activated, possibly by DAG (Hardie, 2003), and the TRPCs are the most closely related to the archetypal TRP in the whole superfamily, the hypothesis is that the TRPC subfamily would have the same activation mechanism, however despite the majority of publications involving the TRP superfamily and more specifically TRPCs involving the functional nature of the

proteins, this is a highly controversial area of study. The general view of the functional activation is summarised in Table 1.3:

TRPC	SOC or SMOC?
TRPC1	SOC
TRPC2	SOC/SMOC
TRPC3	SMOC
TRPC4	SOC
TRPC5	SOC
TRPC6	SMOC
TRPC7	SMOC

Table 1.3: A generalised view of functional activation of the TRPCs. Adapted from Zitt *et al* 2002.

However, this general view is over simplified, the sheer number of functional studies carried out on all of the TRPCs highlights how complex this subject area has become (Zitt et al., 2002).

Most functional experiments carried out on TRPCs have utilised calcium imaging with Fura 2-acetomethyl ester (Fura-2AM) or electrophysiological recording (patch clamp) techniques and a common experimental problem appears to be the failure to fully account for the sometimes relatively high constitutive activity of the channels. This problem can be amplified under conditions in which intracellular Ca^{2+} buffering is reduced, for example during the use of intracellular Ca^{2+} pump inhibitors (Putney, Jr., 2004). There are other short comings of previous functional experiments, so an ideal way of examining any of the TRPCs would be to look at the endogenous form of the protein and performing functional experiments involving blocking of the channel. An example of this were experiments carried out by Xu and Beech on TRPC1 in rabbit arteriolar cells using an inhibitory antibody, the result of this study was that TRPC1 was store-operated (Xu and Beech, 2001). Other studies have used an over-expression system to express the TRPC; this in itself is not ideal as the cell type used may not naturally express the protein and may express it in a way that would not reflect the function of the endogenous protein.

Also, those experiments that use the TRPC from a species that is different to the cell type it is being over-expressed in may also not reflect the function of the endogenous protein, for example Okada et al expressed murine TRPC7 in a HEK293 (human) cell line.

1.5.2.1 - TRPC1

The apparent store-operated activation of TRPC1 has been observed in cell lines and cell types endogenously expressing TRPC1, namely salivary gland and platelets (Liu et al., 2000; Rosado et al., 2002; Zhu et al., 1996). TRPC1 (as well as TRPC4 and 5) may be associated with lipid raft microdomains or a signalplex similar to that seen with *Drosophila* TRP, TRPC1 has been detected in lipid raft domains and TRPC1 SOC signals are inhibited upon cholesterol depletion of lipid rafts in submandibular gland cells (Lockwich et al., 2000). When co-expressed, TRPC1 co-immunoprecipitated with INAD (Goel et al., 2002). It is also known that TRPC1 has activity inhibited by Ca^{2+}, this may be due to the action of CaM (Beech et al., 2003). Stimulation of TRPC1 by the second messenger DAG, independently of store release of Ca^{2+} has been detected in the absence of extracellular Ca^{2+} but not in its presence (Delmas et al., 2002; Lintschinger et al., 2000). Much of the research involving TRPC1 has concluded that it is a SOC, however it has been difficult to obtain reliable results, possibly due to a large fraction of over expressed TRPC1 in cell lines localising to intracellular membrane compartments and not the PM (Beech et al., 2003; Brereton et al., 2001; Hofmann et al., 2002). It is possible that in order to form a functional channel TRPC1 may require other TRPC subunits or other proteins (Beech et al., 2003). Recent research involving electrophysiological recordings, membrane fractionation and Western blotting has identified TRPC1 as a component of a mechanosensitive cation channel (Maroto et al., 2005). They also found that by transfecting *trpc1* into the Chinese Hamster Ovary K1 (CHO-K1) cell line significantly increased the mechanosensitive cation channel expression (Maroto et al., 2005).

1.5.2.2 - TRPCs 4 and 5

The TRPC subgroup that contains TRPCs 4 and 5 is currently thought to form SOCs. When the bovine forms of the channels were originally identified they were named CCE1 and CCE2 (Philipp et al., 1998). The majority of studies on TRPC4 have shown the channel to be a SOC; TRPC4 knockout mice, while showing no outwardly obvious abnormalities, display changes in endothelium mediated signalling and SOC activity is absent from the aortic endothelium (Freichel et al., 2001). Also, lung vascular endothelial cells from TRPC4 knockout mice had a decreased Ca^{2+} response to agonists (Tiruppathi et al., 2002). Expression of antisense TRPC4 in adrenal cells reduces store dependent currents (Philipp et al., 2000). However, Wu et al have found no evidence for SOC activity of TRPC4 and believe it to be receptor activated (Wu et al., 2002). TRPC5, originally thought to be a SOC (Philipp et al., 1998), appears to be controversial in its mechanism of activation. Much of the research carried out on mTRPC5 (97% identical to hTRPC5) seems to suggest that the channel is receptor activated (Okada et al., 1998; Schaefer et al., 2000). However, a recent study has found that DAG has no effect on hTRPC5, indeed hTRPC5 appears to be a Ca^{2+} dependent SOCs with Ca^{2+} release helping activation of the channels (Zeng et al., 2004). TRPCs 4 and 5 are expressed in many brain regions and it has been found that TRPC4 may have a critical role to play in the Ca^{2+} influx that controls GABA release from interneuronal dendrites on to thalamic relay cells (Munsch et al., 2003).

1.5.2.3 - TRPCs 3, 6 and 7

The subgroup containing TRPC3, 6 and 7 is largely thought of as being activated by a second messenger, DAG, and although most of the published work on this subgroup has focused on their Ca^{2+} permeability it is known that TRPC3, 6 and 7 have a relatively low selectivity for Ca^{2+} over Na^{+} (Hofmann et al., 1999; Okada et al., 1999). This section will concentrate on the current understanding of TRPC3 and 6, TRPC7 will be discussed further in section 1.6. TRPCs 3 6 and 7 have varying levels of constitutive activity and this may be due to possible glycosylation at various sites on the N-terminal region; TRPC3 is predicted to be monoglycosylated in the first extracellular loop and has high

constitutive activity; TRPC6 is dually glycosylated at the first and second extracellular loops and is tightly regulated; however, TRPC7 has considerable basal activity despite a predicted glycosylation site at the first and second extracellular loops (Okada et al., 1999; Vazquez et al., 2004). Hofmann et al used Chinese hamster ovary cells to over-express TRPCs 3 and 6 and by patch clamp techniques they determined that both channels were second messenger activated by DAG (Hofmann et al., 1999). For TRPC6 there seems to be little evidence to support activation by store depletion and all studies carried out on TRPC6 have shown it to be a SMOC. An initial experiment, designed to identify SOCs, was carried out on TRPC6 transfected HEK293 cells and found that there was no response to the depletion of stores by TRPC6 (Boulay et al., 1997). Since then, in platelets and human T-cells, TRPC6 has been shown to form at least part of a channel activated by DAG (Gamberucci et al., 2002; Hassock et al., 2002). TRPC6 has also been shown to be regulated by muscarinic ACh receptors involving DAG (Zhang and Saffen, 2001) and TRPC6 has been implicated as being a component of the α_1-adrenoceptor-activated Ca^{2+} permeable cation channels in vascular smooth muscle, where it is activated by second messengers, independent of store depletion (Inoue et al., 2001). TRPC3 is a different matter; much work has been carried out on this protein and the general consensus in most review publications is that it is a receptor activated channel, however a review by Zitt et al showed a comparison of all functional studies on the channel to the date of the publication (numbering almost 20) have shown a fairly even split of individual groups showing the activation either being by the receptor via a second messenger or by store depletion (Zitt et al., 2002). For example; patch clamp experiments showed the channel to be activated by DAG (Hofmann et al., 1999) and TRPC3 stably expressed in HEK293 cells are receptor activated via PLC (Trebak et al., 2002). In 2004 a group identified TRPC3 in chicken muscle and osteoblasts as being a component of the SOC entry pathway in response to vitamin D_3 (Santillan et al., 2004). Also a recent report suggests that TRPC3 is modulated by protein kinase G (PKG) and is store operated, they also hypothesise a role for PKG in the modulation of TRPCs 6 and 7 (Kwan et al., 2004).

A current theory that allows for the observed and reported differences in regulation of the TRPC channels is that at lower levels of expression TRPCs combine with a limited

number of other cellular proteins and possibly other channel subunits to form SOCs and the statistical likelihood of forming a complete, correctly formed channel might decrease if the concentrations are increased (Putney, Jr., 2004). In other words, the 'correct' conformation of a TRPC is as a heteromer and in this conformation it is a SOC, the incorrect conformation of a TRPC is a homomer and in this conformation it is a SMOC (Putney, Jr., 2004). This theory has come about due to work carried out by Vasquez et al; they showed that an increased level of TRPC3 leads to a mode of channel regulation not seen at lower levels of expression, i.e. low levels of expression (stable transfection) the channel is a SOC and high levels of transfection (transient transfection) the channel is a RAC (Vazquez et al., 2003). This current hypothesis has also been applied to TRPC7 (Lievremont et al., 2004), this is discussed further in section 1.6.5, and recent work on TRPC5 has suggested that the activation mechanism could vary due to levels of expression (Zeng et al., 2004).

It is clear from the work carried out to assess the functional nature of TRPC channels that there is still a great deal of ambiguity surrounding what regulates them and perhaps the use of over expression systems (either stable or transient transfections) are inadequate for the assessment of regulation of these channels. The absence of specific and potent channel blockers for TRPCs only leaves ribonucleic acid interference (RNAi) studies or gene knockout studies in mice.

1.5.3 - Tissue Expression and Cellular Localisation of the TRPCs

Several groups have carried out analysis of mRNA expression of the TRPCs in different tissues by reverse transcriptase polymerase chain reaction (RT-PCR) and overall the data obtained corresponds with each other. Data compiled by Riccio et al (2002) appears to be the most thorough and comprehensive study of tissue distribution of the human TRPCs (except hTRPC2) to date. By performing RT-PCRs on various brain regions they found that all of the hTRPCs are expressed at relatively low levels in many brain regions however, hTRPC5 appears to be the only one expressed at moderate levels in almost all of the regions tested (Riccio et al., 2002b). Pituitary was also analysed and it was found

that hTRPC1, 3 and 7 are highly expressed whereas hTRPC4, 5 and 6 have relatively low levels of expression (Riccio et al., 2002b). The cerebellum displayed high levels of expression of hTRPC1 and 5 but low levels of hTRPC3, 4, 6 and 7 (Riccio et al., 2002b). The spinal cord was found to have low levels of expression of all hTRPCs (Riccio et al., 2002b). Other tissues were also analysed; lung, pancreas, kidney and adipose displayed low level expression of all hTRPCs with the exception of hTRPC6, which was highly expressed in lung and moderately expressed in pancreas (Riccio et al., 2002b). However, recent Northern blot data has indicated that hTRPC7 is also highly expressed in the pancreas (P Chen Unpublished data). The heart was also investigated and was found to have a moderate expression level of hTRPC1 but low expression levels of all the other hTRPCs (Riccio et al., 2002b). RT-PCRs were also carried out on several cell lines including COS7 and HEK293, COS7 cells displayed high expression of hTRPC1 and 7, low expression of hTRPC4 and 6 and no expression of hTRPC3 and 5 (Riccio et al., 2002b). HEK293 cells gave high expression of hTRPC3, 5 and 6, low expression of hTRPC1 and 4 and no expression of hTRPC7 (Riccio et al., 2002b). There are some discrepancies between the mRNA expression of some TRPCs in different species, for example mTRPC7 is expressed more in the peripheral tissues and less in the CNS, (Okada et al., 1999) as discussed further, below in section 1.6.3.

There has been relatively little identification of the specific cellular localisation pattern of the TRPCs; TRPC1 has been shown by immunocytochemistry to localise to the PM of the chicken cell line DT40 (Mori et al., 2002) and by electron microscopy to the spine membrane, peri-synaptic region and post synaptic membrane of rat cerebellar Purkinje neurons, furthermore TRPC1 was shown to co-localise with the metabotrophic glutamate receptor 1 (mGluR1) in these cells (Kim et al., 2003). Over-expression of hTRPCs 3 and 4 in HEK293 cells showed both to localise at or near the PM with hTRPC4 showing considerable staining of the Golgi apparatus, there was also significant co-localisation of both TRPC 3 and 4 with β-integrin, a focal adhesion protein (McKay et al., 2000). Finally TRPC5 has been localised in rat hippocampal neurons, it has a punctate appearance along the hippocampal neuronal processes that resemble cytoplasmic transport packets and also localises to neuronal growth cones (Greka et al., 2003).

1.5.4 - TRPC Channel Subunit Associations

Most of the studies on the possible heteromerisation of TRPCs have used co-immunoprecipitation, immunocytochemistry and fluorescence resonance energy transfer (FRET) methods, and have shown that TRPC1 localises to intracellular membrane compartments when over expressed in HEK293 cells, whereas TRPCs 3, 4, 5 and 6 all give PM staining. However, when TRPC1 is co-expressed with TRPC4 the localisation of TRPC1 changes to PM, but this is not the case when TRPC1 is co-expressed with TRPC3 or 6 (Hofmann et al., 2002). Also, a TRPC6 mutant that does not go to the PM gave PM staining when it was co-expressed with TRPC3 or WT TRPC6, but this was not the case with co-expression with TRPCs 4 and 5 (Hofmann et al., 2002). FRET analysis of TRPCs indicated direct protein-protein interaction within the TRPC subgroups and with the same TRPC type showing that the proteins do form heteromers and homomers, summarised in Table 1.4:

TRPC	Association with...	No Association with...
TRPC1	TRPC4 and 5	TRPC3, 6 and 7
TRPC3	TRPC6 and 7	TRPC1, 4 and 5
TRPC4	TRPC1 and 5	TRPC3, 6, and 7
TRPC5	TRPC1 and 4	TRPC3, 6 and 7
TRPC6	TRPC3 and 7	TRPC1, 4 and 5
TRPC7	TRPC3 and 6	TRPC1, 4 and 5

Table 1.4: Heteromeric associations between the TRPCs. Compiled using data from Hofmann *et al* 2002.

Goel et al has also carried out co-expression immunoprecipitation experiments in Sf9 cells and has shown their results to agree with those of Hofmann et al, they also looked at endogenous expression of the TRPCs in rat cortex and cerebellum and again the results agreed with Hofmann et al, however they did state that TRPC7 was difficult to detect in cortex (Goel et al., 2002). They also suggest that TRPCs 1, 4 and 5 interact with INAD like PDZ containing proteins whereas TRPCs 3, 6 and 7 do not (Goel et al., 2002). However immunoprecipitation experiments do not allow for any other protein that may form a link between two TRPCs, and recent research has shown that combining three

different subunits; TRPCs 1, 4 or 5 and 3 or 6, led to the co-assembly of DAG sensitive and insensitive channels (Strubing et al., 2003). They showed that the presence of TRPC1 and TRPC4 or 5 is necessary for the association with TRPC3 or 6 and there is as yet an unidentified fourth subunit to complete the tetramer (Strubing et al., 2003). These mixed subunits are either present in undetectable levels or not present in the adult brain but may occur in embryonic brain and may reflect a degree of developmental regulation (Strubing et al., 2003).

The apparent interactions between TRPCs 1, 4 and 5 and TRPCs 3, 6 and 7 appear to be the accepted TRPC interactions however, recent research by Liu et al (2005) has identified an interaction between TRPC1 and TRPC3. This group showed by immunoprecipitation and yeast-2 hybrid screens, cells that endogenously express TRPCs 1, 3 and 4 displayed an interaction between TRPC1 and TRPC3 but not TRPC4 and they demonstrated that this interaction was via the N-terminal regions of the proteins (Liu et al 2005).

1.5.5 - Other Associated Proteins

All of the TRPCs have CaM and $InsP_3R$ binding domains on their C-terminal region (Figures 1.10 and 1.12). TRPC4 has two CaM binding domains on its C-terminal region, and it is known that its first CaM binding domain and an $InsP_3R$ binding domain overlap, this is known as the CaM $InsP_3R$ binding domain (CIRB domain), and is conserved in all TRPCs (Tang et al., 2001). From their studies, Tang et al found that $InsP_3R$ interacts with TRPC3 and that CaM and $InsP_3R$ compete for binding of the TRPCs (Tang et al., 2001). CaM has varying affinities to the TRPCs depending on which TRP it is binding, it also inhibits the binding of $InsP_3R$ however the extent at which it does so varies from TRPC to TRPC; CaM is more easily displaced from TRPCs 3, 6 and 7 than TRPCs 1, 4 and 5, this suggests that TRPCs 3, 6 and 7 may be more sensitive to activation by $InsP_3R$ (Tang et al., 2001). CaM appears to act as a negative control for conformational coupling involving $InsP_3R$; this may be a primary mechanism for gating SOCs (Tang et al., 2001).

INAD is an associative PDZ protein for Drosophila TRP (see Section 1.3.5 of this chapter), using database searches an attempt has been made to find a mammalian homologue and in 1997 human INAD-like (hINADL) was identified and cloned (Philipp and Flockerzi, 1997), however it is currently not known to associate with any of the TRPCs.

Members of the TRPC subfamily have a conserved proline rich domain on their C-termini, this domain is very similar to the binding domain of an adaptor protein family called Homer (Yuan et al, 2003). Homer family proteins bind to proline rich sequences in RyRs and $InsP_3Rs$ and crosslinks into macromolecular complexes that display enhanced signalling properties (Yuan et al, 2003). Yuan et al (2003) demonstrated that Homer facilitated an interaction between TRPC1 and the $InsP_3R$ by crosslinking the two proteins.

Immunophillins have recently been found to interact with TRPCs; it is already known that they interact with *Drosophila* INAD and TRPL (see Section 1.3.5), and the putative binding domain in TRPL is found in TRPCs. The first LP dipeptide is conserved between TRPCs 1, 3, 4, 5, 6 and 7, however a second LP found in TRPL is changed to an IP in TRPCs 1, 4 and 5 and to a VP in TRPCs 3, 6 and 7 (Sinkins et al., 2004). A study was designed to find whether mammalian homologues of FKBP; FKBP12 and FKBP52 interacted with TRPCs. FKBP12 and FKBP52 were cloned from HEK293 cells and co-expressed with each of the TRPCs in Sf9 cells, it was found that FKBP12 interacts with TRPCs 3, 6 and 7 and FKBP52 interacts with TRPCs 1, 4 and 5 (Sinkins et al., 2004). Furthermore, the immunosupressant drug FK506 could displace the immunophillins from the TRPC and FK506 inhibited the receptor-mediated activation of TRPC6 channels stably expressed in HEK293 cells (Sinkins et al., 2004).

A mammalian PDZ protein, Na^+/H^+ exchanger regulatory factor (NHERF) is thought to interact with TRPCs 4 and 5 in a similar way to the interactions of INAD and TRP (Tang et al., 2001). NHERF has two PDZ domains and TRPC4 and 5 activation and/or PM

localisation may require the assembly with NHERF, $InsP_3R$ and other regulatory and scaffold proteins (Mery et al., 2002; Tang et al., 2001).

A novel TRPC associating protein has recently been identified by Sutton et al. Enkurin was identified in mouse sperm and was shown to bind CaM in a Ca^{2+} dependent manner. It was also shown to bind TRPCs 1, 2 and 5, following the identifcation of TRPCs 1, 3 and 5 in sperm (Sutton et al., 2004) and TRPC2 in a previous study (Jungnickel et al., 2001), discussed further in section 1.5.6. Immuno-localisation demonstrated that TRPCs 1, 2 and 5 were found in the anterior region of the mouse sperm and it is thought that these three proteins account for the Ca^{2+} influx when stimulated by the egg glycoprotein ZP3 (Sutton et al., 2004). TRPC3 was identified in the posterior region (flagellum) of sperm and it is hypothesised that it may have a role in the flagellar motility of sperm (Sutton et al., 2004). Enkurin was also identified in anterior and posterior regions of sperm, however the results of a binding assay carried out in yeast showed enkurin to bind TRPCs 1, 2 and 5 but not TRPC3 (no other TRPCs were tested). Enkurin was also identified at high levels in the vomeronasal organ (VNO), at lower levels in ovary, heart, lung and brain and not detected in several cell lines; HEK293; HD57 and COS (Sutton et al., 2004).

1.5.6 - TRPC2 – A Pseudogene in Humans

TRPC2 was first identified alongside TRPCs 1 and 3 in 1995, however; it was thought that the human form was a pseudogene due to the presence of a stop codon halfway along its open reading frame (Wes et al., 1995). *mtrpc2* was cloned and sequenced in 1996 and was found not to have the stop codon that *htrpc2* had, it was also shown to have 93 base pairs (bp) encoding 31 amino acids that the human form does not have (Zhu et al., 1996). The bovine form of *trpc2* was studied and like *mtrpc2* is not a pseudogene, it is 96% identical to *mtrpc2* and 82% identical to *htrpc2*; *btrpc2* also has the same 93bp insertion as *mtrpc2* (Wissenbach et al., 1998). From Northern blot data there was a suggestion that *trpc2* has splice variants (Wissenbach et al., 1998), this was later confirmed in mouse (see Table 2). The structure of TRPC2 (see Figures 1.10 and 1.11) has been shown to

follow the same general structure as all the TRPCs however, unusually (with the exception of TRPC4) TRPC2 has two CaM binding domains, moreover one of them is on the N-terminal region, N-terminal of the three ankyrin repeats, all other TRPCs have CaM binding domains on the C-terminal region (Yildirim et al., 2003).

Bovine TRPC2 was present in testis, spermatocytes, liver and spleen, and expression in the testis was specific to some seminiferous tubules (Wissenbach et al., 1998). In rat TRPC2 was localised to the VNO; the VNO is adjacent to the ventral septum and is thought to play a key role in the detection of pheromones (Liman et al., 1999). In research leading on from these observations TRPC2 has been implicated in male-male aggression and sex discrimination in mice. Sensory activation of the VNO requires TRPC2, mice deficient in TRPC2 fail to display male-male aggression and they initiate sexual and courtship behaviours toward both male and female mice (Stowers et al., 2002). TRPC2 has also been implicated in sperm-egg interactions during fertilisation (Jungnickel et al., 2001).

Functional analysis of TRPC2 was carried out by transiently over expressing the protein in COS-M6 cells. It was found that TRPC2 enhanced Ca^{2+} entry by a receptor independent store depletion induced pathway, it was concluded from this that the channel is a SOC (Vannier et al., 1999). However, further work by Lucas et al has shown that TRPC2 may be receptor activated, regulated by DAG. A DAG activated channel in the VNO neuronal dendrites (activated upon stimulation by pheromones) is defective in TRPC2 knock out mice, indicating that TRPC2 may form the principal subunits of a DAG gated channel (Lucas et al., 2003).

1.6 - TRPC7

1.6.1 - Identification of TRPC7

TRPC7 was first identified by Okada et al in 1999 in mice, the human form was later identified (in 2002) by Riccio et al and to date those two studies remain the main sources of information on TRPC7 (Okada et al., 1999; Riccio et al., 2002a). Our laboratory also

isolated hTRPC7 from human brain mRNA (Accession number: AJ272034). Mouse TRPC7 (mTRPC7) was cloned from brain cDNA and was found to bear the most similarity to TRPCs 3 and 6 because of this TRPC7 now shares the same subgroup as TRPCs 3 and 6 (see Table 1.5).

TRP	% Identity to TRPC7	% Similarity to TRPC7
mTRPC1	34	56
mTRPC3	81	89
mTRPC4	40	60
mTRPC5	40	60
mTRPC6	75	84
dTRP	32	53
dTRPL	33	53
TRPV1	13	34

Table 1.5: The percentage of identity and similarity with other TRPs. (Data Okada *et al* 1999)

The protein was found to have 862 amino acid residues and TRPC7 shares many of the characteristic features of the TRP superfamily (see Figures 1.10 and 1.11); it has eight hydrophobic regions making up the hydrophobic domain 1 or coiled coil region on the N-terminus, six transmembrane segments and the pore region between S5 and S6 that collectively make up the channel domain and both N and C termini are cytoplasmic (Okada et al., 1999). hTRPC7 was identified by performing homology searching against the GenBank sequence database using the hTRPC3 protein sequence (Riccio et al., 2002a). The group found an unfinished sequence (AC008661) that had sequence homology to both hTRPC3 and mTRPC7, although the initiation sequence from this was missing a newer sequence had been deposited (AC063980) and the identification of an additional exon at the 5' end was made, it was found that the initiation codon, ATG, was split between exons 1 and 2. hTRPC7 has an open reading frame of 2589 base pairs encoding protein sequence of 862 amino acids, the same as the mTRPC7. The protein was predicted to have a molecular mass of 99.6kD (Riccio et al., 2002a). hTRPC7 is 98%

identical to mTRPC7 (Riccio et al., 2002a). There is a discrepancy in the deposited amino acid sequences; the sequence deposited from our laboratory (AJ272034) was identical to the deposited sequence by Riccio et al (AC063980) except in their sequence there was an amino acid change of leucine to proline, respectively, at position 111 (L111P), this was shown by Riccio et al that this was not a cloning derived artefact and by Lievremont et al that this has no significant functional significance (Lievremont et al., 2004; Riccio et al., 2002a).

1.6.2 - TRPC7 Splice Variants

In addition to the full length sequence of mTRPC7 three alternatively spliced forms were also identified; p7β, has deletions in nucleotides encoding amino acid sequence 322-376, p7γ/λa11 at 261-376 and p7δ has a 382 base pair deletion which leads to a frame shift that changes residue 322 from phenylalanine to a glutamate and thus terminates translation of the protein at that point (Okada et al., 1999). Riccio et al have mentioned no splice variants in their publication however there are currently five splice variants published on EMBL/GenBank/DDBJ databases, three, named hTRPC7 A, B and C and accession numbers are; AJ549088, AJ549089 and AJ549090 respectively deposited by Dr A. Wolstenholme. They appear to be the same as the mTRPC7 variants. Two have been deposited by Xu and Beech and are named hTRPC7 β and γ, hTRPC7β appears to be the same as hTRPC7B however hTRPC7γ appears to be a combination of hTRPC7A and B (Table 1.6 and Figure 1.10).

hTRPC7 Variant	Nucleotide Deletion	Amino Acid Deletion	Predicted MW (kD)
hTRPC7A	781-963	261-321	92.4
hTRPC7B	964-1128	322-376	93.4
hTRPC7C	781-1345	261-488	29.9
hTRPC7γ	781-1128	261-376	86.3

Table 1.6: Splice variants of hTRPC7.

Like the corresponding mTRPC7 variant, p7δ, the deletion in hTRPC7C causes a stop codon in the nucleotide sequence leading to a change from glycine to glutamate and preventing the protein sequence from being translated past amino acid 260.

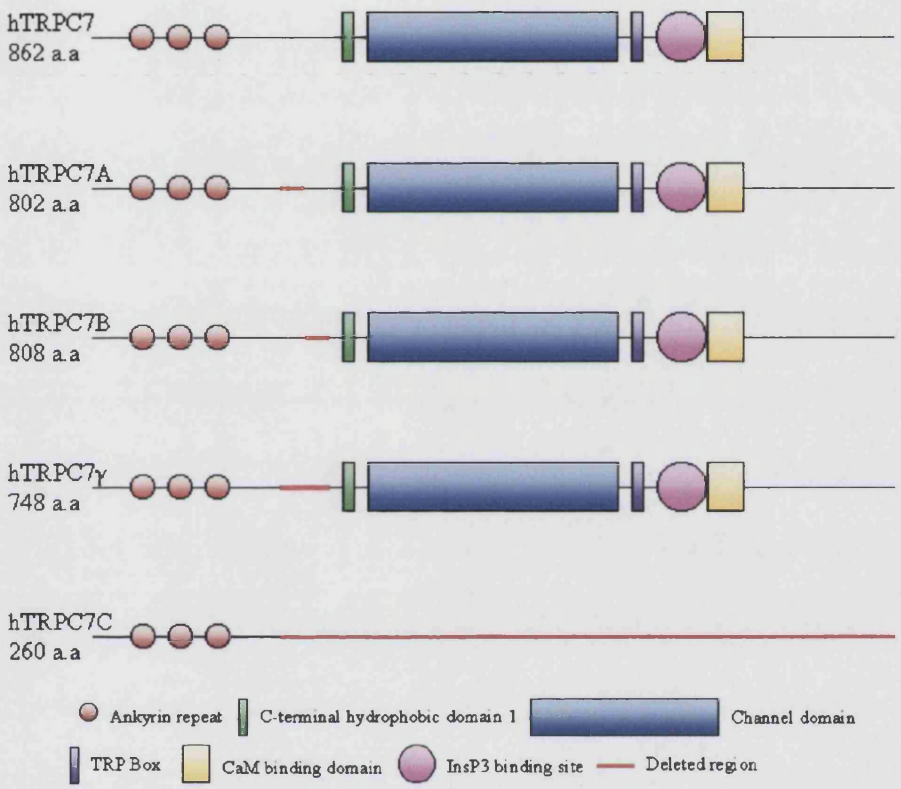

Figure 1.10: Schematic diagrams (not to scale) of all four known hTRPC7 splice variants.

1.6.3 - Tissue distribution of TRPC7

Okada et al used Northern blot analysis (Figure 1.11) to determine the tissue distribution of mTRPC7 RNA, they found that mTRPC7 was most abundant in the heart, lung and eye and also present in lower levels in the brain, spleen and testis.

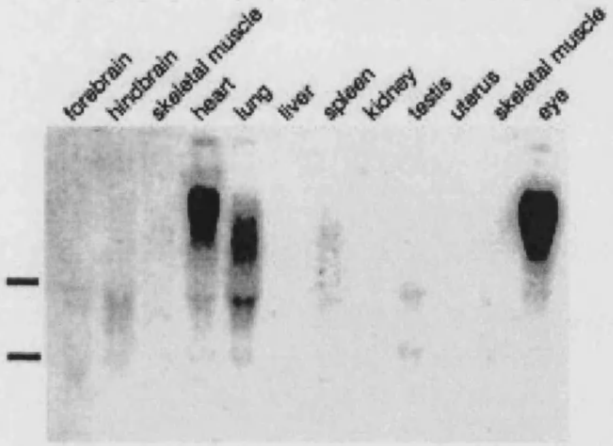

Figure 1.11: Full-length TRPC7 Northern blot carried out on mouse tissue (Okada *et al* 1999).

In order to find the specific brain regions and cell types therein expressing the lower levels of mTRPC7 in comparison to the periphery, Okada et al carried out *in situ* hybridisation, using complementary RNA (cRNA) probes specific to mTRPC7. In 8-week-old mouse brain, they found cerebellar purkinje cells to be the most prominent site of expression; intense mTRPC7 signals were also detected in the mitral layer of olfactory bulb and hippocampal neurons. Signals were also found, more diffusely in regions including the cerebellar nuclei, pons and cerebral cortex (Okada et al., 1999).

The tissue distribution data of mTRPC7 from Okada et al is in direct contrast to the tissue distribution of hTRPC7 found by Riccio et al (Figure 1.12), they carried out TaqMan real time RT-PCR to determine hTRPC7 mRNA distribution. They found hTRPC7 widely expressed in the CNS, with highest expression in this area to be in the nucleus accumbens and lower levels in the putamen, striatum, hypothalamus, caudate nucleus, locus coeruleus and medulla oblongata. Peripheral tissues showed a high level of expression in

the kidney with lower levels of expression in the intestine, prostate and cartilage. Highest over all expression was in the pituitary gland (Riccio et al., 2002a).

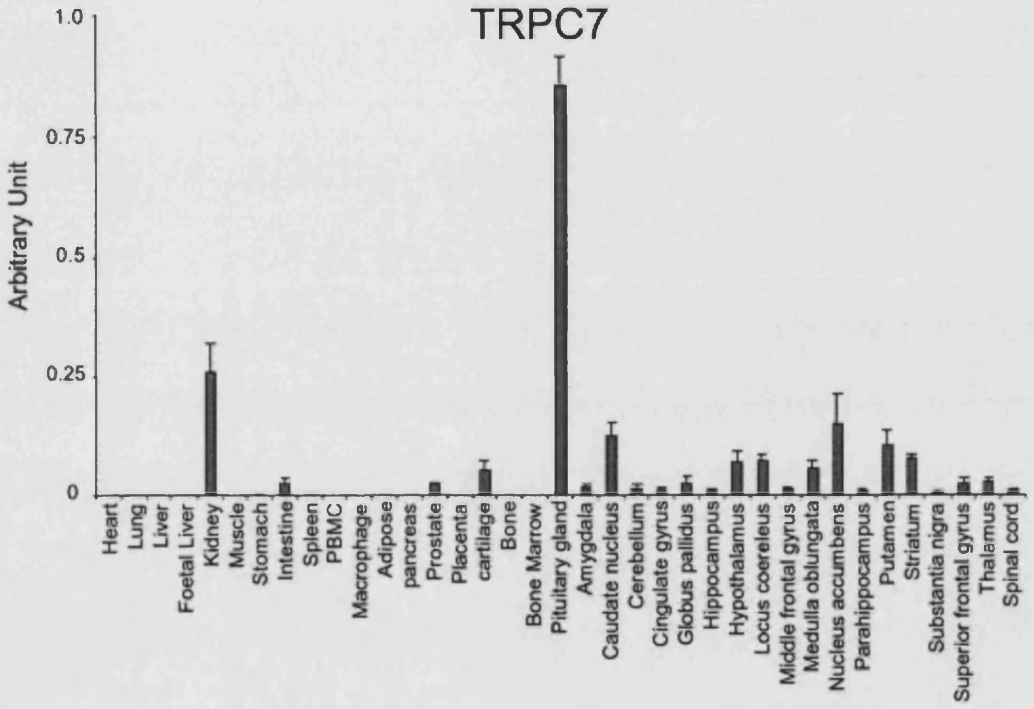

Figure 1.12: RT-PCR results of full-length TRPC7 mRNA from human tissue (Riccio *et al* 2002).

Riccio et al also tested a number of cell lines by RT PCR for the presence of hTRPC7, both found the presence of hTRPC7 in COS7 cells and the absence in HEK293 cells (Figure 1.13) (Riccio et al., 2002a).

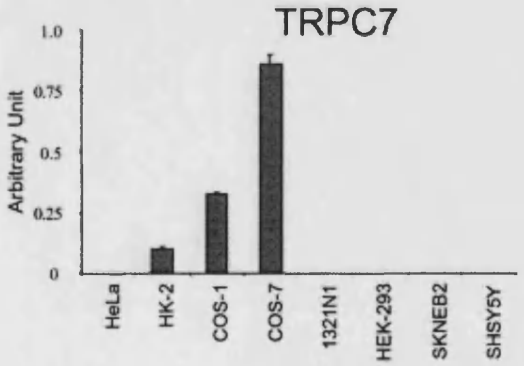

Figure 1.13: RT-PCR results of full-length hTRPC7 mRNA from various cell lines (Riccio *et al* 2002).

A recent Northern blot of human tissue (Figure 1.14) has shown the endogenous expression of hTRPC7 to be very high in the pancreas, skeletal muscle, thymus, brain, spleen and kidney and with much lower levels of expression in the placenta, heart, liver and lung (P Chen, Unpublished Data).

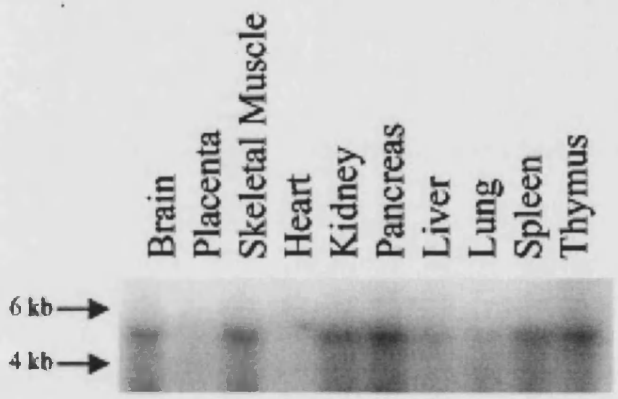

Figure 1.16: Northern blot carried out on human tissue shows *htrpc7* to be highly expressed in the brain, skeletal muscle, kidney, pancreas, spleen and thymus (Chen, Unpublished Data).

The information shown by the Northern blot gives no indication of which, if any, of the splice variants, may be present.

1.6.4 - Expression of TRPC7

HEK293 cells make an excellent expression system for the over expression of hTRPC7, due to the fact there is no endogenous protein present. Riccio et al cloned hTRPC7 into a pFLAG vector. For the purpose of immuno-localising the over expressed protein, they FLAG tagged the N-terminus of the protein in order to be able to visualise the protein and stably expressed the protein in HEK293 (Riccio et al., 2002a). They found that hTRPC7 was localised to the PM and sub-PM, furthermore only in cells that had been permeablised was there staining, consistent with the N-terminus of hTRPC7 being intracellular (Riccio et al., 2002a).

Three groups thus far have looked into the endogenous expression of hTRPC7 along-side other members of the TRPC subfamily, their findings will be discussed in more depth in Chapter 5.

1.6.5 - Functional Characterisation of TRPC7

As with many of the TRP superfamily the functional data produced thus far is controversial. Okada et al and Riccio et al have produced conflicting evidence on the functional mechanism of TRPC7. Okada et al concluded that mTRPC7 is a receptor-activated channel independent of store depletion of calcium (Okada et al., 1999), whereas, Riccio et al found that hTRPC7 is activated through a receptor independent store depletion pathway (Riccio et al., 2002a).

Okada et al cloned the full-length mTRPC7 and all splice variants separately in to pCI-neo vectors for the purpose of carrying out functional experiments on the proteins over expressed in HEK293 cells. Having transiently transfected *mtrpc7* into HEK293 cells, they found that mTRPC7 is still activated by ATP after treatment by TG and that mTRPC7 is activated by ATP at one order of magnitude lower concentration than TRPC3 and TRPC5. They suggest that this evidence points toward an enhancement of calcium influx activity of mTRPC7 via receptor stimulation occuring independently of the depletion of calcium stores (Okada et al., 1999). They also showed that DAG derivatives 1-oleoyl-2-acetyl-*sn*-glycerol (OAG) and 1,2-dioctanoyl-*sn*-glycerol (DOG) induce the cation influx activity of mTRPC7 (Okada et al., 1999). This has previously been seen in TRPC3 and 6 (Hofmann et al., 1999) and suggests that DAG maybe the activator of these channels, generated by stimulation of GPCRs (Hofmann et al., 1999; Okada et al., 1999). They also showed that intracellular Ca^{2+} plays a role in the activation of mTRPC7 by stimulation of the ATP receptors (Okada et al., 1999), as previously shown for TRPC5 (Okada et al., 1998). Their results suggest an involvement of the Ca^{2+}-CaM pathway; there is suppression of Ca^{2+} influx through mTRPC7 by the action of the Ca^{2+}-CaM antagonist W-13 (Okada et al., 1999).

Riccio et al generated an hTRPC7 expressing HEK293 stable cell line to investigate the functional role of hTRPC7. It was found that hTRPC7-expressing cells displayed significantly increased TG stimulated Ca^{2+} influx in the absence of Ca^{2+} compared with control cells, the effect was also abolished upon transfection with antisense hTRPC7 (Riccio et al., 2002a). They concluded that their data suggested that, following emptying

of intracellular Ca^{2+} stores, hTRPC7 is activated in a store depletion dependent manner and therefore hTRPC7 is a SOC (Riccio et al., 2002a). But unlike Okada et al there is no report of any constitutive activity (activity in the absence of apparent stimulation). They suggested that the differences between the mouse and human forms of TRPC7 could be explained by amino acid differences located in the C-terminal region of the proteins (Riccio et al., 2002a). It is suggested that these differences could affect the interaction of the channels with components of signal tranduction machinery, such as CaM, NHERF and $InsP_3Rs$ (Boulay et al., 1999; Kiselyov et al., 1998; Riccio et al., 2002a; Tang et al., 2001).

A recent paper by Lievremont et al (2004) attempted to reconcile the functional differences seen by Okada et al and Riccio et al. It was noted that although essentially the same sequences were used in both studies, Riccio et al used the sequence where Leucine 111 had been replaced by a Proline (leucine 111 is conserved in all of the TRPCs). In addition Riccio et al had used stably transfected HEK293 cells whereas Okada et al had used transiently transfected HEK293 cells. In order to investigate the discrepancies between the two studies, Lievremont et al stably and transiently expressed both types of TRPC7 in HEK293 cells. They used Ba^{2+} instead of Ca^{2+} to avoid complications of buffering Ca^{2+} and experiments were performed in the presence of Gd^{3+}, which completely blocks store depletion induced Ba^{2+} entry in wt-HEK293 cells but does not block any other known Ca^{2+} channel, including TRPC7 (Trebak et al., 2003). Therefore, the presence of Gd^{3+} ensured that the entry of cations occurring in TRPCs 3, 6 or 7 transfected HEK293 cells upon store depletion could be attributed only to the expression of those channels and not to endogenous receptor regulated or store operated Ba^{2+} entry (Lievremont et al., 2004). Their results showed that stable expression of hTRPC7 with the L111P point mutation gave a TG induced Ba^{2+} entry insensitive to $10\mu M$ Gd^{3+} showing that L111P-TRPC7 forms channels that are activated by store depletion when stably expressed in HEK293, confirming the data shown by Riccio et al (Lievremont et al., 2004). They went on to show no difference between TRPC7 and L111P-TRPC7, both appeared to be store operated when stably expressed (Lievremont et al., 2004). Transiently transfected HEK293 cells with TRPC7 or L111P-TRPC7 showed that neither

TRPC7 nor L111P-TRPC7 exhibited TG activated Ba^{2+} entry in the presence of Gd^{3+}, and further experimentation using OAG showed that HEK293 cells transiently transfected with TRPC7 or L111P-TRPC7 are activated by DAG indicating the channels are receptor operated (Lievremont et al., 2004).

The conclusion to be drawn from this is that the function of TRPC7, be it mouse or human, appears to depend upon expression levels, for TRPC7, the higher expression levels of the transient transfection reveal the channel to be operated independently of stores and the lower expression levels shown by stably expressed cells shows the channels activation to be store dependent. This phenomenon has been observed before in the TRPC subfamily where Vazquez et al demonstrated that when expressed in avian B cell line DT40 TRPC3 could be store operated if expressed in low levels and receptor operated if expressed in high levels (Vazquez et al., 2003).

1.7 - Aims

- As relatively little is known about hTRPC7 and its splice variants, the main aim of this project has been to produce an antibody to hTRPC7 and using this, characterise the expression and localisation of TRPC7 and the splice variants in an over-expression system (using the vectors out lined in the appendix, sections A1.1 and A1.2).

- There are still many conflicting reports of how the TRPCs are activated, therefore, using the over-expression system of TRPC7, I aimed to investigate the functional properties of hTRPC7 and the splice variant hTRPC7A.

- Most of the other TRPCs have been localised to various tissues, for example TRPC5 has been localised to the growth cone of hippocampal neurons (Greka et al., 2003). This localisation has lead to identification of function in many cases, therefore a further aim of this project was to identify and localise the endogenous form of the protein in various tissue types by use of the antibody specific to TRPC7, using the localisation possible functions of the channel and a role for Ca^{2+} signalling may be implicated.

Chapter 2
Materials and Methods

2.1 - List of Suppliers

Name of Supplier	Address	Abbreviation
AbCam	Cambridge, UK	ABC
Amersham Biosciences	Buckinghamshire, UK	AB
American Type Culture Collection	Manassas, VA, USA	ATCC
ATTO Corporation	Tokyo, Japan	ATTO
BD Bioscience	San Diego, CA, USA	BD
BDH/Merk	Leicester, UK	BDHM
Beckman	Buckinghamshire, UK	BK
BioGenesis	Poole, UK	BG
BioRad Laboratories Inc.	Hercules, CA, UK	BR
Boehringer Mannheim Gmbh	Mannheim, Germany	BM
Calbiochem	Nottingham, UK	CB
Chemicon International	Temecula, CA, USA	CI
Clontech	Palo Alto, CA, USA	CT
European Collection of Cell Cultures	Salisbury, UK	ECACC
Fisher Scientific	Loughborough, UK	FS
Gibco BRL	Paisley, UK	GBRL
GRI	Braintree, UK	GRI
Harlan Sera-Labs	Loughborough, UK	HSL
Heraeus Instruments	Hertfordshire, UK	HI
Hettich Zentrifugen	Tuttlingen, Germany	HZ
ICN Biomedicals	Ohio, USA	ICN
Invitrogen Life Technologies	Paisley, UK	ILT
J. M. Loveridge plc	Southampton, UK	JML
Millipore Corporation	Bedford, MA, USA	MLP
Molecular Probes	Leiden, The Netherlands	MP
New England Biolabs	Hertfordshire, UK	NEB
Pall Corporation	Pensacola, FL, USA	PC
Perkin Elmer	Cambridgeshire, UK	PE
Pierce Biotechnologies Inc.	Rockford, IL, USA	PB
Promega	Madison, WI, USA	P
Roche	Lewes, UK	R
Sigma	Poole, UK	S

Upstate Biotechnologies	Charlottesville, VA, USA	UB
Vector Laboratories	Burlingame, CA, USA	VL
Warner Instrumentation Corporation	Hamden, CT, USA	WIC
Zeiss	Hertfordshire, UK	Z

All suppliers will be referenced by abbreviation.

2.2 - Materials

All solutions made up in MilliQ grade H_2O unless otherwise stated.

2.2.1 - General Buffers

Buffer	Components	pH
Borax	100mM Sodium tetraborate ($Na_2B_4O_7$)	8.3
TBE	0.89M Tris (hydroxymethyl) methylamine (Tris) –Hydrochloride (HCl) 0.89M Boric acid (H_3BO_3) 20mM Diaminoethane-tetra-acetic acid disodium salt (EDTA)	8.0
PBS	137mM Sodium chloride (NaCl) 2.7mM Potassium chloride (KCl) 10mM Disodium hydrogen orthophosphate (Na_2HPO_4) 2mM Potassium dihydrogen orthophosphate (KH_2PO_4)	7.4

2.2.2 - Bacterial Culture Medium and Antibiotics

Culture Medium/ Antibiotics/ Bacterial Strains	Components	Supplier
Luria Bertani (LB) Medium	25g LB, powdered in 1L Sterilised by autoclaving	S
LB Medium containing 20mM Magnesium sulphate ($MgSO_4$)	25g LB, powdered in 1L + 20mM $MgSO_4$ Sterilised by autoclaving	S
LB Agar	25g LB, powdered with 15g BactoAgar in 1L Sterilised by autoclaving	S / BD
Kanamycin	50mg/ml stock in sterile H_2O, stored at -20°C	S
Ampicillin	50mg/ml stock in sterile H_2O, stored at -20°C	S
TFB1	30mM Potassium acetate (CH_3COOK) 10mM Calcium chloride ($CaCl_2$) 50mM Manganese chloride ($MnCl_2$) 100mM Rubidium chloride (RbCl) 15% (v/v) Glycerol pH 5.8 with 1M Acetic acid	S S S S FS FS

	Filter sterilised with 0.2μm syringe filter	MLP
TFB2	10mM 3-[N-morpholino]propanesulphonic acid (MOPS)	S
	75mM $CaCl_2$	S
	10mM RbCl	S
	15% (v/v) Glycerol	FS
	pH 6.5 with 1M potassium hydroxide (KOH)	S
	Filter sterilised with 0.2μm syringe filter	MLP

2.2.3 - Bacterial Strains and Plasmids

Strain/ Plasmid	Genotype	Supplier
E. coli XL-1 Blue	*SupE*44 *hsdR*17 *recA*1 *endA*1 *gyrA*46 *thi relA*1 *lac*$^-$ F' [*proAB*$^+$ *lacI*^{q} *lacZ ΔM*15 *Tno* (*tet*^{r})]	NEB
pIRES2-EGFP	CMV, Kan^r, 5.3 kb	CT
pFLAG-CMV-2	CMV, Amp^r, 4.7kb	S

2.2.4 - DNA Preparation Reagents

The GenElute™ MiniPrep kit purchased from Sigma was used for the preparation of DNA.

2.2.5 - Electrophoresis Reagents

Reagent	Components	Supplier
Electrophoresis grade agarose	0.8-1.5% (w/v) in TBE buffer	ILT
Ethidium bromide (EtBr)	10mg/ml Aqueous stock solution	S
6X loading buffer	12ml H_2O	
	25ml Glycerol	FS
	10ml 50mM EDTA pH 8.0	S
	50mg Bromophenol blue	S
	50mg Xylene cyanol	S

1kb DNA ladder	Stored at -20°C	P
Submerged horizontal gel tank	Sub-Cell	BR

2.2.6 - Cell Line Culture Reagents

Cell Type	Cell Supplier	Culture Medium Components	Supplier
Human embryonic kidney 293 (HEK293)	ECACC 85120602	Dulbecco's modified eagles medium (DMEM) supplemented with:	S
		10% (v/v) Foetal bovine serum (FBS)	S
		1% (v/v) 200mM Glutamine (Gln)	S
		1% (v/v) Penicillin/streptomycin (P/S)	S
COS7	ECACC 87021302	DMEM (S) supplemented with:	S
		10% (v/v) FBS	S
		1% (v/v) 200mM Gln	S
		1% (v/v) P/S	S
Panc-1	ECACC 87092802	DMEM supplemented with:	S
		20% (v/v) FBS	S
		1% (v/v) 200mM Gln	S
		1% (v/v) P/S	S
Capan-1	ATCC HTB-79	DMEM supplemented with:	S
		20% (v/v) FBS	S
		1% (v/v) 200mM Gln	S
		1% (v/v) P/S	S
GH4C1	ATCC CCL-82.2	DMEM supplemented with:	S
		10% (v/v) FBS	S
		1% (v/v) 200mM Gln	S
3T3-L1	ATCC CL-173	DMEM supplemented with:	S
		10% (v/v) Newborn calf serum (NCS)	GBRL
		1% (v/v) 200mM Gln	S
		1% (v/v) P/S	S
		For differentiation;	
		DMEM supplemented with:	S
		10% (v/v) Myoclone FBS	GBRL
		1% (v/v) P/S	S
		1% (v/v) 200mM Gln	S

		0.2μM Dexamethasone 0.5mM Isobutylmethylxanthine (IBMX) 0.2μM Insulin.	S S S
P3X63Ag8.653	ECACC 85011420	Maintenance medium; RPMI 1640 supplemented with: 10% (v/v) Hybridoma fetal calf serum 1% (v/v) 200mM Gln 1% (v/v) Tylosin 1% (v/v) OPI media supplement 8-Aza guanine. Cloning medium: As maintenance medium, supplemented with: 1% (v/v) Hybridoma cloning factor (HCF) Hypoxanthine aminopterin thymidine (HAT) Hypoxanthine thymidine (HT)	 S S S S S S FS S S

Other Cell Culture Reagents	Composition	Supplier
Freezing medium	50% (v/v) FBS 30% (v/v) DMEM 20% (v/v) Dimethyl sulphoxide (DMSO) cell culture grade	S
Trypsin EDTA	1X bottle, stored at -20°C	S
PBS	Sterilised by autoclave Stored at 4°C	
LipofectAMINE™2000	Stored at 4°C	ILT
Serum and antibiotic free medium	DMEM supplemented with: 1% (v/v) 200mM Gln	S
Antibiotic free medium	DMEM supplemented with: 10% (v/v) FBS 1% (v/v) 200mM Gln	S

2.2.7 - Primary Cell Culture Reagents

Tissue	Mammal of Origin	Culture Medium Components	Other Materials
Adult Pancreas	Human, adult female	—	—
Embryonic Pancreas	Mouse, (MF1 albino) male and female	Basal medium Eagle (BME) (S) with: Earle's medium (S) 10% (v/v) FCS (S) 1X Gln (ILT) 50μg/ml Gentamycin sulphate (S)	BME with Hanks's salts (S) 2% (v/v) 3-Aminopropyltriethoxysilane (APTS) in acetone (S) 50μg/ml Bovine fibronectin in sterile H_2O (ILT)
Embryonic Cardiomyocytes	Rat, (Sprague-Dawley) male and female	Maintained in DMEM (S) supplemented with: 10% (v/v) FBS (S) 1% (v/v) 200mM Gln (S) 1% (v/v) P/S (S)	1M Glucose (S) 1mg/ml DNAse 1 in PBS with 1mM $MgCl_2$ and 2mM $CaCl_2$ (S) 10X Trypsin (S) 1μg/ml Laminin (S) in borax buffer
Embryonic Spinal Cord	Rat, (Sprague-Dawley) male and female	Maintained in; Neurobasal™ Medium (GBRL) supplemented with: 2% (v/v) B27 (S) 1% (v/v) 200mM Gln (S) 1% (v/v) P/S (S)	1M Glucose (S) 1mg/ml DNAse 1 in PBS with 1mM $MgCl_2$ and 2mM $CaCl_2$ (S) 10X Trypsin (S) FBS (S) 5μg/ml Poly-L-lysine (PLL) (S) in borax buffer
Embryonic Cortex	Rat, Sprague-Dawley male and female	Maintained in; Neurobasal™ Medium (GBRL) supplemented with: 2% (v/v) B27 (S) 1% (v/v) 200mM Gln (S) 1% (v/v) P/S (S)	1M Glucose (S), 1mg/ml DNAse 1 in PBS with 1mM $MgCl_2$ and 2mM $CaCl_2$ (S) 10X Trypsin (S) FBS (S) 5μg/ml PLL (S) in borax buffer.

2.2.8 - Reagents for the Isolation of Cardiomyocytes

Solution	Composition	Supplier
Cardiomyocytes Krebs-Ringers HEPES buffer (cKRH buffer)	6mM KCl 1mM Na_2HPO_4 1.4mM $MgSO_4$ 128mM NaCl 10mM HEPES pH 7.4	S
Buffer A	cKRH buffer supplemented with: 5.5mM Glucose 2mM Ultrapure pyruvic acid 2mM Inosine	S
Buffer B	Buffer A supplemented with: 0.7% (w/v) Bovine serum albumin (BSA) Fraction V 1.1mg/ml collagenase (Worthington) 2.65 mg/ml Hyaluronidase Type 1-S 15mM 2,3-Butanedione monoxime (BDM)	 BM S S
Buffer C	Buffer A supplemented with: 0.2 mg/ml DNAse 1 15mM BDM 200μM $CaCl_2$ 2% (w/v) BSA Fraction V	 BM S S BM
Buffer D	Buffer A supplemented with: 1mM $CaCl_2$ 2% (w/v) BSA Fraction V	 S BM
Buffer E	Buffer A supplemented with: 1mM $CaCl_2$ 0.5% (w/v) Fatty acid free BSA (FAF-BSA) Fraction V	 S BM
Heparin Solution	Heparin grade 1A isolated from porcine intestinal mucosa, reconstituted in 0.9% (w/v) NaCl (2000 Units/ml) Filter sterilised with 0.2μm syringe filter Aliquots were stored at 4°C	S MLP
Pentobarbitone sodium b.p.	60mg/ml	JML

2.2.9 - Antibodies

2.2.9.1 - Peptide Conjugation Reagents

Reagent	Composition	Supplier
Peptide 7(K)	NH_2-KNLNKDHLRVNKGKDI-*COOH*	Dr G. Bloomberg, University of Bristol.
Keyhole Limpet Haemocyanin (KLH)		ICN
Glutaraldehyde	Grade I, 25% (v/v)	S
Glycine ethyl ester (GEE)	1M GEE	S
0.1M sodium hydrogen carbonate ($NaHCO_3$)	pH 8.3	S
0.9% (w/v) NaCl		S

2.2.9.2 - Monoclonal Antibody Production Reagents

Reagent	Components	Supplier
Male Balb/C mice		
Alum adjuvant		S
Polyethylene glycol 4000 (PEG 4000)	80% (w/v) PEG 4000 in PBS	BDHM

2.2.9.3 - Polyclonal Antibody Production Reagents

Reagent	Components	Supplier
New Zealand white rabbits	Barrier reared	HSL
Freunds complete adjuvant (FCA)		HSL
Freunds incomplete adjuvant (FIA)		HSL

2.2.9.4 - Antibody Purification Reagents

Reagent/Buffer	Components	Supplier
Cyanogen bromide (CNBr) Activated Sepharose 4B		S
HCl	1mM HCl pH 2-3	S
Coupling buffer	0.1M $NaHCO_3$ 0.5M NaCl	S

	pH 8.3	
Tris-HCl	0.1M Tris-HCl pH 8	S
Sodium acetate (CH_3COONa)	0.1M CH_3COONa pH 4 0.5M NaCl	S
High salt wash	0.1M Tris-HCl pH 8 0.5M NaCl	S
Storage buffer	20mM Na_2HPO_4 0.5M NaCl 0.01% Sodium azide (NaN_3)	S
BSA	5mg/ml	S
Wash Solution	20mM Na_2HPO_4	S
Elution Solution	50mM Glycine HCl pH 2.3	S
Neutralisation Solution	1M Tris, pH 10.8	S
Polyethylene glycol 20000 (PEG 20000)	PEG 20000	BDHM

2.2.9.5 - General Antibodies

Antibody	**Animal raised in**	**Supplier**
Anti-α-Manosidase II	Mouse (monoclonal)	Dr B. Reaves, University of Bath
Anti-β-Tubulin	Mouse (monoclonal)	S
Anti-focal adhesion kinase (FAK)	Mouse (monoclonal)	BD
Anti-FLAG M2	Mouse (monoclonal)	S
Anti-G29 (trans Golgi network [TGN] Marker)	Rabbit	Dr B. Reaves, University of Bath
Anti-glial fibrillary acidic protein (GFAP)	Mouse (monoclonal)	CI
Anti-green fluorescent protein (GFP)	Rabbit (serum)	MP

Anti-glucose transporter 4 (GLUT4)	Mouse (monoclonal)	BG
Anti-human transient receptor potential canonical 7 (hTRPC7)	Rabbit	HSL
Anti-microtubule associated protein (MAP2 a & b)	Mouse (monoclonal)	CI
Anti-Myc	Mouse (monoclonal)	S
Anti-P58 Golgi marker	Mouse (monoclonal)	ABC
Anti-Paxillin	Mouse (monoclonal)	UB
Anti-trans Golgi network 38 (TGN38)	Mouse (monoclonal)	Dr B. Reaves, University of Bath
Rhodamine-Phalloidin	NA	MP
Anti-mouse IgG fluorescein linked whole antibody	Sheep	AB
Anti-mouse IgG Texas Red™ linked whole antibody	Sheep	AB
Anti-rabbit IgG fluorescein linked whole antibody	Donkey	AB
AlexaFluor 568 anti-mouse IgG (H and L)	Goat	MP
AlexaFluor 488 anti-rabbit IgG (H and L)	Goat	MP
AlexaFluor 546 anti-rabbit IgG (H and L)	Goat	MP
Anti-rabbit IgG horseradish peroxidase linked whole antibody	Donkey	AB

2.2.10 - Enzyme Linked Immunoassay (ELISA) Reagents

Reagent/Buffer	Components	Supplier
Coating Buffer	15mM Sodium carbonate (Na_2CO_3), 35mM $NaHCO_3$ 50mg NaN_3 pH 9.6	S
PBS Tween (PBST)	PBS 0.1% (v/v) Tween-20	S

Blocking Buffer (PBSTM)	PBS Tween 5% (w/v) Marvel (dried non-fat milk)	S Sainsburys
Tetramethyl benzidene (TMB)	10mg/ml in DMSO	S
CH_3COONa / Citrate ($C_6H_5Na_3O_7$) Buffer	1M CH_3COONa 0.02M $C_6H_5Na_3O_7$ pH 6.0	S
Hydrogen peroxide (H_2O_2)	30% (v/v)	S
Substrate Stock	1M CH_3COONa / $C_6H_5Na_3O_7$ buffer pH 6.0 diluted to 1:20	S
Substrate Working	49.5ml of substrate stock 0.5ml stock TMB 10µl H_2O_2	S S S
2M Sulphuric acid (H_2SO_4)		S

2.2.11 - Immunocytochemistry Reagents

Reagent	Components	Supplier
Paraformaldehyde (PFA)	2% or 4% (w/v) PFA in PBS	S
Methanol	Stored at -20°C	FS
MEMFA	10% (v/v) Formalin 0.1M MOPS pH 7.4 2mM Ethylene glycol-bis (2-aminoethylether)-N, N, N', N' tetra acetic acid (EGTA) 1mM $MgSO_4$	S
Triton X-100	0.01% (v/v) Triton X-100 in PBS	S
Permeablisation buffer	0.1% (w/v) Saponin 3% (v/v) FBS 1% (w/v) BSA	S

	In PBS	
Block buffer	10% (v/v) FBS in PBS	S
Mowiol mounting media	0.2M Tris-HCl pH 8.5 50% (w/v) Glycerol 20% (w/v) Mowiol 4-88 50% (v/v) ddH_2O	S FS CB
Vector Shield	Mounting media	VL
Confocal Microscope	Zeiss Axiovert LSM510	Z

2.2.12 - Cell Harvesting Reagents

Reagent	Components	Supplier
(4-bromo) Phenylmethyl sulphonylfluoride (PMSF)	0.1M PMSF in isopropanol	S / FS
EDTA	0.1M EDTA	S
Mini complete EDTA free, protease inhibitor tablets	1 tablet in 10ml	R
Protease inhibitor cocktail for lysis	20ml PBS pH 7.4 20µl 0.1M PMSF 200µl 0.1M EDTA 2 Mini complete EDTA free Stored at –20°C	S FS S R

2.2.13 - Protein Quantitation Reagents

Reagent	Components	Supplier
BSA	2mg/ml in PBS	PB
Coomassie® Plus Reagent		PB

2.2.14 - SDS-PAGE Reagents

Reagent	Component	Supplier
30% Acrylamide mix	30% (w/v) Acrylamide, 0.8% (v/v) bis acrylamide	S
4X Tris-HCl	1.5M Tris-HCl, pH 8.8	S
4X Tris-HCl	0.5M Tris-HCl, pH 6.8	S
Sodium dodecyl sulphate (SDS)	10% (w/v) SDS	S
Ammonium persulphate (APS)	10% (w/v) APS	S
N, N, N, N'- Tetramethyl ethylenediamine (TEMED)		S
2X SDS loading buffer	0.125M Tris-HCl 4% (w/v) SDS 20% (v/v) Glycerol 0.2M Dithiothreitol (DTT) 0.02% (w/v) Bromophenol blue	S S FS S S
Precision Protein Standard	Molecular weight marker	BR
1X Running Buffer pH 8.3	0.025M Tris 0.192M Glycine 0.1% (w/v) SDS	S FS S
Vertical Gel tank	Mini Atto	ATTO
Coomassie Blue solution	50% (v/v) Methanol 0.05% (w/v) Coomassie Brilliant Blue R 10% (v/v) Acetic acid (CH_3COOH) The Coomassie Brilliant Blue R was dissolved in methanol before adding acetic acid and water.	FS S FS
Destaining solution	5% (v/v) Methanol 7% (v/v) CH_3COOH	FS FS

2.2.15 - Western Blotting and Immunoprobing Reagents

Reagent	Components	Supplier
BioTrace®NT protein transfer nitrocellulose membrane		PC
Extra Thick Filter paper		BR
Transfer buffer	25mM Tris, 192mM Glycine 20% (v/v) Methanol pH 8.3	S S FS
Western Blotter	Mini Trans-Blot Cell	BR
Ponceau S	Stock solution: 1% (w/v) Ponceau S 5% (v/v) CH_3COOH	 S FS
Rabbit IgG Vectastain ABC kit	Biotinylated anti-rabbit IgG, Avidin DH reagent (reagent A) Biotinylated horseradish peroxidase H reagent (reagent B)	VL
Mouse IgG Vectastain ABC kit	Biotinylated anti-mouse IgG A reagent B reagent	VL
Peroxidase substrate DAB kit	Made according to manufacturers instructions	VL

2.2.16 - Immunoprecipitation Reagents

Reagent	Components	Supplier
2X RIPA Buffer	100mM Tris, 300mM NaCl 2% (w/v) IGEPAL CA-630 1% (w/v) Deoxycholic acid (DOC) 0.2% (v/v) SDS pH 7.4 Stored at 4°C	S
Sepharose 4B-Protein G Beads	Stored in PBS containing 0.01% (w/v) NaN_3, at 4°C	S
Sepharose 4B-Protein A Beads	Stored in PBS containing 0.01% (w/v) NaN_3, at 4°C	S

2.2.17 - Functional Reagents

Reagent	Details	Supplier
Fura 2-AM	Stock solution: 3mM in DMSO containing: 20% (w/v) Pluronic acid Stored at –20°C in the dark	S
Cyclopiazonic acid (CPA)	100mM CPA stock in DMSO Stored at –20°C Used, diluted to 10μM in 2mM Ca^{2+} PSS or 0mM Ca^{2+} PSS	S
1-oleoyl-2-acetyl-sn-glycerol (OAG)	100mM OAG stock in DMSO Stored at –20°C Used, diluted to 100μM in 2mM Ca^{2+} physiological saline solution (PSS) or 0mM Ca^{2+} PSS	S
2mM Ca^{2+} PSS	140mM NaCl 5mM KCl 1mM $MgCl_2$ 2mM $CaCl_2$ 10mM Glucose 15mM HEPES	S
0mM Ca^{2+} PSS	140mM NaCl	S

	5mM KCl 1mM $MgCl_2$ 10mM Glucose 15mM HEPES 100μM EGTA	
In-line heater		WIC
Heated chamber		WIC
Concord Microscope	Zeiss Axiovert epiflourescence microscope	Z
Merlin	A live cell imaging and real time recording computer program	PE

2.3 - Methods

2.3.1 - DNA Methods

2.3.1.1 - Preparation of Competent Cells

Using materials from sections 2.2.2 and 2.2.3, a single colony of *E. coli* XL-1 Blue cells from an LB agar plate was inoculated into 2.5ml of LB medium and incubated overnight at 37°C at 250rpm in a shaking incubator. The entire overnight culture was used to inoculate 250ml of LB medium containing 20mM $MgSO_4$. The cells were grown in a 1L flask for approximately 5-6 hours, until the optical density at 600nm (OD600) reached 0.4-0.6. The cells were centrifuged in a Mikro 22R (HZ) bench top fixed angle rotor at 4500 x g (gravitational force), (6050rpm) for 5 minutes at 4°C, the supernatant was removed and the cells were gently resuspended in 0.4 volumes (of the original culture volume) of ice cold TFB1. From this point onwards, the cells were kept on ice and all pipettes, tubes and flasks were chilled before use. The resuspended cells were incubated on ice for 5 minutes. The cells were then centrifuged at 4500 x g for 5 minutes at 4°C. The supernatant was removed and the cells were gently resuspended in 1/25 of the original culture volume of ice cold TFB2. The cells were then incubated on ice for 15-60 minutes before they were divided into 200µl aliquots, frozen in a dry ice/ isopropanol bath and stored at –80°C.

2.3.1.2 - Transformation

Using materials from sections 2.2.2 and 2.2.3, competent *E. coli* XL-1 Blue cells were defrosted on ice for 5 minutes, then divided into 100µl aliquots in cold micro-centrifuge tubes. 500 – 1000ng of plasmid DNA was added to an aliquot and mixed gently by flicking the tubes. The cells were incubated on ice for 5 minutes. To allow the plasmid to enter the bacteria, the samples were heat shocked at 42°C for 45 - 60 seconds and were replaced back on ice for 5 minutes. 400µl of warmed LB medium (37°C) was added to each tube, these were then incubated at 37°C for approximately one hour in a shaking incubator at 250rpm. LB Agar plates were prepared previously with the appropriate antibiotic, ampicillin or kanamycin, diluted to 50µg/ml. Transformed cells were plated onto warmed LB agar with a sterile plastic spreader, two plates were used per sample, one for an 80% of transformed cells and the other

for 20% of the transformed cells. Each plate was inverted and incubated over night at 37°C. A single discrete colony was then picked from each plate and used to inoculate 5ml LB medium containing the appropriate antibiotic for the plasmid. These were then incubated overnight at 37°C in the shaking incubator. The growth from this was used in preparation of frozen stocks and plasmid purification preparations.

2.3.1.3 - Preparing Frozen Stocks

500µl of an overnight culture was removed and mixed it thoroughly with 500µl glycerol in a cryovial and stored at –80°C.

2.3.1.4 - Preparation of cDNA

DNA was prepared for transfection by the use of the GenElute™ MiniPrep kit (see Section 2.2.4), using all solutions and reagents provided in the kit and with no changes to the protocol.

2.3.1.5 - Analysis of cDNA

The purity of the DNA was determined by spectrophotometric analysis of the DNA by determining the absorbance ratio of A_{260} and A_{280}, a ratio reading of between 1.8 and 2.0 was taken to indicate acceptable purity.

DNA concentrations were calculated using the following equation:

$$\text{Dilution factor} \times 50 \times \text{Absorbance}_{260} = \mu\text{g/ml DNA}$$

2.3.1.6 - Agarose Gel Electrophoresis

Using materials from section 2.2.5, agarose gels were made by dissolving 0.8 – 1.5% (w/v) agarose in 100ml TBE (see Section 2.2.1) buffer by heating in a microwave. The agarose was cooled and EtBr was added to a final concentration of 7µg/ml and swirled to mix. The gel solution was poured in to the pre-assembled gel tank, comb inserted and the gel was allowed to set. The tank was flooded with TBE buffer, samples and a 1kb DNA ladder was mixed with 6X gel loading buffer and 10µl of each sample was loaded in to the wells. The DNA was separated at 100V and then visualised by ultra violet (UV) light.

2.3.2 - Cell Culture

2.3.2.1 - Cell Passaging

All cultured cell types were passaged by the same method and all reagents used (see Section 2.2.6) were pre-warmed to 37°C. Culture medium was aspirated off and 3ml of sterile PBS (see Section 2.2.1) was added to the flask to wash, this was then aspirated off and 1ml of trypsin-EDTA was added to remove the cells from the flask, this was incubated at room temperature for 1 minute. 9ml of fresh medium was then added to the flask and the cells were gently resuspended by pipette action. The cells were split by removing 0.5-2ml of resuspended cells to 9.5ml of fresh medium in a $75cm^2$ flask. The cells were split when they reached 80% confluency. For the 3T3-L1 fibroblasts, medium was replaced every 2 days and cells were split every 7-10 days at approximately 90% confluency. Cells were viable for differentiation up to passage number seven. All cultured cells were incubated at 37°C and in an atmosphere of 5% (v/v) carbon dioxide (CO_2), except the 3T3-L1 fibroblasts, they were incubated at 37°C and in an atmosphere of 10% (v/v) CO_2.

2.3.2.2 - 3T3-L1 Fibroblast Differentiation

Fibroblasts were grown to confluency after revival from liquid nitrogen stores (see Section 2.3.2.4), after 1-2 passages cells were ready for differentiation into adipocytes. Fibroblasts were dissociated from the culture flask as previously described for passaging and seeded in fresh medium at a density of approximately 50000 cells per 35mm dish containing a coverslip and approximately 70000 cells per 90mm dish. After 10 days the cells were confluent and medium was replaced with medium for differentiation (see Section 2.2.6): this was day 0. After two days the cells had begun to differentiate and the medium was replaced with differentiation medium without dexamethasone or IBMX for a further two days. Following this, the medium was changed for normal culture medium every two days until day thirteen.

2.3.2.3 - Cell Storage

All cells were washed and detached as previously described (section 2.3.2.1), they were then each resuspended in 10ml of medium, transferred to a 15ml centrifuge tube and spun in a bench top Mikro 22R (HZ) centrifuge using a fixed angle rotor at 270 x g, (1500rpm) for 5 minutes at room temperature. The supernatant was then aspirated

off and the cell pellet was resuspended in 1ml freezing medium. This suspension was then transferred to cryovials and kept in liquid nitrogen vapour for 24 hours before transferring to liquid nitrogen for long term storage.

2.3.2.4 - Cell Revival

All cells were revived by removing the cryovial from the liquid nitrogen store and rapidly defrosting by placing in a 37°C waterbath. The cells were then transferred by pipette to a 90mm diameter dish containing the appropriate medium (see Section 2.2.6), they were then incubated for 24 hours at 37°C in an atmosphere containing 5 or 10% (v/v) CO_2. Medium was then aspirated off, replaced with fresh medium and incubated at 37°C in an atmosphere containing 5 or 10% (v/v) CO_2 until the cells needed passaging.

2.3.2.5 - HEK293 and COS7 Transfection

Using materials from section 2.2.6, HEK293 and COS7 cells were resuspended in antibiotic free medium and seeded at approximately 50% confluency on to a 22 x 22mm coverslip in a 35mm culture dish and incubated at 37°C, 5% (v/v) CO_2 over night, so that the following day the cells were approximately 60-70% confluent. For each 35mm culture dish, 4µg of DNA was added to 250µl of serum and antibiotic free medium in a sterile tube, and in a second sterile tube 10µl of LipofectAMINE™2000 was added to 250µl of serum and antibiotic free medium, both tubes were mixed gently and incubated for 5 minutes at room temperature. The two tubes were then gently mixed together and incubated for a further 20 minutes at room temperature. The mixture was then added drop wise to the 35mm culture dish containing the cells and 2ml serum and antibiotic free medium, this was then rocked gently to ensure even distribution and incubated at 37°C, 5% (v/v) CO_2 for approximately 5 hours. The transfection medium was removed from the cells and replaced with normal medium. Cells were incubated for 24-48 hours at 37°C, 5% (v/v) CO_2. For larger scale transfection, the volumes involved were scaled up accordingly.

2.3.3 - Primary Cell Culture

2.3.3.1 - Primary Human Pancreas Cell Culture

Primary human pancreatic cells were supplied by Dr David Tosh, University of Bath.

2.3.3.2 - Embryonic Mouse Pancreatic Tissue Culture

This method was carried out using materials from section 2.2.7. Prior to the culture of the pancreatic tissue glass coverslips were prepared as follows. 22 x 22mm glass coverslips were immersed in 2% (v/v) APTS in acetone overnight. The coverslips were then rinsed in 1X acetone, twice in sterile water, air dried and then baked for at least 3 hours at 180°C. The coverslips were then placed in a 35mm culture dish and a drop of bovine fibronectin (50μg/ml) was applied to the centre, to promote attachment of the pancreatic tissue, and allowed to dry in a flow hood for several hours.

Mouse embryos were generated by timed matings and the day of the formation of the vaginal plug was taken as day 0.5. At day 11.5 the pregnant mice were killed by cervical dislocation and the uterus was removed to ice cold PBS. The deciduas were removed and the embryos were transferred to ice-cold BME medium with Hank's salts and, with the aid of a microscope, the gut was dissected out. The dorsal pancreatic bud was removed from the posterior end of the stomach using fine forceps and a tungsten needle.

After the pancreatic tissue was isolated, a cloning ring was placed over the fibronectin coated area on the coverslip and supplemented BME medium was added to the inside of the cloning ring and around the culture dish up to a volume of 2.5ml. The pancreatic tissue was then dropped into the centre of the cloning ring. To ensure the attachment and spread of the tissue, the tungsten needle was used to turn the pancreas so the cut surface lay downwards. The cultures were then grown at 37°C, 5% (v/v) CO_2 for 7 days, until use (Percival and Slack, 1999).

2.3.3.3 - Embryonic Rat Spinal Cord Culture

This method was carried out using materials from section 2.2.7. Prior to seeding of cells, all coverslips and plates were coated with PLL (5μg/ml) for 24 hours at 37°C, 5% (v/v) CO_2 and then washed with PBS.

At approximately 15 days into gestation the pregnant rat was killed by cervical dislocation and up to 15 rat embryos were removed and placed in room temperature PBS. Using a microscope to observe the foetus, the head was removed. The foetus was placed on its belly and using hooked tweezers, the skin was removed down the whole length of the back. The spinal cord was removed from the rest of the foetus; this procedure was carried out as quickly as possible in order to keep the cells viable. The intact spinal cord was placed in 3ml of sterile filtered PBS with 50mM glucose. Nine foetal spinal cords removed in this way gave approximately 3-5 million cells per ml, enough material for 48 coverslips and six 90mm dishes. The spinal cords were cut into small fragments using butterfly scissors and using a Pasteur pipette the fragments were placed in a 15ml tube containing 150µl DNAse 1 and then mixed gently. Following this 10X trypsin was added to a final concentration of 0.5X (v/v), mixed gently and the tube was placed in a 37°C water bath for 20 minutes, mixing gently after 10 minutes. A small amount of supplemented Neurobasal™ Medium was added to the spinal cords to inactivate the trypsin. The spinal cords were mixed gently and spun for 5 minutes at room temperature in a Mikro R22 (HZ) bench top centrifuge with a fixed angle rotor at 270 x g, (1500rpm). The supernatant was removed and the pellet was resuspended in 3ml medium and gently triturated to break up the fragments. The cell suspension was diluted 1:50 in supplemented Neurobasal™ Medium and mixed gently and approximately 0.5ml was added to each coverslip (approximately 50000 cells/cm^2 per coverslip). The cells were incubated at 37°C, 5% (v/v) CO_2 for 2 hours before flooding the well with 2ml supplemented Neurobasal™ Medium. Plates were seeded at higher density of approximately 4 million cells per plate. After approximately 5 hours all medium containing FBS was removed and cells were cultured in the FBS free Neurobasal™ Medium at 37°C, 5% (v/v) CO_2 for a total of three weeks. (Adapted from (Digby et al., 1985).

2.3.3.4 - Embryonic Rat Cortical Culture

This method was carried out using materials from section 2.2.7. Prior to seeding of cells, all coverslips and plates were coated with PLL (5µg/ml) for 24 hours at 37°C, 5% (v/v) CO_2 and washed with PBS.

At approximately 18.5 days into gestation the pregnant rat was killed by cervical dislocation and up to 15 rat embryos were removed and placed in room temperature PBS. Using a microscope to observe the foetus the head was removed. The skin covering the brain was removed and the brain was removed, the cortices were dissected out and meninges removed; this procedure was carried out as quickly as possible in order to keep the cells viable. The intact cortices were placed in 3ml of sterile filtered PBS with 50mM glucose. Nine pairs of foetal cortices were removed; this gave approximately 10 million cells per ml, enough material for 48 coverslips and six 90mm dishes.

At this point the cortices were treated and cultured exactly the same way as the embryonic rat spinal cord (section 2.3.3.3). (Adapted from (Digby et al., 1985).

2.3.3.5 - Embryonic Rat Cardiomyocyte Culture

This method was carried out using materials from section 2.2.7. Prior to seeding of cells, all coverslips and plates were coated with laminin (1μg/ml) for 24 hours at 37°C, 5% (v/v) CO_2 and washed with PBS.

At approximately 18.5 days into gestation the pregnant rat was killed by cervical dislocation and up to 15 rat embryos were removed and placed in PBS. Using the microscope to observe the foetus, the head was removed the foetus was placed on its back and using hooked tweezers, the skin was removed down the whole length of the thorax. The heart was then removed and placed in 3ml of sterile filtered PBS with 50mM glucose. This procedure was carried out as quickly as possible in order to keep the cells viable. Nine foetal hearts were removed; this gave approximately 3-5 million cells per ml, enough material for 48 coverslips and six 90mm dishes. The ventricles were dissected from the rest of the heart and cut into small fragments. Using a Pasteur pipette the fragments were placed in a 15ml tube containing 150µl DNAse 1 and then mixed gently. Following this 10X trypsin was added to a final concentration of 0.5X (v/v) and mixed gently. The tube was placed in a 37°C water bath for 20 minutes with gentle mixing after 10 minutes. The trypsin was inactivated by the addition of DMEM supplemented with 10% (v/v) FBS, 1% (v/v) 200mM Gln and 1% (v/v) P/S. The cell suspension was then mixed gently and spun at room temperature for 5 minutes using a bench top Mikro 22R (HZ) centrifuge with a fixed angle rotor at 270 x g, (1500rpm).

The supernatant was removed and the pellet was resuspended in 3ml medium and gently triturated to break up the fragments. The cell suspension was diluted 1:50, mixed gently and approximately 0.5ml was added to each coverslip (50000 cells/cm^2 per coverslip). The cells were incubated at 37°C, 5% (v/v) CO_2 for 2 hours before flooding the well with 2ml medium. Plates were seeded at higher density of approximately 4 million cells per plate. Cells were cultured for one week at 37°C, 5% (v/v) CO_2. (Adapted from (Digby et al., 1985).

2.3.3.6 - Isolation of Adult Rat Cardiomyocytes

Using materials from section 2.2.8, adult male Wistar rats (260-280 g) were anaesthetised with 350 µl Pentobarbitone Sodium b.p. (60mg/ml) before administration of 500 units of heparin solution via the tail vein. After 5 minutes the neck was dislocated and the heart rapidly removed into semi-frozen Buffer A (0-4°C). The heart was immediately mounted on to a catheter via the aorta and perfused with Buffer A, at 37°C, for 5 minutes to remove blood and metabolites from the coronary vessels and atrial and ventricular chambers. The perfusion was then switched to Buffer B equilibrated with oxygen and was re-circulated by means of a peristaltic pump.

After approximately 30 minutes 100 µM $CaCl_2$ was added to the re-circulating buffer. The $CaCl_2$ concentration was raised to 200 µM after a further 2-3 minutes. The heart was perfused for approximately 40 minutes prior to its' removal from the catheter. The heart tissue was dissociated in a buffer containing 10 ml Buffer B and 10 ml Buffer C prewarmed to 37°C and under an oxygen atmosphere. The calcium concentration was increased in 200 µM steps until the final concentration was 800 µM.

The digested suspension was filtered through a 250 μm^2 nylon gauze (Lockertex,) and the cardiomyocytes were allowed to settle for 3-4 minutes to form a loose pellet. The supernatant was removed and the cells resuspended in 30 ml Buffer D. The cells were allowed to settle again for 3-4 minutes at room temperature and the supernatant was removed. The pellet was resuspended in 25 ml Buffer E and the cell suspension was incubated for 20 minutes at 37°C under an oxygen atmosphere to allow the cells to

recover from the isolation procedure. Viability was assessed by counting the number of rod-shaped (viable) versus round-shaped (dead) cells under the light microscope (Fischer et al., 1991).

2.3.4 – Antibody Production

2.3.4.1 - Antigen Preparation

The peptide termed 7(K) was identical to the final 16 amino acids of the C-terminus of the hTRPC7 protein (sequence: *NH_2*-KNLNKDHLRVNKGKDI-*COOH*) and synthesised by Dr G. Bloomberg, University of Bristol. The peptide was coupled to the carrier protein KLH via the lysine residues.

Using reagents from section 2.2.9.1, the KLH and 7(K) were dissolved in 0.1M $NaHCO_3$ pH 8.3 to a final concentration of 2 mg/ml of KLH and 7(K). Fresh glutaraldehyde was added to the solution at a final concentration of 0.05% (v/v). The sample was mixed by rotation in a glass tube overnight at room temperature. 0.1 volumes of 1M GEE, pH 8.0 was added and mixed for 30 minutes at room temperature. The KLH/7(K) conjugate was dialysed into 0.9% (w/v) NaCl, overnight at 4°C. The dialysed sample was adjusted to 1mg of KLH and 7(K) /ml.

2.3.4.2 - Monoclonal Antibody Production

Using reagents from section 2.2.9.2, two male Balb/C mice (7J and 7K) were immunised with the KLH/7K conjugate adjusted to 200μg/ml with PBS and mixed with an Alum adjuvant at a ratio of 1:1 (v/v). The mice were given one initial immunisation and 4 boosts at one week intervals. ELISAs were carried out on serum samples to analyse how well the mice had responded (section 2.3.6.3).

The P3X63Ag8.653 hybridoma cell line (see Section 2.2.6) used in the production of monoclonal antibodies, were grown in maintenance media containing 8-Aza, the 8-Aza was omitted 2 weeks before use with B cells.

One to three days before fusion of the P3X63Ag8.653 hybridoma cell line with the B cells from the spleens of the immunised mice, a macrophage feeder layer was

prepared. This was carried out by harvesting macrophages from the abdominal cavities of five non-immunised male Balb/C mice into PBS and irradiating with γ-rays from a cobalt source to prevent the macrophages from dividing. Macrophages were then plated out in 5 x 96 well plates in maintenance medium.

The final boost was given to the mice 3-5 days prior to the fusion and on the day of fusion the mice were bled in order to collect as much serum as possible, then as quickly as possible the spleen was removed from the mouse. The spleen was washed out with 10ml PBS and as many of the cells as possible were removed from it using a needle. Cells were transferred to a 50ml tube and 20 million log phase P3X63Ag8.653 hybridoma cells were added. The mixture was then spun down at 200 x g, (1300rpm) for 15 minutes at room temperature in a bench top Mikro 22R (HZ) with a fixed angle rotor. The supernatant was discarded and 1ml of warm PEG4000/PBS was added drop wise over 1 minute with constant agitation. A further 1ml of PBS was added in the same fashion and then the volume was then increased to 20ml with PBS. This was again spun down, the supernatant was discarded and the pellet was resuspended in 20ml of cloning medium (see Section 2.2.6). Cells were dispensed into two $25cm^2$ flasks and incubated overnight at 37°C, 5% (v/v) CO_2. The cells were then pooled, spun at 200 x g for 5 minutes at room temperature and resuspended in 50ml cloning medium with HAT supplement, (see Section 2.2.6; this selects for hybridoma cells fused with B cells from the spleen of the mouse by using aminopterin to block De Novo nucleic acid synthesis, forcing the cells to utilise the Salvage pathway, which requires hypoxanthine and thymidine). This medium was dispensed over the five macrophage-conditioned plates, 100µl per well and incubated at 37°C 5% (v/v) CO_2 for 5 days. Every 3 days the medium was replaced with fresh cloning medium supplemented with HAT. When colonies began to appear, the supernatant from each colony was removed and screened by ELISA (see Section 2.3.5.3), the cells were transferred to a 24 well plate with fresh cloning media and replacing HAT with HT (see Section 2.2.6) to continue growing. From then on the plates were fed every 3 days with cloning media supplemented with HT.

The criterion for the identification of a positive antibody producing colony was that it has at least 50% of the activity of the serum taken at the time of fusion. Positive

colonies were cloned by diluting them to one cell per 200µl per well of a 96 well plate. The cloned plate was fed and screened for further positive colonies in the same manner as before.

2.3.4.3 - Polyclonal Antibody Production

The KLH/7(K) conjugate was sent to Harlan Sera-Labs for the production of hTRPC7 antibodies in barrier reared, New Zealand white rabbits. Four 1mg/ml frozen aliquots were sent, the samples were then processed according to their protocols. Briefly, samples were diluted to 200µg/ml in PBS and then mixed 1:1 with adjuvant before injection (see Section 2.2.9.3). The following table describes the protocol:

Day	Procedure
0	Pre bleed 5ml + immunization KLH/7(K) + FCA 1ml
14	Boost 1- KLH/7(K) + FIA 1ml
28	Boost 2- KLH/7(K) + FIA 1ml
35	Test bleed 1
42	Boost 3- KLH/7(K) + FIA 1ml
49	Test bleed 2
56	Boost 4- KLH/7(K) + FIA 1ml
63	Test bleed 3
70	Boost 5- KLH/7(K) + FIA 1ml
77	Terminal bleed

Serum was prepared, frozen and sent the day after the test bleeds.

2.3.5 - Antibody Purification

2.3.5.1 - Column Preparation

Using reagents from section 2.2.9.4, the column for the purification of antibodies was made using CNBr-activated Sepharose 4B. To make a 5ml column, 1.5g of CNBr-activated Sepharose 4B was added to 100ml 1mM HCl, pH 2-3. This was washed on a sintered glass filter for 15 minutes with several aliquots of 1mM HCl, (this was done

in order to remove the additives and preserve the active groups). The Sepharose was then washed with several aliquots of ddH_2O and then washed with the coupling buffer, pH 8.3. Peptide 7(K) was dissolved in 5ml of the coupling buffer to a concentration of 2mg/ml. The washed gel was then added to the peptide solution and mixed via rotation overnight at 4°C. Following this the Sepharose was washed with 5 gel volumes of coupling buffer (to wash away excess peptide) and then washed in 0.1M Tris-HCl, pH 8 and left to stand for 2 hours at room temperature in 0.1M Tris-HCl, to block any remaining active sites. The Sepharose-peptide conjugate was transferred to a 1ml column and was washed with three alternating cycles of 0.1M CH_3COONa pH 4 with 0.5M NaCl and the high salt wash pH 8, using at least 5 gel volumes of each. The column was stored at 4°C in 20mM Na_2HPO_4 with 0.5M NaCl and 0.01% (w/v) NaN_3.

2.3.5.2 - Antibody Purification

Prior to purification of the antibody, the column was attached via capillary tubing to a pump and spectrophotometer (set to measure at 280nm with an output to a trace recorder). The trace recorder was then calibrated using 5mg/ml BSA. The whole procedure was carried out at 4°C, using reagents from section 2.2.9.4. The column was pre-washed with 20mM Na_2HPO_4 to establish a stable 280nm baseline. Approximately 6ml of serum per 1ml of column volume was added to the column and cycled overnight at approximately 4ml/minute. The post column serum was collected and retained for ELISA and the column washed with 20mM Na_2HPO_4 until the trace recorder had returned to baseline levels. The column was washed further with 20mM Na_2HPO_4 and when a stable baseline was reached the antibody was then eluted by applying 50mM glycine HCl pH 2.3 and the monitored protein peaks were collected in 1ml aliquots. Each aliquot was neutralised with 20µl 1M Tris pH10.8. Collection ceased when the peak had dropped back down to baseline levels.

A small amount of each aliquot of the eluted antibody was dotted onto BioTrace®NT protein transfer nitrocellulose membrane (see Section 2.2.15) and stained with diluted Ponceau S (see Section 2.2.15; 9 parts ddH_2O to 5 parts Ponceau S stock solution), washed in ddH_2O and dried, to determine which aliquots contained the most protein. Aliquots containing the most protein were pooled, and placed in dialysis tubing and

dialysed against 5L PBS overnight at 4°C. The dialysed antibody was then concentrated in PEG20000 to a final volume of approximately 500µl. An aliquot was retained for ELISA and the antibody was stored at -20°C.

The column was then regenerated by washing with 20mM Na_2HPO_4 for at least 1 hour, then three alternating cycles of 0.1M CH_3COONa pH 4 with 0.5M NaCl and the high salt wash, pH 8, using at least 5 gel volumes of each. The column was then stored at 4°C in 20mM Na_2HPO_4 with 0.5M NaCl and 0.01% (w/v) NaN_3 until further use.

The amount of antibody present was determined by carrying out a protein assay using dilutions of 500µg anti rabbit IgG for the standard curve (see Section 2.2.9.5). 10µl of each standard and affinity purified antibody samples were pipetted into the appropriate wells of a microwell plate, 10µl of the diluent, 20mM Na_2HPO_4 was used as a blank, (each standard and sample was done in triplicate). 300µl of the Coomassie® Plus Reagent was added to each well and the plate was placed on a shaker for 30 seconds, the absorbance was then measured at 595nm. The values were blank corrected and a standard curve was plotted of absorbance against protein concentration. The unknowns were read off from the standard curve.

2.3.5.3 - Enzyme Linked Immunosorbent Assay (ELISA)

Using reagents from section 2.2.10, 100µl of 10mg/ml solution of peptide or the conjugate KLH (diluted in coating buffer) were placed in wells of a 96 well plate and incubated overnight at 4°C. The plates were washed 3 times with PBST then blocked with 300µl per well of PBSTM, this was incubated at room temperature for 1 hour. The plates were washed twice with PBST then 100µl of a 1:100 dilution of the serum or purified antibody in PBST was added to the wells, 1:100 serial dilutions of the serum or purified antibody were then performed and plates incubated with antibody at room temperature for 2 hours. The plates were then washed 3 times in PBST and 100µl of the secondary antibody, anti-Rabbit IgG horseradish peroxidase diluted 1:1000 in PBST, was applied to each well and incubated at room temperature for 2 hours. The plates were then washed 3 times in PBST and twice in PBS. The substrate was then added at 100µl per well for 5 to 15 minutes at room temperature. The

reaction was stopped with 50µl of 2M H_2SO_4 and the plates were read at an optical density of 450nm (values were calculated by subtracting background readings of 700nm).

2.3.6 - Protein Methods

2.3.6.1 - Cell Culture for Immunofluorescent Staining

All cells used for immunofluorescent staining, with the exception of adult cardiomyocytes, were cultured on sterile 22 x 22mm coverslips in 35mm diameter cell culture dishes.

2.3.6.2 - Fixation and Immunofluorescent Staining

Using reagents from section 2.2.11, the coverslips containing; HEK293, COS7, Panc-1, Capan-1, human primary pancreas, 3T3-L1, embryonic cortical and spinal cord cultures cells were washed 3 times with PBS and fixed with 2% (w/v) PFA in PBS, 2ml per coverslip, incubated at room temperature for 20 minutes. The coverslips were then washed 3 times with PBS and permeablised with 0.1% (v/v) Triton-X 100 at room temperature for 5 minutes. Coverslips containing GH4C1 cells were fixed and permeablised in methanol for 5 minutes at -20°C. Coverslips containing cultured embryonic mouse pancreatic tissue were fixed in MEMFA at room temperature for 40 minutes, then washed in PBS for 30 minutes, before permeablisation in 5% (v/v) Triton-X 100 for 10 to 15 minutes at room temperature.

From this point all cell types were treated in the same way and all stages were carried out at room temperature. Coverslips were again washed 3 times in PBS before blocking with blocking buffer for 20 minutes. The primary antibody was prepared at an appropriate dilution in blocking buffer and 70µl was applied as a drop to Parafilm, the coverslips were then inverted on to the primary antibody and incubated at room temperature for at least 1 hour. The coverslips were then floated off the Parafilm with PBS and replaced back in the plates and washed twice in blocking buffer and twice in PBS for 5 minutes each. The following steps were carried out in the dark; the appropriate secondary antibodies were then prepared, diluted 1:100 or 1:200 in blocking buffer, the coverslips were inverted onto 70µl of secondary antibody solution and incubated at room temperature for 20 minutes. Unless otherwise stated the secondary antibody used with anti-hTRPC7, the pre-immune serum or peptide

control solution was anti-rabbit IgG conjugated to Alexa Fluor 488. The coverslips were removed to their dish as described and washed twice in blocking buffer and twice in PBS for 5 minutes each. The coverslips were then dipped in water and mounted onto a glass slide with 30µl of Mowiol mounting medium and left to dry overnight at room temperature and stored at 4°C until observed by confocal microscopy.

2.3.6.3 - Immunofluorescence Staining of Adult Rat Cardiomyocytes

Cells treated with insulin were washed once in 15ml PBS containing the same amount of insulin used to stimulate the cells, cells not stimulated with insulin were washed once in 15 ml PBS alone. Cells were left to stand for 1 minute until the cells settled, and the supernatant was removed. Using materials from section 2.2.11, cells were fixed in 7.5ml 4% (w/v) PFA for 20 minutes on a rocker at room temperature, cells were again left to stand for 1 minute and the supernatant removed. Cells were then washed three times in PBS allowing the cells to settle between washes for 1 minute. Cells were blocked and permeablised in 7.5ml of permeablisation buffer at room temperature for 45 minutes on a rocker. Cells were allowed to settle for 1 minute and the supernatant was removed leaving approximately 250µl of buffer with the cells, they were then transferred to microfuge tubes. A 1:50 dilution of primary antibodies was made in the permeablisation buffer, 250µl was added to the cells to make a final dilution of 1:100. This was incubated for 1 hour 30 minutes at room temperature on the rocker. The cells were left to settle for 1 minute and the supernatant was removed, they were then washed three times in permeablisation buffer allowing cells to settle between washes. From this point on samples were kept in the dark. A 1:50 dilution of secondary antibodies was made up in permeablisation buffer 250µl was added to the cells already in 250µl buffer, to make a 1:100 dilution of secondary antibodies. This was incubated for 1 hour at room temperature, in the dark on the rocker. Keeping them in the dark, the cells left to settle and the supernatant was removed, cells were then washed six times in permeablisation buffer allowing the cells to settle between each wash. The supernatant was removed and the cells were resuspended in 150µl of permeablisation buffer. A drop of Vector Shield mounting medium was applied to a glass coverslip, to this 10µl of cells were added, a glass coverslip was lowered over

the top which was held in place by the application of clear nail varnish around the sides. The cells were then stored at 4°C until analysis by confocal microscopy.

2.3.6.4 - Preparation of Cell Lysates

Cultured cells, approximately 80-90% confluent, were harvested by washing 3 times in PBS and scraping the cells using a cell scraper in to 1ml of ice-cold protease inhibitor cocktail (see Section 2.2.12). The collected cells were then sonicated on ice with 3 x 15 second bursts of 15-18kHz. Adult rat cardiomyocytes were prepared by re-suspending the freshly isolated cells in 1ml of the ice-cold protease inhibitor cocktail and quickly frozen in liquid nitrogen. The protein concentration was measured using the Coomassie® plus Protein Assay Reagent. Samples were prepared for SDS-PAGE by adding 2X loading buffer and denatured by incubation in a boiling water bath for 5 minutes and spun in a Biofuge 13 (HI) bench top centrifuge at 13000rpm for 3 minutes at room temperature.

2.3.6.5 - Membrane Preparation

Sonicated cell lysates were transferred to 10ml ultracentrifuge tubes and centrifuged in a floor standing Beckman ultra centrifuge using a 70.iTi rotor at 54000 x g, (28000rpm) for 30 minutes at 4°C. The resulting pellet was resuspended in 1ml ice cold protease inhibitor cocktail. The protein concentration was measured using the Coomassie® plus Protein Assay Reagent (see Section 2.3.6.6). Samples were prepared for SDS-PAGE as described (see Section 2.3.6.7).

2.3.6.6 - Protein Concentration Measurements

Coomassie® Plus Protein Assay Reagent (see Section 2.2.13) was used to determine the total protein obtained from all cell lysate preparations. A standard curve was made by serial dilutions of 2mg/ml BSA (see Section 2.2.13) in protease inhibitor cocktail. 10µl of each standard and cell lysate samples were applied to the appropriate wells of a microwell plate, 10µl of the diluent was used as a blank, (each standard and sample was done in triplicate). 300µl of the Coomassie® Plus Reagent was added to each well and the plate was placed on a shaker for 30 seconds, the absorbance was then measured at 595nm. The values were blank corrected and a standard curve was plotted of absorbance against protein concentration. The unknowns were read off from the standard curve.

2.3.6.7 - SDS-Polyacrylamide Gel Electrophoresis (SDS-PAGE)

SDS-PAGE was carried out using materials from section 2.2.14. For the preparation of two 10% separating gels the following was mixed together:

Volume	Reagent
10ml	Acrylamide mix
7.5ml	1.5M Tris-HCl pH 8.8
300µl	10% (w/v) SDS
12.1ml	ddH_2O
150µl	10% (w/v) APS
10µl	TEMED

The gel mix was transferred by pipette to two pre-assembled Atto™ mini-gel rigs, over laid with isopropanol and left for approximately one hour to polymerise. The isopropanol was then removed and the top of the gel washed with water. A 4% stacking gel was then prepared by mixing the following:

Volume	Reagent
1.33ml	Acrylamide mix
2.5ml	0.5M Tris-HCl pH6.8
100µl	10% (w/v) SDS
6ml	ddH_2O
50µl	10% (w/v) APS
5µl	TEMED

The gel mix was poured on to the separating gel, the combs were inserted and the gels were left for 1 hour to polymerise.

The gels were placed in the vertical gel tank and running buffer was added. The combs were removed and the wells were washed out with running buffer. Samples of a known amount of protein and Precision protein marker were loaded into the wells; the gels were run at a constant voltage of 200V until the dye front just ran off the bottom of the gel.

The gels were either stained with Coomassie Blue solution for 30 minutes to 1 hour and destained with destaining solution until the background stain was removed, or the gels were soaked in transfer buffer ready for Western blotting, described below in section 2.3.6.8.

2.3.6.8 - Western Blot

Western blotting was carried out using materials from section 2.2.15. For each gel one piece of nitrocellulose membrane and two sheets of extra thick filter paper were cut to the same size as the gel. The nitrocellulose was wetted in water for 2 minutes the water was poured off and transfer buffer was added. The gel, filter paper and support pads were also placed in transfer buffer and were gently agitated on a rocker for 15 minutes. One of the support pads was placed on the open cassette, on top of which was placed one sheet of filter paper, the gel, the nitrocellulose membrane, the remaining sheet of filter paper and finally the support pad. Air bubbles were removed between layers by rolling a pipette on top of the sandwich. The cassette was then closed and placed in the blotting chamber in the correct orientation (gel on cathode side and nitrocellulose membrane on anode side) and enough transfer buffer was then added to submerge the sandwich. The blotter was then connected to the power supply and the transfer was run at a constant current of 200mA for 2 hours.

2.3.6.9 - Immunoprobing and Detection

After Western blotting the nitrocellulose membrane was stained with diluted Ponceau S (for dilution see Section 2.3.5.2) for approximately 1 minute and destained in ddH_2O to visualise the protein, after this the Ponceau was totally removed by washing in PBST. Unbound sites were blocked with PBST (see Section 2.2.10) containing 5% (w/v) BSA overnight at 4°C. For all the following stages the blot was incubated at room temperature, on a rocker with constant agitation. The membranes were then washed 3 times with PBST for 10 minutes each wash. The primary antibody, diluted to the appropriate concentration in PBST was added to the membrane and incubated for 2 hours. The membrane was then washed 3 times in PBST, 10 minutes each wash. The secondary antibody from the Vectastain kit (see Section 2.2.15) diluted to 1:1000 in PBST was then added to the membrane and incubated for 1 hour. The ABC reagent was also made at this time and incubated, in a 50ml tube on the belly dancer for 1

hour. The membrane was then washed with PBST 3 times, 10 minutes each wash and the blot was then incubated in the ABC reagent for 1 hour. The membrane was then washed twice with PBST and twice with PBS for 5 minutes each. The substrate DAB (see Section 2.2.15), was then applied according to the manufacturers instructions; this was incubated for up to 15 minutes. The reaction was stopped with copious amounts of ddH_2O. Membranes were dried and stored in the dark at room temperature.

2.3.6.10 - Immunoprecipitation

Cells were cultured in 90mm cell culture dishes and transfected, if required as previously described (Section 2.3.2.5). Cells were then washed, harvested and lysed in 600µl ice cold protease inhibitor cocktail as previously described (in Section 2.3.6.4). 100µl of the sonicate was mixed with 2X SDS-PAGE loading buffer, boiled for 5 minutes and stored at -20°C. To the remaining sonicate, 500µl 2X RIPA buffer (see Section 2.2.16) was added, this was mixed for three to four hours at 4°C to solubilise membrane proteins. 50µl of Protein G beads (see Section 2.2.16) were washed twice with cold PBS by spinning in a Mikro 22R (HZ) bench top centrifuge with a fixed angle rotor at 490 x g, (2000rpm) for 5 minutes each at 4°C. To the beads 50µl of antibody was added and mixed for 3 hours at 4°C. The beads were spun again and supernatant removed, the beads were then washed three times in cold, 1X RIPA buffer by spinning to remove unbound protein. The solubilised sonicate was then added to the beads and mixed overnight at 4°C. The beads were pelleted as described above and the supernatant removed which was then mixed with 2X SDS-PAGE loading buffer, boiled for 5 minutes and stored at -20°C. The beads were then washed three times in cold 1X RIPA buffer by spinning, 2X SDS-PAGE loading buffer was added to the beads, which were then boiled for 5 minutes and stored at -20°C. Samples were separated by SDS-PAGE and protein detected by Western blot and immunodetection, as described (in Sections 2.3.6.7, 2.3.6.8 and 2.3.6.9).

2.3.7 - Functional Methods

2.3.7.1 - Cell Culture for Functional Methods

25mm diameter coverslips sterilised by washing in 100% ethanol and then autoclaved. The sterile coverslips were placed in 35 mm culture dishes and HEK293 cells were

seeded on the coverslips, grown overnight and subsequently transfected, as described (Section 2.3.2.5).

2.3.7.2 - Calcium Re-addition Protocol: Experimental Set Up

Using reagents from section 2.2.17, the experimental solutions were placed in the solution reservoirs (Figure 2.1) and allowed to feed down the capillary tubing by gravity and all air bubbles were removed. Cultured HEK293 cells were washed three times in 2mM Ca^{2+} PSS and incubated for 30 minutes in 3μM Fura 2-AM, then washed for 10 minutes in 2mM Ca^{2+} PSS. Excess cells were carefully removed from the edges of the coverslip and by the use of vacuum grease the coverslip was then loaded on to the heated chamber (heated to 37°C) (Figure 2.1). The capillary tubing from the manifold was attached to the in line heater to heat the solutions to 37°C, this was then attached to the chamber at the solution inflow end and capillary tubing leading to a vacuum pump was attached at the solution out flow end to remove the out flow liquid (Figure 2.1).

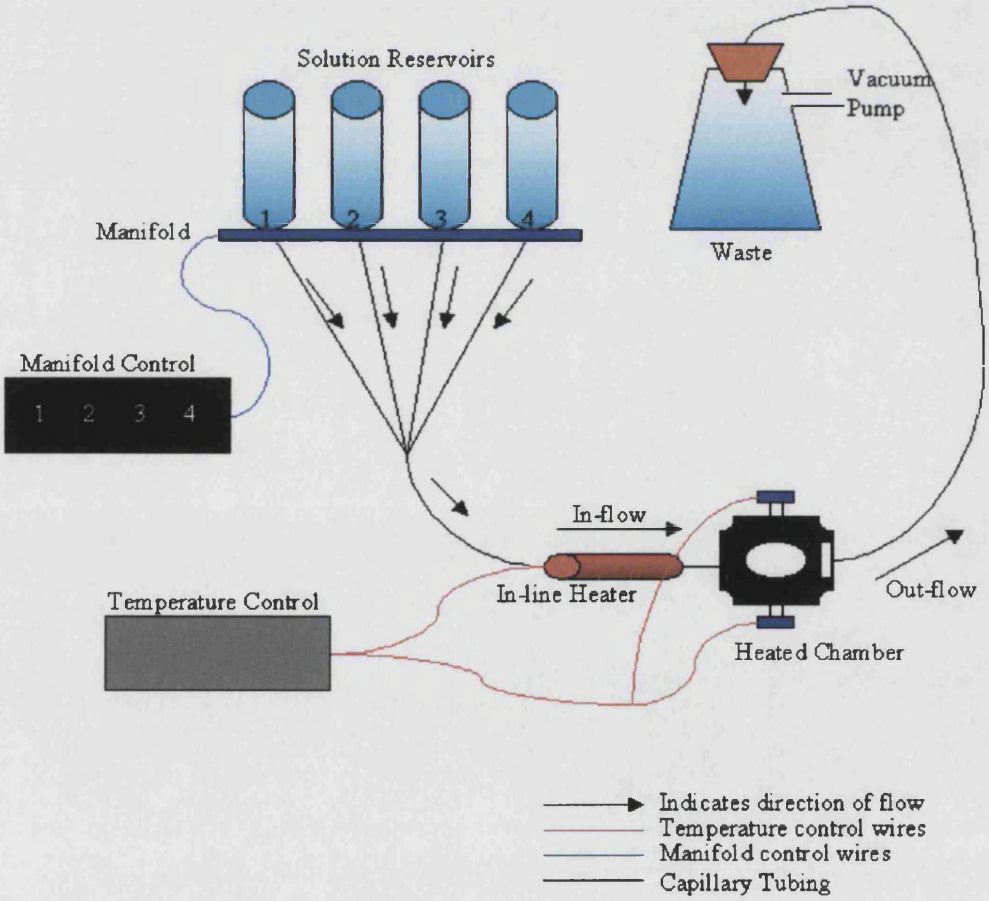

Figure 2.1: A schematic diagram of the equipment set up for the Calcium Re-addition Protocol.

Once a flow of 2mM Ca^{2+} PSS through the chamber was established and air bubbles removed, the chamber was then clamped in place on the microscope and using the x40 oil immersion objective the cells were visualised.

2.3.7.3 - Calcium Re-addition Protocol

If cells were transfected using pIRES2-EGFP, pIRES2-EGFP-htrpc7 or pIRES2-EGFP-htrpc7A, the EGFP positive cells were visualised using the GFP filter. A short recording was taken with the Spectramaster laser set to illuminate at 488nm, (emission at 535nm) to establish where the EGFP positive cells were. The filter was then switched to the Fura 2 filter and laser settings were changed to illuminate at a ratio of 340nm and 380nm at a ratio of 1:3 (and to measure emission at 510nm). The calcium re-addition protocol was followed; either CPA or OAG was used in a single calcium re-addition experiment.

Calcium re-addition protocol:

Treatment	**Time**
PSS + calcium	2 min
PSS no calcium	5 min
PSS no calcium + 10μM CPA or 100μM OAG	5 min
PSS + calcium + 10μM CPA or 100μM OAG	15 min

A background recording was taken at the end of each experiment by moving to another part of the coverslip with no cells present.

Fluorescent Ca^{2+} indicators are molecules whose optical properties change when they bind Ca^{2+}, and they can be classed as single or dual wavelength indicators. Fura 2-AM is an example of a dual wavelength or ratiometric indicator. When Ca^{2+} binds to Fura 2-AM the emission spectrum changes, the Ca^{2+} free molecule emits optimally at 380nm whereas the Ca^{2+} bound molecule has a peak emission at 340nm. By calculating the ratio of emission at the two wavelengths a measure of Ca^{2+} can be made that is independent of indicator concentration. It is due to this ratioing that it is not as important to carry out calibration with these types of indicators as it is with single wavelength indicators (Tepikin, 2000). Fura 2-AM is a common choice of

indicator and, using this dye, 50 – 90% of it can be sequestered in intracellular organelles. Once the indicator is in the cytoplasm of the cell, the ester groups are cleaved by endogenous esterases and a Ca^{2+} sensitive form of the dye is released, slowing leakage from the cells (Tepikin, 2000).

Experiments are usually carried out using specific inhibitors to the sarco-endoplasmic reticulum Ca^{2+} ATPase (SERCA) pump such as thapsigargin (TG) or cyclopiazonic acid (CPA; Figure 2.2), or agonists such as 1-oleoyl-2-acetyl-*sn*-glycerol (OAG; Figure 2.3), an analogue of diacyl glycerol (DAG), in the presence or absence of Ca^{2+} (where Ca^{2+} is chelated by EGTA) (Putney, Jr. and McKay, 1999). TG and CPA activate calcium entry by depleting intracellular stores of Ca^{2+} through inhibition of the ER Ca^{2+} re-uptake pump, SERCA (Putney, Jr. and McKay, 1999).

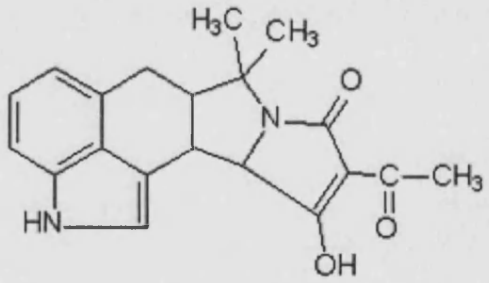

Figure 2.2: Structure of cyclopiazonic acid.

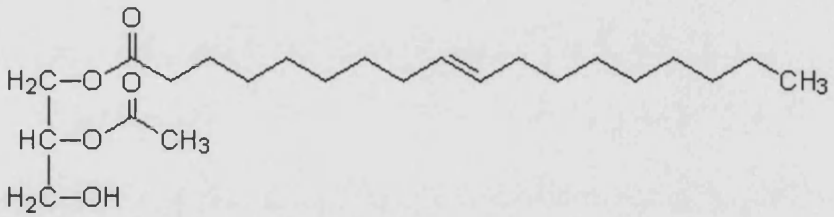

Figure 2.3: Structure of 1-oleoyl-2-acetyl-*sn*-glycerol

Chapter 3
Production and Characterisation of Anti-hTRPC7 Antibodies

3.1 - Introduction

3.1.1 - Antibodies

Antibodies are useful tools to study proteins, and can be used to detect specific proteins using a number of methods, including immunocytochemistry or Western blotting. Antibodies are produced by B lymphocytes, each one of which expresses a surface receptor specific for a particular antigen (Roitt et al., 1998).

Polyclonal antibodies (usually isolated from the serum) are a mixed group of antibodies that identify different sites on the same antigen. Because there is an increased chance that they may recognise different antigens polyclonal antibodies can give a lot of non-specific cross reactivity. However, purification using the peptide the antibody was raised to will usually to reduce much of the non-specificity. Monoclonal antibody production generates an immortal clone of cells that manufacture a single antibody of defined specificity and affinity (Roitt et al, 1998).

3.1.2 - Antibodies to TRPC7

It can be difficult to produce specific antibodies against hTRPC7 due to the high level of homology with the other hTRPCs, specifically hTRPCs 3 and 6. There are several published reports of the use of an anti-TRPC7 antibody: first a group, lead by William Schilling, raised antibodies to all of the TRPCs with varying levels of success. They used the antibodies to look into associations of the TRPC proteins with other TRPCs and PDZ proteins (Goel et al., 2002). Using the same TRPC7 antibody a second study was carried out to determine, by immunocytochemistry, the endogenous localisation of all the TRPC proteins in the rat carotid chemosensory pathway (Buniel et al., 2003). Another group have carried out siRNA studies of TRPC7 and other TRPCs using Western blotting techniques with an anti-TRPC7 (purchased from AbCam, later withdrawn, discussed later in Chapter 5 Section 5.3) to identify the presence or absence of TRPC7 in H19-7 hippocampal neurons (Wu et al., 2004). Goel et al and Bunniel et al raised their own

antibody to TRPC7. As there was no available commercial antibody to hTRPC7 it was decided to raise an antibody specific to hTRPC7 for this current study. The results in this chapter will demonstrate the production of this antibody and its full characterisation in an over expression system.

3.1.3 - Protein Expression

The HEK293 cell line is often used as an expression system for a variety of proteins. HEK293 cells are originally an epithelial cell line derived from human embryonic kidney, which were transformed with sheared human adenovirus 5 (Ad5) DNA (ECACC). HEK293 cells are especially of interest as a system for over expression of *htrpc7* because it was found, by RT-PCR that there is no endogenous hTRPC7 mRNA in HEK293 cells (Riccio et al., 2002).

3.2 - Results

3.2.1 - Amino Acid Sequence Alignment

There are several different ways in which to raise an antibody. The whole of the protein of interest may be used, either by immunising an animal with the entire protein (for example, by creating a fusion protein), alternatively a smaller region of the protein may be used in immunising the animals to obtain an antibody, either by using a fusion protein of part of the sequence or a synthetic peptide. Immunisation with large segments of the protein as a fusion or whole proteins can present problems with specificity of the resulting antibody. For example, if the entire hTRPC7 protein was used to raise an antibody the cross reactivity between the other hTRPCs would be high due to the high level of sequence similarity throughout the group. In addition, there can be significant technical problems associated with the production and purification of sufficient quantities of the antigen. For these reasons a peptide corresponding to a small region of hTRPC7, that was not homologous with other hTRPCs, was used to raise an antibody to hTRPC7. In order to determine the optimum peptide for use, an alignment of the amino acid sequences of the mammalian TRPC polypeptides was examined (Dr A. Wolstenholme, personal communication). This revealed that the extreme C-terminus was poorly conserved between the TRPC sub-family and so this sequence was chosen (Figure 3.1). Highlighted in bold is the sequence the hTRPC7 antibody was raised to, the sequence is conserved between mice and humans with mTRPC7 showing only one amino acid difference for hTRPC7.

```
hTRPC7      942QQLSEKFGKN LNKDHLRVNK GKDI......966
mTRPC7        QQLSEKFGKN LNKDHLRVNQ GKDI......
hTRPC3        HKLSEKLNPS M....LRCE* ..........
hTRPC6        RELGEKLSME PNQEETNR.. ..........
hTRPC5        PRSFSTSSTE LSQRDDNNDG SGGARAKSKS
hTRPC4        SANASKESSN SADSDEKSDS EGNSKDKKKN
hTRPC1        PRN*...... .......... ..........
```

Figure 3.1: A comparative amino acid sequence alignment of hTRPC7, mTRPC7 and all other hTRPCs, highlighted in bold is the 16 amino acids at the very C-terminus of hTRPC7 indicating where the hTRPC7 antibody from this study was raised to (Dr A. Wolstenholme, personal communication).

3.2.2 - Polyclonal Antibody Production in Mice

The peptide was named 7(K), it was conjugated to the carrier protein KLH (see Chapter 2, Section 2.3.4.1) and was first injected into mice 7J and 7K. By immunising with the 7(K) peptide conjugated to KLH a good titre of antibodies against the peptide was obtained in both mice, measured by ELISA (Figure 3.2; see Chapter 2, Section 2.3.5.3). After the fifth boost the titre of antibody to the 7(K) peptide had increased in both mice, this shows an increased affinity of the antibody to antigen at lower dilutions. Mouse 7J appeared to have a higher titre of antibodies in its serum after 5 boosts.

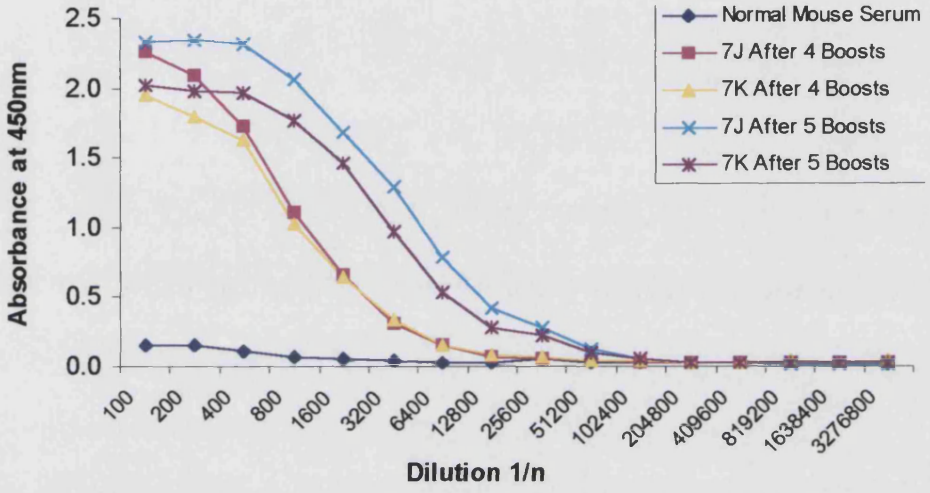

Figure 3.2: The responses of mice 7J and 7K to the 7(K) peptide after 4 boosts and after 5 boosts in comparison to a non-immune, normal mouse serum. 'Dilution 1/n' indicates the ratio of dilution of sample to dilutent where n is the amount in parts of dilutent.

A second ELISA (Figure 3.3) was carried out to analyse the level of immunity to the carrier protein, KLH. KLH appears to be more immunogenic than 7(K) as the results showed a stronger immune response in all cases in comparison to the 7(K) ELISA, this is usual when KLH has been used as the carrier protein. This result indicated that the apparent response by the mice to the 7(K) peptide was 'real' as the mice responded to the carrier protein.

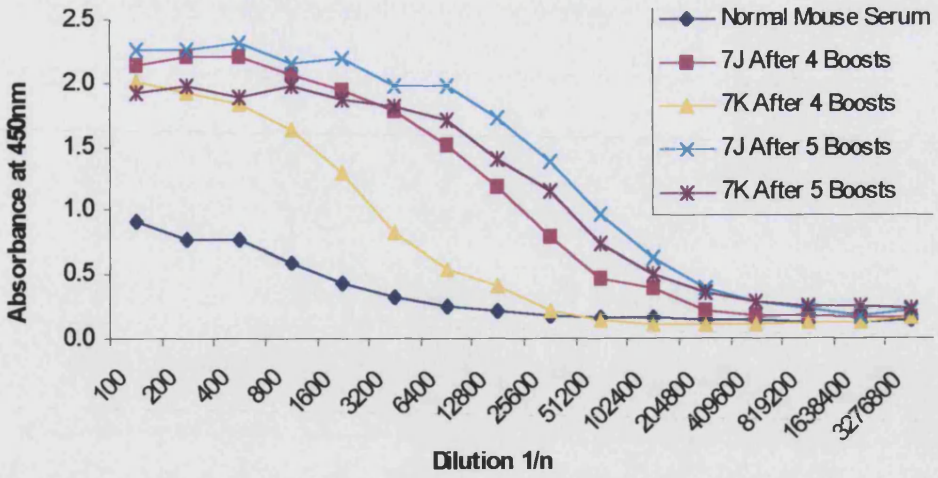

Figure 3.3: The responses of mice 7J and 7K to the carrier protein, KLH, after 4 boosts and after 5 boosts, at the time of fusion. In comparison to a non-immune, normal mouse serum. 'Dilution 1/n' indicates the ratio of dilution of sample to dilutent where n is the amount in parts of dilutent.

3.2.3 - Immunocytochemistry Using 7J and 7K Serum on HEK293 Cells Over Expressing hTRPC7

The sera from both mice was tested on pIRES2-EGFP-*htrpc7* transfected HEK293 cells.

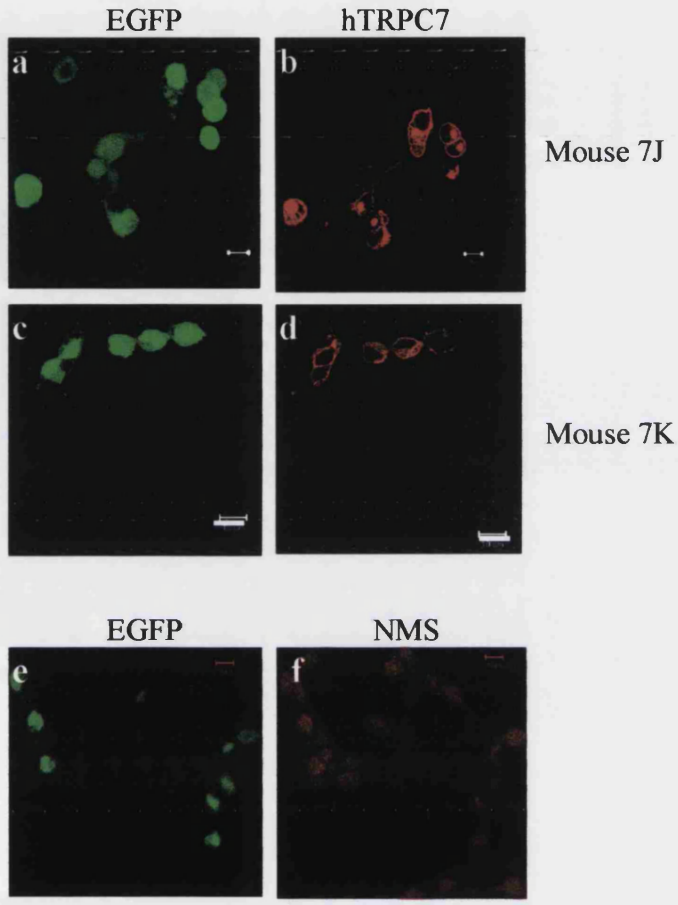

Figure 3.4: Serum test of 7J and 7K. Images **a** to **e** show HEK293 cells transfected with pIRES2-EGFP-*htrpc7*, the EGFP fluorescence (**a, c** and **e**) is confirmation of a positive transfection. **b** shows immunofluorescent staining of the same cells as **a** by serum from mouse 7J (1:100). **d** shows the same cells as **c** immunofluorescently stained with serum from mouse 7K (1:100). **f** shows the same cells as **e**, stained with a non-immune mouse serum (NMS) (1:100). All secondary antibodies used were anti-mouse Texas Red (1:100) and all size bars are 10μm.

The serum from both mice recognises the pIRES-EGFP-*htrpc7* transfected HEK cells (Figure 3.4). The EGFP localises to the nucleus and is used as an indicator of positive transfection, it is not tagged to hTRPC7 (See Appendix Section A1). The positively

transfected cells show staining by the sera from mice 7J and 7K, located in the plasma membrane (PM) region, and with some intracellular staining adjacent to the nucleus.

3.2.4 - Monoclonal Antibody Production

After the final bleed of the mice, the B cells from the spleens of the immunised mice were fused to the P3X63Ag8.653 hybridoma cell line to begin the process of monoclonal antibody production.

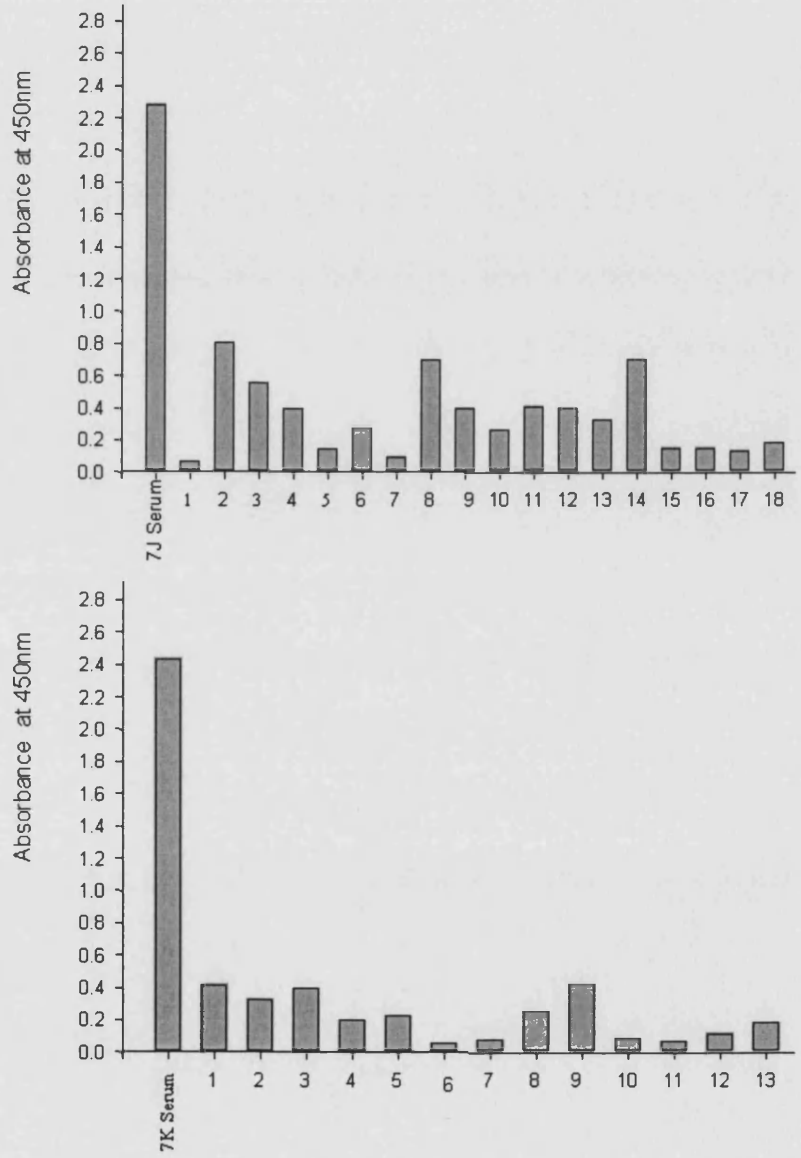

Figure 3.5: The results from the monoclonal antibody production of anti-hTRPC7 from mice 7J and 7K, the positive controls are 7J and 7K Serum and the colonies tested number 1-18 and 1-13 for 7J and 7K respectively.

To produce monoclonal antibodies, the media from colonies were required have at least 50% of the level of antibodies of the fusion serum, and if this was the case the cells would then be propagated to produce a clonal population producing antibodies. However, after four months none of the colonies produced the required 50% activity and therefore, no monoclonal antibodies were produced (Figure 3.5). This was probably due to a low fusion efficiency, it would be useful to attempt to make anti-hTRPC7 monoclonal antibodies again, however, due to time constraints, this was not possible.

3.2.5 - Polyclonal Antibody Production in Rabbits

The ELISA and immunocytochemistry results were encouraging, showing a good polyclonal antibody had been produced; therefore polyclonal antibodies were then produced on a larger scale. The 7(K) peptide conjugated to KLH was sent to Harlan Sera-Labs for immunisation in rabbits, they returned the all test bleed sera and the final bleed sera of the two immunised rabbits for testing by ELISA (described in Chapter 2 Section 2.3.5.3).

The ELISA carried out against peptide 7(K) (Figure 3.6) show high titres of antibodies produced by rabbit 89 to the 7(K) peptide. The antibody binding affinity to the antigen did not decrease until approximately a 1:12800 dilution in rabbit 89.

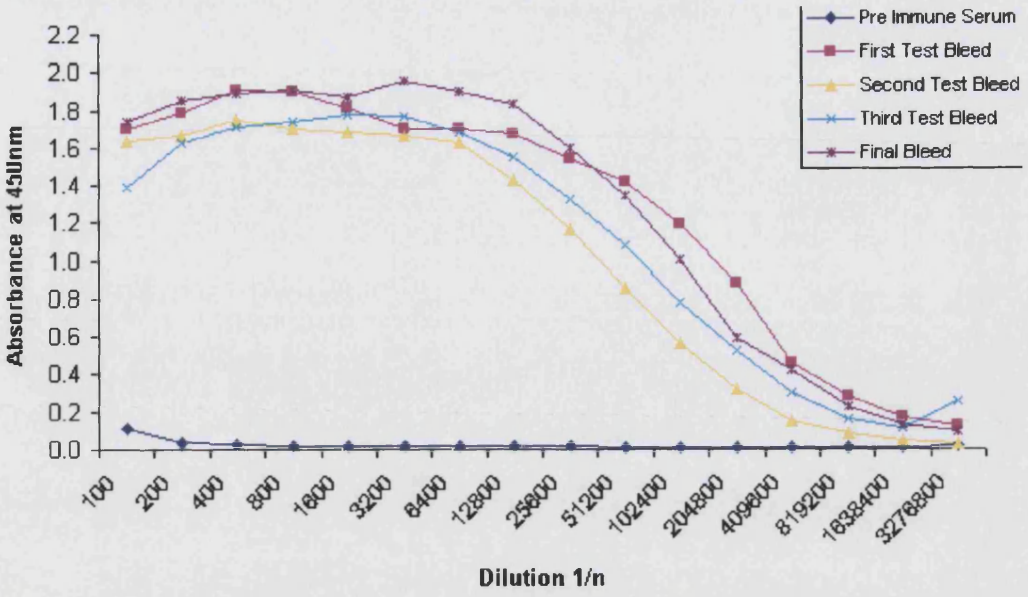

Figure 3.6: The immune response of rabbit 89 to the 7(K) peptide, before the initial immunisation and after the subsequent boosts. 'Dilution 1/n' indicates the ratio of dilution of sample to dilutent where n is the amount in parts of dilutent.

An ELISA was carried out to analyse the level of immunity to the carrier protein, KLH (Figure 3.7). These results showed a similar immune response in all cases in comparison to the 7(K) ELISA.

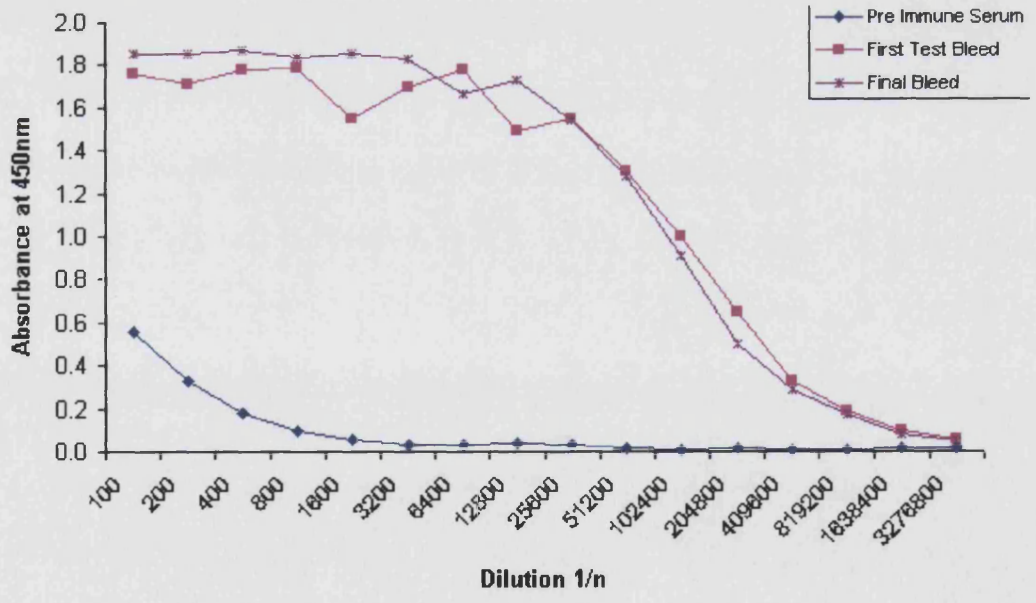

Figure 3.7: The immune response of rabbit 89 to the carrier protein KLH, before the initial immunisation and after the subsequent boosts. 'Dilution 1/n' indicates the ratio of dilution of sample to dilutent where n is the amount in parts of dilutent.

The ELISA carried out against peptide 7(K) (Figure 3.8) show high titres of antibodies produced by rabbit 90 to the 7(K) peptide. The amount antibody did not decrease until approximately a 1: 25600 dilution in rabbit 89.

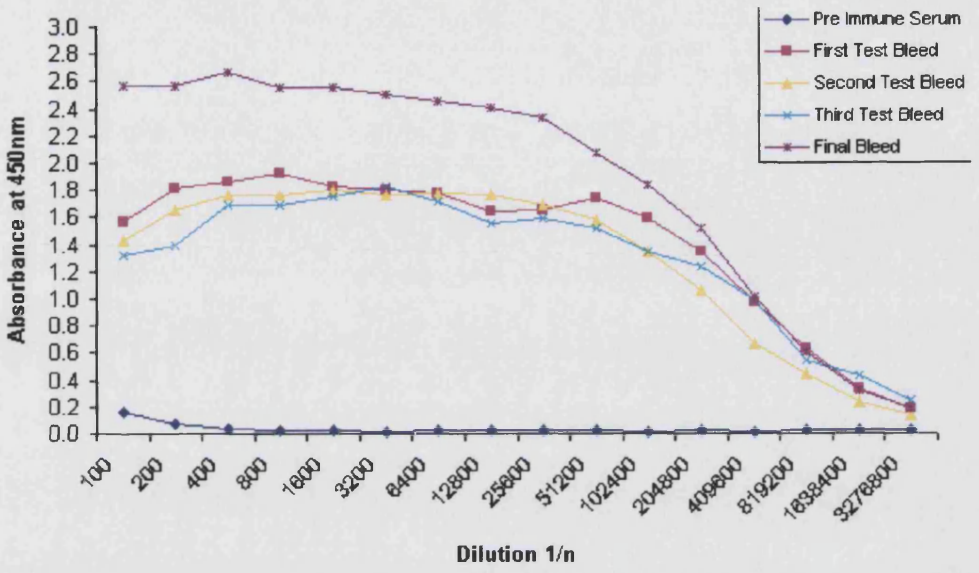

Figure 3.8: The immune response of rabbit 90 to the 7(K) peptide, before the initial immunisation and after the subsequent boosts. 'Dilution 1/n' indicates the ratio of dilution of sample to dilutent where n is the amount in parts of dilutent.

An ELISA was carried out to analyse the reactivity to KLH (Figure 3.9). These results showed a similar immune response in all cases in comparison to the 7(K) ELISA.

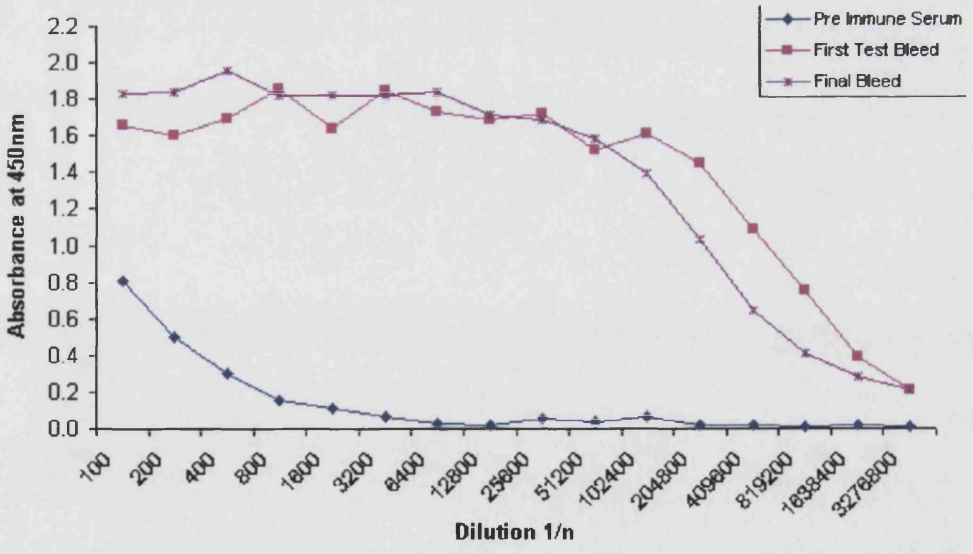

Figure 3.9: The immune response of rabbit 90 to the carrier protein, KLH, before the initial immunisation and after the subsequent boosts. 'Dilution 1/n' indicates the ratio of dilution of sample to dilutent where n is the amount in parts of dilutent.

3.2.6 - Antibody Purification

Purification of serum from rabbit 90 was carried out on an affinity column coupled to the 7(K) peptide to isolate the antibodies to hTRPC7. The serum from rabbit 90 was used in the purification process because of the increased titre as a result of the final boost (Figure 3.8).

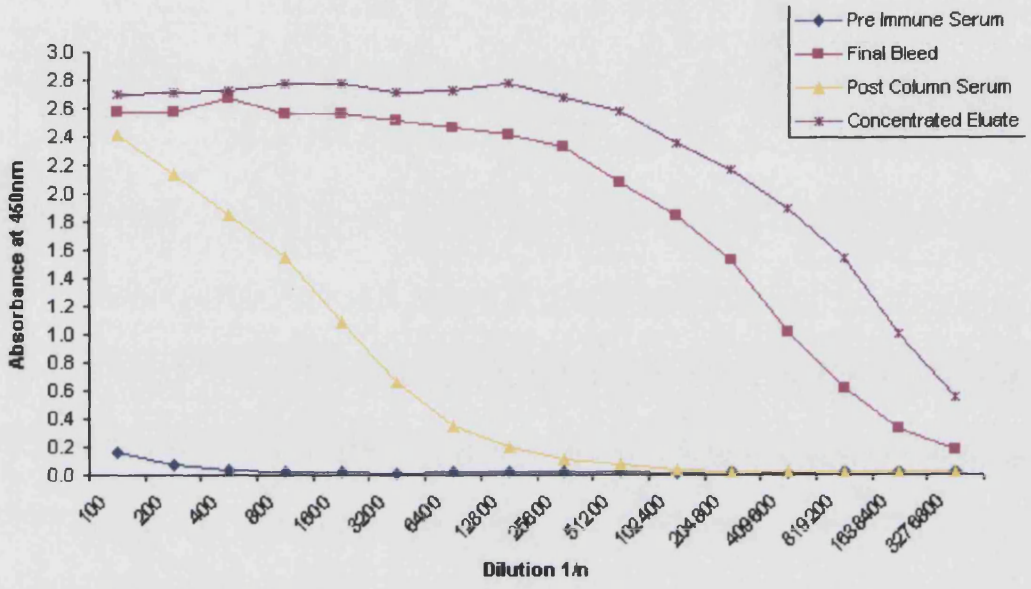

Figure 3.10: The results of an ELISA carried out on samples taken at various stages of affinity purification of rabbit 90 serum. 'Dilution 1/n' indicates the ratio of dilution of sample to dilutent where n is the amount in parts of dilutent.

An ELISA was performed on a plate coated with peptide 7(K) to assay the affinity-purified serum (Figure 3.10). This showed that showed the antibody levels in the final bleed serum were at approximately the same as the concentrated eluate. The post column serum shows a reduction in the antibody levels, but these levels were not down to pre-immune serum levels, suggesting there were some hTRPC7 antibodies remaining in the serum. From this result it showed that the column may have been overloaded with serum and for future purifications the serum could be diluted with PBS and less applied to the column.

3.2.7 - Over Expression of pIRES-EGFP-htrpc7 in HEK293

Immunocytochemistry studies were carried out on transiently transfected HEK293 cells, in order to characterise the purified hTRPC7 antibody.

Immunofluorescent staining of HEK293 cells transfected with pIRES2-EGFP-*htrpc7* (Figure 3.11) reveals staining pattern similar to that of the mouse serum. Positively transfected cells showed localisation of the protein in the PM region with a small amount of staining localised to intracellular organelles, possibly the Golgi apparatus (Figure 3.11). The differential interference contrast (DIC) images (Figure 3.11 j, k and l) show that not every cell is transfected and the antibody only stains the cells transfected with pIRES2-EGFP-*htrpc7*. The level of transfection also appeared to be important, as lower levels of EGFP appeared to have lower levels of hTRPC7.

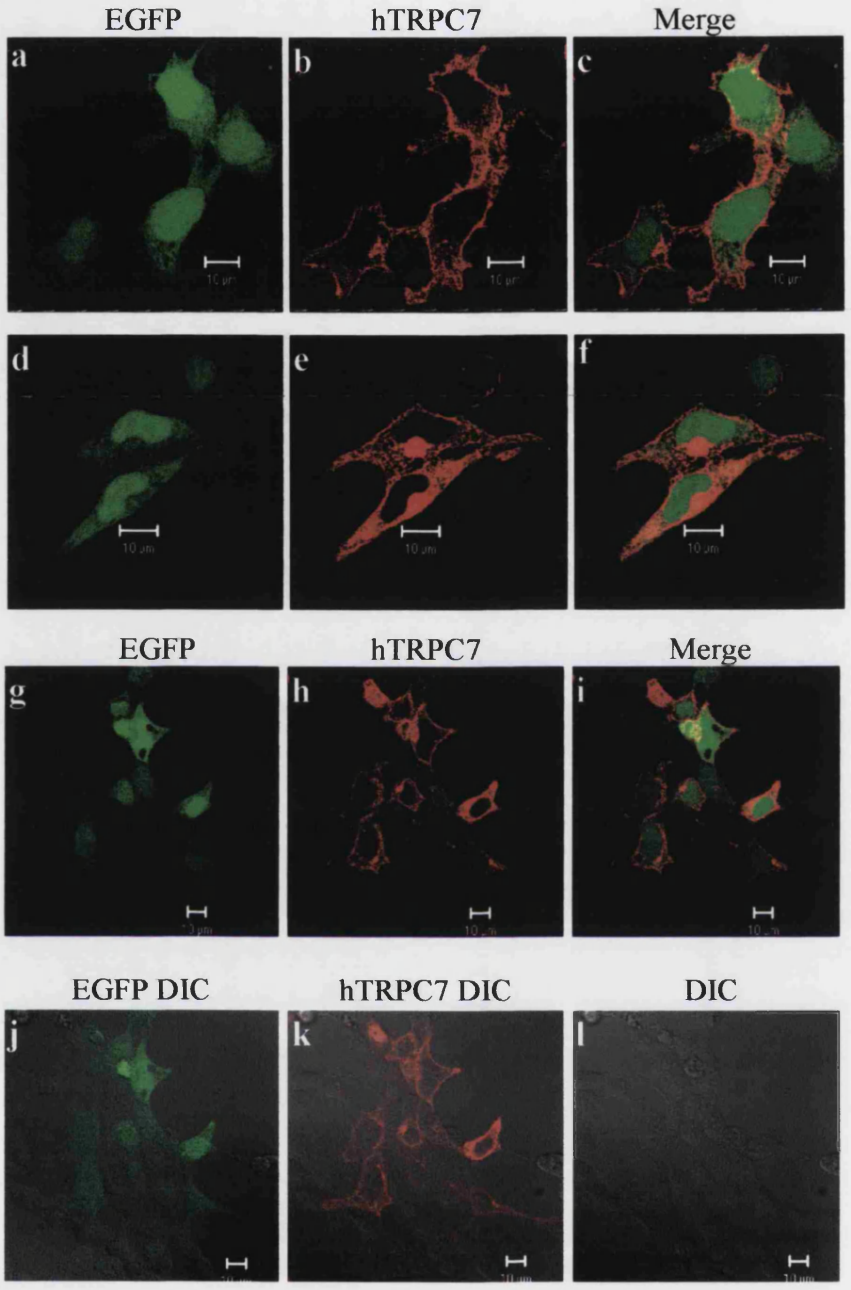

Figure 3.11: HEK293 cells transfected with pIRES2-EGFP-*htrpc7*, images **a, d** and **g** shows positive transfections, images **b, e** and **h** shows the same group of cells as **a, d** and **g** respectively, stained with the affinity purified hTRPC7 antibody from rabbit 90 (anti-hTRPC7), **c, f** and **i** are the merged images of **a** and **b**; **d** and **e** and **g** and **h** respectively. Images **j, k** and **l** are the DIC images of **g, h** and **i** respectively. Anti-hTRPC7 was used at a dilution of 1:100. All size bars 10μm.

Control immunocytochemistry was carried out using HEK293 cells transiently transfected with pIRES-EGFP-*htrpc7* stained with the pre-immune serum from rabbit 90 (Figure 3.12). The staining pattern as observed in Figure 3.11 did not occur and only low-level background staining was apparent (Figure 3.12 a, b and c). Also, similarly transfected cells were stained with anti-hTRPC7 (1:100) which had previously been pre-incubated with the peptide 7(K) for 3 hours at room temperature. Again, only background staining was observed (Figure 3.12 d, e and f).

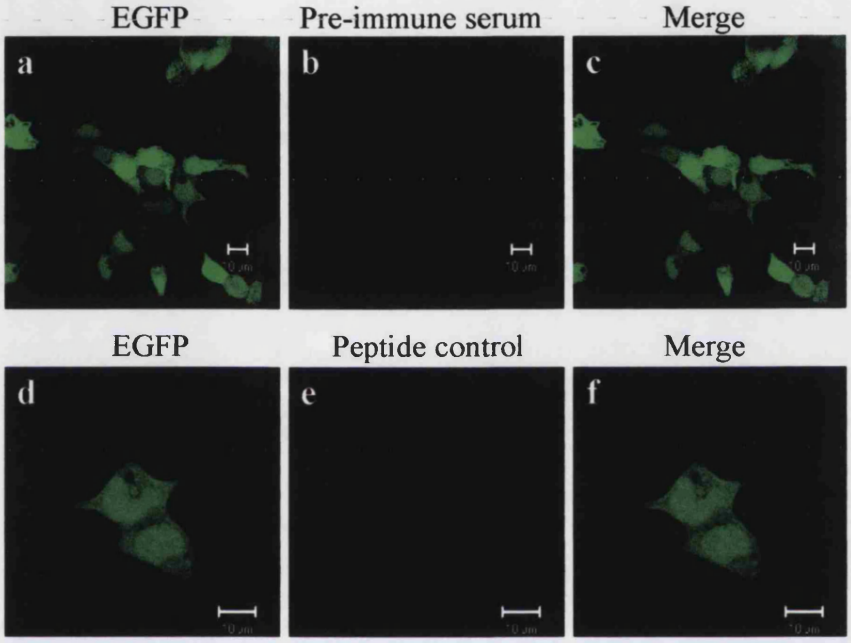

Figure 3.12: control images of two groups of HEK293 cells transfected with pIRES2-EGFP-*htrpc7*, **a** and **d** shows positively transfected cells, **b** shows the same group of cells as **a** stained with pre-immune serum (1:100) from rabbit 90 and **e** shows the same cells as **d** stained using anti-hTRPC7 pre-incubated with the 7(K) peptide (peptide control solution). **c** and **f** are the merged images of **a** and **b** and **d** and **e** respectively.. All size bars 10μm.

As a further control HEK293 cells were transiently transfected with the pIRES-EGFP vector only. Though the same nuclear localisation for EGFP was seen, there was no staining with the anti-hTRPC7 antibody (Figure 3.13a to f). Those cells that were treated with the pre-immune serum or peptide control solution did not show the same staining pattern as those transfected with *htrpc7* and stained with anti-hTRPC7 (Figure 3.13e to l).

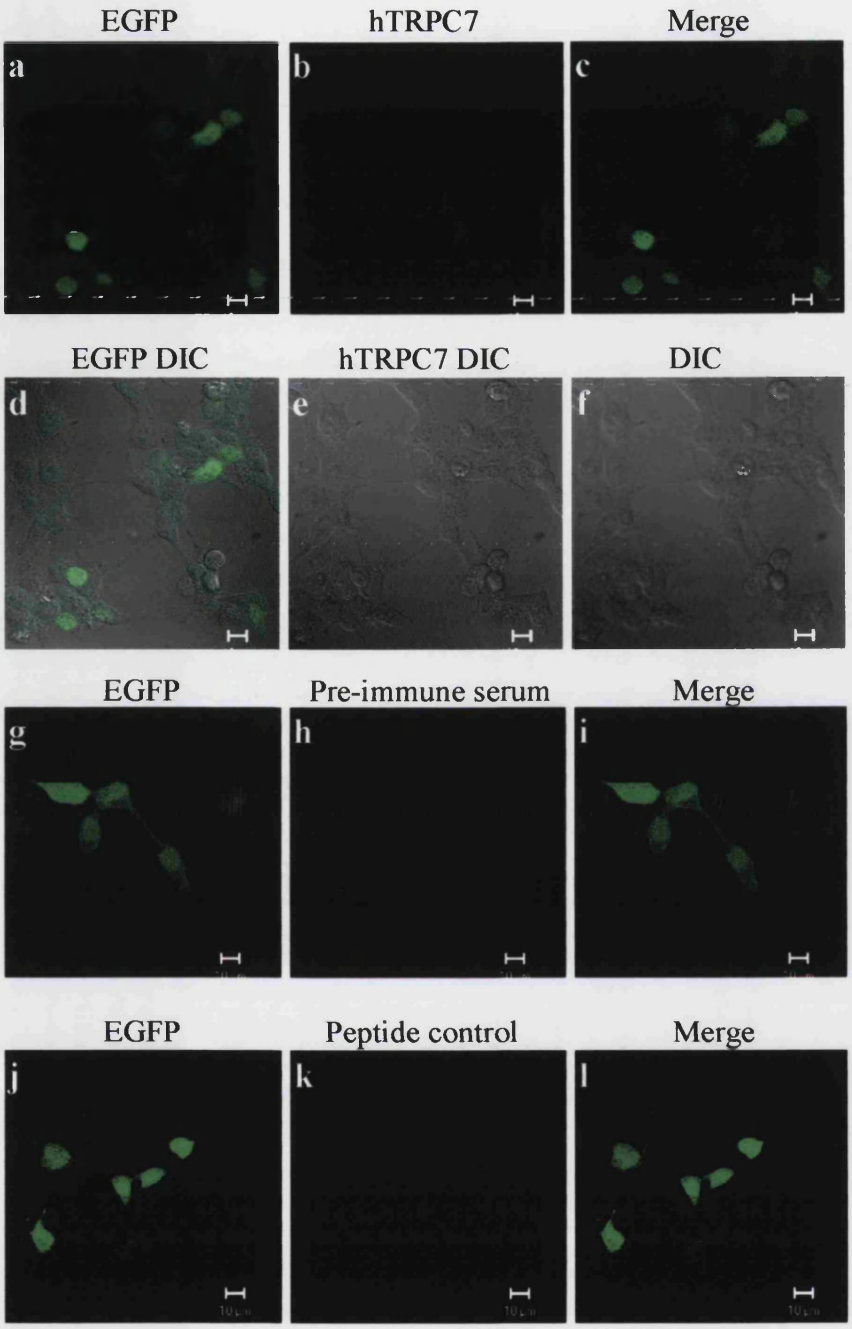

Figure 3.13: HEK293 cells that have been positively transfected with pIRES2-EGFP (vector only), image **a** shows a group of positively transfected cells, **b** shows the same group of cells immunofluorescently stained with anti-hTRPC7 (1:100), **c** shows the merged image of **a** and **b**. Images **d**, **e** and **f** show the DIC images of **a, b** and **c** respectively. Images **g** and **j** show the positive transfections, **h** shows the same group of cells as **g** stained with the pre-immune serum (1:100) from rabbit 90 and **k** shows the peptide control staining of cells in image **j**. **i** and **l** are the merged images of **g** and **h** and **j** and **k** respectively. All size bars 10μm.

In the control staining of non-transfected HEK293 cells, there was no indication of hTRPC7 expression (Figure 3.14a to d), confirming that HEK293 cells do not express hTRPC7 (Riccio et al., 2002).

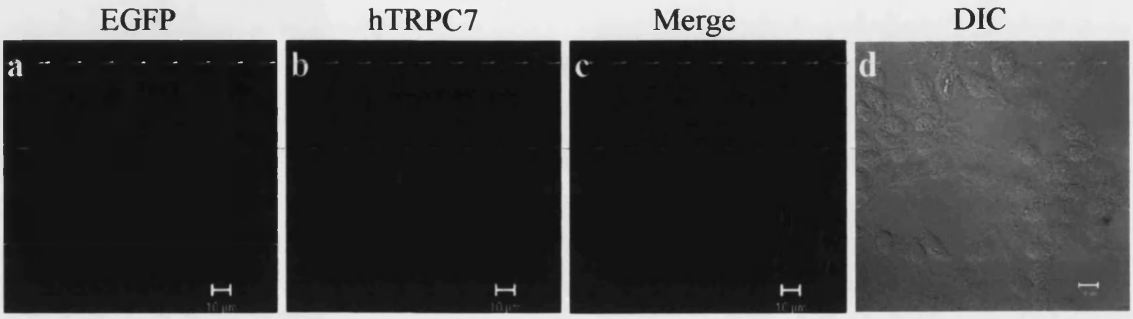

Figure 3.14: Non-transfected HEK293 cells, image **a** shows no presence of EGFP confirming no transfection has taken place, **b** shows immunofluorescent staining by anti-hTRPC7 (1:100), **c** shows the merged image of **a** and **b**. **d** shows a DIC image confirming the presence of cells. All size bars 10μm.

3.2.8 - Over Expression of FLAG-tagged htrpc7 in HEK293

A FLAG-tagged *htrpc7* construct (See Appendix Section A1) was used as a further control in addition to pIRES2-EGFP-*htrpc7* transfections to see if the same pattern of staining could be observed.

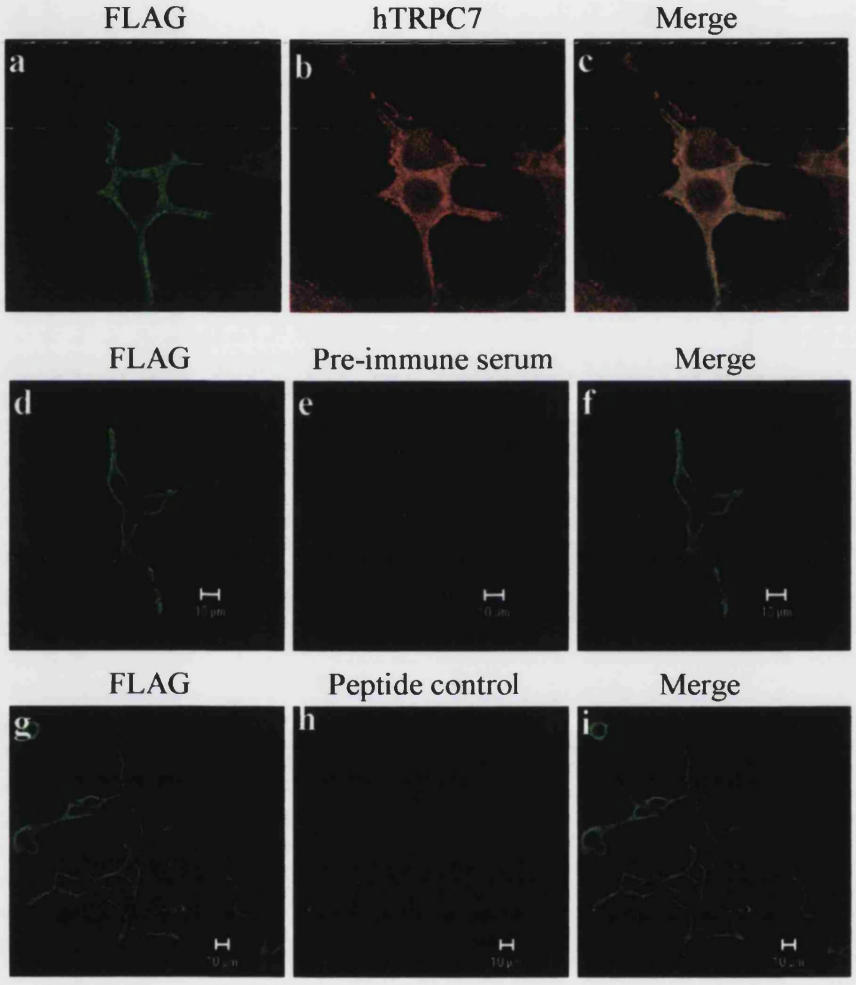

Figure 3.15: HEK293 cells transfected with pFLAG-*htrpc7*, images **a, d** and **g** show immunostaining by anti-FLAG (1:500) giving an indication of a positive transfection, **b** shows the same cell as **a** immunostained by anti-hTRPC7 (1:100), **e** shows the same cells as **d** stained with the pre-immune serum (1:100) from rabbit 90 and **h** shows the peptide control staining. **c, f** and **h** are the merged images of **a** and **b, d** and **e** and **g** and **h** respectively. Secondary antibody for anti-FLAG was anti-mouse FITC. All size bars 10μm.

HEK293 transfected with a FLAG tagged *htrpc7* showed almost complete co-localisation between the FLAG antibody and anti-hTRPC7 and a similar PM region pattern of

staining to the pIRES2-EGFP-*htrpc7* transfected HEK293 cells (Figure 3.15 a, b and c). Control staining of the HEK293 cells transiently transfected with pFLAG-*htrpc7* showed the localisation of hTRPC7 was still evident through the anti-FLAG staining and the pre-immune serum from rabbit 90 gave no staining. Also, similarly transfected cells that were treated with the peptide control solution did not display any staining (Figure 3.15d to i).

3.2.9 - Western Blots of Over-Expressed hTRPC7 in HEK293

Western blots of lysed HEK293 cells that had been transiently transfected with pIRES-EGFP-*htrpc7* showed the presence of a band at approximately 100kD when the blot was probed with anti-hTRPC7 (Figure 3.16a); faint background bands at approximately 60kD and 25kD were also observed. This 100kD band was not present in the lanes containing non-transfected HEK293 lysate or vector only transfected HEK293 lysate. The blots probed with pre-immune serum and peptide control solution (prepared in the same way as the peptide control solution for immunocytochemistry) showed no 100kD band in the lanes containing pIRES-EGFP-*htrpc7* transfected HEK293 lysate (Figure 3.16 c and d) and only faint background bands. The presence of 25kD bands of lanes 2 and 3 of the Western blot probed with anti-GFP confirms the transfection was successful (Figure 3.16b). This 25kD band was much less intense in the lane with vector only transfected HEK293 cell lysate despite that all the lanes were loaded with equal amounts of protein.

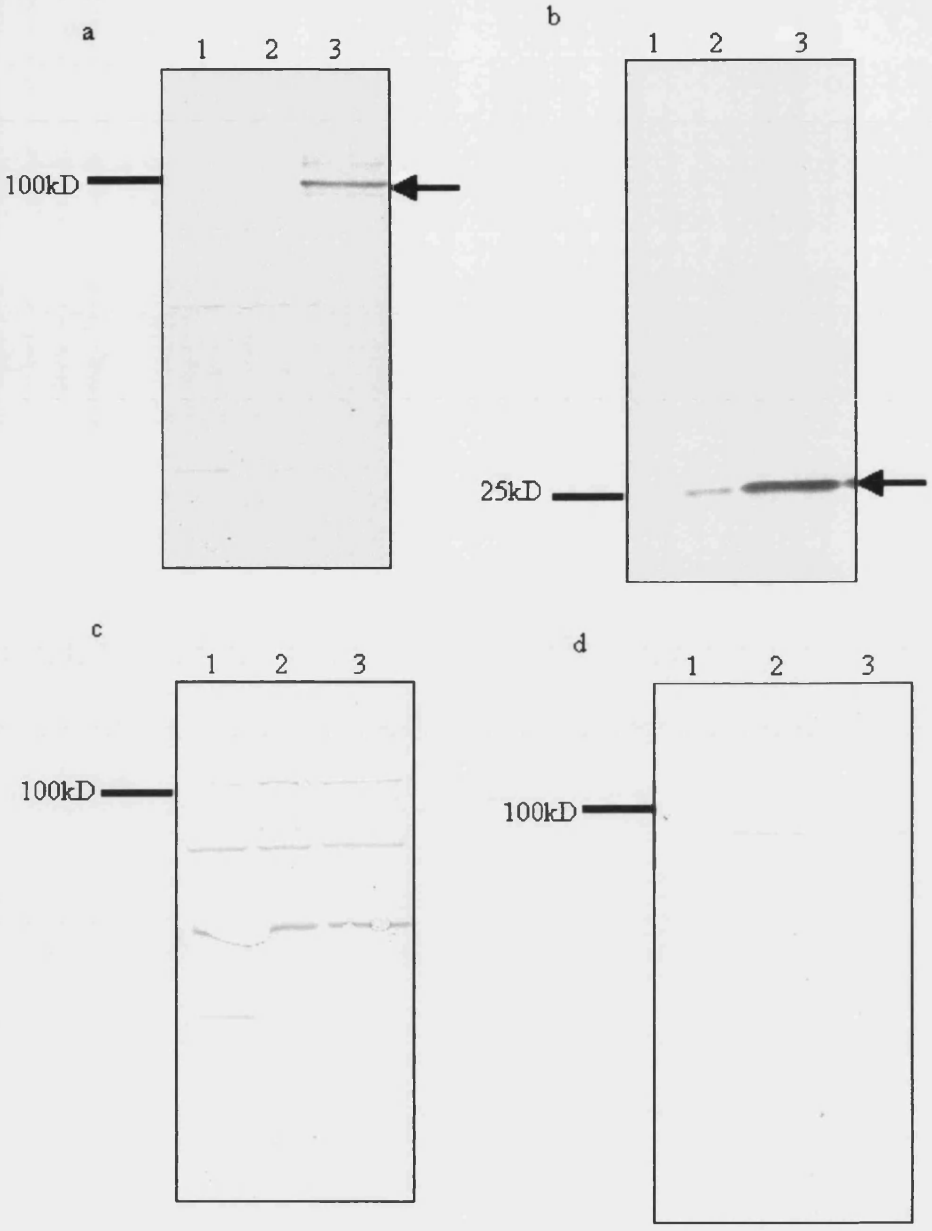

Figure 3.16: Western blots showing; lane 1 non-transfected HEK293 lysate; lane 2 vector only transfected HEK293 lysate; lane 3 pIRES-EGFP-*htrpc7* transfected HEK293 lysate. 5μg of protein was loaded into each lane. Blot **a** shows the Western blot immunoprobed with anti-hTRPC7 (1:1000), **b** shows the Western blot immunoprobed with anti-GFP (1:1000) to indicate positive transfection. **c** and **d** are control Western blots, **c** shows the Western blot immunoprobed with pre immune serum from rabbit 90 (1:1000) and **d** shows a peptide control Western blot.

3.2.10 - Testing Cross-Reactivity of the Anti-hTRPC7 Antibody with Other Members of the hTRPC Subfamily

Transfecting HEK293 cells with *htrpc1*, *3* or *6* cDNAs and staining with the anti-hTRPC7 antibody (Figures 3.17, 3.18 and 3.19 respectively) would reveal any cross-reaction between hTRPC7 and the other TRPCs, though the portion of hTRPC7 used to design the peptide is divergent in other TRPCs, so no cross reaction should occur.

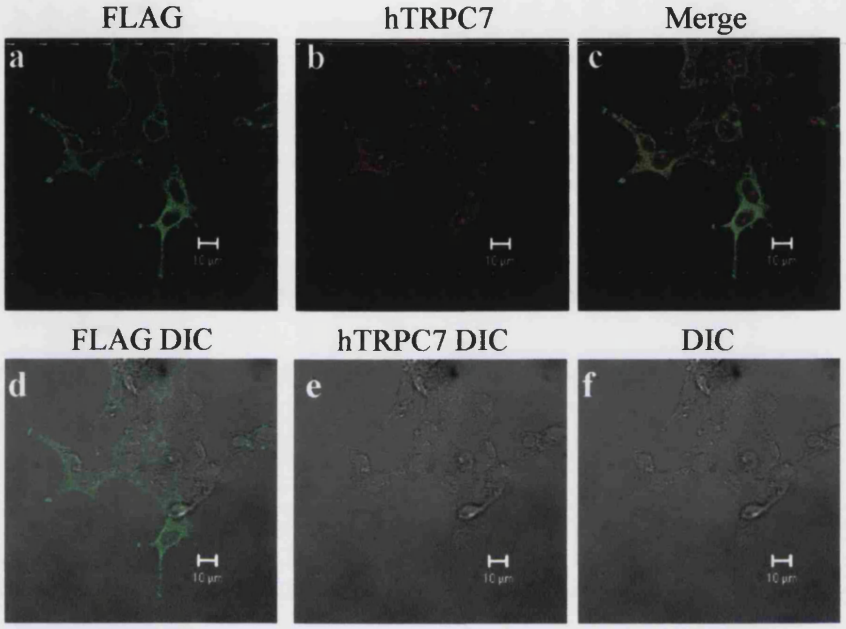

Figure 3.17: HEK293 cells transfected with pFLAG-*htrpc1*, **a** shows immunostaining by anti-FLAG (1:500) with anti mouse FITC secondary antibody (1:100), **b** shows the same group of cells immunostained with anti-hTRPC7 (1:100), **c** shows the merged image of **a** and **b**. **d**, **e** and **f** are the DIC images of **a, b** and **c** respectively. All size bars 10μm.

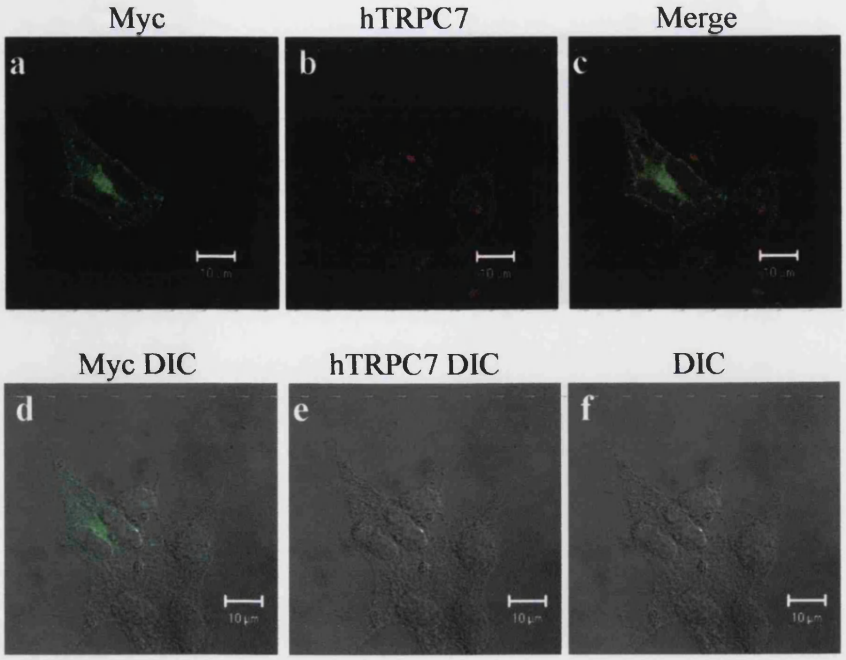

Figure 3.18: HEK293 cells transfected with Myc tagged *htrpc3*, **a** shows immunostaining by anti-myc (1:100) with anti mouse FITC secondary antibody (1:100), on a group of cells, **b** shows the same group of cells immunostained with anti-hTRPC7 (1:100), **c** shows the merged image of **a** and **b**. **d**, **e** and **f** are the corresponding DIC images. All size bars 10μm.

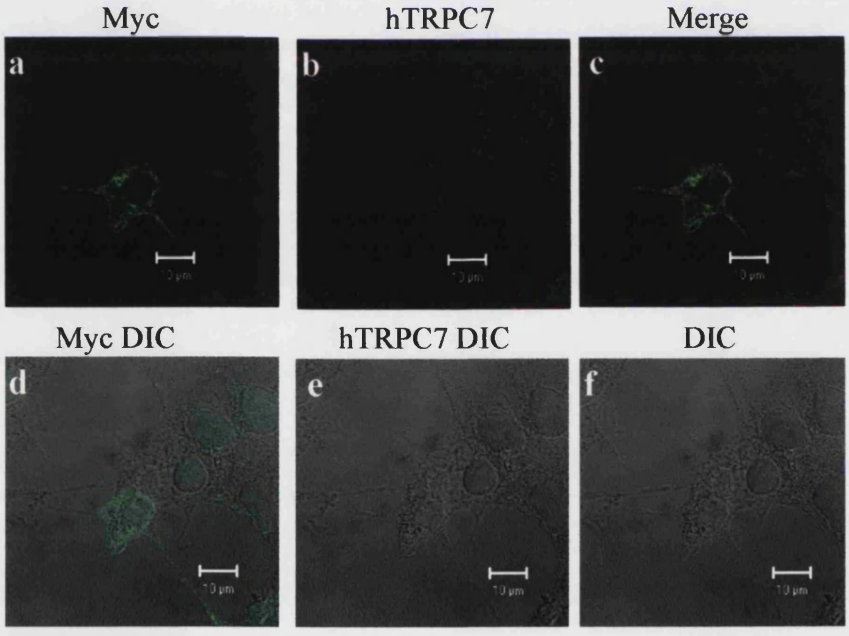

Figure 3.19: HEK293 cells transfected with Myc tagged *htrpc6*, **a** shows immunostaining by anti-Myc (1:100) with anti mouse FITC secondary antibody (1:100), on a group of cells, **b** shows the same group of cells immunostained with anti-hTRPC7 (1:100), **c** shows the merged image of **a** and b. **d**, **e** and **f** are the corresponding DIC images. All size bars 10μm.

Immunofluorescent staining by anti-hTRPC7 on cells transiently transfected with either *htrpc1*, *3* or *6* cDNAs showed no specific staining by anti-hTRPC7 indicating that anti-hTRPC7 did not cross react with other members of the TRPC subfamily. The images taken using the laser set to scan Alexa Fluor 488, were deliberately overexposed in order to confirm that there was no cross reaction between the TRPC sub-type and anti-hTRPC7 antibody.

3.3 - Discussion

A polyclonal antibody was raised in mice that displayed good specificity for the peptide antigen when tested by ELISA and immunocytochemistry (Figures 3.2, 3.3 and 3.4). Unfortunately monoclonal antibody production was unsuccessful (Figure 3.5). However, a rabbit polyclonal anti-hTRPC7 antibody was produced, purified and characterised in an over-expression system. It was shown to be specific for hTRPC7 and did not cross react with TRPCs 1, 3 and 6 (Figures 3.6 to 3.19).

The ELISAs carried out on peptide 7(K) coated 96 well plates showed high levels of hTRPC7 antibodies were produced by the two rabbits, 89 and 90 (Figures 3.6 and 3.8), this high titre continued in each test bleed sent and so rabbit 90 anti-hTRPC7 serum antibodies were purified. Purification was carried out using an affinity column coupled to peptide 7(K), there was no apparent loss of antibody specificity through this process, there was actually a gain in antibody specificity (Figure 3.10). However, not all the antibodies may have been retrieved from the serum. It is most likely that the column may have been over loaded and in future purifications could be performed with less serum diluted in PBS.

Characterisation of the antibodies took place using HEK293 cells transfected with the mammalian expression vectors pIRES-EGFP-*htrpc7* and pFLAG-*htrpc7*. Control transfections were carried out using an empty pIRES-EGFP vector, no vector or with expression of other TRPC proteins. Staining by the hTRPC7 antibody on pIRES-EGFP-*htrpc7* (Figure 3.11) and pFLAG-*htrpc7* (Figure 3.15) showed the hTRPC7 to be present on the PM region and possibly in the Golgi apparatus. Riccio *et al* (2002) have previously FLAG tagged the N-terminus of the hTRPC7 in order to visualise the protein by use of anti-FLAG antibody and stably expressed the protein in HEK293. They found that hTRPC7 was localised to the PM region (Riccio et al., 2002), which corresponds well with the results in the current study. Western blots carried out on the HEK293 cells over expressing pIRES-EGFP-*htrpc7* detected a band of approximately 100kD (Figure 3.16), which is close to the predicted molecular weight for hTRPC7 (99.6kD). The band

described was the most prominent on the blot and appeared first during development, other background bands developed later. This band was not present in any of the control lanes (non-transfected and vector only), probed with anti-hTRPC7 and was also not present on any of the control probed blots (pre-immune serum or the peptide control solution). A loading control (such as β-tubulin) was not used and may be advantageous here to demonstrate equal loading. Vector only transfection of the same amount of DNA as pIRES-EGFP-*htrpc7* was often less efficient, this was observed in immunocytochemistry experiments also. However this does not alter the conclusion that, the 100kD band seen in these experiments represented the over-expressed hTRPC7 and in conclusion the antibody is suitable for detecting hTRPC7 by Western blotting. Immunoprecipitation experiments have been carried out using the anti-hTRPC7 antibody; under the conditions used this was unsuccessful, and therefore the antibody may not suitable for immunoprecipitation experiments.

All immunocytochemistry of control transfections (Figures 3.12 to 3.14 and 3.17 to 3.19) were negative indicating that anti-hTRPC7 does not cross react with other TRPC proteins or other endogenous proteins in the HEK293 cell.

An antibody dilution of 1:100 was used for the immunocytochemistry despite the ELISAs displaying a high titre of antibody as the ELISA only showed the affinity of the antibody for the peptide it was raised against therefore it did not give any indication of affinity or avidity for the protein expressed in cells. Affinity is the measure of strength of the binding of an epitope to an antibody (Harlow and Lane; 1999). Avidity is the measure of overall stability of the complex between antibodies and antigens and is governed by three factors: affinity of an antibody for the epitope, valency of the antibody and antigen and geometric arrangement of interacting components (Harlow and Lane; 1999). Varying dilutions of antibody were tested by immunocytochemistry (results not shown) and 1:100 was found to give the best signal, this dilution was used for all subsequent immunocytochemistry with the anti-hTRPC7 antibody. For Western blotting it is common that a lower dilution of antibody is used to detect the protein of interest, this is because the protein is denatured and epitope exposed, therefore the affinity and avidity of

the antibody for the antigen is higher and less antibody is required (Harlow and Lane; 1999). It is for this reason that a 1:1000 dilution of the anti-hTRPC7 antibody was used on Western blots. However, background bands were apparent on the Western blots probed with the anti-hTRPC7 antibody, although cross-reactions by the secondary antibody can occur, giving background bands, it is common to have other bands present as well as the band of interest when using a polyclonal antibody. Polyclonal antibodies are a mixed population of antibodies raised to many different sites on the epitope (in this case the peptide) this mixed population of antibodies may recognise other antigens in the sample (to varying affinity and avidity) giving other bands of different molecular weights (Harlow and Lane; 1999). However, because the molecular weight of the protein of interest is known and interactions of the antibody with the protein of interest usually has the highest affinity and avidity, it is fair to conclude that the anti-hTRPC7 antibody is specific for hTRPC7 as shown by immunocytochemistry and reflected in the results from Western blotting.

The results presented in this chapter show that a specific antibody to hTRPC7 has been raised and characterised, in an over-expression system. The anti-hTRPC7 antibody was then used study the over-expression of the splice variant hTRPC7A (see Chapter 4) and the expression of endogenous TRPC7 (see Chapters 5, 6 and 7).

Chapter 4

Localisation and Functional Characterisation of hTRPC7 and Splice Variants in an Over Expression System

4.1 - Introduction

4.1.1 - Splice Variants of hTRPC7

hTRPC7 has four splice variants, in addition to the full-length version, termed hTRPC7A, hTRPC7B, hTRPC7γ and hTRPC7C. All are described in Section 1.6.2 of Chapter 1. The anti-hTRPC7 antibody produced and characterised in Chapter 3 was raised to the very C-terminus of full-length hTRPC7 and, based on sequence analysis, it should also recognise three of the four splice variants; hTRPC7A, hTRPC7B and hTRPC7γ. However, it was not expected to recognise hTRPC7C, as this protein is a highly truncated version of the protein that consists of the N-terminus only. Previously this type of protein has been shown to disrupt or suppress the expression of the full size form of the protein, for example co-expression of the archetypal TRP with an N-terminal fragment of itself led to suppression of protein function (Xu et al., 1997b). None of the hTRPC7 splice variants have been investigated for their expression, localisation or functional roles.

The COS7 cell line is a kidney fibroblast cell line from the African Green Monkey; the original cells were derived from CV-1 simian cells transformed by an origin-defective mutant of SV40 (ECACC). It has been found by RT-PCR that *trpc7* mRNA is endogenously expressed in COS7 cells (Riccio et al., 2002f) and further to this it has been found that the splice variant *trpc7C* mRNA is also expressed in COS7 cells along side the full-length *trpc7* (A. Wolstenholme, Unpublished data).

4.1.2 – Investigating Function

Many groups studying the functional roles of TRPC channels utilise HEK293 cells as they serve as an excellent heterologous expression system in which to study functional properties of recombinant TRP channels, due to the low endogenous activity of store operated CCE channels (Okada et al., 1998; Okada et al., 1999d). To investigate the hypothesis that TRPC proteins form putative Ca^{2+} entry channels, Ca^{2+} influx is usually measured using fluorescent Ca^{2+} indicators or by electrophysiological measurements of

transmembrane ion fluxes (Parekh and Penner, 1997; Putney, Jr., 2004; Zacharias et al., 2000).

4.1.3 – Functional Roles of hTRPC7

Using TG and OAG, it was concluded that mTRPC7 was a receptor-activated channel activated by OAG independently of the depletion of stores (Okada et al., 1999c). However, in contrast, using TG, Riccio et al deduced that hTRPC7 was a store-operated channel (Riccio et al., 2002e). Lievremont et al (2004) studied these conflicting reports in detail recently and they concluded that the reason for such a stark difference between the two previous studies was the expression levels of the protein (Lievremont et al., 2004c). By further experimentation they showed that transient transfections typically giving high expression levels of the protein and lead to the formation of a receptor activated channel, whereas a stable transfection with a lower expression level led to a store-operated channel (Lievremont et al., 2004b). A discussion of these studies is given in Section 1.6.5 of Chapter 1.

The experiments described in this chapter will involve a comparison of the localisation and function of over-expressed splice variant hTRPC7A compared to that of hTRPC7 in HEK293 cells. Also the localisation of endogenous hTRPC7 is probed in COS7 cells using the anti-hTRPC7 antibody and the identification of any changes in localisation when hTRPC7 and hTRPC7A are over expressed also using the anti-hTRPC7 antibody.

4.2 - Results

4.2.1 - Localisation of hTRPC7A

In order to compare the localisation and expression of hTRPC7 (previously shown in Chapter 3) and hTRPC7A in an over-expression system, pIRES-EGFP-*htrpc7A* (see Appendix section A1) was transiently transfected into HEK293 cells and immunocytochemical studies using the anti-hTRPC7 antibody, characterised in Chapter 3, were carried out. HEK293 cells positively transfected with pIRES-EGFP-*htrpc7A*, reacted to the anti-hTRPC7 antibody (Figure 4.1). Non-transfected cells in the culture did not display staining by the antibody and only a very low-level background fluorescence was observed. The hTRPC7A in positively transfected cells appeared to be at the PM region with a small amount of perinuclear staining. The over expression of hTRPC7A in HEK293 cells was similar to that of hTRPC7 in HEK293 cells (see Chapter 3). These images confirmed that anti-hTRPC7 did recognise hTRPC7A.

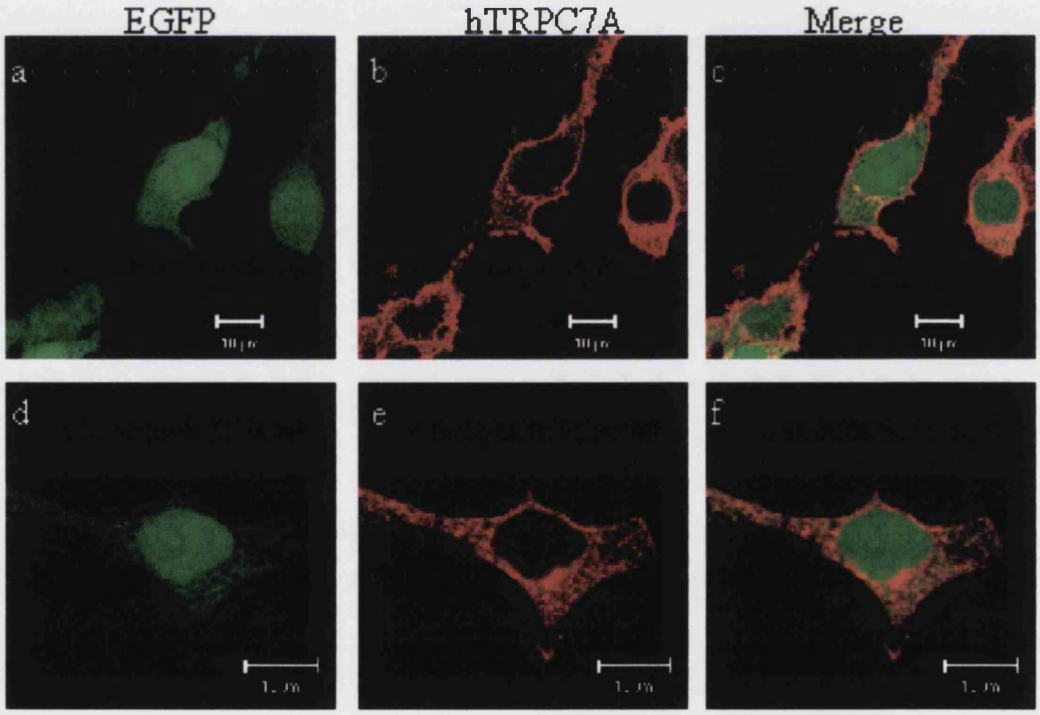

Figure 4.1: HEK293 cells expressing pIRES-EGFP-*htrpc7A*, image **a** and **d** show positive transfections, images **b** and **e** show the same cells as **a** and **d** respectively and show staining by anti-hTRPC7 (1:100), **c** and **f** are the merged images of **a** and **b; d** and **e;** respectively. All size bars 10μm.

Control staining was carried out on pIRES-EGFP-*htrpc7A* transfected HEK293 cells, by using pre-immune serum and peptide control solution (see Chapter 3, Section 3.2.7 for preparation).

HEK293 cells transiently transfected with pIRES-EGFP-*htrpc7A* were stained with the pre-immune serum (Figure 4.2a to c). The results showed that the staining pattern as those stained with the anti-hTRPC7 antibody did not occur, only low level background staining was apparent. Also, similarly transfected cells were incubated with the peptide control solution (Figure 4.2d to f): the results showed no specific staining confirming that the antibody to hTRPC7 is specific for the splice variant hTRPC7A as well as full-length hTRPC7.

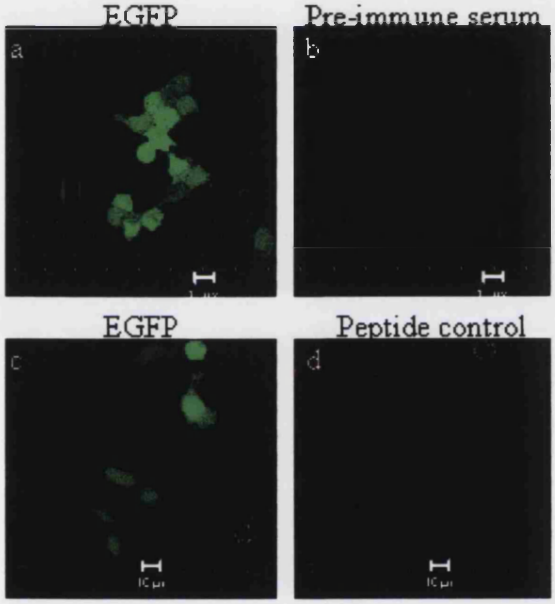

Figure 4.2: HEK293 cells expressing pIRES-EGFP-*htrpc7A*, images **a** and **c** show positive transfection, images **b** and **d** shows the same cells as **a** and **d** respectively, **b** is stained with pre-immune serum (1:100) and **d** is stained with peptide control solution. All size bars 10μm.

4.2.2 - Endogenous and Over-Expression of hTRPC7 in COS7 Cells

COS7 cells are known to endogenously express both hTRPC7 and hTRPC7C (A. Wolstenholme Unpublished data). Immunocytochemistry experiments were carried out to identify the localisation of endogenous hTRPC7 and to observe the effects of over-expressing hTRPC7 and hTRPC7A.

4.2.2.1 - Endogenous Expression of hTRPC7

Non-transfected COS7 cells were stained for hTRPC7 using the anti-hTRPC7 antibody to localise endogenous expression of hTRPC7.

Results showed a low-level of background stain (Figure 4.3a), this was not apparent in non-transfected cells stained with pre-immune serum (Figure 4.3b). These results suggest that the anti-hTRPC7 antibody could not detect the endogenous TRPC7 expressed by COS7 cells.

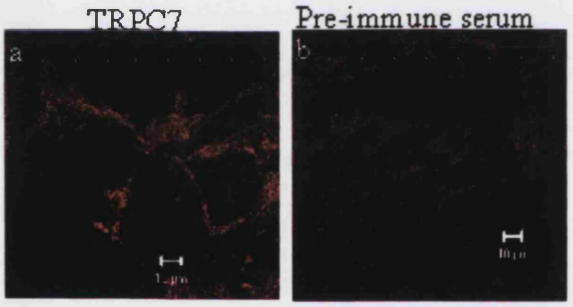

Figure 4.3: Non-transfected COS7 cells, image **a** shows immunofluorescent staining by anti-TRPC7 (1:100), **b** shows immunofluorescent staining by pre-immune serum (1:100). All size bars 10μm.

4.2.2.2 - Over-Expression of hTRPC7 in COS7 Cells

COS7 cells were then transiently transfected with pIRES-EGFP-*htrpc7* to observe the localisation of over-expressed hTRPC7.

COS7 cells transiently transfected with pIRES-EGFP-*htrpc7* and stained with anti-hTRPC7 shows bright, mainly intracellular staining with very little PM staining (Figure 4.4a to f). This was different to the localisation of over-expressed hTRPC7 in HEK293 cells where the staining was largely PM and only a small amount of intracellular localisation. When the control staining (pre-immune serum and peptide control solution) was carried out on the transfected COS7 cells there was no evidence of specific staining however, there was background staining in both cases (Figure 4.4g and h).

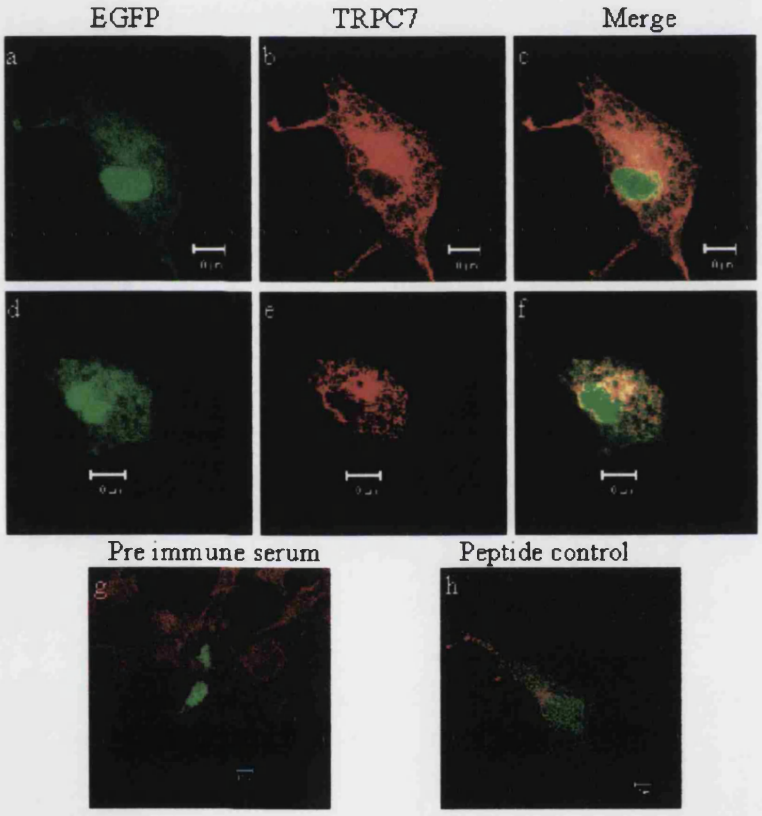

Figure 4.4: Immunofluorescent staining in COS7 cells transfected with pIRES2-EGFP-*htrpc7*. Images **a** and **d** shows positive transfections, images **b** and **e** are the same cells as **a** and **d** respectively and show staining by anti-hTRPC7 (1:100). Images **c** and **f** are the merged images of **a** and **b**; **c** and **d** respectively. Images **g** and **h** show merged images of positively transfected COS7 cells stained with pre-immune serum (1:100) and peptide control solution respectively. Size bars 10μm.

4.2.2.3 - Over-Expression of hTRPC7A in COS7 Cells

The over-expression of hTRPC7A in COS7 cells was carried out to observe differences in localisation of hTRPC7A compared to over-expressed hTRPC7 in COS7 cells. COS7 cells transiently transfected with pIRES-EGFP-*htrpc7A* (Figure 4.5a to f) showed a predominantly intracellular localisation of hTRPC7A with very little PM expression this staining was absent when cells were treated with pre-immune serum or peptide control solution, both controls gave a high level of background staining (Figure 4.5g and h). The pattern of staining was not dissimilar to that of hTRPC7 over-expressed in COS7 cells (Figure 4.4) however, it was different from the pattern of staining of hTRPC7A over-expressed in HEK293 cells, where there is very little intracellular staining and mainly PM region localisation of hTRPC7A (Figure 4.1).

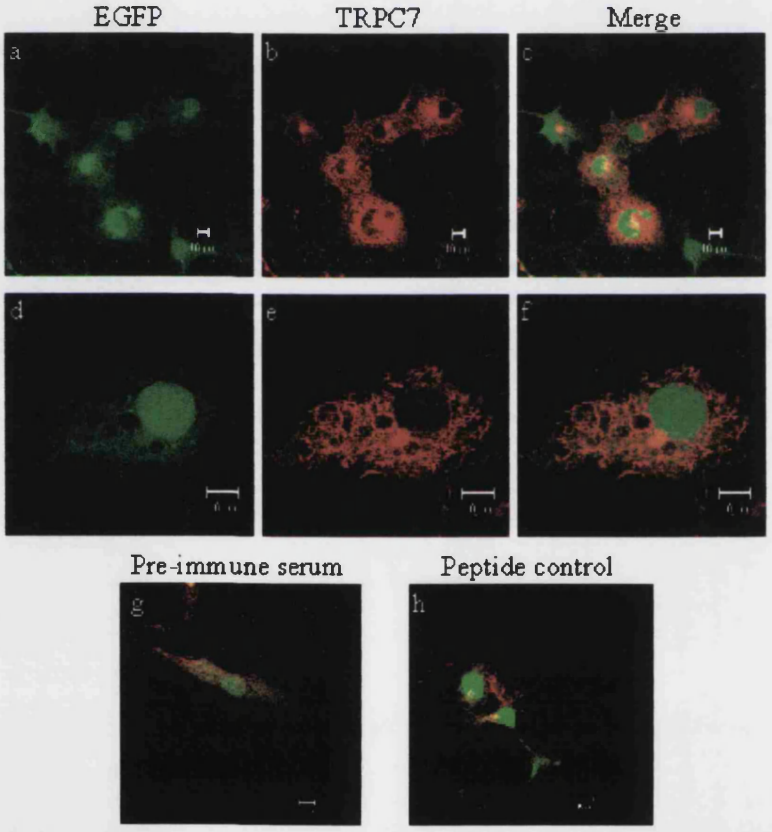

Figure 4.5: Immunofluorescent staining in COS7 cells transfected with pIRES2-EGFP-*htrpc7A*. Images **a** and **d** shows positive transfections, images **b** and **e** are the same cells as **a** and **d** respectively and show staining by anti-hTRPC7 (1:100). Images **c** and **f** are the merged images of **a** and **b**; **c** and **d** respectively. Images **g** and **h** show merged images of positively transfected COS7 cells stained with pre-immune serum (1:100) and peptide control solution respectively. Size bars 10μm.

4.2.3 - Functional Characterisation of hTRPC7 and hTRPC7A

Having found no apparent difference between the intracellular localisation of over-expressed hTRPC7 and hTRPC7A, it was important to find if there was any functional difference between the two proteins. Therefore, functional experiments were carried out to assess any differences between full-length hTRPC7 and hTRPC7A. These were carried out by a Ca^{2+} re-addition protocol involving either CPA (SERCA pump inhibitor (Goeger et al., 1988) or OAG (analogue of DAG).

4.2.3.1 - SOC Activity of hTRPC7 and hTRPC7A

Previous experiments have indicated that mTRPC7 may be a receptor-activated channel (Okada et al., 1999b) and that hTRPC7 may be a store-operated channel (Riccio et al., 2002d), or both depending on the level of expression (Lievremont et al., 2004a). Previous data from our laboratory has not agreed with the findings of Riccio et al but suggested that hTRPC7 may be a receptor-activated like its mouse homologue (H. Aptel Unpublished Data). It was found that when a Ca^{2+} re-addition protocol was carried out in the presence of 10μM CPA there was no increase in size of releasable stores in cells that over-expressed hTRPC7 in comparison to a vector only control, indeed there was a reduction in the size of releasable stores (H. Aptel Unpublished Data).

The current study involved the same experimental protocol of Ca^{2+} re-addition in the presence of 10μM CPA, the responses of cells with hTRPC7A over-expression will be compared to cells over-expressing hTRPC7 and a vector only control. Previously, higher concentrations of CPA (50μM and 100μM) have been tested in a Ca^{2+} re-addition protocol carried out on hTRPC7 over-expressing HEK293 cells, however no difference was observed between the three concentrations of CPA (results not shown). It was therefore decided to use 10μM CPA.

The graph in Figure 4.9 represents the mean results from Ca^{2+} re-addition experiments on HEK293 cells over-expressing hTRPC7 (6 experiments; approximately 42 transfected cells), hTRPC7A (5 experiments; approximately 51 transfected cells) or the vector alone (4 experiments; approximately 20 transfected cells). Comparing all experiments shows

that the size of the store release peak (first peak) in each experiment was larger or the approximately the same size as that of the Ca^{2+} influx peak (second peak) of the same experiment. Also the store release peak in the vector alone trace was larger than the equivalent peaks in both hTRPC7 and hTRPC7A traces, this indicated that the Ca^{2+} store was larger in the vector only control. The trace generated by the vector only transfected experiments showed a slightly larger peak of Ca^{2+} influx in comparison to hTRPC7 and hTRPC7A, and in addition hTRPC7 and hTRPC7A appeared to have a slower rate of Ca^{2+} influx than the vector only control. The opposite would be expected if hTRPC7 and hTRPC7A were SOCs.

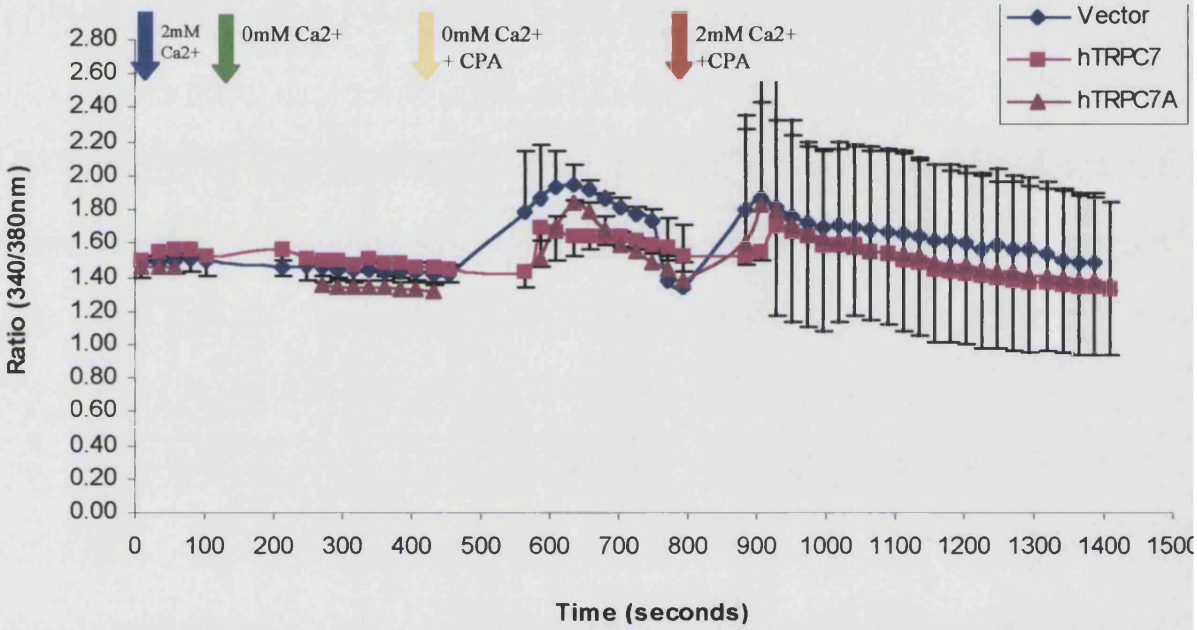

Figure 4.9: Ca^{2+} re-addition protocol using 10μM CPA carried out on HEK293 cells over-expressing hTRPC7 (n=6 experiments, approximately 42 cells) and hTRPC7A (n=5 experiments, approximately 51 cells) with a vector only transfected control (n=4 experiments, approximately 20 cells). Error bars are SEM of each experiment. Some of these data were generated with the kind help of Dr A Rogers.

4.2.3.2 - Statistical Analysis

In order to get an accurate comparison of the function of vector only control, hTRPC7 and hTRPC7A when over-expressed and the Ca^{2+} re-addition protocol applied in the presence of 10μM CPA, statistical analysis was carried out comparing the amount of Ca^{2+} influx after addition of CPA in the presence of Ca^{2+}. The amount of Ca^{2+} influx (ratio

values) after addition of CPA was found by calculating the area under each peak after time point 800 seconds (addition of CPA) until the end of the experiment, data summarised in Table 4.1 and Figure 4.10.

	Amount of Ca^{2+} Influx (340/380nm); μ	**Standard Deviation (s)**	**Number of Experiments (n)**
Vector (V)	41.55	0.11	4
hTRPC7 (7)	36.83	0.12	6
hTRPC7A (7A)	38.01	0.13	5

Table 4.1: Summary of the amount of Ca^{2+} influx after addition of 10μM CPA of HEK293 cells transfected with vector only, pIRES-EGFP-*htrpc7* or pIRES-EGFP-*htrpc7A*

Figure 4.10: Bar graph summarising the data in table 4.1; showing the average amount of Ca^{2+} influx (Ratio values) gained from stimulation by 10μM CPA. Error bars are standard deviation of each experiment.

Calculations for the t-test were carried out for $\mu_V = \mu_7$, $\mu_V = \mu_{7A}$ and $\mu_7 = \mu_{7A}$ however, there was no significant difference of the amount of Ca^{2+} influx as a result of 10μM CPA stimulation between hTRPC7 and hTRPC7A expressing cells however there was significantly more influx in the vector only controls.

t-test for $\mu_7 = \mu_{7A}$:

1. Over all estimate of variance (s^2):

$s^2 = [(n_7-1) * s_7^2 + (n_{7A}-1) * s_{7A}^2] / (n_7 + n_{7A} - 2)$

$s^2 = [(6-1) * 0.013 + (5-1) * 0.018] / (6 + 5 - 2)$

$s^2 = 0.015$

2. Standard error (SE) of the difference between the sample means:

$SE(\mu_7 - \mu_{7A}) = \sqrt{s^2} * (1/n_7 + 1/n_{7A})$

$SE(\mu_7 - \mu_{7A}) = \sqrt{0.015} * (1/6 + 1/5)$

$SE(\mu_7 - \mu_{7A}) = 0.045$

3. Test statistic (t_s):

$t_s = (\mu_7 - \mu_{7A}) / SE(\mu_7 - \mu_{7A})$

$t_s = (0.54 - 1.10) / 0.51$

$t_s = -26.26$

$\mu_7 = \mu_{7A}$

$t_s = -26.26$ Comparing this value with critical values of 't' (t_α) for 9 degrees of freedom (3 + 2 – 2) at P = 0.05, $t_s < t_\alpha$. Therefore the average amount of Ca^{2+} influx induced by 10μM CPA between 821.7 and 890.5 seconds of experimental recording is not significantly different between *htrpc7* and *htrpc7A* expressing cells.

4.2.3.3 - RACC Activity of hTRPC7 and hTRPC7A

Okada et al (1999) have shown that mTRPC7 is activated by DAG analogues OAG and DOG, concluding that mTRPC7 may be a receptor-activated channel. DAG is thought to directly activate the TRPC channel following stimulation of a receptor (Okada et al., 1999e) or regulate activation of the channel via activation of PKC (Spassova et al., 2004). However, Riccio et al did not perform experiments on hTRPC7 with OAG, they concluded that, following experiments with the SERCA pump inhibitor, TG, that hTRPC7 is a store-operated channel (Riccio et al., 2002c). However, as previously

discussed, Lievremont et al (2004) confirmed the findings from both groups citing protein expression levels as the explanation for the discrepancy.

The current study involved, for consistency sake, the Ca^{2+} re-addition protocol in the presence of 100μM OAG however there was not expected to be a Ca^{2+} release peak as OAG was supposed to act directly upon the Ca^{2+} influx channel. This was applied to HEK293 cells expressing the vector only, hTRPC7 and hTRPC7A.

The graph in Figure 4.11 represents the mean results from Ca^{2+} re-addition experiments on HEK293 cells over-expressing hTRPC7 (3 experiments; approximately 25 transfected cells), hTRPC7A (3 experiments; approximately 30 transfected cells) or the vector alone (2 experiments; approximately 20 transfected cells). The peaks observed from all traces indicated activation of channels by OAG to different extents, channels in the vector only control are activated and allow the influx of more Ca^{2+} than the HEK293 cells expressing hTRPC7 (shown by the height of the peak), whereas cells expressing hTRPC7A are activated and allow more Ca^{2+} entry than vector and hTRPC7 transfected HEK293 cells. This indicated that OAG may not have activated hTRPC7 but did activate hTRPC7A, but statistical analysis was required to assess this observation (see Section 4.2.3.4 below). In addition a decrease in activity was noted in cells over-expressing hTRPC7 and hTRPC7A when the cells were placed in Ca^{2+} free medium after the baseline recording, this indicated that they have constitutive activity, as previously reported in cells over-expressing mTRPC7 and hTRPC7 (Okada et al., 1999a; Riccio et al., 2002b).

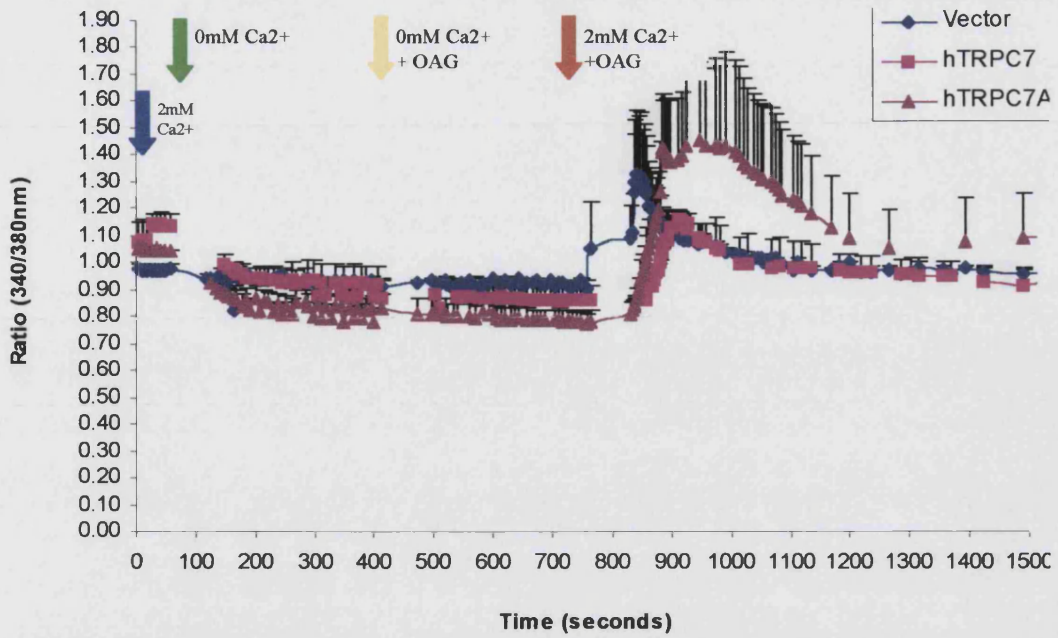

Figure 4.11: Ca^{2+} re-addition protocol using 100μM OAG carried out on HEK293 cells over-expressing hTRPC7 (n=3 experiments) and hTRPC7A (n=2 experiment) with a vector only transfected control (n=2 experiments). Error bars are SEM.

4.2.3.4 - Analysis

In order to compare of the function of vector only control, hTRPC7 and hTRPC7A when over-expressed and the Ca^{2+} re-addition protocol applied in the presence of 100μM OAG, statistical analysis was carried out comparing the amount of Ca^{2+} influx after addition of OAG. The amount of Ca^{2+} influx (ratio values) after addition of OAG in the presence of Ca^{2+} was found by calculating the area under each peak after time point 700 seconds (addition of CPA) until the end of the experiment, data summarised in Table 4.2 and Figure 4.12.

	Amount of Ca^{2+} Influx (340/380nm)	Standard Deviation	Number of Experiments
Vector (V)	86.02	0.09	2
hTRPC7 (7)	81.61	0.08	3
hTRPC7A (7A)	97.58	0.2	3

Table 4.2: Summary of average Ca^{2+} influx values gained from the stimulation by 100μM OAG of HEK293 cells transfected with vector only, pIRES-EGFP-*htrpc7* or pIRES-EGFP-*htrpc7A*.

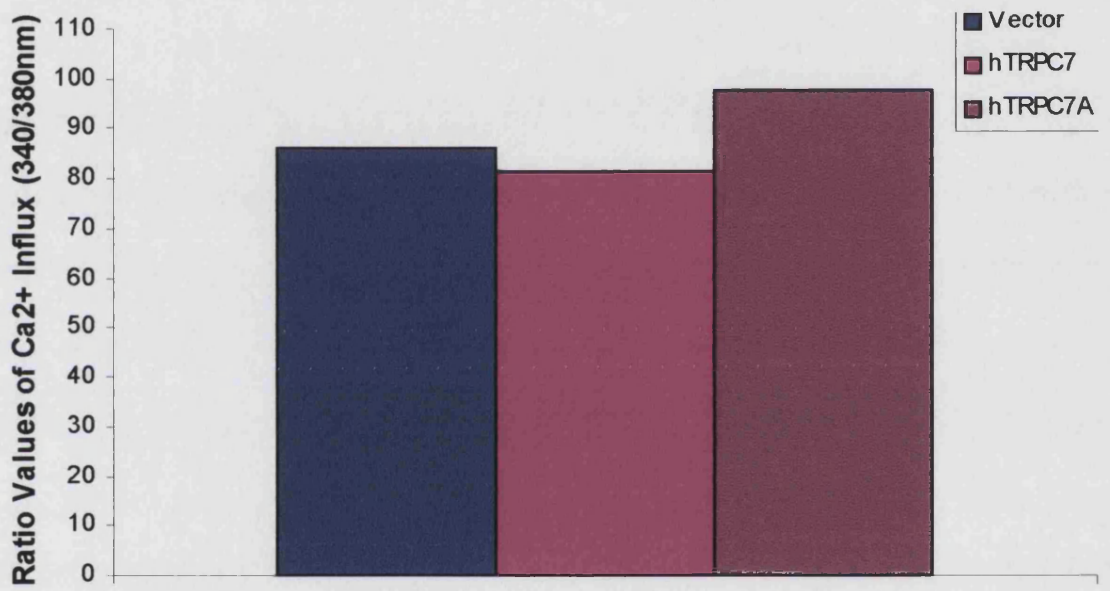

Figure 4.12: Bar graph showing the amount of Ca^{2+} influx (Ratio values of Ca^{2+} influx) between time points 764.1 and 861.4 seconds after stimulation by 100μM OAG. Error bars are SEM.

Unfortunately due to limited resources it was not possible to increase the number of experiments for this section, therefore, because of the small data set in each experiment it was not possible to carry out any statistical analysis for these experiments.

4.3 - Discussion

4.3.1 - Localisation of Over-Expressed hTRPC7 and hTRPC7A in HEK293 Cells

The splice form of hTRPC7, hTRPC7A has a small deletion of nucleotides that leads to a small deletion of amino acids in the N-terminal region, there is no frame-shift of nucleotides and the rest of the sequence remains homologous to the full-length version (Murphy, Unpublished data). Therefore, as the anti-hTRPC7 antibody was raised to the very C-terminus of hTRPC7 it was expected to detect hTRPC7A. Over-expression of hTRPC7A in HEK293 cells has shown very similar staining to full-length hTRPC7 when detected with the anti-hTRPC7 antibody (Figure 4.1). The pattern of staining was predominantly PM with a small area of perinuclear staining; again this may indicate Golgi localisation of hTRPC7A when over-expressed. Control staining by pre-immune serum and peptide control solution gave no specific staining pattern, only low-level background staining was observed (Figure 4.1). These results indicate that the anti-hTRPC7 antibody recognised over-expressed hTRPC7A and over-expressed hTRPC7A has an apparently identical subcellular localisation pattern to full-length hTRPC7 when over-expressed in HEK293 cells.

4.3.2 - Localisation of Over-Expressed hTRPC7 and hTRPC7A in COS7 Cells

COS7 cells express endogenous *trpc7* and *trpc7C*, however when non-transfected COS7 cells were stained using the hTRPC7 antibody (Figure 4.3) an intracellular pattern of mitochondrial-like staining is observed. It may be that there was no protein for the antibody to identify and as such targets the mitochondria (this as well as nuclear or nucleolar staining can be a common phenomenon where antibodies cannot find their specific targets). Immunofluorescent staining carried out on COS7 cells over expressing pIRES-EGFP-*htrpc7* with the antibody to hTRPC7 (Figure 4.4) showed a large amount of intracellular staining with relatively little PM staining in comparison to the HEK293

cells (Chapter 3). COS7 cells transfected with pIRES-EGFP-*htrpc7A* (Figure 4.5) showed the localisation of hTRPC7A to be predominantly intracellular with very little PM region staining, again this is very similar to the full-length hTRPC7 expressed in COS7 cells (Figure 4.4), and also in contrast to HEK293 cells over-expression hTRPC7A (Chapter 3). It is well known that COS7 cells are not efficient at processing and inserting membrane proteins and in this case may not be an adequate over-expression system. Western blots carried out on COS7 cells showed many contaminating, background bands especially one at 100kD in all samples run, including non-transfected and vector only transfected controls (results not shown). These results indicate that the antibody was not able to detect endogenous TRPC7 in COS7 cells, suggesting that the protein is expressed at very low levels if at all despite the high level of *trpc7* mRNA detected by RT-PCR (Riccio et al., 2002a); A. Wolstenholme Unpublished data).

An explanation for the apparent lack of endogenous staining in COS7 cells and the apparently suppressed expression of hTRPC7 and hTRPC7A when co-transfected into HEK293 cells may be that the *htrpc7C* splice variant is an N-terminal dominant negative protein, and thus prevents the expression of the full length TRPC7. Dominant negative N-terminal fragments are a common phenomenon and has previously been observed in other TRP proteins. For example, it was first observed in the archetypal TRP and TRPL originally used as a tool to study N-terminal interactions when Xu et al co-expressed full length TRP or TRPL with N terminal fragments of TRP or TRPL, it was found that the interaction of the N-terminal fragments with the full length versions dominantly suppressed the function of TRP. However at the time localisation experiments were not carried out so it is unknown whether this interaction prohibited channel formation and membrane insertion (Xu et al., 1997a). It is possible that a similar disruption happens in COS7 cells with TRPC7 and TRPC7C and, although over expression of the full length hTRPC7 is not greatly affected by endogenous TRPC7C, the localisation may have been changed.

4.3.3 - Function of Over-Expressed hTRPC7 and hTRPC7A in HEK293 Cells

HEK293 cells transfected with the *htrpc7*, *htrpc7A* and the vector only were subjected to the Ca^{2+} re-addition protocol with 10μM CPA. The data generated (Figure 4.6) indicated that, when stimulated with 10μM CPA in the absence of Ca^{2+}, the stores of Ca^{2+} were released. The sizes of these first peaks gave an indication of the sizes of the Ca^{2+} stores and demonstrated that the vector only transfected HEK293 cells have larger intracellular stores than hTRPC7 and hTRPC7A over-expressing cells, this has been seen previously in a comparison of *htrpc7* and vector only transfected cells (H. Aptel Unpublished Data). Statistical analysis of the Ca^{2+} influx peaks have shown no significant difference between the cells over-expressing hTRPC7 and hTRPC7A groups, however cells expressing the vector alone had a significantly more Ca^{2+} influx. This indicated that hTRPC7 and hTRPC7A did not function as store-operated channels under these conditions.

The Ca^{2+} re-addition protocol was also applied to HEK293 cells over-expressing hTRPC7 or hTRPC7A using 100μM OAG to stimulate the influx of Ca^{2+}. The data obtained (Figure 4.11) showed no Ca^{2+} release peak, as OAG does not stimulate the release of Ca^{2+} from the stores, instead it directly stimulates the ion channel to allow the influx of Ca^{2+}. This is demonstrated by the large peaks seen when 100μM OAG is added in the presence of Ca^{2+}. Due to the small number of experiments for this test it was not possible to carry out statistical analysis. However, the preliminary data (Figures 4.11 and 4.12) suggests that cells over-expressing hTRPC7A may allow more entry of Ca^{2+} than cells over-expressing hTRPC7, this may indicate that hTRPC7A at least may be a receptor-activated channel. However, the trace obtained from the vector only transfected cells appears to be anomalous as it does not mirror those given by hTRPC7 and hTRPC7A, the trace appears to spike very quickly when cells were administered with OAG in the presence of Ca^{2+}, it is therefore difficult to give an accurate interpretation of these results in the absence of an adequate control. The experiments could be repeated again as readings may be found to be significantly different between vector only and hTRPC7 and hTRPC7A. However, further controls need to be carried out in order to fully assess and back up the preliminary results presented here. Are the same amounts of

hTRPC7 and hTRPC7A expressed? Immunocytochemistry carried out on HEK293 under the same conditions suggested that similar amounts of the two proteins are expressed however, Western blotting should be carried out to confirm this.

There were some draw backs to the system used to generate these results, Fura 2-AM, the Ca^{2+} indicator dye and EGFP, the marker for positive transfection have a very similar emission frequency (Figure 4.13 and 4.14) and may have led to a distortion of results by EGFP interfering with the signal generated by Fura 2-AM. Due to the limitations of the system used it was not possible to use a different Ca^{2+} indicator dye or a different marker for positive transfection.

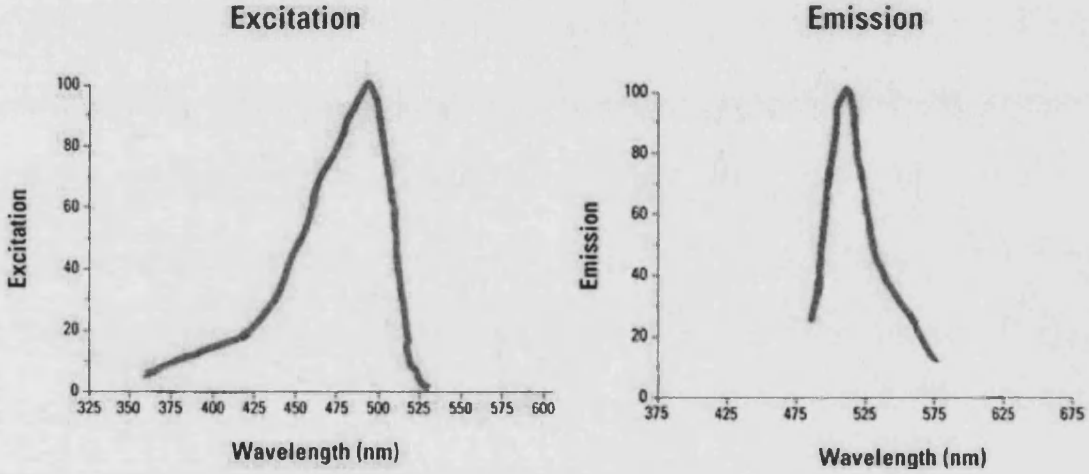

Figure 4.13: Excitation and emission frequencies of GFP (Molecular Probes).

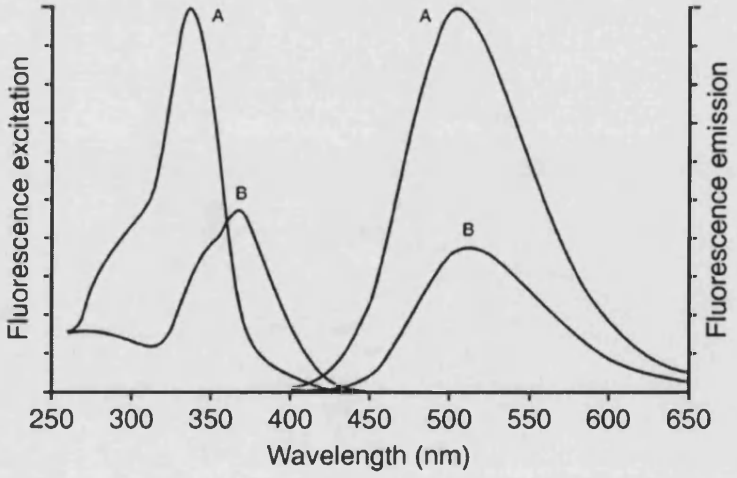

Figure 4.14: Excitation and emission frequencies of Fura 2-AM, A refers to free Fura 2-AM, B refers to bound Fura 2-AM (Calbiochem).

Another limitation may be that Ca^{2+} rather than Ba^{2+} was used to assess channel activation. The use of Ca^{2+} can lead to the wrong conclusion that a channel is store-operated because the cell may lack the ability of the ER to buffer Ca^{2+} entering through the channels, due to irreversible block of SERCA produced by TG (Trebak et al., 2002a; Trebak et al., 2003a). This can exaggerate constitutive calcium entry occurring through ion channels expressed in living cells (Trebak et al., 2002b; Trebak et al., 2003b). The variable nature of the HEK293 cells, made obtaining reliable functional and calibration results difficult, therefore calibration of the functional experiments was not carried out. The choice of indicator dye used, Fura 2-AM meant it was not necessary to calibrate as the measured Ca^{2+} was independent of dye concentrations, as discussed in the introduction to this chapter (Tepikin, 2000). However, for future experiments it may be beneficial to calibrate the data in order to assess how much Ca^{2+} is being allowed in by the channels.

In conclusion, it has been demonstrated that the anti-hTRPC7 antibody, characterised in Chapter 3 recognised both hTRPC7 and hTRPC7A. Localisation studies have shown that both hTRPC7 and hTRPC7A have a similar pattern of localisation when over-expressed in HEK293 cells; predominantly PM with a small region of peri-nuclear localisation. However, endogenous expression of hTRPC7 in COS7 cells was not detected using the anti-hTRPC7 antibody and when over-expressed, hTRPC7 had a different localisation in COS7 cells compared to over-expression of the protein in HEK293 cells. This poses the question; does hTRPC7C have a role in hTRPC7 localisation? Functional experiments carried out on hTRPC7 and hTRPC7A over-expressing HEK293 cells has shown that hTRPC7 and hTRPC7A are probably not store-operated channels.

Chapter 5

Endogenous Expression of TRPC7 in the Exocrine Pancreas

5.1 - Introduction

The pancreas is made up of two types of tissue, exocrine and endocrine. The endocrine portion of the pancreas is known as the Islets of Langerhans and makes up 2% of the total pancreatic mass (Berne and Levy, 1998a). The cells of the Islets of Langerhans secrete the hormones insulin, glucagon, somatostatin and pancreatic polypeptide (Berne and Levy, 1998b). Insulin and glucagon are the major hormones; insulin is secreted by the β cells, which comprise 60 to 70% of the Islets, glucagon is secreted by the α cells, which comprise 20 to 25% of the Islets (Berne and Levy, 1998b). Together they co-ordinate the flow and metabolic fate of endogenous glucose, free fatty acids, amino acids and other substrates to ensure the energy needs are met in the basal state and during exercise (Berne and Levy, 1998b). The main function of the exocrine pancreas is to produce the pancreatic juices that enter the digestive system at the duodenum and aid digestion (Berne and Levy, 1998a). Each part of the pancreas (exocrine and endocrine) is supplied by separate capillary networks (Berne and Levy, 1998a). The exocrine pancreas contains many blind-ended tubules that are surrounded by polygonal acinar cells, they are organised into lobules (acini) and the primary function of the acini is to secrete the enzyme component of the pancreatic juice (Berne and Levy, 1998a).

There are immortalised cell lines available to study the function of pancreatic cells, two of which were used in the present study, namely Panc-1 and Capan-1. These cell lines are both human pancreatic cell lines in origin and they are both adherent and epithelial in morphology. The Panc-1 cell line originates from a ductal carcinoma of the pancreas and the Capan-1 cell line is from a metastatic site of liver adenocarcinoma in the pancreas (ATCC, ECACC).

Previously in our laboratory studies of human tissue probed by Northern blotting showed relatively high levels of hTRPC7 mRNA in the pancreas (Chen, Unpublished Data; see Chapter 1, Figure 1.16). In this chapter the hTRPC7 antibody (characterised in Chapter 3) was used to identify the expression and localisation of hTRPC7 in the two pancreatic cell

lines described above and primary human pancreatic tissue. Further to this, the presence of TRPC7 in mouse pancreatic tissue was identified by use of the antibody.

5.2 - Results

5.2.1 - hTRPC7 Expression in Panc-1 Cells

Immuno-localisation of hTRPC7 in Panc-1 cells displayed a specific punctiform pattern of staining (Figure 5.1), which appeared to be localised to the periphery of the cells and on the protrusions extended by the cells, but with no apparent staining of any intracellular organelles. No specific staining pattern was observed when using the pre-immune serum or peptide control solution (Figure 5.1) indicating that anti-hTRPC7 was specific for endogenous hTRPC7 expressed by the Panc-1 cells.

Figure 5.1: Image **a** shows a group of Panc-1 cells immunostained with the anti-hTRPC7 antibody (1:100), **b** shows Panc-1 cells immunostained using the pre-immune serum (1:100), and **c** shows a group of Panc-1 cells stained by the peptide control solution, anti-rabbit FITC (1:100) was used as the secondaryantibody in all cases. All size bars are 10µm.

Panc-1 cells were immuno-stained using the anti-hTRPC7 antibody and anti-β-tubulin antibodies. The anti-β-tubulin was used as a general cell marker, it localises to the cytoskeletal protein tubulin, which is expressed in many cell types. In Panc-1 cells tubulin appears as fine intracellular filaments, some of which appear to lead to the cellular protrusions expressing hTRPC7 (Figure 5.2).

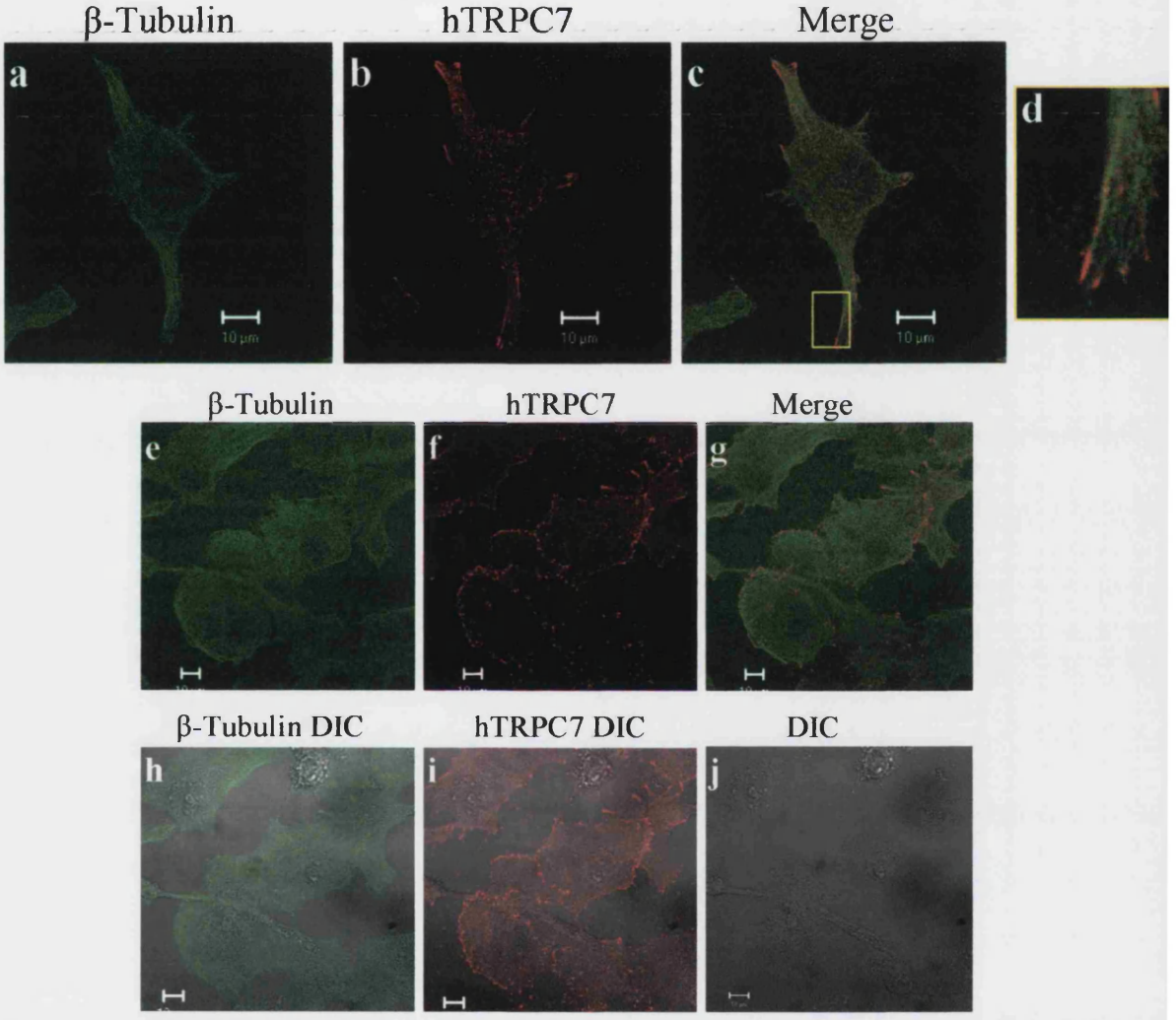

Figure 5.2: Image **a** and **e** show immunostaining by β-Tubulin (1:200) with anti-mouse FITC (1:100) secondary, **b** and **f** show staining by anti-hTRPC7 (1:100). **c** and **g** are the merged imaged of **a** and **b**; **e** and **f** respectively. **d** is the magnified image of the boxed area in **c**. **h, i** and **j** are corresponding DIC images of **e, f** and **g**. All size bars 10μm.

Panc-1 cells stained with anti-hTRPC7 were z-sectioned at 0.63μm intervals using the confocal microscope, from the base of the cells to the top of the cells (Figure 5.3). The sections show that hTRPC7 expression is mainly restricted to the basal membrane of the Panc-1 cell, where the cell adheres to the extracellular matrix, in this case the glass coverslip.

Figure 5.3 (opposite): z-sections of Panc-1, the sections run from the basal membrane (**a**) to the apical membrane (**t**) the cells were stained with anti-hTRPC7 (1:100).

Basal Membrane

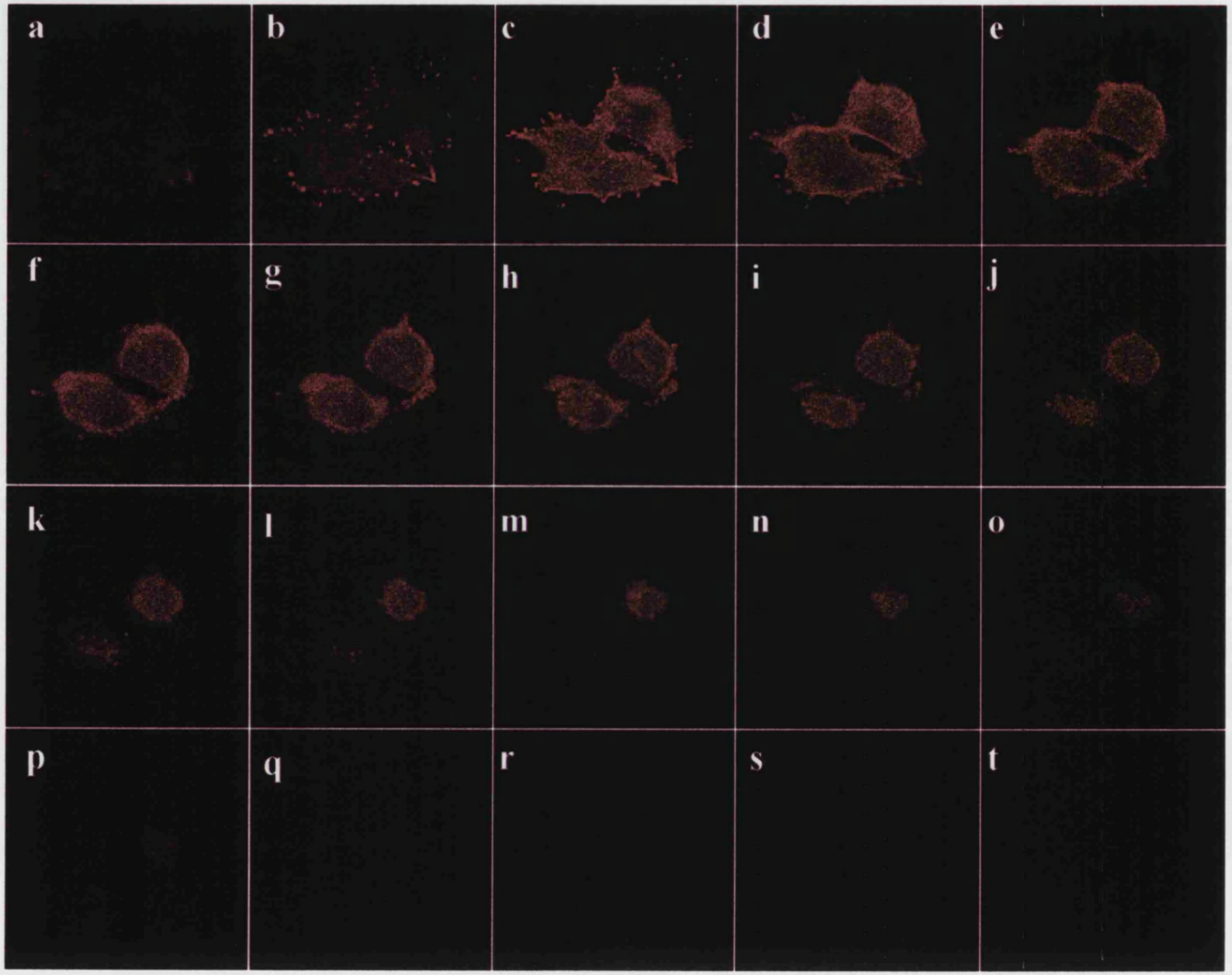

Apical Membrane

Panc-1 cells were also immuno-stained for hTRPC7 and F-actin. Phalloidin, here conjugated to rhodamine, was used as a general marker for the cytoskeletal protein F-actin. Some F-actin was observed at the periphery of the cell where it appeared to co-localise with hTRPC7, indicated by the arrows (Figure 5.4).

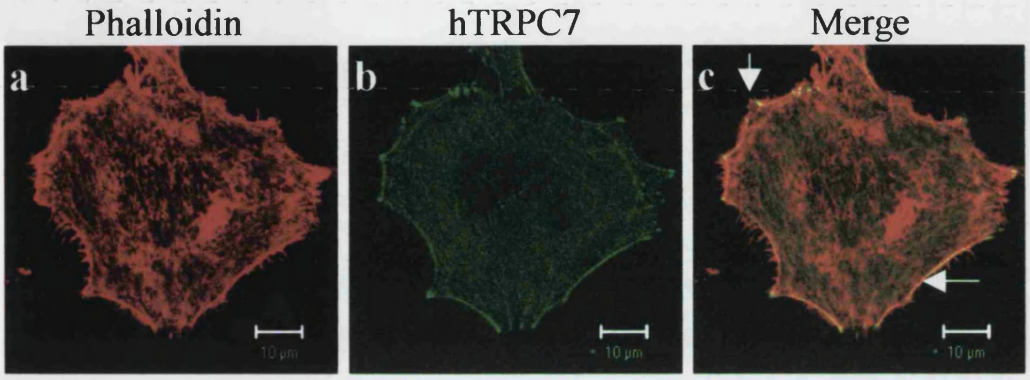

Figure 5.4: Image **a** Panc-1 immunostained with Rhodamine conjugated Phalloidin (1:500), image **b** is the same cell as **a** stained with anti-hTRPC7 (1:100), **c** is the merged image of **a** and **b**. All size bars are 10µm.

5.2.2 - hTRPC7 Co-localises with Focal Adhesion Kinase (FAK)

The staining pattern of hTRPC7 in Panc-1 cells (Figure 5.1, 5.3 and 5.4) was highly reminiscent of staining by focal adhesion markers in other cell types. Therefore Panc-1 cells were stained for both hTRPC7 and FAK (Figure 5.5). FAK is a focal adhesion molecule, involved in the formation of focal adhesion complexes in many cell types. The images show complete co-localisation of hTRPC7 and FAK.

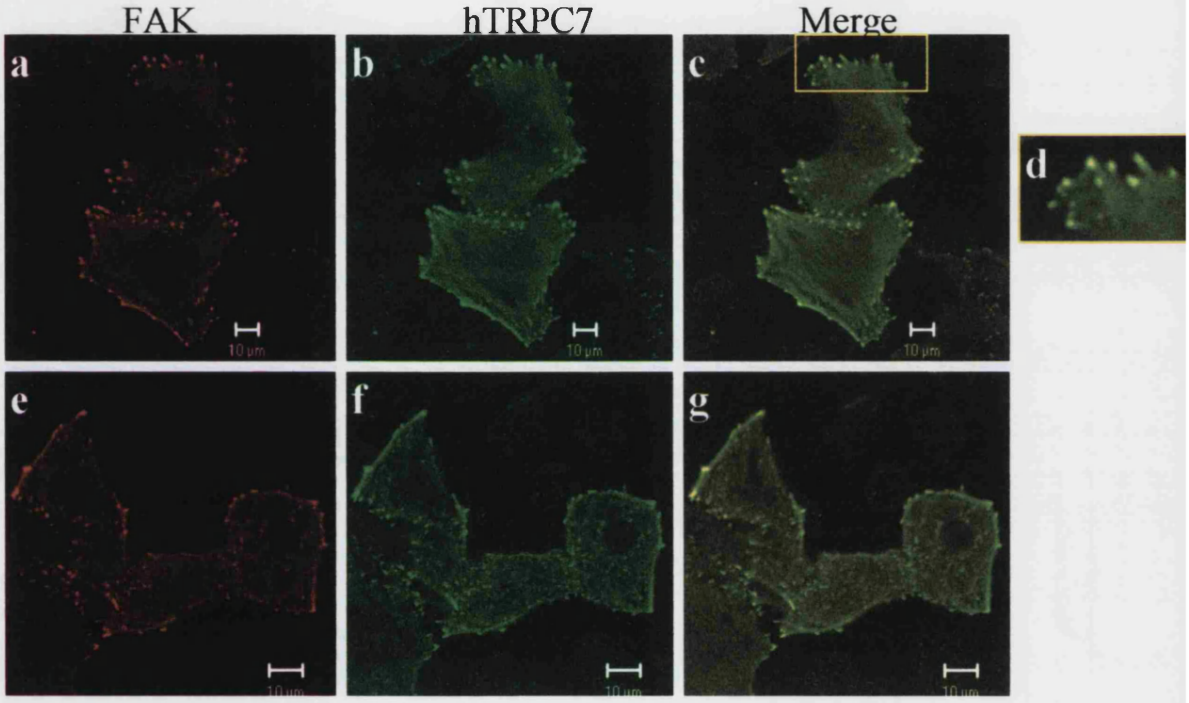

Figure 5.5: Images **a** and **e** stained with anti-focal adhesion kinase (FAK; 1:50) with anti-mouse IgG conjugated Alexa Fluor 568 secondary. Images **b** and **f** stained with anti-hTRPC7 (1:100) with anti-rabbit IgG conjugated Alexa Fluor 546 secondary, **c** and **g** are merged images of **a** and **b**; **e** and **f** respectively. **d** is a magnified image of the boxed area in image **c**. All size bars are 10µm.

5.2.3 - hTRPC7 Expression in Capan-1 Cells

The second pancreatic cell line used in this study was Capan-1. The staining pattern given by anti-hTRPC7 in Capan-1 cells (Figure 5.6) was similar to that seen in Panc-1 cells where hTRPC7 localised predominantly to protrusions on the basal PM. However, Capan-1 cells grow in clusters and not every cell in the cluster appeared to express hTRPC7. Mainly it was the cells at the periphery of the clusters that expressed hTRPC7 and in these cells the protein was more prominent on the protrusions produced by the cells. Neither the pre-immune serum nor peptide control solution gave the specific staining pattern seen by the hTRPC7 antibody (Figure 5.6). This indicated that anti-hTRPC7 may be specific for endogenous hTRPC7 expressed by the Capan-1 cells.

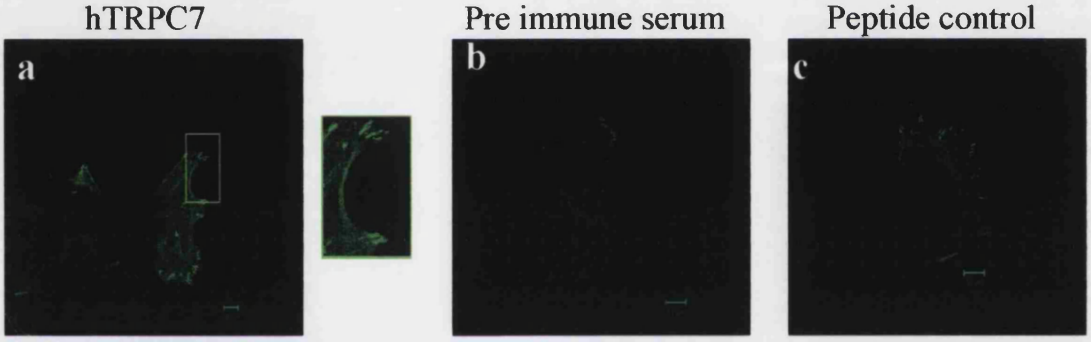

Figure 5.6: Image **a** shows staining by the anti-hTRPC7 antibody (1:100), **b**, pre-immune serum (1:100) and **c** shows staining by the peptide control solution with anti-rabbit FITC (1:100) secondary antibody in all cases. All size bars 10μm.

The anti-β-tubulin antibody was again used as a general cell marker, and in Capan-1 cells tubulin appears as fine intracellular filaments, which appear to lead to the cellular protrusions expressing hTRPC7 (Figure 5.7).

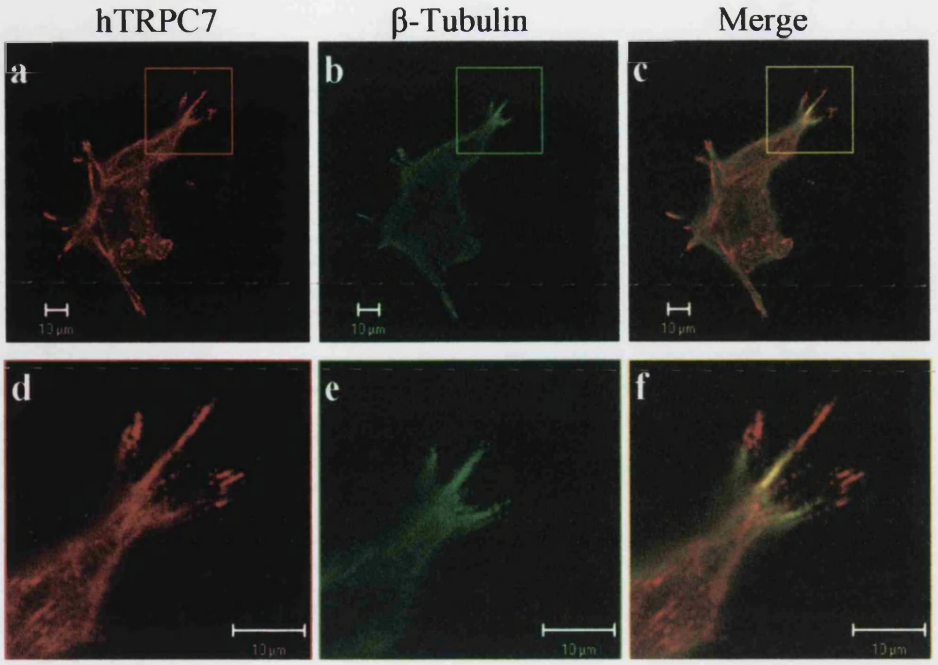

Figure 5.7: Image **a** shows cells stained with anti-hTRPC7 (1:100), image **b** is stained with anti-β-Tubulin (1:200) with anti-mouse FITC (1:100) secondary. Image **c** is the merged image of **a** and **b**. **d**, **e** and **f** are magnified images of the corresponding boxed areas in **a**, **b** and **c**. Size bars 10μm.

5.2.4 - Capan-1 Co-localisation Studies

It was not possible to carry out co-localisation studies on Capan-1 cells with anti-FAK as problems were encountered while culturing this cell type, in particular a high susceptibility to infection. However, anti-paxillin was used, paxillin is a focal adhesion molecule that is involved in the structure of the multi-molecular focal adhesion complexes in some cell types (discussed further in Section 5.3). Staining with anti-Paxillin and anti-hTRPC7 in Capan-1 cells (Figure 5.8) showed that the two proteins did not co-localise. Paxillin was present in the cells at a different focal plane to hTRPC7, it appeared to be more intracellular than the apparently basal membrane localised hTRPC7.

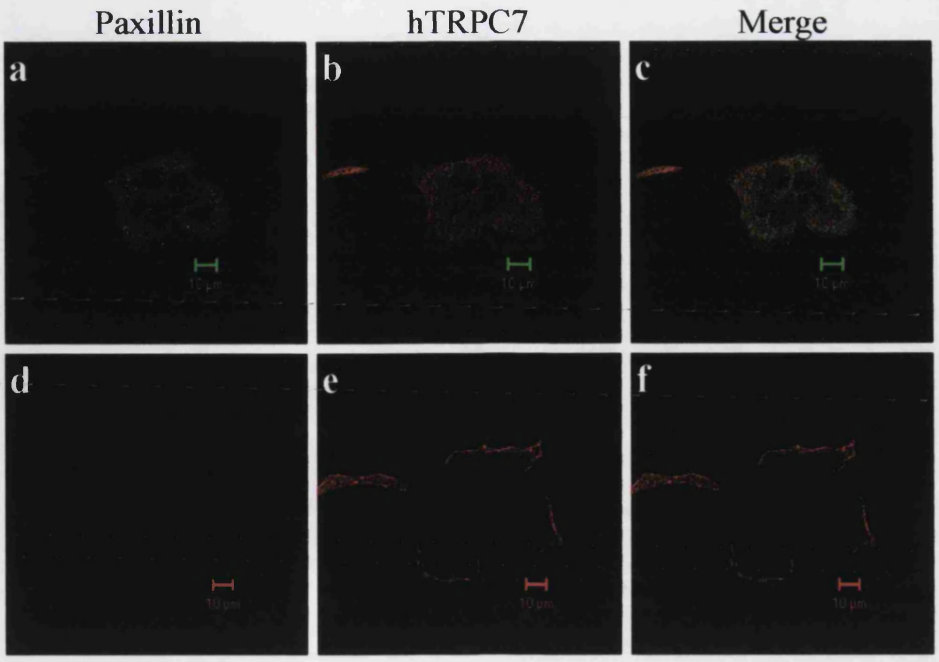

Figure 5.8: Image **a** shows a group of cells stained with anti-paxillin (1:100) with anti-mouse FITC (1:100) secondary, **b** shows the same group of cells stained with anti-hTRPC7 (1:100) and **c** shows the merged image of **a** and **b**. **d**, **e** and **f** shows the same group of cells as **a, b** and **c**, however the image was taken in a different focal plane, on the basal membrane of the group of cells. All size bars 10μm.

5.2.5 - Expression of hTRPC7 in Primary Human Pancreatic Cells

The opportunity arose to use the hTRPC7 antibody on primary human adult pancreatic cells that had been dissociated from the tissue and subsequently cultured. Primary human pancreatic cells in culture for one day (Figure 5.9) were stained for hTRPC7. Approximately 5% of the mixed population of cells were stained and the staining pattern appeared to be predominantly of the PM region, particularly on the feathery protrusions produced by the cell. The staining pattern was unlike that of hTRPC7 in Panc-1 (Figure 5.1) and Capan-1 cells (Figure 5.6) where the cell lines displayed bright, punctate staining for hTRPC7 on the basal PM, the staining of these cell types was more generalised over the entire cell. The extremely bright areas of staining were autofluorescing debris that, as seen by the microscope appeared yellow, however the scan gave them a false green colour.

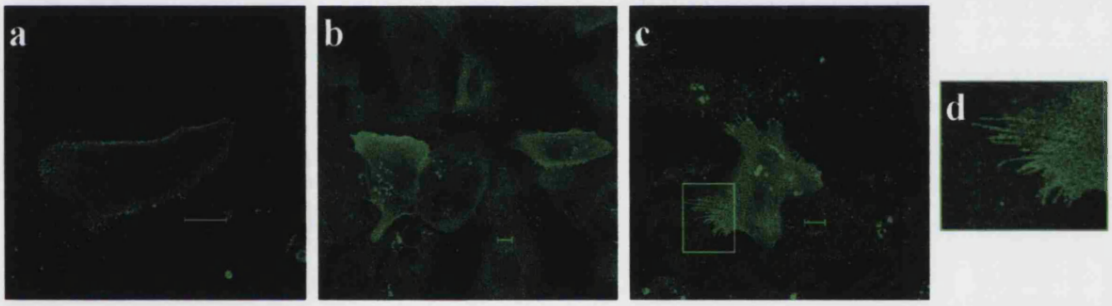

Figure 5.9: Images, **a**, **b**, **c** and **d** show primary human pancreatic cells in culture for 1 day stained with anti-hTRPC7 (1:100) with anti-rabbit FITC (1:100) secondary. **d** is a magnified image of the boxed area in image **c**. All size bars 10μm.

Primary human pancreatic cells were cultured for a further seven days and showed similar results to the 1 day culture (Figure 5.9). The culture displayed staining for hTRPC7 over approximately 5% of the population of cells, the staining pattern appeared to be predominantly PM region and on the protrusions extended by the cells (Figure 5.10).

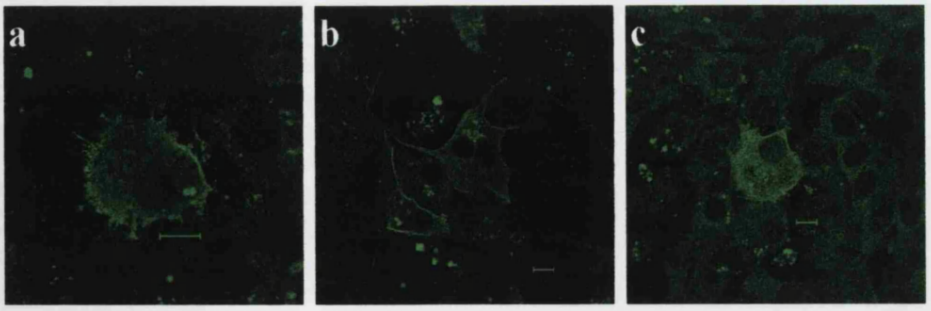

Figure 5.10: Images **a**, **b** and **c** are primary human pancreatic cells in culture for 7 days stained with anti-hTRPC7 (1:100) with anti-rabbit FITC (1:100) secondary. All size bars 10μm.

A pre-immune serum control stain was carried out on cells in culture for seven days, no specific staining was observed however; the autofluorescing bodies were still present (Figure 5.11).

Pre immune serum

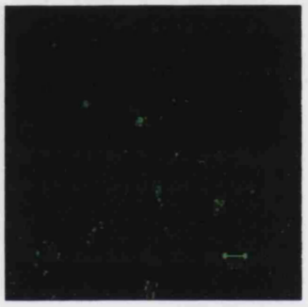

Figure 5.11: Primary human pancreatic cells in culture for 7 days, immunostained with pre-immune serum (1:100) with anti-rabbit FITC (1:100) secondary. Size bar 10μm.

5.2.6 - Western Blots

Western blotting was carried out in order to determine if the 100kD, hTRPC7 band could be observed from Panc-1, Capan-1 and primary human pancreatic cell lysates to back up the hTRPC7 expression detected by immunofluorescence.

Western blots probed with anti-hTRPC7 (Figure 5.12a) showed an approximately 100kD band present in Panc-1 membrane, Capan-1 lysate and primary human pancreas lysate. The bands are strong in both Panc-1 and primary human pancreas (Figure 5.12a, d and g) however the hTRPC7 band given by Capan-1 lysate was much fainter by comparison (Figure 5.12a). The 100kD band was not present in lane 1 of the blot in figure 5.12g as HEK293 cells do not natively express hTRPC7, there was also no 100kD band present with any of the blots probed with the pre-immune serum (Figure 5.12b, e and h) or peptide solution controls (Figure 5.12c, f, i).

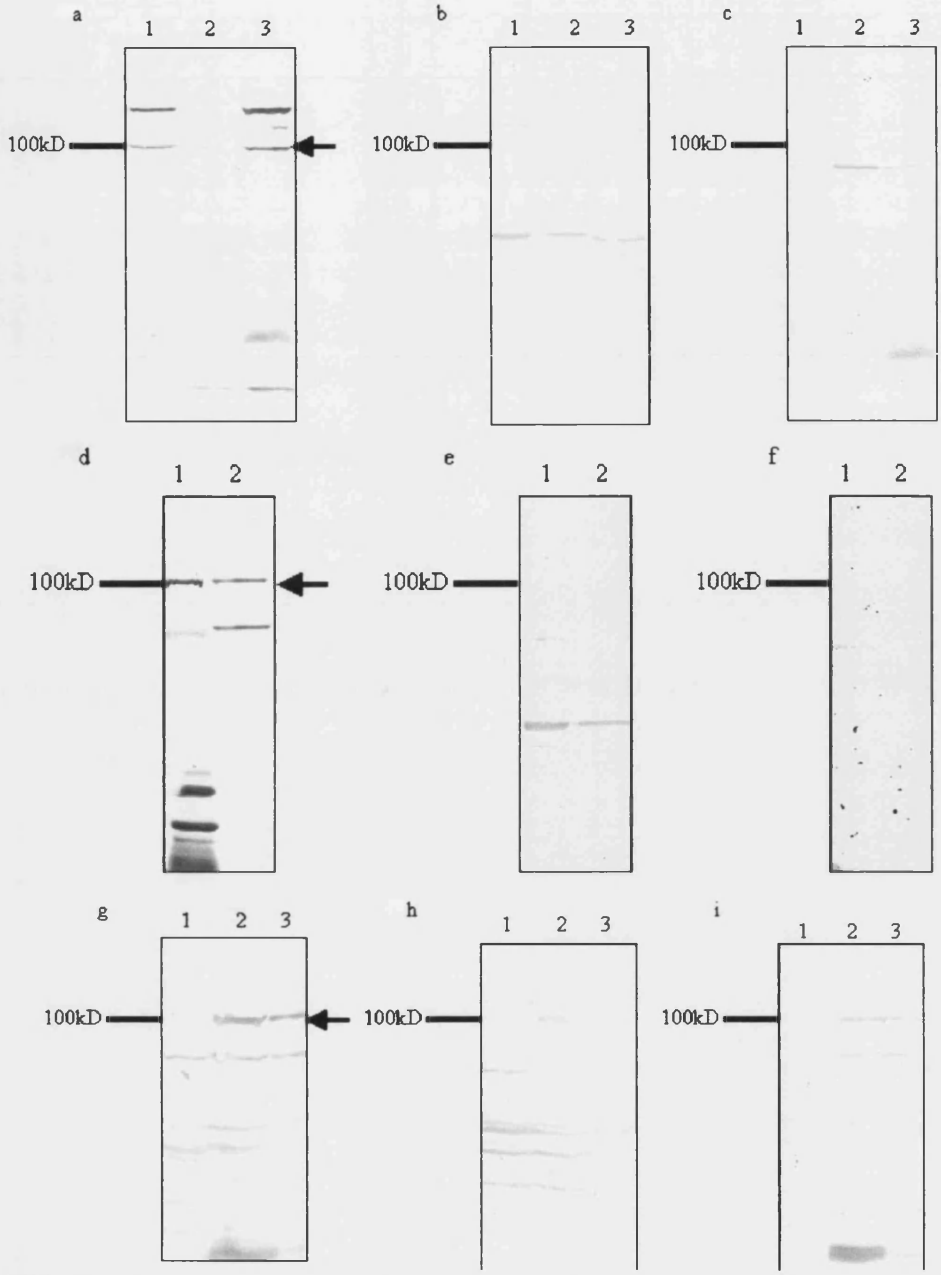

Figure 5.12: Western blots **a**, **b** and **c** lane 1 Panc-1 membrane; lane 2 Capan-1 lysate; lane 3 primary human pancreas lysate (10μg of protein was loaded in each lane). Western blots **d**, **e** and **f** lane 1 primary human pancreas lysate; lane 2 Panc-1 membrane (10μg of protein was loaded in each lane). Western blots **g**, **h** and **i**, lane 1 non-transfected HEK293 cells; lane 2 primary human pancreas lysate; lane 3 Panc-1 membrane (20μg of protein was laded in each lane). Blots **a, d** and **g** have been immuno-probed with anti-hTRPC7 (1:1000), blots **b, e** and **h** have been immuno-probed with pre-immune serum (1:1000), blots **c, f** and **i** have been immuno-probed with the peptide control solution.

5.2.7 - Immunoprecipitation

Due to the apparent co-localisation of hTRPC7 and FAK in Panc-1 cells, an immunoprecipitation using the FAK antibody was carried out on Panc-1 lysates.

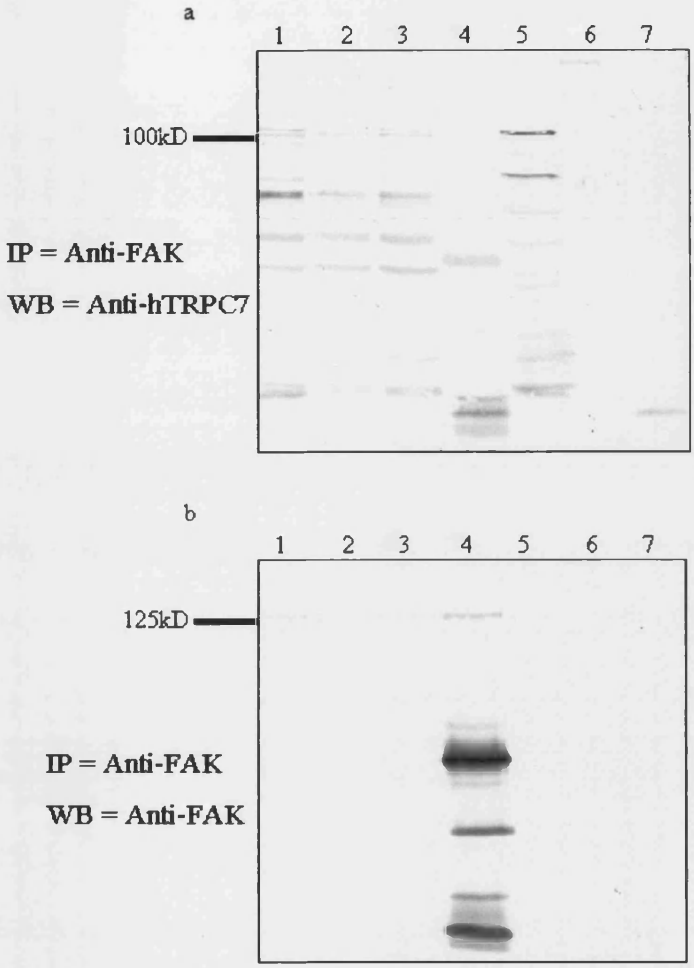

Figure 5.13: Western blots of an IP carried out on Panc-1 cells with anti-FAK. Lane 1 Panc-1 lysate; lane 2 Panc-1 supernatant after IP with anti-FAK; lane 3 Panc-1 supernatant after negative control IP; lane 4 Panc-1 IP with anti-FAK; lane 5 Panc-1 membrane; lane 6 molecular weight ladder; lane 7 negative control IP. Blot **a** has been probed with anti-hTRPC7 (1:1000), blot **b** has been probed with anti-FAK (1:1000). (IP = Immunoprecipitation, WB = Western blot).

Western blots of the IP, carried out with anti-FAK, and probed with anti-hTRPC7 showed a 100kD band in lane 1 (Panc-1 lysate) but no 100kD band was observed in the lane containing the anti-FAK immunoprecipitate (Figure 5.13a). Probing the Western blot with anti-FAK showed a 125kD (FAK) band in lanes 1 and 4, however there was no band

in lane 5 which contained Panc-1 membrane. Figure 13a and b lane 4 shows strong bands at lower molecular weights, these are the IgG heavy and light chains and are commonly observed in immunoprecipitations.

5.2.8 - Expression of TRPC7 in Mouse Pancreatic Tissue

There is no published data on the expression of TRPC7 in mouse pancreatic tissue however, the opportunity arose to use the antibody on primary cultured embryonic mouse pancreatic tissue.

Preliminary results from the staining of cultured embryonic mouse primary pancreatic tissue (Figure 5.14) clearly showed ductal-like structures (arrows) in the tissue expressing TRPC7, image 5.14a shows the structure in transverse section and images 5.14b and c show the structures in longitudinal section. There was also no apparent staining of structures resembling the Islets of Langerhans however, due to restricted amounts of tissue it was not possible to carry out pre-immune serum control staining or co-localisation with other proteins known to be expressed in the embryonic mouse pancreas such as insulin and glucagon.

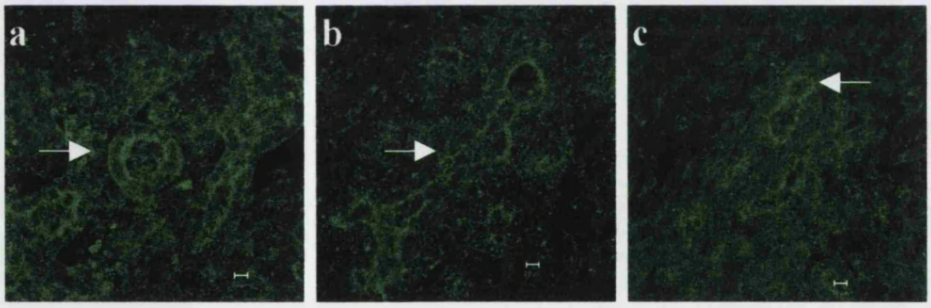

Figure 5.14: Images **a**, **b** and **c** show mouse pancreatic tissue, cultured for 7 days stained with anti-TRPC7 (1:100) with anti-rabbit FITC (1:100) secondary. All size bars 10μm.

5.3 - Discussion

The current study has shown that Panc-1 and Capan-1 cell lines endogenously express hTRPC7 protein (Figures 5.1, 5.6 and 5.9), and that this is detected by the anti-hTRPC7 antibody. This confirmed that the antibody could recognise not only the over-expressed protein but also the endogenous protein.

Three groups thus far have looked into the expression of TRPC7 by primary cells. In separate studies, groups lead by Diana Kunze and William Schilling carried out expression and localisation studies of all seven TRPC proteins using antibodies that had been raised to each member of the TRPC subfamily (Buniel et al., 2003; Goel et al., 2002). Schilling's group used the antibodies to look into associations of the TRPC proteins with other TRPCs and PDZ proteins. Their TRPC7 antibody was raised to an amino acid peptide human sequence corresponding to 843 to 857 amino acids; this part of the human sequence does not differ from that of the mouse (Goel et al., 2002). They used over expression of TRPC7 in the insect cell line, Sf9, and endogenous expression in rat brain preparations to characterise their TRPC7 antibody (Goel et al., 2002). Upon characterisation of this antibody by Western blot only, they state that the antibody recognised TRPC7 by the production of a band at the correct predicted molecular mass and did not recognise other endogenous proteins in the Sf9 (Goel et al., 2002). Further to this, it did not recognise any of the other TRPC proteins over expressed in the Sf9 cells and from endogenous expression in rat brain preparations (Goel et al., 2002). However, the marked absence of control experiments in this study leave the results open to some debate.

In an immuno-localisation study of TRPC proteins in the rat carotid sensory pathway using the same antibodies as the previous study, it was found that TRPC7 was not expressed in any of the sensory fibres but was expressed in the petrosal neurons throughout the ganglia as well as 'supportive satellite' cells (Buniel et al., 2003). However, there was no co-localisation with any other TRPCs (Buniel et al., 2003). The staining of the cells by their TRPC7 antibody in the figures shown appears to be a low

level staining of all cell types under investigation, which may possibly mean there is a lack of specificity of the antibody. This is further confirmed by the presence of nuclear staining of the satellite cells, which is indicative of non-specific staining. The marked absence of any control experiments or other supportive data, such as Western blot or RT-PCR, to confirm the presence or absence of TRPC7 in these cell types also leaves these results open to some debate. It is possible that the antibody may be adequate for the detection of TRPC7 by Western blot of cells over expressing TRPC7 however on the evidence shown, this antibody may not have been ideal for immunocytochemistry studies.

A third group have carried out small interfering RNA (siRNA) studies of TRPC7 and other TRPCs using Western blotting techniques to identify the presence or absence of the protein (Wu et al., 2004). The study was largely of a functional nature as an assessment of SOC in H19-7 hippocampal neurons, however the use of a TRPC7 antibody on Western blots showed the presence of a TRPC7 band in those cells that had not undergone siRNA and no band in cells that had (Wu et al., 2004). The TRPC7 antibody was reportedly purchased from AbCam raised in goat (ab2658) this however, was removed from sale in August 2003 after it was found that the antibody was unfit for use due to poor characterisation results (AbCam, personal communication) specifically, it was withdrawn due to a very low titre by ELISA and high concentrations of the antibody needed on Western blots (AbCam, personal communication). Despite this the results of the study did appear to be valid as there was supportive data from RT-PCR, unfortunately there was no immunocytochemistry data to show the localisation of the protein on this cell type, it may be that the antibody was not suitable for immunocytochemistry.

The pattern of staining given by my anti-hTRPC7 antibody (produced in this study) in Panc-1 cells was bright and specific in a punctiform pattern mainly localised to the edges of the cells (Figure 5.1). Control staining with the pre-immune serum and peptide control solution, in the Panc-1 cells showed no evidence of any staining other than a low-level background (Figure 5.2). The staining pattern by anti-hTRPC7 was shown by z-sectioning to be mainly restricted to the basal membrane of the cell where the cell

interfaced with the glass coverslip it was attached to (Figure 5.3). It was also evident that there was not any other intracellular structure that appeared to be labelled by anti-hTRPC7, this was in contrast to the staining pattern of over-expressed hTRPC7 (Chapters 3 and 4) where hTRPC7 appeared to be localised to the Golgi as well as the PM. Where Panc-1 cells were stained with both anti-hTRPC7 and anti-β-tubulin (Figure 5.1) the fibrillary structure of the cytoskeletal protein tubulin was evident and, while it did not co-localise with hTRPC7, it appeared that the tubulin fibres led to some of the punctate hTRPC7, particularly where the cell has extended protrusions. These cells are quite dynamic (like many epithelial adherent cell lines) and move across the extracellular matrix by PM protrusions. These protrusions have staining for hTRPC7 at their very tips. The staining of Panc-1 cells for hTRPC7 and F-actin (Figure 5.4) showed some co-localisation at the periphery of the cell. This may indicate that actin filaments (which are involved in cell shape and membrane protrusions; (Wozniak et al., 2004) may be involved with hTRPC7 at the protrusions of the cells. The pattern of staining by anti-hTRPC7 in Panc-1 cells is highly reminiscent of staining for focal adhesion proteins in other cell types. Therefore, dual staining with anti-hTRPC7 and anti-FAK was carried out which, revealed complete co-localisation of these two proteins (Figure 5.5). Immunoprecipitation experiments were carried out to determine whether or not the two proteins were physically linked. The resulting Western blots (Figure 5.12) indicated that this was not so with the conditions used as no detectable hTRPC7 was recovered from the IP of Panc-1 lysates. Interestingly, the Western blot probed with anti-FAK (Figure 5.12b) revealed the 125kD FAK band in Panc-1 lysate (and recovered in the IP) but not in Panc-1 membrane preparation. This indicates that FAK is not a membrane protein, as hTRPC7 clearly seems to be, but is instead recruited to focal adhesion complexes formed at the PM and sub-PM (Wozniak et al., 2004), this process may involve hTRPC7 or the Ca^{2+} that goes through hTRPC7.

Capan-1 cells also express endogenous hTRPC7, as demonstrated by immuno-staining with the anti-hTRPC7 antibody. These cells exhibited a similar localisation of hTRPC7 to the Panc-1 cells, displaying a punctiform staining pattern localised to the PM with no evidence of hTRPC7 expression in any intracellular structures (Figure 5.6). However,

only a small fraction of cells in culture actually appeared to be expressing the protein. Capan-1 cells grow in clusters of approximately 20 or more cells, and the hTRPC7 appears to be largely at the periphery of these cell clusters, with no apparent expression of hTRPC7 in cells at the centre of the clusters. It was also evident that the level of expression of hTRPC7 in Capan-1 cells was lower than in Panc-1 cells, possibly because fewer cells express the protein. The same 100kD band was identified on Western blot of Capan-1 cell lysates. However, despite equal protein loading the hTRPC7 band was much less intense in the Capan-1 lane (Figure 5.12a). Control experiments with pre-immune serum and peptide control solution, as with the Panc-1 cells, did not show the specific staining seen with anti-hTRPC7 and only a low-level background stain was apparent (Figure 5.7). It was not possible to use the FAK antibody to co-localise hTRPC7 and FAK in Capan-1 cells due to problems with the Capan-1 culture (described in section 5.2.4). However, an antibody to paxillin (a scaffolding protein involved in the formation of focal adhesion complexes) was used in a co-localisation study with anti-hTRPC7 on Capan-1 cells. The staining pattern of hTRPC7 and paxillin did not co-localise, there was very little evidence of paxillin in Capan-1 cells and where it was evident it appeared to be intracellular unlike the PM localisation of hTRPC7 (Figure 5.8). The same experiment was carried out in Panc-1 cells however there was no evidence of paxillin expression in Panc-1 cells (results not shown). As described below in more detail paxillin is recruited to focal adhesion complexes as a scaffold molecule, however it is not always a component of every focal adhesion complex whereas FAK is a very important general molecule of focal adhesions (Wozniak et al., 2004). It may be that paxillin is not a component of the focal adhesion complexes in Panc-1 and Capan-1 cells that hTRPC7 appears to be associated with.

Evidence gathered in the current study indicates that hTRPC7 may be involved in focal adhesion complexes of some cell types. Focal adhesions are diverse and include scaffolding molecules, GTPases and enzymes such as kinases, phosphatases and lipases (Wozniak et al., 2004). Different types of focal adhesions are defined by their subcellular localisation, size and composition and they can be split into four different structures; focal complexes, focal adhesions, fibrillar adhesions and 3-dimensional matrix adhesions

(Wozniak et al., 2004). Focal complexes are small and situated at the periphery of spreading or migrating cells and are regulated by the small GTPases, Rac and Cdc42 (Nobes and Hall, 1995). Focal adhesions are situated on the periphery and central areas of cells and are regulated by the activity of Rho, a GTP binding protein; focal adhesions are also associated with ends of stress fibres in cells cultured on 2D rigid surfaces (Chrzanowska-Wodnicka and Burridge, 1996; Hotchin and Hall, 1995; Ridley and Hall, 1992). It is not clear what distinguishes focal complexes from focal adhesions however, the localisation results presented in this chapter appear to indicate that hTRPC7 is associated with focal adhesions.

Cell migration is essential for normal embryonic development, wound healing, tumour invasion, metastatis and the inflammatory response(Wozniak et al., 2004). Adhesive contacts are highly dynamic structures that undergo regulated assembly at the cell front, disassembly at the cell rear and translocation in both stationary and migratory cells (Huttenlocher et al., 1995; Katz et al., 2000; Lauffenburger and Horwitz, 1996; Smilenov et al., 1999; Zamir et al., 1999). Focal adhesions are clusters of integrin (a family of heterodimeric cell surface receptors), a compex of tyrosine kinases, phosphatases and scaffold or adaptor proteins (talin, α-actinin, filamin and paxillin) that links the extra cellular matrix (ECM) to the actin cytoskeleton (Schoenwaelder and Burridge, 1999; Wozniak et al., 2004). Assembly of focal adhesions occurs as the cell migrates; the leading edge membrane protrusion is stabilised by small adhesive foci that initially contain paxillin then α-actinin (Edlund et al., 2001; Laukaitis et al., 2001), the foci grow into focal complexes abundant in tyrosine phosphorylation and contain integrin, talin, paxillin, vinculin and FAK (Laukaitis et al., 2001; Zaidel-Bar et al., 2003). Zyxin and tensin are subsequently recruited to stabilise the protrusion and the complexes remodel into focal adhesion (Zaidel-Bar et al., 2003). It is believed that this is all regulated by small GTPases, initially by Rac and later by Rho for maturation of the focal adhesions (Ballestrem et al., 2001; Kiosses et al., 2001; Rottner et al., 1999). The scaffold proteins function as signalling scaffolds for other components of focal adhesions, they complex in a manner that brings together all kinases and substrates to elicit changes in cell morphology and behaviour (Wozniak et al., 2004). Cells are able to continuously remodel

focal complexes into focal adhesions and vice versa to migrate. Src and FAK are important regulators in focal adhesion turnover, it is known that Src generally causes a reduction in focal adhesions and decreased cell adhesion, this suggests that tyrosine phosphorylation of focal components by Src causes focal adhesion turnover (Wozniak et al., 2004).

Ca^{2+} dependent calpain appears to have a role in the regulation of focal adhesions/ complexes; specifically, calpain is involved in the disassembly of focal adhesion complexes. Calpain is a protease whose substrates include integrin, FAK, ezrin and talin. It has been shown that calpain inhibitors reduce cell migration rates and cell detachment rates during migration (Huttenlocher et al., 1998). Furthermore, calpain cleavage of FAK is enhanced by Src (Carragher et al., 2003). Calpain inhibition stabilises peripheral adhesive complexes that contain vinculin and integrin (Huttenlocher et al., 1998; Palecek et al., 1998). Disruption of other proteins (FAK and Src) also promote formation of strong focal adhesions at the cell periphery (Ilic et al., 1995; Klinghoffer et al., 1999; Sieg et al., 1999). Calpain, FAK and Src may be acting by related mechanisms to regulate cell migration (Bhatt et al., 2002). It is possible that hTRPC7 may be involved in the disassembly of focal adhesion complexes as a means of providing Ca^{2+} for the Ca^{2+}-dependent calpain regulated disassembly of focal adhesions.

There is very little known about the role of ion channels in the control of focal adhesions, or indeed the control of ion channels by focal adhesions. It is known that phosphorylation can alter Ca^{2+} channel gating properties (voltage sensitivity and Ca^{2+} sensitivity) and can therefore control the electrophysiological properties of a cell, there is recent evidence to suggest that ion channels are regulated by tyrosine phosphorylation, just as many of the focal adhesion components are (Davis et al., 2001). Tyrosine phosphorylation is a key signalling event occurring at focal adhesions, regulating the activation of additional kinases and phosphatases. FAK and Src are tyrosine kinases that bind to different partners to regulate focal adhesion dynamics and cell behaviour (Wozniak et al., 2004). Src activation is implicated in many processes: receptor phosphotyrosine kinases, GPCRs and integrins and may indicate a key point of many signal transduction pathways (Davis

et al., 2002). Src kinase has, in a recent study, been implicated in the regulation of another TRPC, TRPC3. HEK293 cells stably expressing TRPC3 are usually activated by DAG however, when Src kinase is pharmacologically inhibited or expressed in a dominant negative form, TRPC3 is not activated by DAG (Vazquez et al., 2004).

Integrins may play a role in directing the localisation of ion channels for example; in neuroblastoma cells neurite outgrowth is initiated by hyperpolarisation subsequent to $\beta 1$ integrin dependent adhesion on ECM (Arcangeli et al., 1993). There is also evidence that integrins play a functional role in ion channel regulation for example; integrin-dependent adhesion initiates Ca^{2+} influx in smooth muscle (Chan et al., 2001) and epithelial cells (Sjaastad et al., 1996). There have been very few studies that define the interactions between a focal adhesion and an ion channel, however a few studies have implicated SOC or non-selective cation channels to be regulated by integrins. A possible SOC in human umbilical vein endothelium has been implicated in adhesion dependent intracellular Ca^{2+} increases (Schwartz, 1993; Schwartz and Denninghoff, 1994) and SOC have been reported to be activated by focal adhesion glycoproteins of platelet PM (Fujimoto et al., 1991). It is possible that hTRPC7 may be a component of these channels, especially as it is expressed in platelets (C. Murphy, Unpublished Data).

The opportunity arose to test the hTRPC7 antibody on primary human pancreatic cells isolated post-mortem and cultured for up to seven days, material, which because of its origin was in very limited supply. The culture was a mixed population of largely exocrine cell types and a small proportion of endocrine cells. Staining by anti-hTRPC7 showed approximately 5% of the mixed population of cell types to be expressing hTRPC7. The staining appeared to be of PM localisation in these cells, at both day one and at day seven of culture (Figures 5.9 and 5.10). The pattern was unlike that seen in Panc-1 and Capan-1 cells, in that it was not punctiform but more uniform. Control staining by pre-immune serum gave low level staining of all cell types in the culture (Figure 5.11). The morphology of these pancreatic cells would have changed a great deal *in vitro* compared to *in vivo* after having been dissociated from its structure and being cultured on glass coverslips. Therefore the staining pattern of hTRPC7 seen may not reflect the true

expression pattern of the protein *in vivo*. Western blots of this tissue showed a prominent 100kD band, comparable to that from the Panc-1 membrane, which was not present when the blots were probed with pre-immune serum or the peptide control solution (Figure 5.12). There were no other bands present on the blots probed with anti-hTRPC7 that would have indicated the presence of the hTRPC7 splice variants in Panc-1, Capan-1 and primary human pancreas. From the limited information gained from these results it is impossible to say what pancreatic cell type hTRPC7 appears to be present in.

Evidence gathered so far leads to the hypothesis that hTRPC7 may be expressed in the exocrine portion of the pancreas, in a specific and as yet unidentified sub-set of ductal cells. This is due, in part, to the expression and localisation evidence shown by the human ductal pancreatic carcinoma cell line, Panc-1 and primary human pancreatic cells, which are a mixed population of largely exocrine cells from the human pancreas. To further confirm the expression of hTRPC7 in these cell types RNAi experiments could be carried out. Evidence from co-localisation studies with FAK in Panc-1 cells suggests that hTRPC7 may be involved in some way with focal adhesion proteins. However, the focal adhesion-like staining of hTRPC7 seen in Panc-1 and Capan-1 cell lines was not observed in the primary human pancreatic cells. Therefore, it is not possible to say that hTRPC7 is associated with focal adhesions in human pancreatic tissue, further immunocytochemistry or immunohistochemistry on the human pancreas involving co-staining with anti-FAK (or other focal adhesion markers) and anti-hTRPC7 should be carried out. The current evidence may suggest that hTRPC7 is associated with focal adhesions in carcinoma tissue. To find whether or not hTRPC7 plays a role in the regulation of focal adhesions (or vice versa) a number of experiments could be undertaken. Cells could be low-level transfected with EGFP tagged *htrpc7*, a chemotactic stimulus placed in the culture and time-lapse confocal microscopy carried out to observe cell movement and any changes in expression of hTRPC7. The ECM in the cell culture could be changed and immunocytochemistry carried out to observe any changes in the localisation of hTRPC7. RNAi could also be carried out and using the experiments outlined above, this could be used to observe whether the adhesion properties of the cell changes.

The hTRPC7 antibody was also used on embryonic mouse pancreatic tissue (Figure 5.14). Although the antibody has been raised against the human epitope, there is only one amino acid difference between that and the corresponding epitope in the published murine sequence of TRPC7 (See Chapter 3 Figure 3.1) and therefore the antibody was expected to cross react with mTRPC7. Where the hTRPC7 antibody has been applied to non-human tissue it is called anti-TRPC7. The staining pattern of anti-TRPC7 on embryonic murine tissue revealed ductal like structures in the embryonic tissue (Figure 5.14), and there was no apparent staining of discrete cells within Islets of Langerhans. It has previously been reported that two splice forms of mTRPC4 and mTRPM2 have been cloned from a mouse insulinoma cDNA library (Qian et al., 2002). They have also identified mTRPC4 in endocrine cells and brain however, the expected currents (previously seen in β-cells) could not be reproduced in stably transfected cells and they deduce from this that to form a functional channel mTRPC4 was probably a heteromer with another as yet unknown protein (Qian et al., 2002). There is no report of the identification of other members of the TRP superfamily in this study, however they believe that mTRPC4 and mTRPM2 may provide a pathway for Ca^{2+} in β-cells and may be targets for manipulating β-cell function (Qian et al., 2002). The current study focuses on the expression of hTRPC7 and mTRPC7 in the exocrine pancreas and it is yet to be ascertained whether or not the protein is expressed in the endocrine portion of the pancreas, as other TRPs appear to be. Future work could involve the use of pancreatic endocrine cell lines and primary tissue to identify the possible expression and localisation of hTRPC7 and mTRPC7 in the endocrine pancreas. The very preliminary data obtained from mouse pancreas may suggest that the hTRPC7 antibody does cross react with mouse TRPC7 due the anti-TRPC7 staining of mouse pancreatic tissue displayed a distinctly ductal-like structure. There is a high degree of dissimilarity between the tissue distributions of hTRPC7 and mTRPC7 however, there is a lack of data on the presence or absence of mTRPC7 in mouse pancreas. Future work could involve ascertaining the presence or absence of TRPC7 and any splice variants in the mouse pancreas. It is possible that TRPC7 may have an important and common role to play in the pancreas that is conserved across species.

It is currently impossible to say what specific pancreatic cell type TRPC7 is expressed in and what function it has however, these results have demonstrated that the antibody to TRPC7 recognises the endogenous protein in human pancreas and results also suggests that it recognises TRPC7 in mouse pancreas. Furthermore, results suggest that hTRPC7 may be involved in focal adhesion complexes, this may be important for the functional role of hTRPC7 in the pancreas.

Chapter 6

TRPC7 in Ventricular Cardiomyocytes and 3T3-L1 Adipocytes

6.1 - Introduction

6.1.1 - Cardiomyocytes

The heart is composed of cells that contract in a co-ordinated fashion: these cells are cardiomyocytes. Cardiomyocytes comprise approximately 80% of cardiac mass, however they represent only 20% of cardiac cells. Other cell types include; fibroblasts, neurons and endothelial cells (Jacobson and Piper, 1986). Cardiomyocytes have a particular significance in Ca^{2+} signalling since it is the generation of regular pulses of Ca^{2+} that drives each heart beat (Bers, 2002). Cardiomyocytes are insulin sensitive and have an abundance of the insulin receptor on their membranes. Insulin stimulation increases entry of glucose into the cell, but may also be involved in mitogenesis and regulation of enzymatic pathways, and it is thought to be cardioprotective (Nystrom and Quon, 1999). Glucose and lactate metabolism produces up to 30% of myocardial ATP (Abel, 2004; Hiraoka, 2003). Glucose is transported into the cell by a group of facilitative glucose transporters known as the Glucose Transporters (GLUTs) and the most abundant GLUT in cardiomyocytes is GLUT4 (Abel, 2004). When stimulated by insulin GLUT4 translocates from the intracellular tubo-vesicular network to the PM to allow the entry of glucose (Abel, 2004). Besides glucose entry, insulin has recently been found to have another action on the cardiac membrane, activating a non-selective cation current in guinea pig ventricular myocytes (Zhang and Hancox, 2003). Zhang and Hancox also found that this channel was directly activated by OAG, a non-hydrolysable form of DAG, and it was suggested that this was a TRP like channel (Zhang and Hancox, 2003). It is known that, in humans, TRPCs 1, 4 and 6 are expressed in the heart to varying degrees and hTRPC7 appears not to be expressed (Riccio et al., 2002b); Chen Unpublished data). However, in mice TRPC7 is abundantly expressed in the heart (Okada et al., 1999), and it seemed likely that it would also be expressed in the rat heart.

6.1.2 - Adipose Tissue

Adipose tissue is the fat storage tissue and is also insulin sensitive, using GLUT4 to facilitate the uptake of glucose for storage as fatty acids (Watson et al., 2004). Insulin

also blocks mobilisation and oxidation of the fatty acids (Berne and Levy, 1998). There is very little understood about Ca^{2+} signalling in adipocytes, and most research on Ca^{2+} signalling in this tissue has centred on the action of insulin and the secretion of leptin (Cammisotto and Bukowiecki, 2004). Leptin acts on the hypothalamus causing decreased food intake and increased energy expenditure and is part of a feedback loop regulating body fat stores (Campfield et al., 1995; Halaas et al., 1995; Pelleymounter et al., 1995). Ca^{2+} does not affect leptin synthesis or exocytosis directly, but excess Ca^{2+} disrupts leptin secretion by interfering with metabolic events that are independent of glucose uptake (Cammisotto and Bukowiecki, 2004). The mouse fibroblastic cell line 3T3-L1 is commonly used in research into adipose tissue as it has the ability to, when stimulated by the glucocorticoid dexamethosone, insulin and IBMX (see Chapter 2 Section 2.3.3.2), differentiate into adipocytes. hTRPC7 was not reported to be present in human adipocytes (Riccio et al., 2002a) and there are not any data concerning the expression of mTRPC7 in adipocytes.

The anti-hTRPC7 antibody, produced and characterised in Chapter 3, was predicted to cross-react with mTRPC7 due to the high sequence homology of the portion of amino acid sequence the antibody was raised to (Chapter 3 Figure 3.1). Also, previous staining using this antibody on mouse pancreatic tissue (Chapter 5 Figure 5.14) further indicated that the antibody was useful for both human and mouse tissue. In the current study insulin sensitive tissues, namely mouse 3T3-L1 cell line and rat embryonic and adult cardiomyocytes, were utilised to study the expression and localisation of TRPC7.

6.2 - Results

6.2.1 - TRPC7 in Embryonic Cardiomyocytes

Embryonic rat cardiomyocytes were cultured for one week and immuno-stained with the anti-TRPC7 antibody. These cells exhibited staining for TRPC7 (Figure 6.1), which appeared to localise to what may be the t-tubules on embryonic cardiomyocytes (Figure 6.1a and b, arrows). Other cell types present in the culture appeared to be predominantly fibroblasts (Figure 6.1c) and showed generally high-level of background fluorescence and nucleolar staining. There were also many cells in the culture that had similar morphology to the cell in Figure 6.1d, these cells had many projections, a 'spotty' pattern of staining and they also had nucleolar staining. Cultured cardiomyocytes can take on three general morphologies; the rod shape of healthy cardiomyocytes, the rounded shape of ischaemic cardiomyocytes (ischaemia can lead to cell death) and the de-differentiated cardiomyocyte that form many pseudopodia (Thum and Borlak, 2000). De-differentiation is a common occurrence in cultures of cardiomyocytes and is thought to be irreversible (Thum and Borlak, 2000). It is possible from the morphology of the cell observed in Figure 6.1d that this cell may be de-differentiating cardiomyocytes.

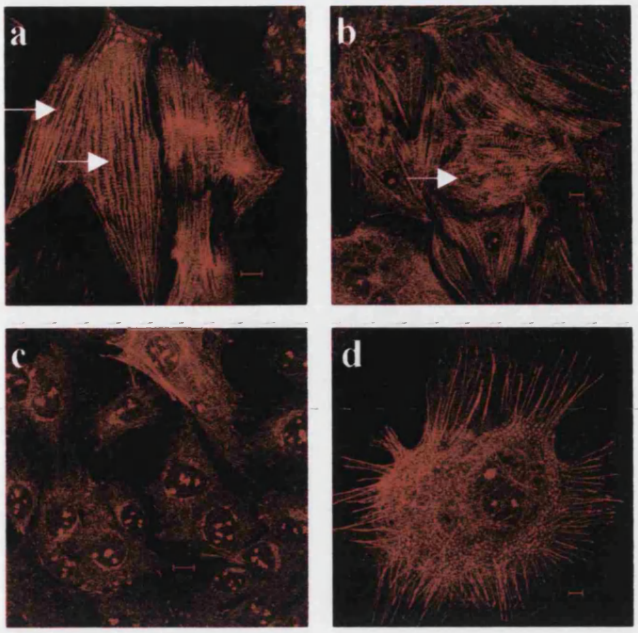

Figure 6.1: Images **a** to **d** show a mixed population of cell types from the same culture of embryonic rat cardiomyocytes that have been cultured for one week, stained using anti-TRPC7 (1:100). All size bars 10μm.

The glucose transporter GLUT4 was used as a general cardiomyocyte marker as it is present in embryonic and adult cardiomyocytes although embryonic cardiomyocytes are not responsive to the actions of insulin. Cells were co-stained with anti-TRPC7 and anti-GLUT4 in order to more readily identify cardiomyocytes and to ascertain that it was just the cardiomyocytes in culture that had the specific staining. Embryonic cardiomyocytes in culture for three days (Figure 6.2) showed similar staining to that observed in the embryonic cardiomyocytes in culture for one week (Figure 6.1). The t-tubule like pattern of TRPC7 did not co-localise with GLUT4, which showed a predominantly peri-nuclear localisation with a small amount of PM staining (Figure 6.2a to c). Control staining by pre-immune serum gave only low-level background fluorescence with no specificity on cultured embryonic cardiomyocytes (Figure 6.2d to f).

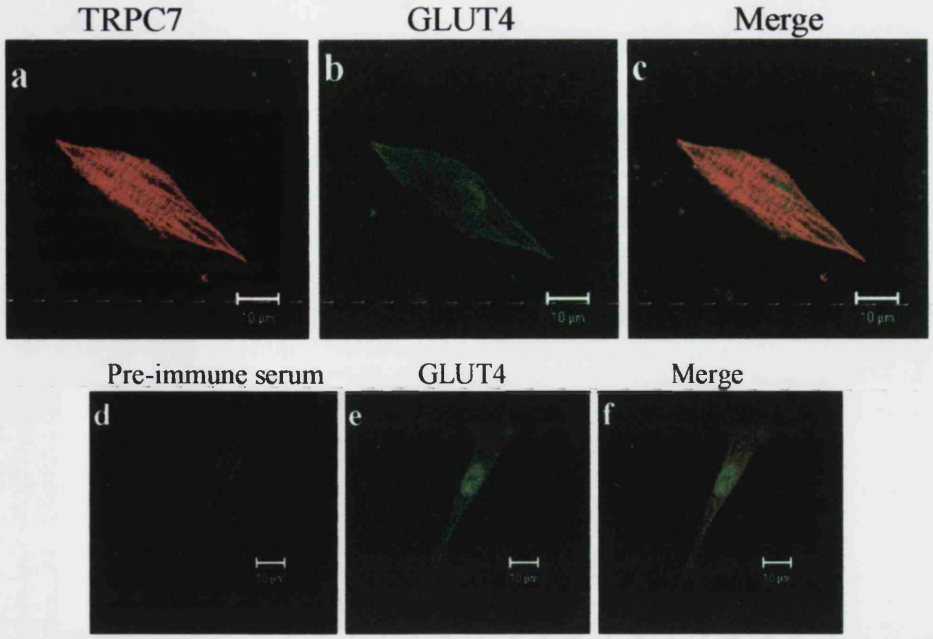

Figure 6.2: Embryonic cardiomyocytes cultured for three days. Image **a** shows a single embryonic cardiomyocyte stained using anti-TRPC7 (1:100). **b** shows the same cells as **a**, stained using anti-GLUT4 (1:200) with anti-mouse FITC secondary (1:100). **c** is the merged image of **a** and **b.** Image **d** was stained using pre-immune serum (1:100). **e** has been stained using anti-GLUT4 (1:200) with anti-mouse FITC secondary (1:100). Image **f** is the merged image of **d** and **e**. All size bars 10μm.

6.2.2 - TRPC7 in Adult Ventricular Cardiomyocytes

After having identified TRPC7 in a primary culture of embryonic rat cardiomyocytes adult rat cardiomyocytes were also investigated for the expression of TRPC7. Cardiomyocytes were immunofluorescently stained immediately after isolation and not cultured in order to obtain a more true representation of TRPC7 localisation *in vivo*. GLUT4 was once again used as a cellular marker. Freshly isolated adult rat cardiomyocytes showed strong staining for TRPC7 with very little background fluorescence apparent (Figure 6.3). The staining pattern appeared to be of PM region, most likely localised to the t-tubules. GLUT4 showed a degree of co-localisation with TRPC7; in the non-insulin stimulated states such as this, GLUT4 usually localises around the nucleus of the cell and has little PM localisation (Abel, 2004). Control staining of the adult cardiomyocyte by the pre-immune serum gave no specific staining and a low-level of background fluorescence (Figure 6.3e).

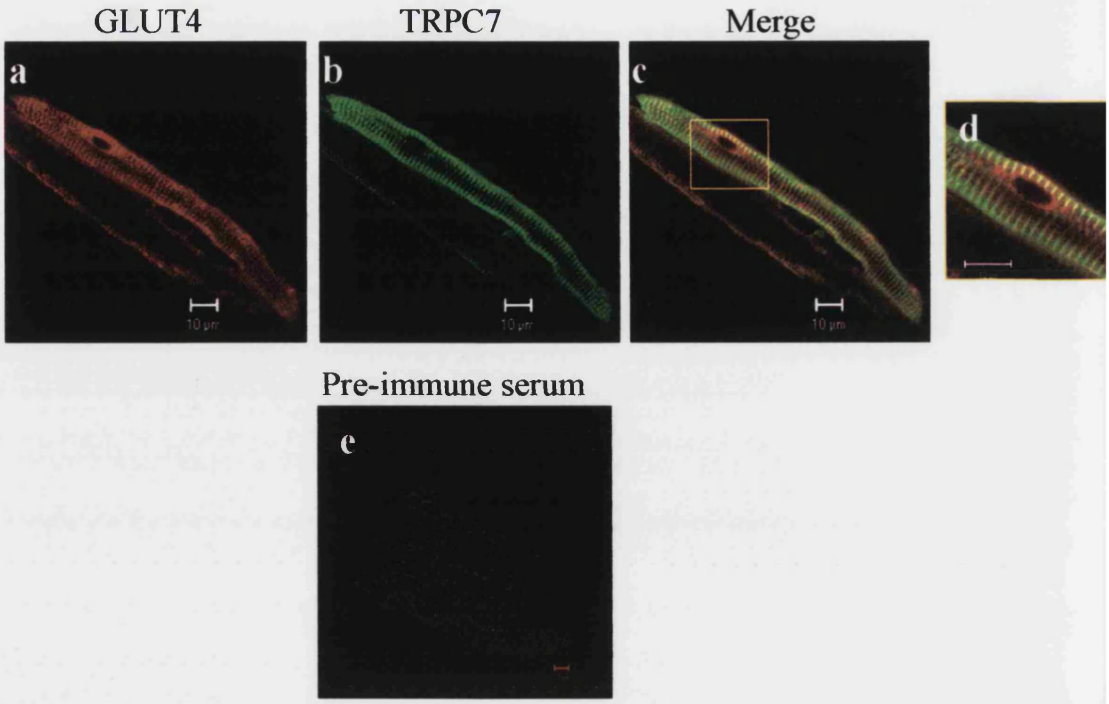

Figure 6.3: Image **a** shows staining by anti-GLUT4 (1:200) with anti-mouse conjugated Alexa Fluor 568 (1:300) secondary, **b** shows staining by anti-TRPC7 (1:100) with anti-rabbit conjugated Alexa Fluor 546 (1:300) secondary, **c** is the merged image of **a** and **b**. Image **d** shows a magnified view of the boxed area of image **c**. Image **e** shows cardiomyocytes stained using pre-immune serum (1:100). All size bars 10μm.

Adult rat cardiomyocytes stained with the anti-TRPC7 antibody were z-sectioned at 1.0μm intervals using the confocal microscope, these cells were not attached to a coverslip and therefore the z-section was taken in longitudinal sections from one side of the cell to the other. Sectioning indicated that the staining of TRPC7 was PM region, most likely in the t-tubules, there was not any intracellular localisation of TRPC7 (Figure 6.4).

Figure 6.4 (Opposite): Z-sections of an adult cardiomyocyte, stained using anti-TRPC7 (1:100). All size bars 10μm.

a
b
c
d
e
f
g
h
i
j
k
l
m
n
o
p
q
r
s
t

6.2.3 - TRPC7 in Insulin Stimulated Adult Cardiomyocytes

Heart cells are responsive to stimulation by insulin, and as previously discussed GLUT4 translocates to the PM upon stimulation by insulin and facilitates entry of glucose. Adult rat cardiomyocytes were stimulated using two concentrations of insulin to observe any differences in localisation of TRPC7 in these conditions compared to the basal conditions (Figures 6.3 and 6.4) and to possibly infer a function for TRPC7 in the heart. The insulin stimulation of adult cardiomyocytes (Figure 6.5) did not appear to change the localisation of TRPC7 at either concentration of insulin. The localisation was still restricted to PM/ t-tubular regions. Both concentrations however, did change the localisation of GLUT4; from peri-nuclear to PM localisation, this change in localisation of GLUT4 indicated that the cells were appropriately stimulated by insulin. Stimulation by insulin led to a greater co-localisation of the two proteins than in the non-insulin stimulated state.

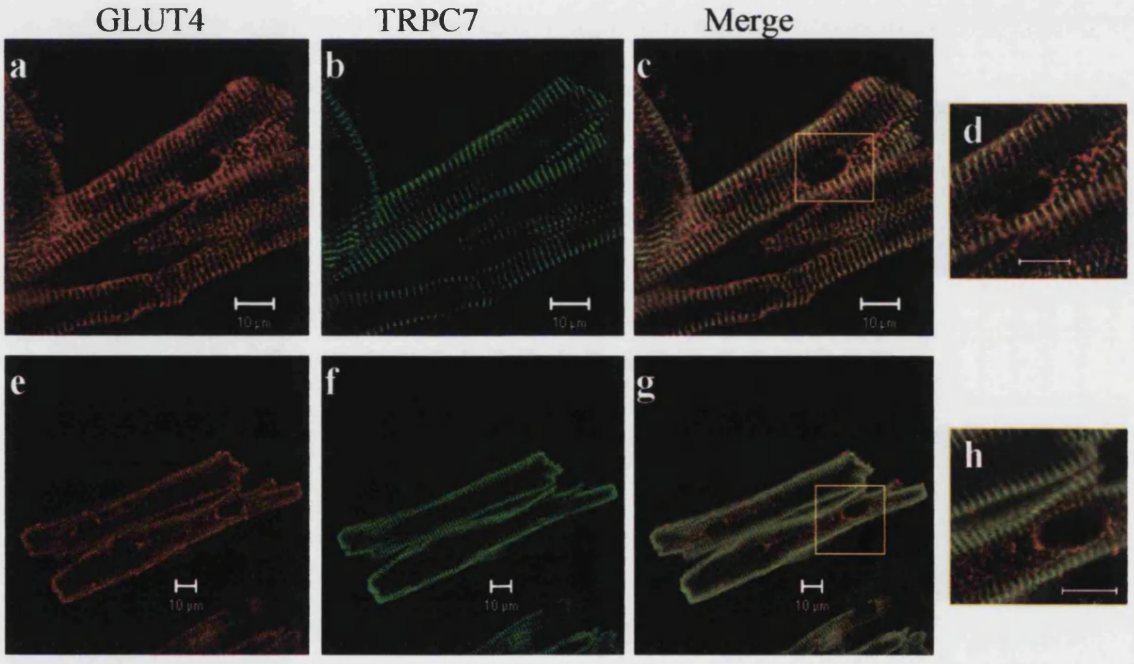

Figure 6.5: The top row of images show a cardiomyocytes that have been stimulated with 30nM insulin and the bottom row of images show cardiomyocytes that have been stimulated with 60nM insulin. Images **a** and **e** stained using anti-GLUT4 (1:200) with anti-mouse conjugated Alexa Fluor 568 (1:300) secondary. Images **b** and **f** stained using anti-TRPC7 (1:100) with anti-rabbit conjugated Alexa Fluor 546 (1:300) secondary. Images **c** and **g** are the merged images of **a** and **b** and **e** and **f** respectively. Images **d** and **h** are magnified views of the boxed areas in images **c** and **g**. All size bars 10μm.

6.2.4 - TRPC7 Co-localisation Studies

Non-stimulated adult rat cardiomyocytes were stained for both TRPC7 and F-actin using the anti-TRPC7 antibody and rhodamine conjugated Phalloidin. This was carried out to observe if there was any co-localisation between the two, inferring a link between TRPC7 and the actin cytoskeleton. The staining of non-insulin stimulated adult cardiomyocytes for TRPC7 and F-actin, gave no co-localisation of the two structures, F-actin showed localisation to intracellular regions and TRPC7 again displayed PM/ t-tubule region staining (Figure 6.6).

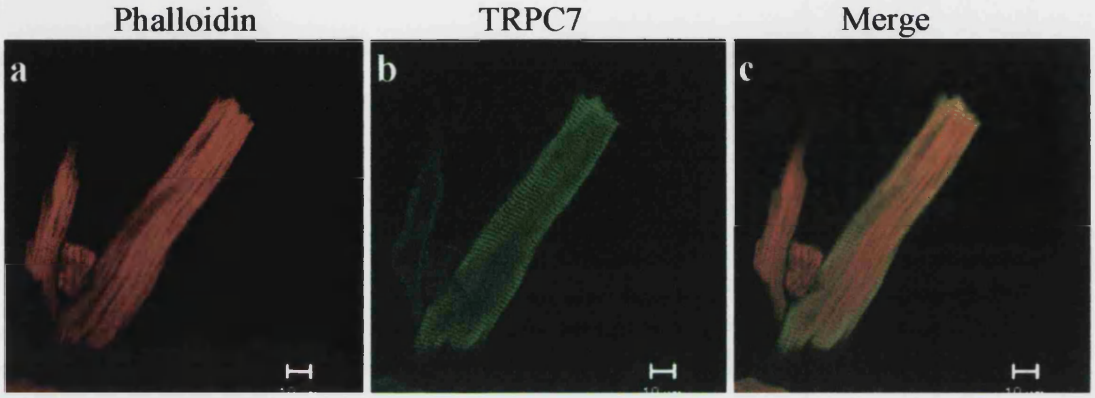

Figure 6.6: Image **a** shows cardiomyocytes stained for F-actin, using Rhodamine conjugated Phalloidin (1:500). Image **b** shows the same cell as **a**, stained using anti-TRPC7 (1:100) with anti-rabbit FITC (1:100) secondary antibody. **c** is the merged images of **a** and **b**. All size bars 10μm.

TRPC7 appeared to be expressed on t-tubules; focal adhesion complexes are also known to be present in the t-tubular structure of cardiomyocytes, acting as part of a scaffold for this structure (with membrane associated proteins and basal lamina proteins) which is usually under constant stresses from excitation-contraction coupling (Brette and Orchard, 2003). The component of focal adhesions, FAK, has been shown previously to co-localise with hTRPC7 in the human pancreatic cell line, Panc-1 (Chapter 5 Figure 5.5). Adult rat cardiomyocytes were therefore stained for TRPC7 and FAK. The staining of non-stimulated adult cardiomyocytes for TRPC7 and FAK (Figure 6.7) showed total co-localisation of the two proteins. Co-localisation between TRPC7 and FAK has been observed previously in Panc-1 cells (see Chapter 5, Section 5.2.2), but due to limitations on resources it was not possible to carry out an immunoprecipitation experiment on cardiomyocytes for these two proteins.

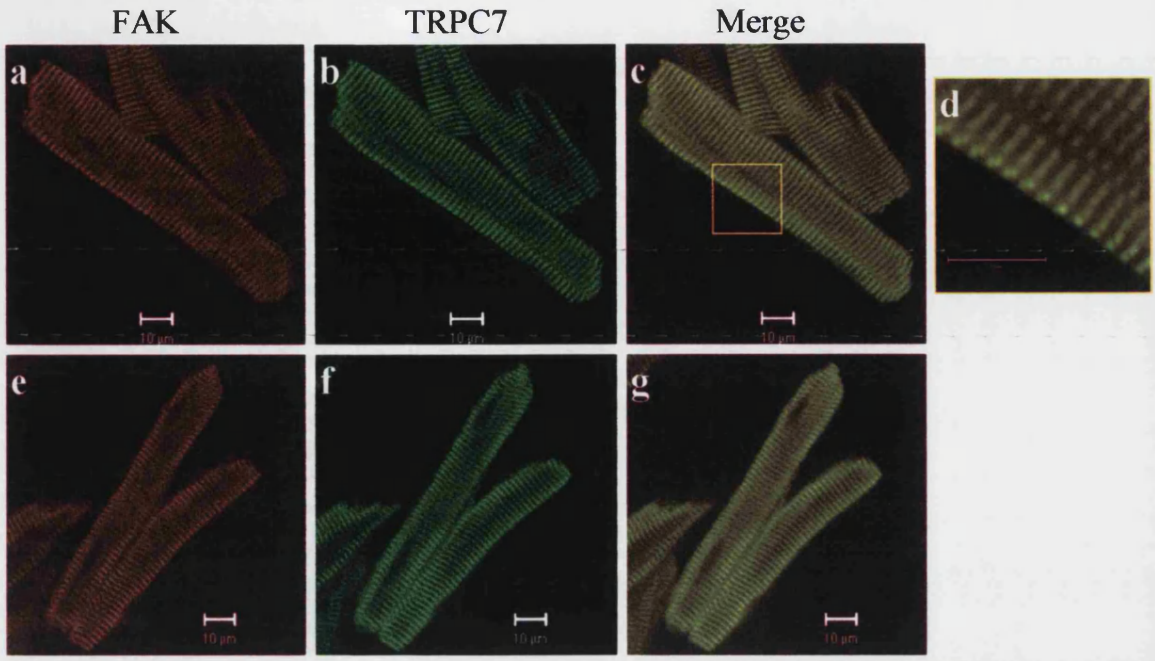

Figure 6.7: Images **a** and **e** show cardiomyocytes stained using anti-FAK (1:50) with anti-mouse conjugated Alexa Fluor 568 (1:300) secondary antibody. Images **b** and **f** are the same cardiomyocytes as **a** and **e** respectively and are stained using anti-TRPC7 (1:100) with anti-rabbit conjugated Alexa Fluor 546 (1:300) secondary antibody. **c** and **g** are the merged images of; **a** and **b**; **e** and **f**; respectively. Image **d** is a magnified view of image **c**. All size bars 10μm.

6.2.5 - Western Blotting

Western blots of adult and embryonic rat cardiomyocyte lysates were carried out, using Panc-1 cell membranes as a positive control. Western blotting was carried out in order to determine if the 100kD TRPC7 band could be observed in adult and embryonic cardiomyocyte lysates as this would reinforce the hTRPC7 expression detected by immunofluorescence.

Western blotting of adult and embryonic rat cardiomyocyte lysates using Panc-1 membrane as a positive control (Figure 6.8) showed that, when probed with anti-TRPC7 a similar band of approximately 100kD as produced by Panc-1 was present in the adult and embryonic cardiomyocytes. This band was not present when blots were probed with the pre-immune serum or peptide control solution.

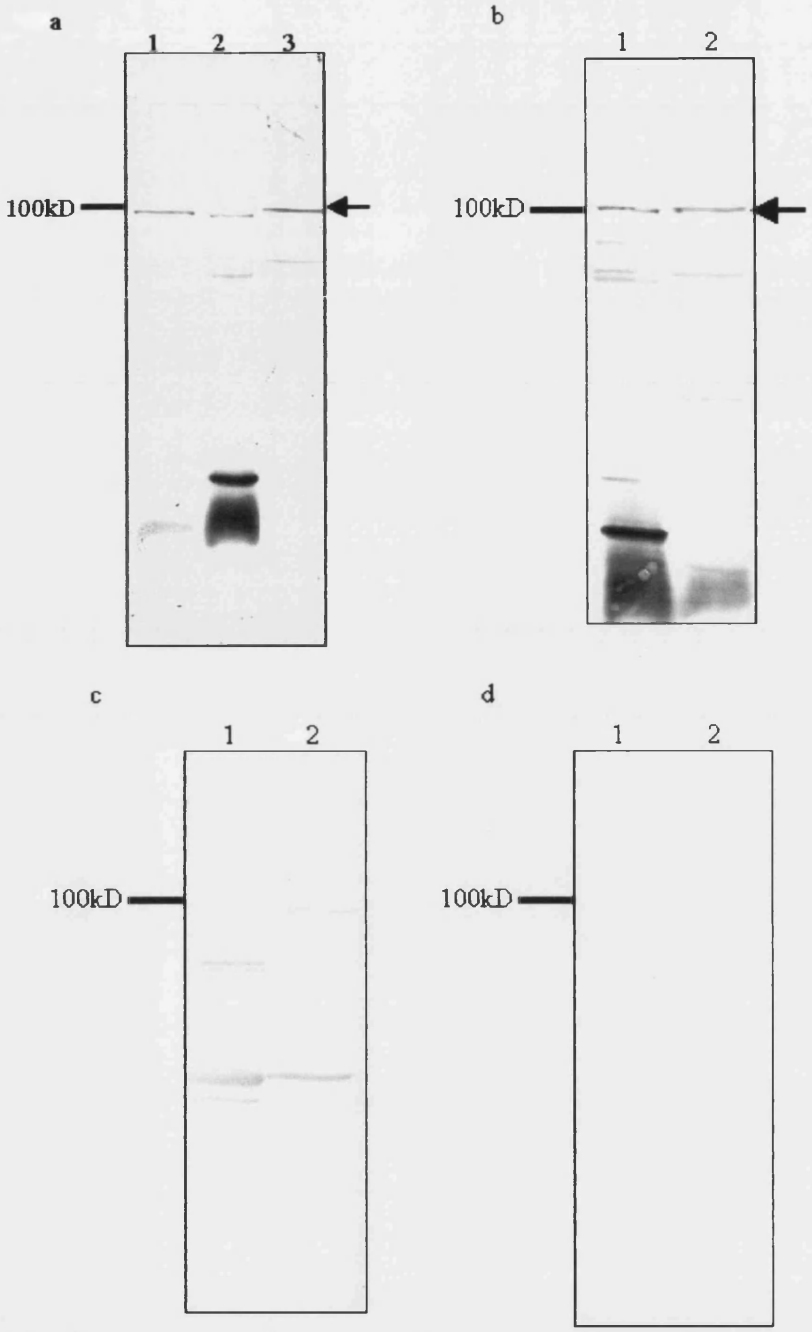

Figure 6.8: Western blot of **a** adult cardiomyocytes in lane 1, cultured embryonic cardiomyocytes in lane 2 and Panc-1 membrane in lane 3 (10μg of protein was loaded into each lane). Blots **b, c** and **d** show cultured embryonic cardiomyocytes in lane 1 and adult cardiomyocytes in lane 2 (10μg of protein was loaded into each lane). Blots **a** and **b** were probed with anti-TRPC7 (1:1000), blot **c** with pre-immune serum (1:1000) and blot **d** with the peptide control solution.

6.2.6 - TRPC7 in 3T3-L1 Adipocytes

3T3-L1 cells are a mouse fibroblastic cell line that is often used as a model for differentiation, as they can be stimulated to differentiate into 3T3-L1 adipocytes. Having observed a difference in expression levels of TRPC7 from the non-insulin responsive embryonic cardiomyocytes (low expression) to insulin sensitive adult cardiomyocytes (high expression) and a difference in localisation of TRPC7 in what were thought to be de-differentiating embryonic rat cardiomyocytes, 3T3-L1 cells were studied for the expression and localisation of TRPC7 at specific time points before, during and after differentiation. GLUT4 has been used in this case as a general cell marker, but not as a marker for differentiation.

Staining for TRPC7 in 3T3-L1 fibroblasts differentiating into adipocytes (Figure 6.9) showed the development of TRPC7 reactivity as the differentiation process occurs. At day 0 there was no indication of TRPC7 expression, however as the cells differentiated into adipocytes they began to express TRPC7. By day 12 of differentiation the 3T3-L1 cells were fully differentiated and staining for TRPC7 showed an intracellular, possibly Golgi apparatus localisation of the protein. GLUT4 expression also increased with differentiation into adipocytes, however the protein did not co-localise with TRPC7 and was diffusely localised throughout intracellular regions. In all cells observed, staining by the anti-TRPC7 antibody appeared to give quite a high level of background fluorescence.

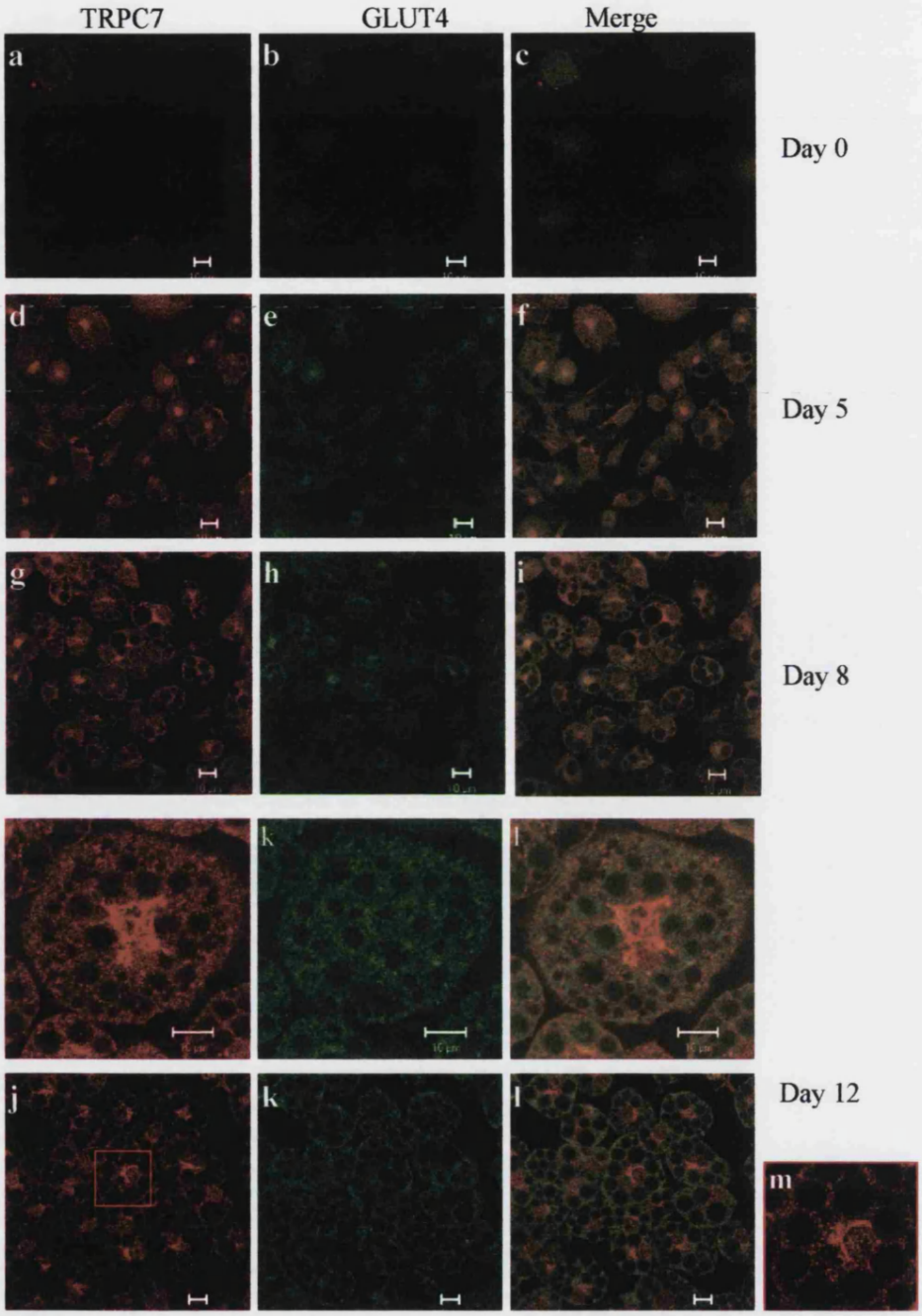

Figure 6.9: 3T3-L1 fibroblast differentiation in to adipocytes. The top row of images show 3T3-L1 fibroblasts at day 0 of the differentiation process. The second row of images shows 3T3-L1 cells at day 5 in the differentiation process and the third row of images shows 3T3-L1 cells at day 8 in the differentiation process and the fourth and fifth rows of images show 3T3-L1 cells at the final day of differentiation. Images **a**, **d, g** and **j** show staining by anti-TRPC7 (1:100). Images **b**, **e, h** and **k** show the same groups of cells stained using anti-GLUT4 (1:200) with anti-mouse FITC (1:100) secondary antibody. Images **c**, **f, i** and **l** are merged images of; **a** and **b**; **d** and **e**; **g** and **h, j** and **k** respectively. Image **m** is a magnified view of the boxed area in image **j.** All size bars 10μm.

No specific staining was observed when using pre-immune serum at each time point of the differentiation process, only a low-level background fluorescence (Figure 6.10a to l). There was also no specific staining given by the peptide control solution on fully differentiated 3T3-L1 cells (Figure 6.10m to o).

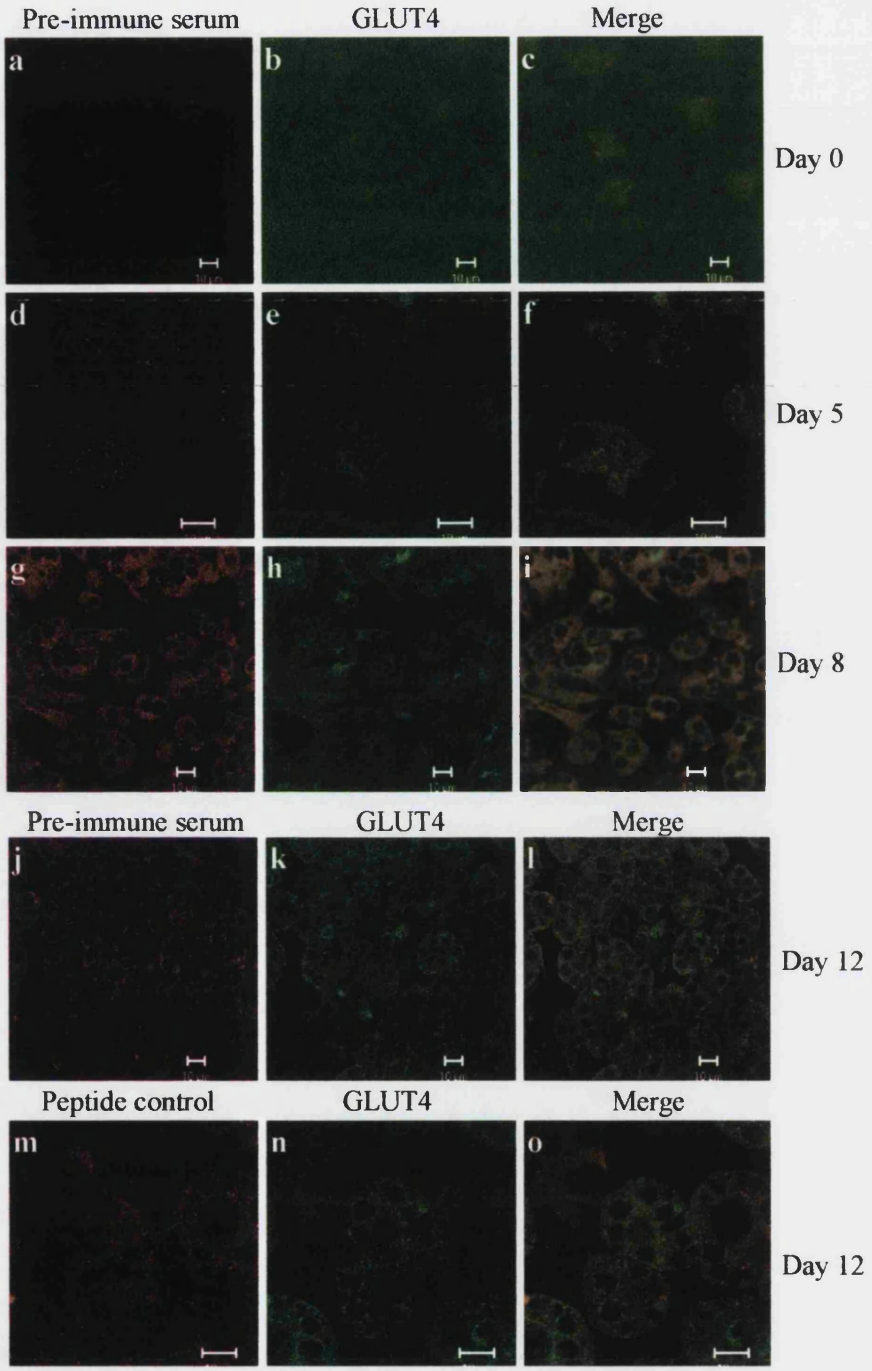

Figure 6.10: The top row of images show 3T3-L1 fibroblasts at day 0 of the differentiation process. The second row of images shows 3T3-L1 cells at day 5 in the differentiation process, the third row of images shows 3T3-L1 cells at day 8 in the differentiation process and the fourth and fifth rows of images show 3T3-L1 cells at the final day of the differentiation process. Images **a**, **d**, **g** and **j** show staining by pre-immune serum (1:100). Image **m** shows staining by the peptide control solution. Images **b**, **e**, **h**, **k** and **n** show the same group of cells stained using anti-GLUT4 (1:200) with anti-mouse FITC (1:100) secondary antibody. Images **c**, **f**, **i**, **l** and **o** are the merged images of; **a** and **b**; **d** and **e**; **g** and **h**; **j** and **k**; and **m** and **n** respectively. All size bars 10μm.

6.2.7 - Co-localisation of TRPC7 with a Golgi Apparatus Protein

Due to the results shown in Figure 6.9 showing an intracellular localisation of TRPC7, co-localisation studies with anti-TRPC7 and a Golgi apparatus marker, anti-58K antibodies, were carried out on undifferentiated and differentiated 3T3-L1 cells. Staining for TRPC7 and the Golgi apparatus (by 58K Golgi marker) of fully differentiated 3T3-L1 adipocytes (Figure 6.11) showed complete co-localisation between TRPC7 and the Golgi apparatus.

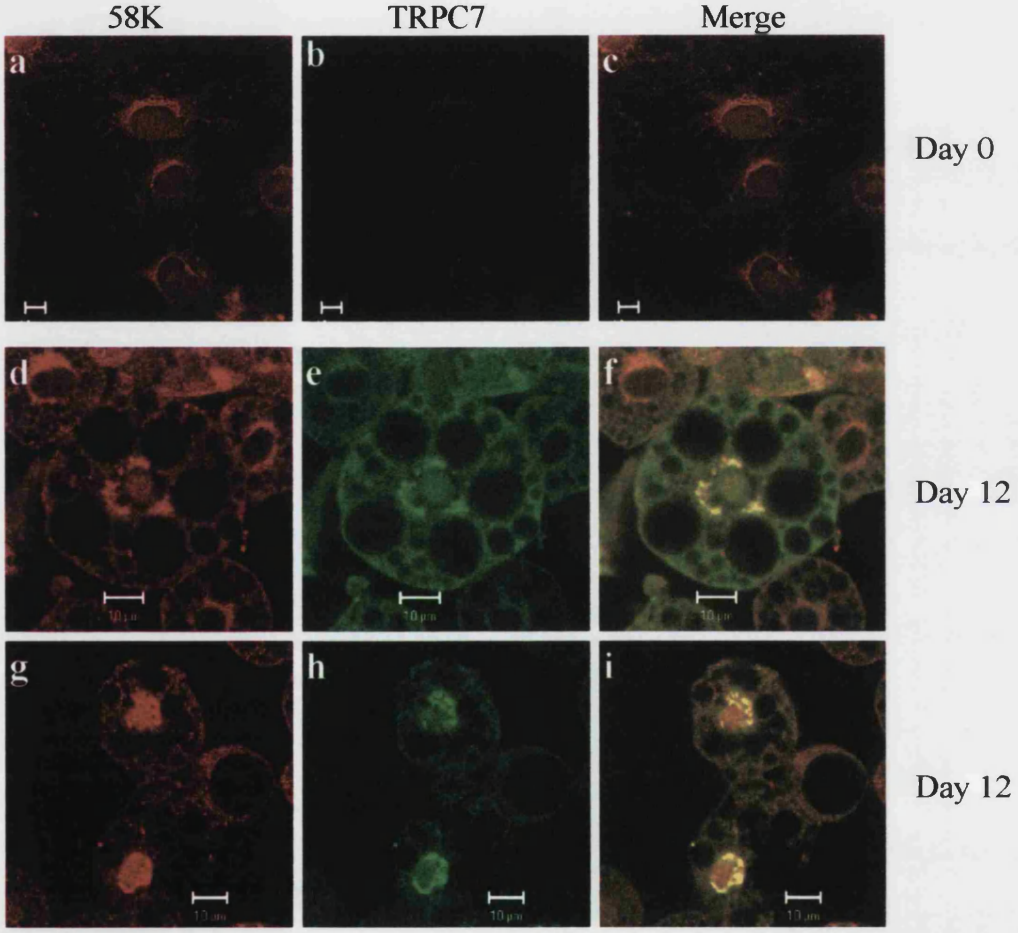

Figure 6.11: The top row of images show 3T3-L1 fibroblasts at day 0 of the differentiation process. The second and third rows of images shows 3T3-L1 adipocytes on the final day of differentiation. Images **a**, **d** and **g** show staining by anti-58K (1:50), a Golgi marker, with anti-mouse conjugated Alexa Fluor 568 (1:300) secondary antibody. Images **b**, **e** and **h** show the same group of cells to **a**, **d** and **g** respectively and are stained using anti-TRPC7 (1:100) with anti-rabbit conjugated Alexa Fluor 546 (1:300) secondary antibody. Images **c**, **f** and **i** are merged images of; **a** and **b**; **d** and **e**; and **g** and **h** respectively. All size bars 10μm.

6.2.8 - Western Blotting

Western blots were carried out on 3T3-L1 cell lysates prepared at the various time points of the differentiation process. Panc-1 cell membranes were used as a positive control. Western blotting of 3T3-L1 cells at the different stages of differentiation (Figure 6.12) showed an increased expression of an approximately 100kD TRPC7 band from day five to the end of differentiation, comparable to that given by Panc-1 membrane, when probed with anti-TRPC7 antibody (Figure 6.12a, d and e). However, the TRPC7 band obtained from the 3T3-L1 lysate appeared to have a slower migration in comparison to the Panc-1 membrane. Controls blots probed with pre-immune serum and peptide control solution showed no presence of the band (Figure 6.12b and c). All blots showed the presence of many background bands, this is reflected in the immunocytochemistry (Figure 6.9) those bands heavier than TRPC7 in the differentiating 3T3-L1 cells also appear to increase in expression as the differentiation time course continues.

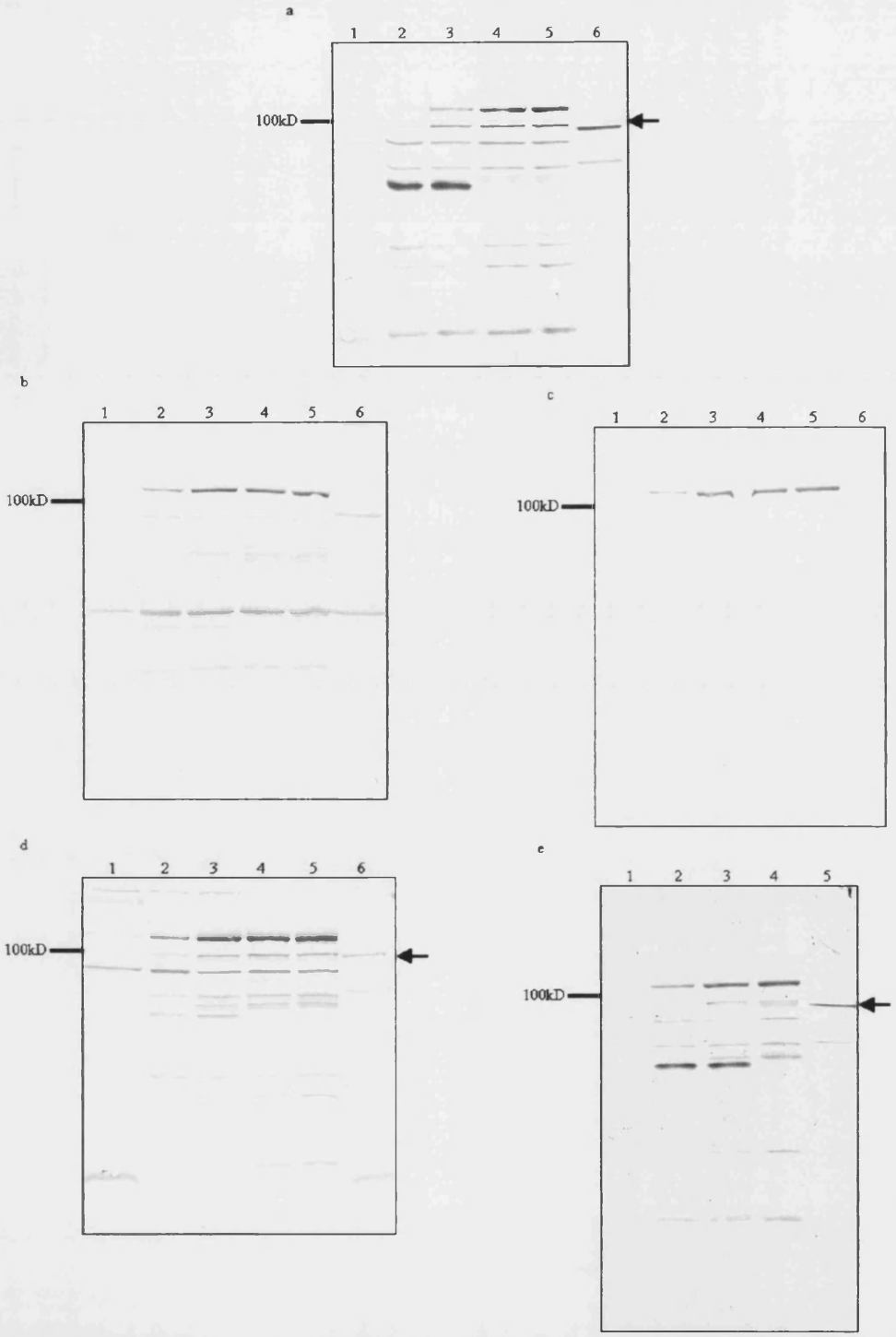

Figure 6.12: Western blots, a, b, c and d show; 3T3-L1 lysates at time points of differentiation; in lane 1, day 0; lane 2, day 5; lane 3, day 8; lane 4, day 12; lane 5, day 12; lane 6, Panc-1 membrane. Blot e shows 3T3-L1 lysates at time points of differentiation in lane 1 day 0; lane 2 day 5; lane 3 day 8; lane 4 day 12; lane 5 Panc-1 membrane. Blots a, d and e were probed with anti-TRPC7 (1:1000). Blot b was probed with pre-immune serum (1:1000) and blot c was probed with the peptide control solution. In all cases 10μg of protein was loaded into each lane. The 100kD band thought to represent TRPC7 is indicated with an arrow.

6.3 - Discussion

The results in this chapter show that embryonic and adult rat cardiomyocytes express endogenous TRPC7 that can be detected by the anti-TRPC7 antibody. Embryonic cardiomyocytes cultured for up to one week showed staining for TRPC7 on a small percentage of two cell types within the culture. One cell type appeared to be a typical rod shaped structure characteristic of the ventricular myocyte; these cells accounted for less than 5% of the culture and usually occurred in small clusters of cells. TRPC7 expression in these cells appeared to be striated in a transverse manner across the cell (Figures 6.1a, b, 6.2a to f). There did not seem to be any co-localisation between TRPC7 and the glucose transporter protein, GLUT4 (Figure 6.2) however, GLUT4 is not highly expressed in embryonic cardiomyocytes, instead the levels increase post-natally (Abel, 2004). Control experiments using the pre-immune serum did not give any specific staining and appeared to be a low-level background stain (Figure 6.2g to i). Other cell types in the culture, the majority of which were probably fibroblasts, showed a low-level background stain; also the nucleoli were often stained in these cell types (Figure 6.1c). The second cell type that displayed expression of TRPC7 were cells that had many 'spiky' membrane protrusions, these cells had punctate staining for TRPC7 on the cell body and all the protrusions were also stained; in addition these cells gave nucleolar staining (Figure 6.1d). These cell types may have possibly been de-differentiating cardiomyocytes, a process which begins with the loss of the typical rod shape morphology, changes in the cytoskeleton such as changes in expression of myosin subtypes leads to the formation of pseudopodial extensions (Thum and Borlak, 2000). Healthy, well cultured cardiomyocytes should not contract however, de-differentiating cardiomyocytes display a change in electrical conductivity and a significant increase of beats per minute (Thum and Borlak, 2000). It is known that embryonic ventricular cardiomyocytes as well as adult atrial cardiomyocytes lack the sophisticated t-tubular system that is characterised by the transverse striations across the cells (Brette and Orchard, 2003). This may explain why the embryonic cardiomyocyte culture had very few cells that displayed the specific pattern of apparently t-tubular staining using the anti-TRPC7 antibody.

Adult rat ventricular myocytes, fixed and stained shortly after isolation, also displayed strong staining for TRPC7 (Figure 6.3a to d), and the expression was confirmed to be in the PM region by z-sectioning the cells (Figure 6.4). The pattern of staining was similar to that of some of the embryonic cardiomyocytes, TRPC7 was in a pattern of transverse striations across the cell membrane and appeared to be localised to the t-tubules. Control staining by the pre-immune serum did not give any staining specificity, only a low-level background stain was apparent (Figure 6.3e).

Atrial and ventricular cells have differing morphologies. Ventricular cells have a t-tubular system that is well established and highly important for function but atrial cells have a sparse t-tubular system (Brette and Orchard, 2003). T-tubules are invaginations of the surface membrane (sarcolemma) of the cardiomyocyte, as the name suggests they occur in a transverse nature over the sarcolemma however, they also have a longitudinal element (Brette and Orchard, 2003). T-tubules develop after birth; there is very little evidence of ventricular t-tubule development in neonatal hearts (Brette and Orchard, 2003). The t-tubule system maintains a remarkable degree of structure considering the forces exerted on it during the contraction cycle, this is largely due to a number of 'scaffold' proteins of focal adhesion molecules, membrane associated proteins and basal lamina proteins (Kostin et al., 1998). Previous results from studies in the pancreas in the current investigation (Chapter 5) hTRPC7, has already been shown to be closely localised to focal adhesions. The localisation to the t-tubules of TRPC7 in rat ventricular myocytes may also reflect an association with focal adhesions.

Western blots carried out on adult and embryonic rat cardiomyocyte lysates (Figure 6.8) both yielded a band of 100kD comparable to that of Panc-1 membrane when probed with anti-TRPC7, confirming the presence of TRPC7. The band was not present when blots were probed with pre-immune serum or peptide control solution. It is clear from the results gained in this study that the full-length version of TRPC7 is expressed, because of the 100kD band obtained from the Western and also from this it indicated that there may not be any expression of the splice variants TRPC7A or B.

Co-staining the adult rat ventricular myocytes for TRPC7 and GLUT4 in a non-insulin stimulated state showed little co-localisation of the two proteins (Figure 6.3). GLUT4 was concentrated in a peri-nuclear region of the cells with very little at the periphery of the cell (Figure 6.3a to d). Stimulation of the cells with insulin at two different concentrations caused the translocation of more GLUT4 to the PM, as expected (Figure 6.5). There was very little difference in the localisation of GLUT4 when stimulated with the more physiological level of insulin (30nM) or the higher concentration (60nM). As previously discussed, the TRPs have been implicated in non-selective cation currents in guinea pig ventricular myocytes, activated in response to insulin (Zhang and Hancox, 2003). From these results it is not possible to offer any correlation between the channels in guinea pig ventricular myocytes and the localisation of TRPC7 in rat ventricular myocytes. Further functional studies are needed (either by patch-clamp or fluorescent indicator dyes) to confirm that in the rat cardiomyocytes a non-selective cation current is generated by insulin stimulation. To further assess the role of TRPC7 in such currents, specific, as yet unknown channel blockers would be required or RNAi carried out on TRPC7 in cardiomyocytes however they have been shown to be a difficult cell type to transfect into. Transfections into cardiomyocytes have been successfully carried out with use of the Lenti virus, however the longer the incubation with the virus for transfection the more the insulin receptors on the cell decrease in their responsiveness to insulin (Blesch, 2004).

As a control, co-staining for TRPC7 and F-actin was carried out on the adult rat cardiomyocytes; F-actin is a cytoskeletal protein and results from this study show it was localised intracellularly and did not show any co-localisation with TRPC7 (Figure 6.6). Co-staining for TRPC7 and FAK revealed total co-localisation between the two proteins on the PM (Figure 6.7). Co-localisation of TRPC7 and FAK has been observed previously in Panc-1 cells (See Chapter 5 Section 5.2.2), but the immunoprecipitation result gained from Panc-1 cells (see Chapter 5, section 5.2.7) did not show any physical link between FAK and TRPC7 and therefore, a similar result might be expected in this case. Co-localisation of TRPC7 and FAK in ventricular myocytes lends weight to the

hypothesis that TRPC7 is expressed in the t-tubules of cardiomyocytes. T-tubules are highly structured invaginations of the surface membrane of cardiomyocytes, and they are known to be supported by a scaffold of focal adhesion molecules, membrane associated proteins and basal lamina proteins (Brette and Orchard, 2003; Kostin et al., 1998). The structure and function of focal adhesions is described fully in Section 5.3 of Chapter 5. Cardiomyocytes have focal adhesions not only at their distal ends for cell-cell adhesion but they also form cytoskeletal-sarcolemmal attachments in register with the t-tubules, known as costameres, that help to support the t-tubules (Sharp et al., 1997). A study of 3 to 4 day old rat pup cultured cardiomyocytes revealed staining by anti-β_1-integrin and anti-vinculin (Sharp et al., 1997) to be very similar to the staining gained in this study using anti-TRPC7 and anti-FAK. Results in the current study suggest that TRPC7 may be involved in some way with the focal adhesion proteins associated with the t-tubular structure of cardiomyocytes. Associations of Ca^{2+} channels and focal adhesions have been discussed in Chapter 5, however at this point it is unclear whether the role of TRPC7 is the same in human pancreas and rat heart. It is possible that TRPC7 in the rat heart may regulate the disassembly of focal adhesions via activation of Ca^{2+}-dependent calpain as it is known that calpain inhibition stabilises focal adhesion complexes that contain vinculin and integrin, two proteins which are integral components of the focal adhesion complex in cardiomyocytes (Huttenlocher et al., 1998; Palecek et al., 1998; Sharp et al., 1997). Alternatively, as previously suggested, the focal adhesions may regulate the localisation and activation of Ca^{2+} channels, for example, TRPC7 (Davis et al., 2001).

The TRPCs have often been implicated in signalling pathways that involve $InsP_3$, however the role of $InsP_3$ and $InsP_3Rs$ in cardiomyocytes is controversial and not fully understood. It is known that both atrial and ventricular myocytes express type II $InsP_3Rs$ and high concentrations of $InsP_3$ can cause Ca^{2+} release (Bers, 2002) and the $InsP_3Rs$ co-localise with junctional RyRs (Lipp et al., 2000). The Ca^{2+} signalling pathway involving $InsP_3$ in cardiomyocytes is the same as described in Chapter 1 Section 1.2.4 and many hormones activate it (eg adrenaline/ noradrenaline) (Bers, 2002). Many believe that $InsP_3$ has little, if any role in cardiac excitation-contraction coupling, but may be involved in

other discrete spatial and functional roles such as transcription regulation pathways (Bers, 2002). However, evidence from Mackenzie et al and Lipp et al suggests that $InsP_3$ may play a modulatory role in cardiac excitation-contraction coupling, the close proximity of RyRs and $InsP_3Rs$ it is thought that the activation of $InsP_3R$ and subsequent release of Ca^{2+} activates RyRs and enhances excitation-contraction coupling (Lipp et al., 2000; Mackenzie et al., 2002). TRPC7 may have some role to play in this enhancement of excitation-contraction coupling either in a capacity as a SOC to replenish SR levels of Ca^{2+} or as a RACC to further increase levels of Ca^{2+} for excitation-contraction coupling.

To further confirm the expression of TRPC7 in cardiomyocytes RNAi experiments could be carried out and to find whether or not TRPC7 plays a role in the regulation of focal adhesions (or vice versa) in cardiomyocytes RNAi of the various focal adhesion proteins could be carried out to observe possible changes in localisation or expression of TRPC7. However, primary rat cardiomyocytes are difficult cells to transfect into and in the absence of a specific channel blocker for TRPC7 it may be difficult to assess the role the channel has to play.

In the 3T3-L1 cells TRPC7 was not present in the undifferentiated form of the cell however upon differentiation into adipocytes TRPC7 staining is observed from approximately day five onwards, increasing in amount until all cells are fully differentiated, although there did appear to be a high-level of background fluorescence in these cells (Figure 6.9). The specific staining was unlike any previously seen in this study, there was not any PM staining and TRPC7 appeared to be totally intracellular mainly localised to the Golgi apparatus (Figure 6.11). There was low-level background fluorescence observed after treatment by either the pre-immune serum or peptide control solution showing that the TRPC7 antibody was responsible for the staining pattern observed (Figure 6.10). Western blotting results confirm the immuno-staining results with the presence of an approximately 100kD band on Western blots probed with the TRPC7 antibody (Figure 6.12). 10μg of protein was loaded in each lane and there was an apparent increase in intensity of the TRPC7 band with the increasing differentiation and the TRPC7 band was not present when blots were probed with pre-immune serum or

peptide control solution. A number of background bands were also observed and are reflected in the high level of background fluorescence in the immunofluorescent staining. The TRPC7 bands in 3T3-L1 lysates migrated more slowly than that of the positive control, Panc-1 membrane, this band has been calculated to be approximately 109kD. There are a number of reasons why TRPC7 in this cell type may be heavier; some form of post-translational modification, for example, phosphorylation or glycosylation of the protein or binding of an unknown protein. There are known binding sites for CaM on TRPC proteins and it has been predicted that the 17kD CaM binds tightly to native TRPC1 causing a slight band shift in comparison to over expressed TRPC1 (Beech et al., 2003). With the current evidence CaM may not be the reason behind the band shift because of the differences in the observed molecular weight.

Ca^{2+} signalling in adipocytes has been studied with a view to determine the signalling events associated with stimulation by insulin to allow the uptake of glucose and secretion of leptin. This Ca^{2+} signalling is mainly carried out through VOCCs (Cammisotto and Bukowiecki, 2004) and is described in Chapter 1 Section 1.2.5.1. However, there appears to be very little else known about other signalling roles of Ca^{2+} and expression of Ca^{2+} channels in adipocytes. The Golgi localisation of TRPC7 in differentiated 3T3-L1 adipocytes could facilitate the entry of Ca^{2+} into or out of the Golgi depending on its orientation in the Golgi membrane, as the Golgi is a known store of Ca^{2+}. This may be linked with a regulatory role associated with the Ca^{2+} signaling involved in insulin stimulation, glucose uptake and leptin secretion. To test this RNAi could be carried out on TRPC7 in differentiated 3T3-L1 adipocytes and functional experiments carried out to analyse the Ca^{2+} levels in response to insulin stimulation, compared to wild type 3T3-L1 adipocytes. It would also be of use to study the expression of TRPC7 in primary adipocytes as a comparison to the 3T3-L1 adipocytes, this may indicate whether TRPC7 has a role to play in differentiation or is an integral part of adipocytes.

Evidence gathered in this current study suggests that the anti-TRPC7 antibody cross-reacts with endogenous TRPC7 in mouse and rat, and that endogenous TRPC7 may be expressed in two important insulin sensitive tissues, the heart and adipose tissue of the rat

and mouse respectively. Recent research goes towards backing up the TRPC7 t-tubule localisation, cellular sub-fractionation experiments involving differential centrifugation and subsequent Western blot analysis showed almost all TRPC7 to be in the same fraction that displaying Ca^{2+}-ATPase activity and contains the majority of myofilaments, TRPC7 probably remained tightly associated with myofilaments and the SR probably in the dyadic structure (S Lawrence Unpublished data). TRPC7 appeared not to be in the PM fraction indicated by the marker protein Na^{+}/K^{+} ATPase (S Lawrence Unpublished data). TRPC7 also appeared not to be present in fractions containing intracellular components such as endosomes (S Lawrence, Unpublished data). However, from these preliminary results gathered it is unclear what role TRPC7 plays in the rat cardiomyocyte. From co-localisation experiments in the current study TRPC7 and FAK have been shown to co-localise, a similar observation has been made in the human pancreatic cell line, Panc-1 (Chapter 5). From the results gathered from Panc-1 cells it was not possible to be certain of an involvement for TRPC7 in focal adhesion complexes and the same is true for cardiomyocytes. TRPC7 may have a similar role to play in cardiomyocytes as hTRPC7 in Panc-1 cells, or it may fulfil a different function. TRPC7 is also endogenously expressed by 3T3-L1 adipocytes and the localisation in 3T3-L1 cells appeared to be predominantly Golgi, this was only apparent after beginning differentiation from fibroblasts into adipocytes. These preliminary results indicate that *trpc7* is up-regulated during differentiation however further analysis is required to establish what role TRPC7 has in this cell type. The current study has utilised rat and mouse tissues to observe expression of TRPC7, and although in human heart and adipose tissues hTRPC7 is thought not to be endogenously expressed to the extent that mTRPC7 is in the equivalent rodent tissues it would be interesting to carry out localisation studies of hTRPC7 in human heart and adipose to compare with the mouse and rat data.

Chapter 7

TRPC7 Expression in the Pituitary Gland and Central Nervous System

7.1 - Introduction

7.1.1 - Pituitary Gland

The pituitary gland is situated below, and attached to, the base of the brain and is gently held in a cradle of bone at the base of the skull (Bear et al., 1996a; Berne and Levy, 1998). The pituitary has two lobes; posterior and anterior, both of which are controlled by the hypothalamus (Bear et al., 1996a; Berne and Levy, 1998). The posterior pituitary is controlled by the magnocellular neurosecretory neurons from the hypothalamus, which release neurotransmitters (NT) directly into the capillaries in the posterior pituitary (Berne and Levy, 1998). These transmitters, oxytocin and vasopressin, act like hormones and as such are termed neurohormones (Bear et al., 1996a; Berne and Levy, 1998). Oxytocin is released during the final stages of childbirth and also stimulates the ejection of milk from the mammary glands; vasopressin (also called anti-diuretic hormone) regulates blood volume and salt concentration (Bear et al., 1996a; Berne and Levy, 1998). The anterior pituitary is an actual endocrine gland; it synthesises and secretes a wide array of hormones that regulates hormone secretions from other endocrine glands in the body (Bear et al., 1996a; Berne and Levy, 1998). Anterior pituitary hormones act on the gonads, thyroid, adrenal glands and mammary glands (Bear et al., 1996a; Berne and Levy, 1998). The hypothalamus regulates the anterior pituitary by secreting hypophysiotropic hormones, which can inhibit or trigger the release of pituitary hormones (Berne and Levy, 1998). Due to its links to the brain and its endocrine function the pituitary is often termed 'neuroendocrine' (Bear et al., 1996a; Berne and Levy, 1998). There are cell lines available to study the pituitary; the GH4C1 cell line is an anterior pituitary tumour cell line from the rat. It is adherent, its morphology is epithelial and it secretes prolactin (PRL) and growth hormone (GH) (somatotrophin) (ECACC).

The role of Ca^{2+} has been researched in many different pituitary cell types and it is largely VOCCs that have been characterised, however SOC may also be implicated in sustained Ca^{2+}influx in some types of pituitary cells (Ashworth and Hinkle, 1996; Bear et al., 1996b; Carew and Mason, 1995).

7.1.2 - Central Nervous System

The cerebral cortex is divided into three types; hippocampus, olfactory cortex and neocortex (Bear et al., 1996b). The neocortex is only found in mammals and is the upper most layer of the cerebral cortex, it is this that is referred to when the term 'cortex' is used (Bear et al., 1996b). The cortex is primarily comprised of neurons and glia. The spinal cord is an area of the CNS that relays information from the peripheral and visceral nervous system to the brain; it is comprised of primarily neurons and glia. Ca^{2+} signalling in the CNS is well documented (Bear et al., 1996b). The release of NTs is mediated by Ca^{2+}, it is triggered by an action potential that depolarises the membrane and causes the VOCCs to open allowing a large, rapid influx of Ca^{2+} (Bear et al., 1996b). The elevation in internal Ca^{2+} causes NTs to be released from synaptic vesicles by exocytosis (Bear et al., 1996b). At the post synaptic membrane of a dendrite or other cell there are many neurotransmitter receptors (NTR), these NTRs can be divided into two subgroups; transmitter gated ion channels and GPCRs (Bear et al., 1996b). Transmitter gated ion channels such as acetylcholine receptor (AChR) and glutamate gated ion channels are relatively non-selective ion channels with five membrane spanning, pore forming subunits that open due to a conformational change elicited by a NT (Bear et al., 1996b). Depending on whether their effect is inhibitory (γ-aminobutyric acid; GABA) or excitatory (glutamate), these channels can cause membrane de- or hyper-polarisation. GPCRs have a longer lasting and more diverse repertoire of post synaptic actions, the NT binds to a GPCR on the post synaptic membrane and initiates the cascade of Ca^{2+} signalling events described in Section 1.2.4 of Chapter 1. When the Ca^{2+} is released from internal stores it goes on to mediate several cellular processes (Bear et al., 1996b).

Tissue distribution studies of hTRPC7 in the pituitary and CNS have shown the mRNA to be present in relatively high amounts in the pituitary and in lower amounts in the CNS (Riccio et al., 2002a); Chen Unpublished data). However, mTRPC7 expression is very low in the mouse CNS and there is no data on the presence of mTRPC7 in the pituitary (Okada et al., 1999). However, *htrpc7* was first isolated and cloned from human brain cDNA (A.Wolstenholme Unpublished Data) and our laboratory has expertise in neuronal cultures of embryonic rat brain. Two areas, cortex and spinal cord, were investigated. The

studies described in this chapter are aimed to examine the expression and localisation of TRPC7 in the rat pituitary and the cultured neurons and glia of the cortex and spinal cord of embryonic rats.

7.2 - Results

7.2.1 - Endogenous Expression of TRPC7 in the GH4C1 Cell Line

To identify any expression of TRPC7 in the rat GH4C1 cell lines, immunocytochemistry was carried out. The immuno-localisation of TRPC7 in GH1C4 rat pituitary cells showed a defined intracellular localisation of a defined structure adjacent to the nuclei of the GH4C1 cells (Figure 7.1a to d). This staining was not apparent when the cells were treated with the pre-immune serum (Figure 7.1e), however there was a high level of background staining.

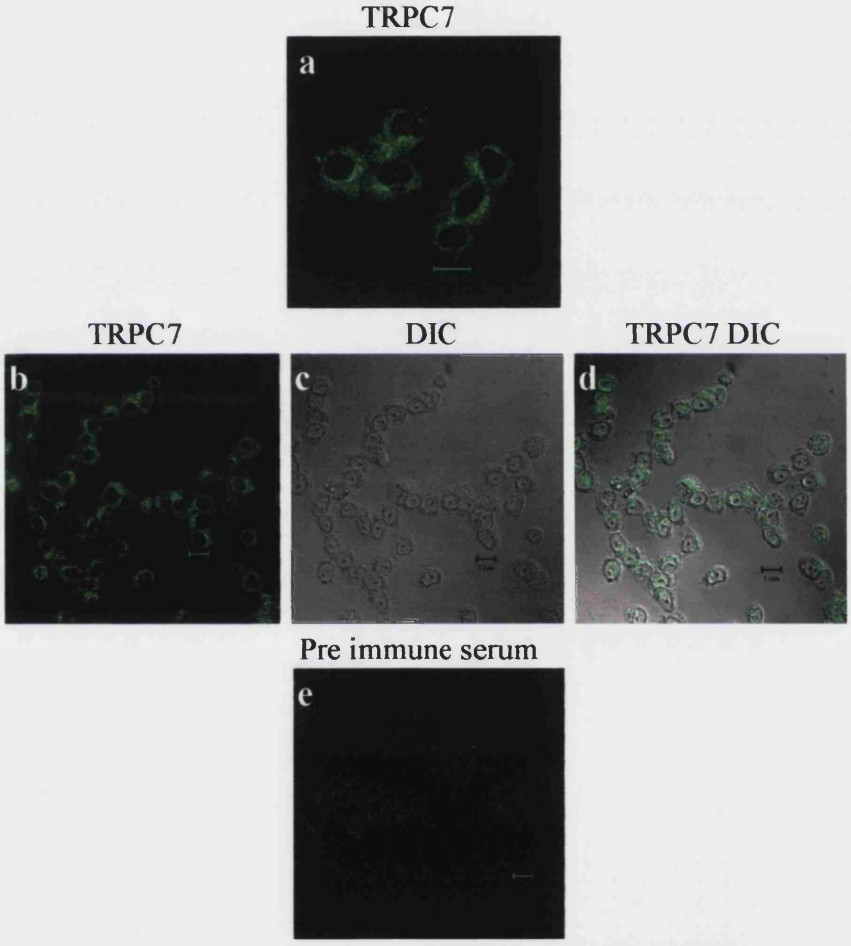

Figure 7.1: Images **a** and **b** are GH1C4 cells stained using anti-TRPC7 (1:100) with anti-rabbit FITC (1:100) secondary. Image **c** is the DIC image of **b** and **d** shows the merged image of **b** and **c**. Control staining of GH1C4 cells. Image **e** shows staining of pre-immune serum (1:100) with anti-rabbit FITC (1:100). All size bars 10μm.

7.2.2 - TRPC7 is Present in the Golgi Apparatus in GH4C1 Cells

The intracellular localisation of TRPC7 was similar to a Golgi apparatus pattern of staining therefore, co-localisation studies were carried out using markers for the *trans*- and *cis*-Golgi networks.

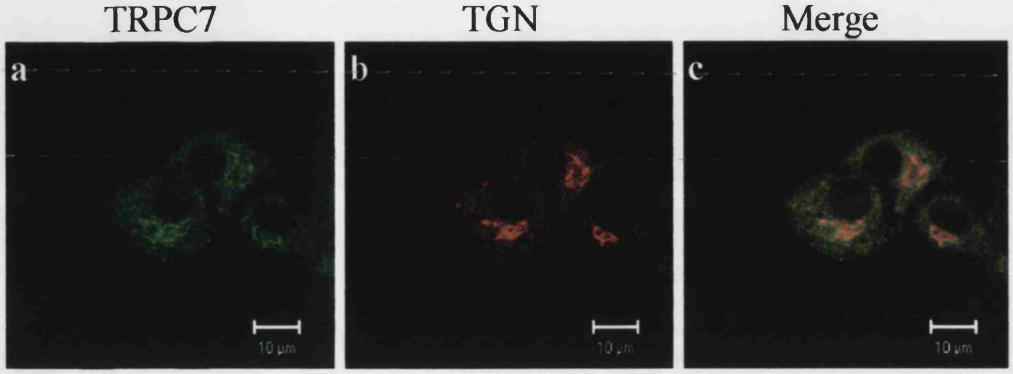

Figure 7.2: Image **a** GH4C1 cells stained with anti-TRPC7 (1:100) with anti-rabbit FITC (1:100); and anti-TGN38 (1:200) staining of image **b**, the same cells as **a**, with anti-mouse Texas Red (1:100) secondary. Image **c** is the merged image of **a** and **b**. Size bars 10µm.

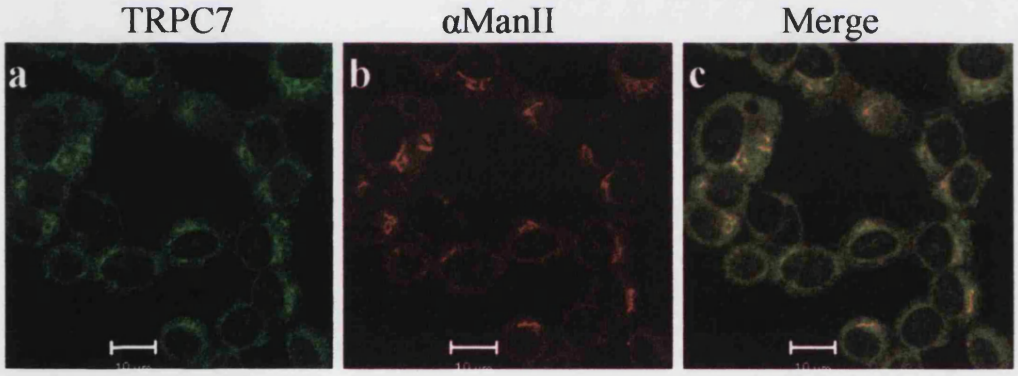

Figure 7.3: Image **a** GH4C1 cells stained with anti-TRPC7 (1:100) with anti-rabbit FITC (1:100); and anti-α-Mannosidase II (neat supernatant) staining of image **b**, the same cells as **a**, with anti-mouse Texas Red (1:100) secondary. Image **c** is the merged image of **a** and **b**. Size bars 10µm.

Co-localisation studies with the *cis*- and *trans*-Golgi markers anti-α-Mannosidase II (αManII, Figure 7.3) and anti-TGN38 (Figure 7.2) respectively, revealed semi co-localisation of TRPC7 and the TGN marker (Figure 7.2). It appeared as though TRPC7 and TGN38 were interlocked but not on the same part of the structure. However, there was almost complete co-localisation of TRPC7 and the *cis*-Golgi marker (Figure 7.3).

7.2.3 - Western Blots

Western blots were carried out to visualise the endogenous expression of TRPC7 in GH4C1 cells as a 100kD band. An equal protein load of Panc-1 membrane was run along side as an endogenous positive control.

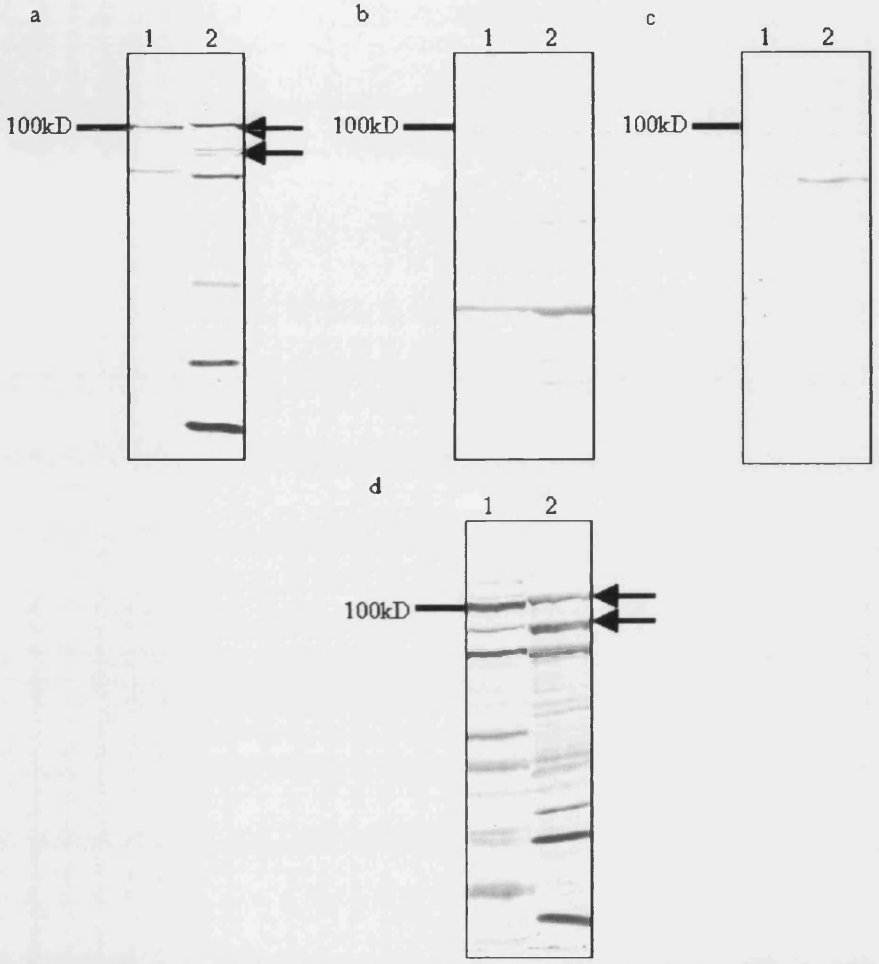

Figure 7.4: Western blot of GH4C1 lysate. Lane 1 Panc-1 membrane; lane 2 GH4C1 lysate. **a**, **b** and **c** have 10μg protein loaded, **d** has 20μg protein loaded. Blots **a** and **d** (**d** is slightly over developed) have been probed with anti-TRPC7 (1:1000), blot **b** has been probed with pre-immune serum and blot **c** has been probed with peptide control solution. Arrows indicate bands of approximately 108kD (upper) and 93kD (lower) for lane 2 of blots **a** and **d**.

Western blots of GH4C1 lysate, probed with anti-hTRPC7 (Figure 7.4) showed a band of approximately 100kD, however in comparison to the band given by Panc-1 membrane (lane 1), it appeared that TRPC7 in GH4C1 has a slightly higher molecular weight, of approximately 108kD. A few other bands developed on the blot and were thought to be back ground bands however, the band indicated by the second (lower) arrow is approximately 93kD and may indicate the presence of splice variants hTRPC7A or B, or both (the same band in Figure 7.4a is a double band). The control blots did not show the presence of a band at 100kD when probed with pre-immune serum or peptide control solution. There were a number of background bands produced by the GH4C1 cell lysate, this was more obvious in the blot that was over developed (Figure 7.4d), some of these background bands were present on the control blots, probed with the pre-immune serum and the peptide control solution (Figure 7.4b and c). The immunocytochemistry carried out also indicated the presence of high-level background staining by the anti-hTRPC7 antibody and the pre-immune serum (Figure 7.1).

7.2.4 - TRPC7 in Embryonic Rat Spinal Cord Cultures

Embryonic rat spinal cords were cultured for up to two weeks and investigated for their expression of TRPC7.

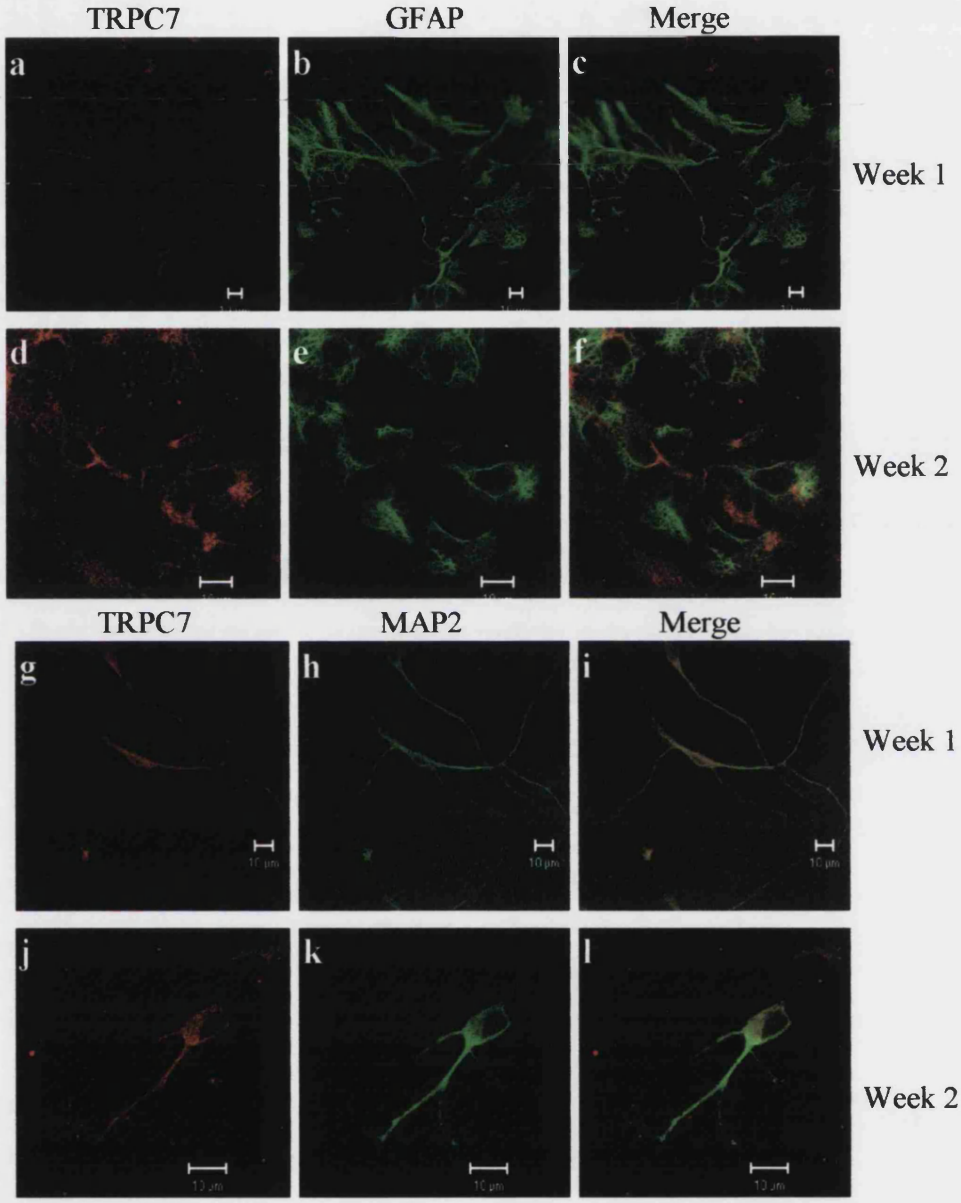

Figure 7.5: Embryonic rat spinal cord cultures, in culture for 1 or 2 weeks. Images **a** and **d** show staining by anti-TRPC7 (1:100). Images **b** and **e** are the same cells as **a** and **d** respectively and show staining by anti-GFAP (1:100) anti-mouse FITC secondary. **c** and **f** show the merged images as **a** and **b**; and **d** and **e** respectively. Images **g** and **j** show staining by anti-TRPC7 (1:100). Images **h** and **k** are the same cells as **g** and **j** respectively and show staining by anti-MAP2 (1:100) anti-mouse FITC secondary. **i** and **l** show the merged images as **g** and **h**; and **j** and **k** respectively. All Size bars 10μm.

The staining of cultured rat embryonic spinal cord for TRPC7 (Figure 7.5) did not show any presence of the protein at week one but by week two there was a small amount of staining in glial cells (shown by the glial marker anti-GFAP). However, the low-level staining was also present in the neurons (indicated by neuronal microtubule marker anti-MAP2). The staining pattern did not appear to be specific and may reflect a high level of background staining.

Control staining of spinal cord by pre-immune serum (Figure 7.6) showed a low-level background fluorescence with no apparent specific pattern, similar to that observed in Figure 7.5.

Figure 7.6: Control staining of embryonic rat spinal cord by pre-immune serum (1:100) anti-rabbit FITC secondary (1:100). Size bar 10μm.

7.2.5 - TRPC7 in Embryonic Rat Cortex

Embryonic rat cortices were cultured for up to two weeks and investigated for their expression of TRPC7.

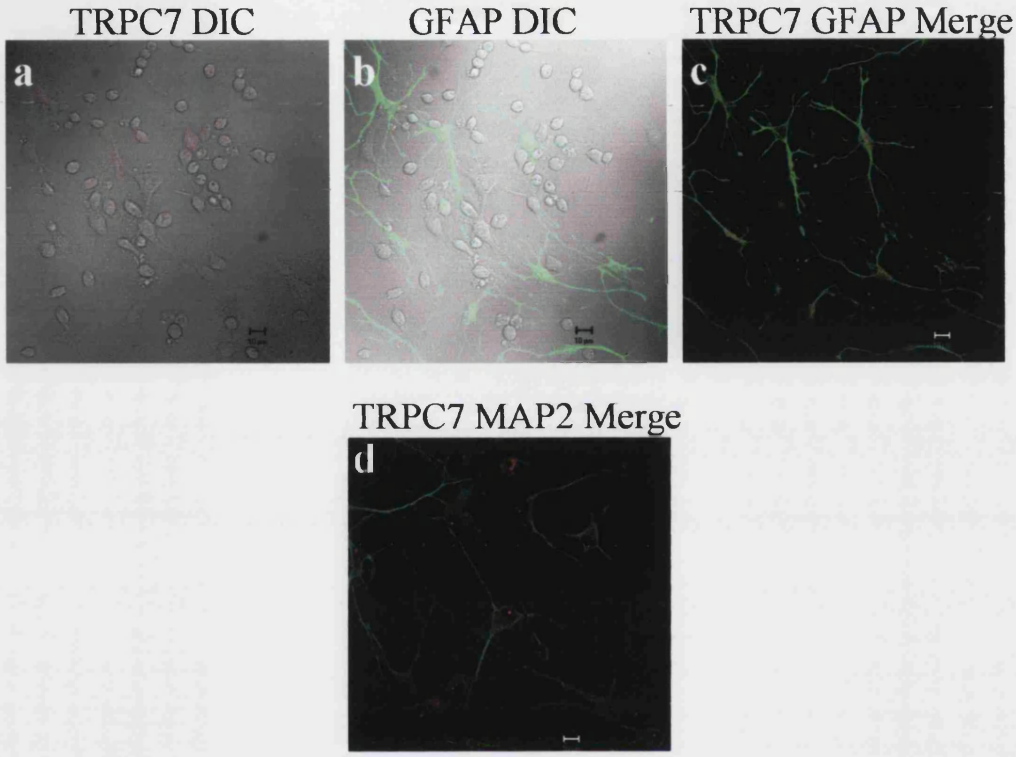

Figure 7.7: Embryonic rat cortical cultures, in culture for 1 week. Image **a** shows staining by anti-TRPC7 (1:100). Image **b** is the same cell as **a** and shows staining by anti-GFAP (1:100) anti-mouse FITC secondary. **c** show the merged image of **a** and **b**. Image **d** is stained using anti-TRPC7 (1:100) and anti-MAP2 (1:100) with anti-mouse FITC (1:100). All Size bars 10μm.

Embryonic rat cortical cultures showed very little staining for TRPC7 (Figure 7.7), though low-level background fluorescence was observed on neuronal and glial cells.

Control staining of the cortical culture was carried out using pre-immune serum and a similar low-level background to that seen in Figure 7.7 was obtained using pre-immune serum (Figure 7.8).

Figure 7.8: Embryonic rat cortical 1 week old culture with staining by pre-immune serum (1:100) Alexa Fluor 488 (1:300) secondary and anti-GFAP (1:100) anti-mouse FITC secondary. All Size bars 10μm.

7.2.6 - Western Blotting

Western blots were carried out to confirm the results of the immunocytochemistry, positive controls used for the Western blotting of spinal cord and cortical lysates were GH4C1 cells and Panc-1 membranes.

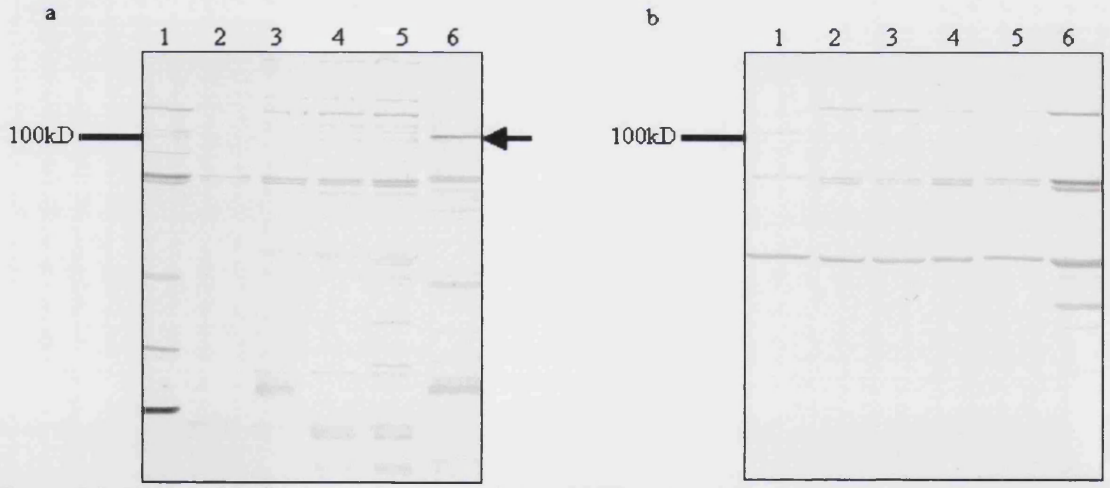

Figure 7.9: Lane 1 GH1C4 lysate; lane 2 week 1 cultured cortex; lane 3 week 2 cultured cortex; lane 4 week 1 cultured spinal cord; lane 5 week 2 cultured spinal cord; lane 6 Panc-1 membrane. Blot **a** was probed with anti-TRPC7 (1:1000) and blot **b** was probed with pre-immune serum (1:1000).

Both GH4C1 lysate and Panc-1 membranes revealed the 100kD TRPC7 band when probed with anti-TRPC7 (Figure 7.9). However, in contrast the spinal cord and cortical

culture lysates showed no TRPC7 band when probed with anti-TRPC7 or the pre-immune serum.

7.3 - Discussion

The results in the present study show that the rat pituitary cell line, GH4C1 expresses TRPC7 and this appeared to be localised to the Golgi apparatus. The *cis*-Golgi network marker co-localised well with TRPC7 (Figure 7.3), whereas the *trans*-Golgi network marker showed an adjacent, interlocking pattern with TRPC7 (Figure 7.2). The Golgi apparatus pattern of staining for TRPC7 has also been observed in differentiated 3T3-L1 adipocytes (see Chapter 6). Control experiments using pre-immune serum (Figure 7.1e) did not show this staining pattern suggesting that the antibody is detecting TRPC7 in the GH4C1 cells. Western blotting of GH4C1 lysate (Figure 7.4) confirmed the presence of TRPC7 giving an approximately 100kD band. However, when compared to the band from Panc-1 membranes, the GH4C1 TRPC7 band ran at a slightly higher molecular weight, which may indicate some form of additional post translational modification, for example, differences in glycosylation between the Golgi and the PM, or binding of an unknown protein. This shift has also been observed with the Western blot of differentiated 3T3-L1 adipocytes (see Chapter 6). There are known binding sites for CaM on TRPC proteins and it has been predicted that the 17kD CaM binds tightly to native TRPC1 causing a slight band shift in comparison to over expressed TRPC1 (Beech et al., 2003). It may be that the band shift of TRPC7 observed in the current study reflects binding by CaM, though the band seen on the Western blot was calculated to be 108kD, indicating a band shift of 8kD so this is currently inconclusive. However, to produce these results a standard SDS-PAGE gel and molecular weight markers that covered a broad range (Precision Protein Standard, BioRad) were used. If more accurate markers could be used, a more accurate molecular weight of TRPC7 in GH4C1 cells could be calculated. The difference between the bands of GH4C1 lysate and Panc-1 membrane may be due to cellular localisation. The western blots appear to be inconclusive for the presence of TRPC7 splice variants A, B or γ as there were many spurious 'background' bands produced, this may be due to anti-hTRPC7 or the secondary antibody used. Two of the most prominent bands were calculated to have molecular weights of approximately 93kD and 78kD, it is unlikely that the 78kD band is a TRPC7 splice variant however, it is possible that the 93kD band may reflect the presence of TRPC7A or B (predicted

molecular weights of 92.4 and 93.4 respectively). Control Western blotting (Figure 7.4) did not give a TRPC7 band when probed with pre-immune serum or the peptide control solution. The Western blots all showed a high level of background bands (Figure 7.4), this is reflected in the immunocytochemistry shown in Figure 7.1 where, as well as the Golgi localisation there is some background intracellular fluorescence apparent. The Golgi localisation of TRPC7 in GH4C1 (the Golgi is a known store of Ca^{2+}) could facilitate the entry of Ca^{2+} into or out of the Golgi depending on its orientation in the Golgi membrane.

In the anterior pituitary gland ATP plays an important role in Ca^{2+} signalling (Koshimizu et al., 2000). Adenosine receptors ($P_{2Y}Rs$) and receptor channels ($P_{2X}Rs$) are expressed on anterior pituitary cells and ATP is the agonist for all $P_{2Y}Rs$ and $P_{2X}Rs$ (Koshimizu et al., 2000). The biological actions of ATP are terminated by ectonucleotidases which degrade extracellular ATP to adenosine, thereby activating G-protein coupled adenosine receptors (Koshimizu et al., 2000). Additionally, GH4C1 cells possess two populations of VOCCs, one is preferentially modulated by dihydropyridine Ca^{2+} channel modulators (Matteson and Armstrong, 1986).

Previously, functional experiments have been carried out on pituitary cells. One study used lactotrophs (adenohypophysical cells that synthesise and secrete PRL), freshly isolated from lactating female rats in order to identify the thyrotropin releasing hormone (TRH)-sensitive Ca^{2+} entry pathway (Carew and Mason, 1995). TRH causes an increase in intracellular Ca^{2+} from the release of Ca^{2+} via intracellular stores and the entry of extracellular Ca^{2+} (Carew and Mason, 1995). The study produced evidence that the influx of Ca^{2+} in these cells was via a SOC (Carew and Mason, 1995) however, no molecular identification of the channel has been made. From the results shown here it is possible that TRPC7 or other members of the TRPC subfamily could contribute to this channel. Future studies could test this hypothesis, for example; RNAi could be carried out on pituitary cells and the calcium re-addition protocol with the use of TG or CPA (detailed in Chapter 2, Section 2.3.7), carried out on them, alongside the WT cells, to determine if there is any difference in the SOC response.

Another study involved GH4C1 cells incubated in Ca^{2+} free medium for several days, which led to the production of PRL being reduced dramatically. Subsequent re-addition of Ca^{2+} caused a large increase in the rate of PRL synthesis (Matteson and Armstrong, 1986). Although in the current study a PRL secreting cell line was used, future work could involve isolation of primary cells from the rat pituitary and identification of TRPC7 and other TRPCs through immunocytochemistry and Western blotting, furthermore RNAi could be applied to assess whether TRPC7 contributes to the production of PRL or other Ca^{2+} signalling pathways.

Tissue distribution of human TRPC mRNAs in the CNS and pituitary has shown TRPCs 1, 3 and 7 to be very highly expressed in the pituitary gland; hTRPC1, 3 and 5 also had high expression in the cerebellum (detailed in Chapter 1 section 1.5.3; Riccio et al 2002 Mol Brain Res). All other brain regions and spinal cord showed relatively low expression of all the TRPCs, in particular TRPCs 6 and 4 showed very low expression in the pituitary, all brain regions and spinal cord (detailed in Chapter 1 section 1.5.3; (Riccio et al., 2002b). In a more specific study involving single cell RT-PCR, Sergeeva et al found all seven TRPCs mRNAs in the rat dorsal raphe and ventral tegmental area neurons and TRPCs 1, 4, 5, 6 and 7 in the neurons of the tuberomamillary nucleus (Sergeeva et al., 2003). Expression of TRPC7 mRNA in the human CNS is relatively low in comparison to other TRPCs (Riccio et al., 2002b); Chen Unpublished data).

Immunocytochemical studies of cultured embryonic rat spinal cord and cortex by anti-TRPC7 (Figures 7.5 and 7.7) showed only faint background staining over neurons and glia in the culture, which appeared to be enhanced after two weeks in the spinal cord culture. The Western blots from spinal cord and cortical cultures (Figure 7.9) did not give a 100kD TRPC7 band as observed in Panc-1 membrane or GH4C1 lysate, when probed with the TRPC7 antibody. From these results TRPC7 is probably not present, or it is present in very low levels, in the neurons and glia of the cortex and spinal cord. These results appear to echo the Northern blot data obtained from mouse, showing relatively small expression levels of TRPC7 in mouse brain (Okada et al., 1999). An investigation

into the expression and selective association of TRPC proteins appears to show (by Western blot) the presence of TRPC7 in adult rat synaptosome preparation from the cerebellum (Goel et al., 2002). Future studies could investigate TRPC7 expression in the culture of embryonic rat cerebellum and immunolocalisation experiments to directly compare adult and embryonic rat cerebellum, if TRPC7 is present, it may not develop until neonatal or adult stages of life.

Other TRPCs have been functionally implicated in various signalling systems of the CNS. Although TRPC7 may not be highly expressed in the CNS, TRPC5 may be important; TRPC5 has been specifically implicated in the regulation of hippocampal neurite length and growth cone morphology in rat neurons, dominant negative TRPC5 expression allowed significantly longer neurites and filopodia to form (Greka et al., 2003). TRPC4 is thought to contribute to the control of GABA release from the dendrites of thalamic interneurones (Munsch et al., 2003). TRPC1 is expressed in peri-synaptic regions of cerebellar parallel fibre-Purkinje cell synapse and is physically linked to and is activated by the metabotrophic glutamate receptor 1 (mGluR1) (Kim et al., 2003). However, TRPC7 expression has been investigated in the peripheral nervous system as has that of many of the other TRPCs. The investigation carried out by Buniel et al was an immunolocaliation study of the rat carotid chemosensory pathway. The authors have interpreted the diffuse, faint staining over all cell types in the study by their TRPC7 antibody (discussed in Chapter 5) as showing TRPC7 to be present in the neurones of the ganglia (Buniel et al., 2003). As there are no supportive results it is not easy to say whether the faint staining seen was that of TRPC7 or background. Other TRP subfamilies have been implicated in the peripheral nervous system, TRPMs have been identified as components of cold and taste sensation pathways (Hofmann et al., 2003; McKemy et al., 2002; Perez et al., 2003) and TRPVs are involved in heat, pain and osmotic sensation (Benham et al., 2002; Caterina et al., 2000; Gunthorpe et al., 2002).

Experiments in this current study have been carried out on a rat pituitary cell line, cortex and spinal cord. It has previously been shown from Northern blot and RT-PCR data that there is a high level of expression of TRPC7 in the human pituitary gland but there was

no data concerning expression in the mouse or rat pituitary gland (Riccio et al., 2002a); Chen Unpublished data). In the absence of human pituitary cells for this study the rat cell line GH4C1 was used and found to have a Golgi localisation of TRPC7. TRPC7 in cultures of embryonic rat cortex and spinal cord was not identified, however, it is known to be present is very small amount in these areas of the mouse brain (Okada et al., 1999). Future work could involve the investigation of the localisation of TRPC7 in human brain structures, particularly the pituitary in view of the extremely high expression levels, it would be interesting to see if the protein has the same sub-cellular localisation in the human pituitary gland as rat.

Chapter 8

Discussion

8.1 - Localisation and Functional Characterisation of Over-expressed hTRPC7 and hTRPC7A

Localisation and functional studies have been carried out on over-expressed hTRPC7 and one of its splice variants, hTRPC7A, in HEK293 cells in order to elucidate any differences between the two. hTRPC7A displayed a very similar PM and perinuclear (possibly Golgi) localisation as hTRPC7, which may reflect a similar function between the two proteins when over-expressed. Results from functional studies have indicated that neither of the two proteins appeared to have store-operated channel activities, in direct contrast to results from Riccio et al who found hTRPC7 to be a store-operated Ca^{2+} channel (Riccio et al., 2002). However, further results cannot confirm whether hTRPC7 and hTRPC7A have receptor activated Ca^{2+} channel activity when transiently over-expressed. Some questions need to be addressed in the light of these results: since hTRPC7 and hTRPC7A have a similar localisation pattern when over-expressed, if co-expressed would they interact or co-localise with each other? Would the presence of hTRPC7A in an hTRPC7-hTRPC7A heteromer have an effect on the level of activation in comparison to a homomer of hTRPC7 or hTRPC7A? *In vivo*, are the two proteins expressed in the same tissues, and if so do they co-localise? Does the function of the proteins vary according to the tissue and species expressing them?

8.2 - Localisation of Endogenous hTRPC7 in COS7 Cells and the Implications of hTRPC7C

Results from immunostaining of COS7 cells by the anti-hTRPC7 antibody showed no evidence of endogenous expression of hTRPC7 despite the RT-PCR suggesting otherwise (Wolstenholme Unpublished data) and may indicate that hTRPC7C (also expressed in COS7 cells) is a dominant negative N-terminal fragment in this cell type. Another explanation for the apparent lack of expression of hTRPC7 at the COS7 PM comes from a recent publication by Lussier et al (2005), it has implicated MxA as a potential regulator of the TRPCs (Lussier et al., 2005b). MxA is a member of the dynamin family of GTPases, and is known to have a role in protection of cells against viral infections, it

was shown to have an interaction with the second ankyrin repeat of TRPC6, this interaction enhanced the activity of TRPC6 (Lussier et al., 2005a). The authors suggest that MxA has a role in trafficking of TRPC6 and other TRPCs (Lussier et al., 2005c), this may have an implications for hTRPC7C. The highly truncated hTRPC7C has all three ankyrin repeats as the full length hTRPC7 does however, it is possible that when co-expressed, hTRPC7C interferes with the binding of MxA to the full-length hTRPC7 by competing for the binding sites. This may in turn have implications for the trafficking of hTRPC7 to the PM and, as observed in COS7 cells hTRPC7 may not be expressed at the PM. However, future work should to be carried out to confirm these findings; for example RNAi targeted to hTRPC7C in COS7 cells may lead to an increase in hTRPC7 expression, this may be difficult to do as hTRPC7C is a small fragment.

8.3 - TRPC7 may be Associated with Focal Adhesions in the Pancreas and Cardiomyocytes

The basal PM localisation pattern of endogenous hTRPC7 in Panc-1 and Capan-1 cells was highly reminiscent of focal adhesions and co-staining for hTRPC7 and FAK in Panc-1 cells revealed total co-localisation. TRPC7 also co-localised with FAK in rat ventricular cardiomyocytes. Focal adhesions are known to be present at t-tubules of cardiomyocytes as they help provide a support for the structure (Brette and Orchard, 2003). These results indicated a possible association between TRPC7 and focal adhesion complexes. There are several hypotheses for the co-localisation of TRPC7 with FAK observed in Panc-1 cells and rat cardiomyocytes. Very little is known about associations between focal adhesions and Ca^{2+} signalling, from the limited information available (see Chapter 5 Section 5.3), it is my hypothesis that hTRPC7 may be involved in the disassembly of focal adhesions by Ca^{2+}-dependent calpain as a means of providing Ca^{2+}. Calpain is a protease whose substrates include the focal adhesion molecules integrin, FAK, ezrin and talin and it appears to have a role in the disassembly of focal adhesions/ complexes (Huttenlocher et al., 1998). I have devised three hypotheses pertaining to the functional association of TRPC7 with focal adhesions. Hypothesis one (Figure 8.1) is that stimulation of integrins at the cell surface may lead to activation of G-proteins by the

small GTPases in focal adhesion complexes may initiate the activation of PLC to cleave PIP_2 into $InsP_3$ and DAG, this would then lead to the influx of Ca^{2+} by two possible pathways. DAG may then directly activate TRPC7 to allow the influx of Ca^{2+} in a store-independent manner, this Ca^{2+} influx would lead to the activation of calpain and the disassembly of focal adhesions. Alternatively, $InsP_3$ may lead to release of Ca^{2+} stores, through activation of the $InsP_3R$ on the ER; Ca^{2+} from the stores would activate calpain for the disassembly of focal adhesions. The depletion of Ca^{2+} in the ER would lead to a signal being produced, activating TRPC7 allowing the influx of Ca^{2+} to replenish the stores. In figure 8.1 the molecule Src is present, this is because Src is a ubiquitously expressed tyrosine kinase that may also be implicated as calpain cleavage of FAK is enhanced by Src (Carragher et al., 2003). It is also known that Src generally causes a reduction in focal adhesions and decreased cell adhesion and it has been suggested that tyrosine phosphorylation of focal components by Src causes focal adhesion turnover (Wozniak et al., 2004). Furthermore, Src kinase has, in a recent study, been implicated in the regulation of stably expressed TRPC3 in HEK293 cells. TRPC3 is the closest relative of TRPC7 and has been found to be a RACC activated by DAG however, when Src kinase is pharmacologically inhibited or expressed in a dominant negative form, TRPC3 is not activated by DAG in these cell types (Vazquez et al., 2004a).

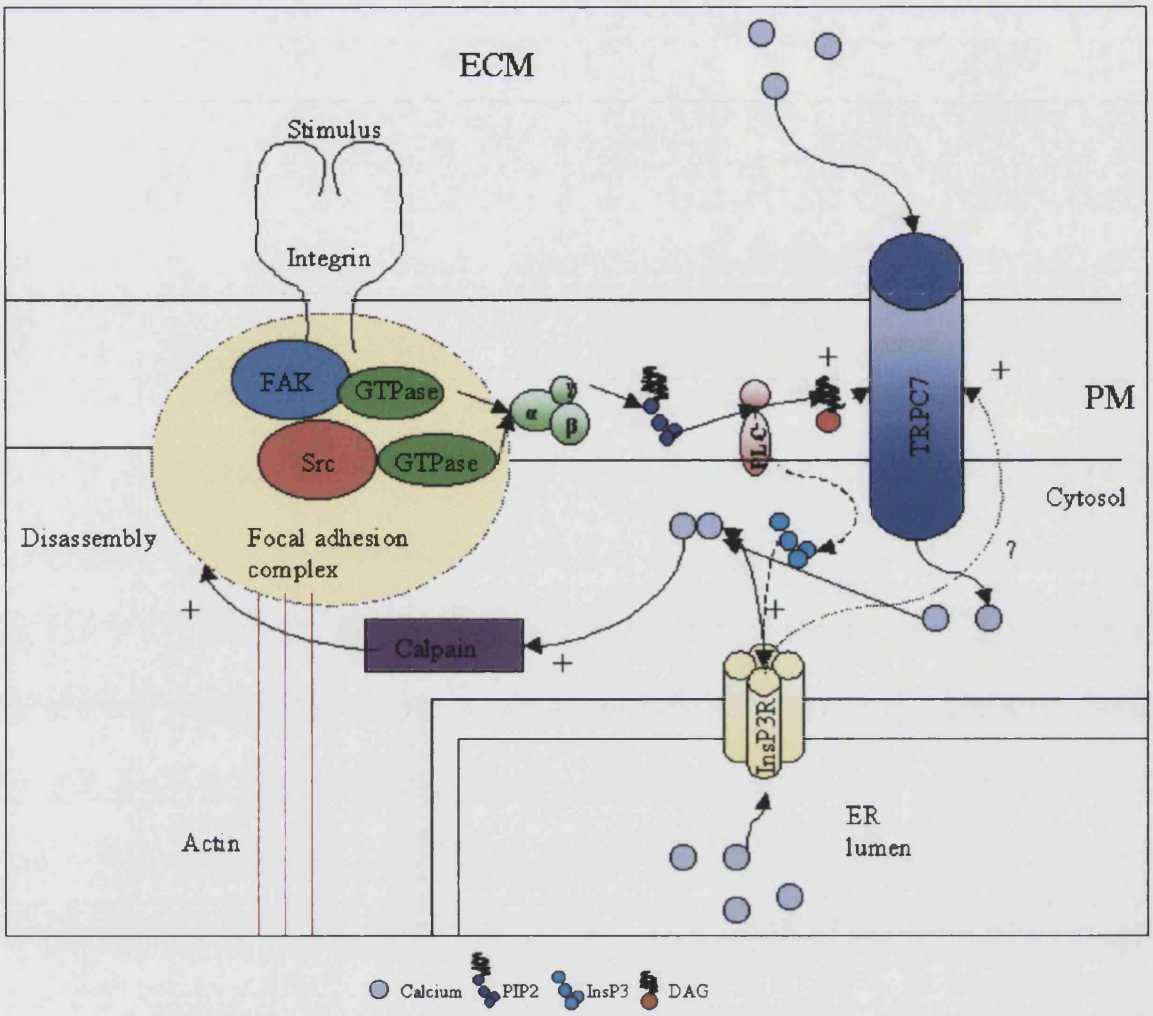

Figure 8.1: Hypothesis one, a schematic diagram of how TRPC7 may be involved in the disassembly of focal adhesions in human Panc-1 cells and rat ventricular myocytes.

Hypothesis two (Figure 8.2) illustrates how direct activation of PLC by the tyrosine kinase, Src, could regulate the channel using the same store depletion dependent or independent pathways as described in hypothesis one.

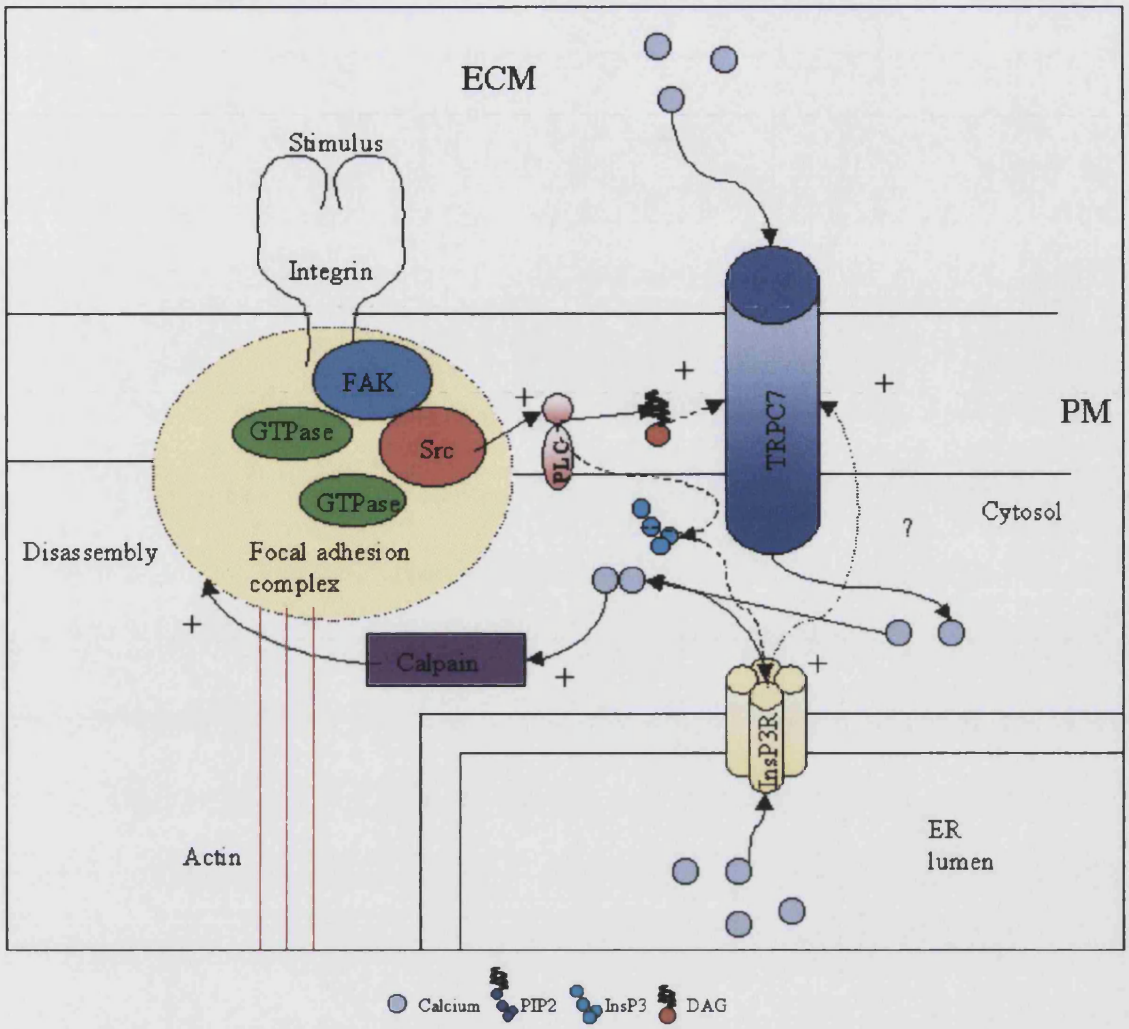

Figure 8.2: Hypothesis two, a schematic diagram of how TRPC7 may be involved in the disassembly of focal adhesions in human Panc-1 cells and rat ventricular myocytes.

Hypothesis three (Figure 8.3) illustrates that Src may in some way directly activate TRPC7 allowing the influx of Ca^{2+} for use by calpain to disassemble focal adhesions.

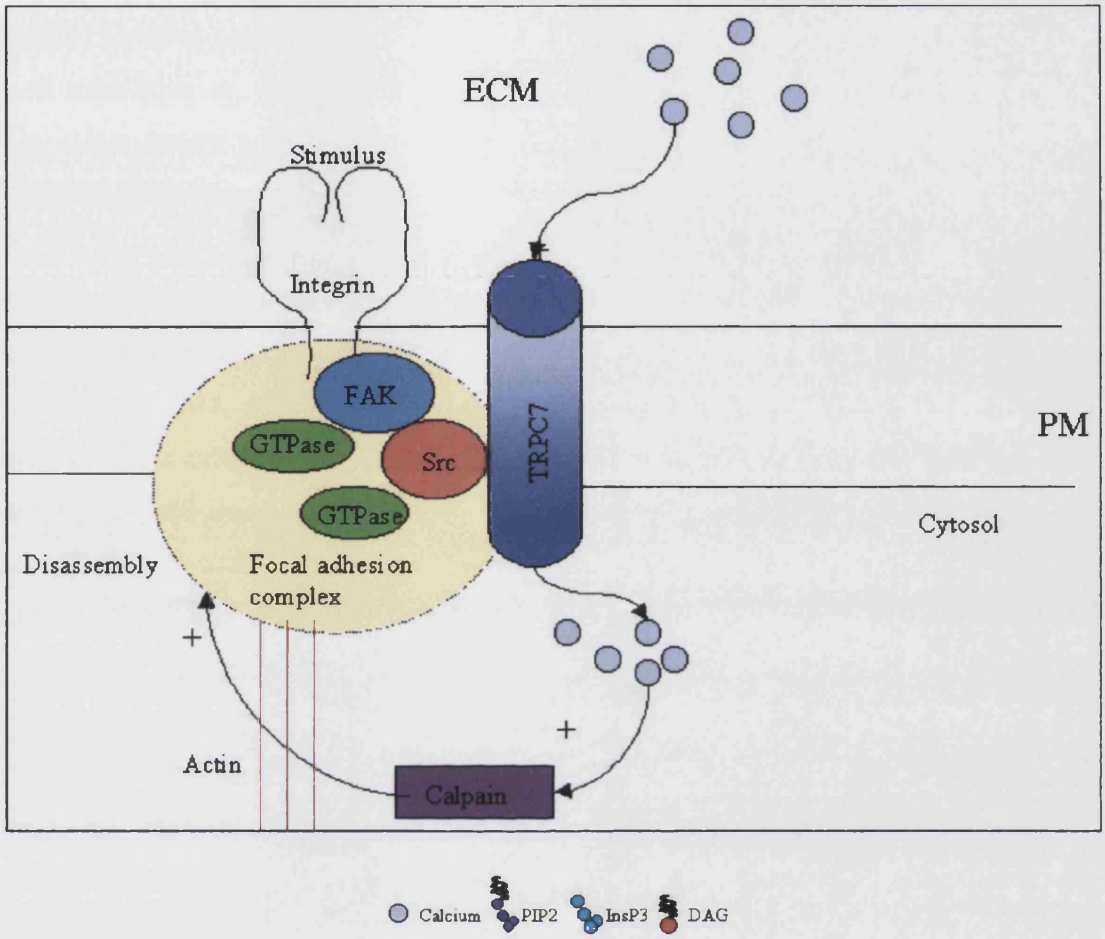

Figure 8.3: Hypothesis three, a schematic diagram of how TRPC7 may be involved in the disassembly of focal adhesions in human Panc-1 cells and rat ventricular myocytes.

Further experimentation is required to ascertain whether TRPC7 is associated with or regulated by focal adhesion complexes or a specific protein of focal adhesions in Panc-1 cells and rat ventricular myocytes. Northern blotting or RT-PCR experiments could be carried out first to confirm the presence of TRPC7 in these cell types and then RNAi could be employed in these cell types to knockdown the expression of TRPC7 to observe any alterations in cell behaviour and focal adhesion localisation. RNAi may prove difficult to do in the rat cardiomyocytes without the use of viral transfection however, a transgenic TRPC7 knockout rat could be made and phenotypic effects could be observed at the global and cellular levels.

Another question associated with this could be asked, could other TRPCs be involved in focal adhesions in other cell types? As previously discussed, TRPC3 in an over-expression system appears to be regulated by Src, an important component of focal adhesions (Vazquez et al., 2004b).

Recent research has identified TRPC1 and TRPA1 to be components of mechanosensitive and stretch activated channels in several different vertebrate cell types (Corey et al., 2004; Maroto et al., 2005). Mechanosensitive and stretch activated channels are involved in cellular functions, such as detection of sound by the ear, regulation of cell volume and cell locomotion (Barritt and Rychkov, 2005). Theories discussed here may put hTRPC7 forward as a candidate to join these TRPs identified as mechanosensitive and stretch activated channel and may indicate a possible involvement in cellular locomotion. The evidence presented by the previous studies relies upon functional analysis but no localisation has been carried out to analyse whether the expression pattern co-localises with known stretch activated channels or associated proteins. However, functional analysis would need to be carried out on TRPC7 in Panc-1 and cardiomyocytes to strengthen the localisation evidence for this theory. As mentioned previously, it is difficult to carry out functional experiments on the endogenous TRPC7 however, in addition to further experiments already outlined the cells could undergo osmotic shock treatment to assess any changes in localisation of the protein and Ca^{2+} influx.

8.4 - TRPC7 may be Involved in the Release of Zymogen Granules in Pancreatic Cells

The pancreas is made up of endocrine islet cells that produce insulin, glugagon, somatostatin and pancreatic polypeptide; and the exocrine cells that secrete the digestive pancreatic juice into the digestive system (Berne and Levy, 1998). The pancreatic juice is made up of aqueous and enzymic components; the aqueous component is secreted by columnar epithelia that line the pancreatic ducts and is made up of Na^+ and K^+ ions that are isotonic to plasma and high levels of bicarbonate and chloride (Berne and Levy,

1998). Acinar cells secrete the enzyme component the polygonal, polarised acinar cells are organised into lobules around the tubules that feed the pancreatic ducts and the enzymes they secrete are important for the digestion of all major foodstuffs (Berne and Levy, 1998). The proteases (secreted in an inactive, zymogen, form) are trypsinogen, chymotrypsinogen and pro-carboxypeptidase (Berne and Levy, 1998). Enteropeptidase in the duodenum activates trypsinogen to trypsin, which in turn activates chymotrypsinogen, and pro-carboxypeptidase to chymotrypsin and carboxypeptidase respectively (Berne and Levy, 1998). Starch molecules are cleaved to oligosaccharides by α-amylase also secreted by the acinar cells, lipases (triacylglycerol hydrolase, cholesterol ester hydrolase and phospholipase A_2) digest lipids, ribonucleases and deoxyribonucleases are also secreted (Berne and Levy, 1998). All enzymes are stored in the zymogen granules in the apical region of the cell before release (Berne and Levy, 1998).

Zymogen granules are released from the cells in response to a stimulus such as hormones or neurotransmitters, this stimulus activates the Ca^{2+} signalling pathway that leads to the release of zymogen granules. Stimulation by an extracellular agonist such as ACh, leads to a rise in apical Ca^{2+} by release of Ca^{2+} from the $InsP_3$ sensitive apical stores by the pathway described in Chapter 1 Section 1.2.4 (Figure 8.4) (Kasai et al., 1993; Thorn et al., 1993). These stores become depleted of Ca^{2+} after stimulation (Sasaki et al., 1996) and must be refilled somehow. It is known that in these cells SOCE occurs predominantly at the basal membrane (Toescu and Petersen, 1995) and by performing patch clamp experiments on pancreatic acinar cells Mogami et al found that by depleting the Ca^{2+} stores in the apical region with thapsigargin, induced focal Ca^{2+} entry through the basal membrane. They hypothesised that an operational tunnel from the basal membrane to the apical stores provided a route for the Ca^{2+} that entered via the SOC (Figure 8.4) (Mogami et al., 1997).

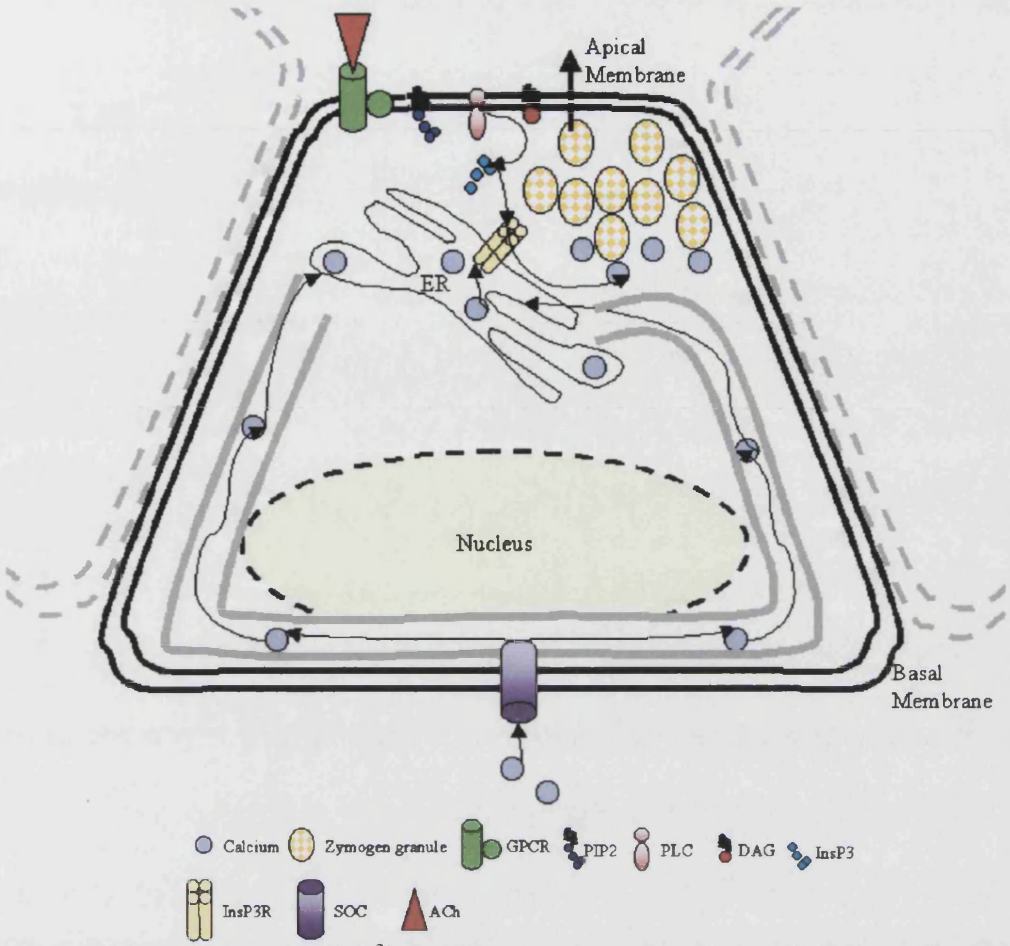

Figure 8.4: A schematic diagram of Ca^{2+} signalling in a pancreatic acinar cell (Not to scale). (Adapted from Mogami *et al* 1997).

Endogenous hTRPC7 expressed by Panc-1 and Capan-1 gave a punctiform staining pattern and was localised to the basal membrane. An alternative hypothesis to explain the pattern of staining on Panc-1 cells I observed is that hTRPC7 could be the focal Ca^{2+} entry channels described by Mogami et al in these cell types and that they refill the Ca^{2+}stores ready for the next stimulation for the release of zymogen granules. However, it is currently unknown whether hTRPC7 is a SOC or a RACC. In order to test this RNAi could be carried out prior to functional experimentation. Also as no candidate protein was put forward or identified by Mogami et al, it would therefore be difficult to carry out co-localisation experiments.

8.5 - TRPC7 may be Involved in Excitation-Contraction Coupling in the Heart

Cardiac excitation-contraction coupling is a process that leads to a heart beat. Ca^{2+} signalling is very important in this process (Bers, 2002a). Ca^{2+} signalling in ventricular myocytes is the combination of Ca^{2+} influx via PM channels and release from the SR at the t-tubules via RyRs to raise the intracellular concentration of Ca^{2+} (Bers, 2002b). The role of $InsP_3$ and $InsP_3Rs$ in cardiomyocytes are not fully understood. $InsP_3Rs$ co-localise with junctional RyRs (Lipp et al., 2000b) and evidence from Mackenzie et al and Lipp et al suggests that $InsP_3$ may play a modulatory role in cardiac excitation-contraction coupling. Because of the close proximity of RyRs and $InsP_3Rs$ it is thought that the activation of $InsP_3R$ and subsequent release of Ca^{2+} activates RyRs and enhances excitation-contraction coupling (Lipp et al., 2000a; Mackenzie et al., 2002). The anti-hTRPC7 antibody was used on insulin sensitive tissue, cardiomyocytes, from rat. There is very little expression of hTRPC7 in human heart, however mouse heart does express high amounts of TRPC7 mRNA (Okada et al., 1999). In treating embryonic rat cardiomyocyte cultures with the anti-hTRPC7 antibody a possibly t-tubular localisation of TRPC7 was observed. Adult rat primary ventricular cardiomyocytes were also treated with the anti-TRPC7 antibody and they were found to have an entirely t-tubular localisation of TRPC7. Due to its localisation, TRPC7 may have some role to play in this enhancement of excitation-contraction coupling either as a SOC to replenish SR levels of Ca^{2+} or as a RACC to further increase levels of Ca^{2+} for excitation-contraction coupling. However, it is not yet known whether endogenous TRPC7 in the rat heart is a SOC or a RACC. RNAi of TRPC7 and subsequent functional studies to ascertain what type of Ca^{2+} entry channel it is in these cell types could be carried out.

8.6 - Golgi Apparatus Localisation of TRPC7

Two different cell types demonstrated the expression of TRPC7 in the Golgi apparatus; the mouse cell line 3T3-L1 showed Golgi localisation of TRPC7 during and after differentiation from fibroblasts to adipocytes and the rat cell line GH4C1 displayed Golgi localisation of TRPC7. An interesting aspect of this observation was that when Western

blotting was carried out on these cell types the resulting TRPC7 bands from both cell types were slightly higher than that given by Panc-1 membranes. Calculations revealed an approximately eight or nine kD difference between the Golgi localised TRPC7 and the PM localised TRPC7. This difference may be due to an additional tightly bound protein (unlikely to be CaM as discussed in Chapters 6 and 7) or post-translational modification. It must be ascertained whether or not TRPC7 in the Golgi of these cells is associated with another protein and if TRPC7 is functional. It may be that in these cells TRPC7 is bound to another protein or has been modified in someway that renders it non-functional and unable to be transported to the PM. However, the Golgi apparatus has been implicated in Ca^{2+} signalling and has been assessed for its capacity to be an intracellular store of Ca^{2+}, and because of its defined intracellular localisation it has been hypothesised to be involved in generating highly localised Ca^{2+} gradients (Rizzuto, 2001). If TRPC7 is a functional channel in the Golgi apparatus of these cells it is possible that it is orientated so that the N- and C-termini are at the cytoplasmic side, this would mean that TRPC7 may channel Ca^{2+} out of the Golgi to be involved in various cellular processes. RNAi could be carried out to observe any functional changes associated with the knock down of TRPC7 in these cell types.

8.7 - Endogenous TRPC7

Endogenous localisation of TRPC7 in the cell types studied can be divided into two groups; those with PM localisation and those with Golgi apparatus localisation. From the results gathered in the current study it appears that the differences in localisation of TRPC7 between diverse cell and species types may reflect a differences in its function. Further work is needed to resolve these possibilities.

References

Abel,E.D. (2004). Glucose transport in the heart. Front Biosci. *9*, 201-215.

Albert,A.P. and Large,W.A. (2003). Synergism between inositol phosphates and diacylglycerol on native TRPC6-like channels in rabbit portal vein myocytes. J. Physiol *552*, 789-795.

Ambudkar,I.S. (2004). Cellular domains that contribute to Ca2+ entry events. Sci. STKE. *2004*, e32.

Arcangeli,A., Becchetti,A., Mannini,A., Mugnai,G., De Filippi,P., Tarone,G., Del Bene,M.R., Barletta,E., Wanke,E., and Olivotto,M. (1993). Integrin-mediated neurite outgrowth in neuroblastoma cells depends on the activation of potassium channels. J. Cell Biol. *122*, 1131-1143.

Ashworth,R. and Hinkle,P.M. (1996). Thyrotropin-releasing hormone-induced intracellular calcium responses in individual rat lactotrophs and thyrotrophs. Endocrinology *137*, 5205-5212.

Ballestrem,C., Hinz,B., Imhof,B.A., and Wehrle-Haller,B. (2001). Marching at the front and dragging behind: differential alphaVbeta3-integrin turnover regulates focal adhesion behavior. J. Cell Biol. *155*, 1319-1332.

Bargal,R., Avidan,N., Ben Asher,E., Olender,Z., Zeigler,M., Frumkin,A., Raas-Rothschild,A., Glusman,G., Lancet,D., and Bach,G. (2000). Identification of the gene causing mucolipidosis type IV. Nat. Genet. *26*, 118-123.

Barritt,G.J. (1998). Does a decrease in subplasmalemmal Ca2+ explain how store-operated Ca2+ channels are opened? Cell Calcium *23*, 65-75.

Barritt,G.J. (1999). Receptor-activated Ca2+ inflow in animal cells: a variety of pathways tailored to meet different intracellular Ca2+ signalling requirements. Biochem. J. *337 (Pt 2)*, 153-169.

Bassi,M.T., Manzoni,M., Monti,E., Pizzo,M.T., Ballabio,A., and Borsani,G. (2000). Cloning of the gene encoding a novel integral membrane protein, mucolipidin-and identification of the two major founder mutations causing mucolipidosis type IV. Am. J. Hum. Genet. *67*, 1110-1120.

Bear, M. F, Connors, B. W, and Paradiso, M. A. Neuroscience Exploring The Brain. Chemical control of brain and behaviour. 402-431. 1996a. Williams and Wilkins.
Ref Type: Generic

Bear, M. F, Connors, B. W, and Paradiso, M. A. Neuroscience Exploring the Brain. Foundations. 1-187. 1996b. Williams and Wilkins.

Beech,D.J., Xu,S.Z., McHugh,D., and Flemming,R. (2003). TRPC1 store-operated cationic channel subunit. Cell Calcium *33*, 433-440.

Beech DJ, Muraki K, Flemming R. (2004). Non-selective cationic channels of smooth muscle and the mammalian homologues of Drosophila TRP. J Physiol *559* (3) 685-706.

Berne, R. M and Levy, M. N. Physiology. Genuth, S. M. The Endocrine System. [4], 779-910. 1998b. Mosby.

Berne, R. M and Levy, M. N. Physiology. Kutchai, H. The Gastrointestinal System. [4], 589-676. 1998a. Mosby.

Berridge,M.J. (1993). Inositol trisphosphate and calcium signalling. Nature *361*, 315-325.

Berridge,M.J. (2002). The endoplasmic reticulum: a multifunctional signaling organelle. Cell Calcium *32*, 235-249.

Berridge,M.J., Bootman,M.D., and Lipp,P. (1998). Calcium--a life and death signal. Nature *395*, 645-648.

Berridge,M.J., Lipp,P., and Bootman,M.D. (2000). The versatility and universality of calcium signalling. Nat. Rev. Mol. Cell Biol. *1*, 11-21.

Bers,D.M. (2002). Cardiac excitation-contraction coupling. Nature *415*, 198-205.

Berven,L.A., Hughes,B.P., and Barritt,G.J. (1994). A slowly ADP-ribosylated pertussis-toxin-sensitive GTP-binding regulatory protein is required for vasopressin-stimulated Ca2+ inflow in hepatocytes. Biochem. J. *299 (Pt 2)*, 399-407.

Bird,G.S. and Putney,J.W., Jr. (1993). Inhibition of thapsigargin-induced calcium entry by microinjected guanine nucleotide analogues. Evidence for the involvement of a small G-protein in capacitative calcium entry. J. Biol. Chem. *268*, 21486-21488.

Birnbaumer,L., Yildirim,E., and Abramowitz,J. (2003). A comparison of the genes coding for canonical TRP channels and their M, V and P relatives. Cell Calcium *33*, 419-432.

Bhatt,A., Kaverina,I., Otey,C., and Huttenlocher,A. (2002). Regulation of focal complex composition and disassembly by the calcium-dependent protease calpain. J. Cell Sci. *115*, 3415-3425.

Blesch,A. (2004). Lentiviral and MLV based retroviral vectors for ex vivo and in vivo gene transfer. Methods *33*, 164-172.

Bode,H.P. and Netter,K.J. (1996). Agonist-releasable intracellular calcium stores and the phenomenon of store-dependent calcium entry. A novel hypothesis based on calcium stores in organelles of the endo- and exocytotic apparatus. Biochem. Pharmacol. *51*, 993-1001.

Bootman,M.D., Collins,T.J., Peppiatt,C.M., Prothero,L.S., Mackenzie,L., de Smet,P., Travers,M., Tovey,S.C., Seo,J.T., Berridge,M.J., Ciccolini,F., and Lipp,P. (2001). Calcium signalling--an overview. Semin. Cell Dev. Biol. *12*, 3-10.

Boulay,G., Brown,D.M., Qin,N., Jiang,M., Dietrich,A., Zhu,M.X., Chen,Z., Birnbaumer,M., Mikoshiba,K., and Birnbaumer,L. (1999). Modulation of Ca(2+) entry by polypeptides of the inositol 1,4, 5-trisphosphate receptor (IP3R) that bind transient receptor potential (TRP): evidence for roles of TRP and IP3R in store depletion-activated Ca(2+) entry. Proc. Natl. Acad. Sci. U. S. A *96*, 14955-14960.

Boulay,G., Zhu,X., Peyton,M., Jiang,M., Hurst,R., Stefani,E., and Birnbaumer,L. (1997). Cloning and expression of a novel mammalian homolog of Drosophila transient receptor potential (Trp) involved in calcium entry secondary to activation of receptors coupled by the Gq class of G protein. J. Biol. Chem. *272*, 29672-29680.

Brereton,H.M., Chen,J., Rychkov,G., Harland,M.L., and Barritt,G.J. (2001). Maitotoxin activates an endogenous non-selective cation channel and is an effective initiator of the activation of the heterologously expressed hTRPC-1 (transient receptor potential) non-selective cation channel in H4-IIE liver cells. Biochim. Biophys. Acta *1540*, 107-126.

Brette,F. and Orchard,C. (2003). T-tubule function in mammalian cardiac myocytes. Circ. Res. *92*, 1182-1192.

Buniel,M.C., Schilling,W.P., and Kunze,D.L. (2003). Distribution of transient receptor potential channels in the rat carotid chemosensory pathway. J. Comp Neurol. *464*, 404-413.

Cammisotto,P.G. and Bukowiecki,L.J. (2004). Role of calcium in the secretion of leptin from white adipocytes. Am. J. Physiol Regul. Integr. Comp Physiol *287*, R1380-R1386.

Campfield,L.A., Smith,F.J., Guisez,Y., Devos,R., and Burn,P. (1995). Recombinant mouse OB protein: evidence for a peripheral signal linking adiposity and central neural networks. Science *269*, 546-549.

Carew,M.A. and Mason,W.T. (1995). Control of Ca2+ entry into rat lactotrophs by thyrotrophin-releasing hormone. J. Physiol *486 (Pt 2)*, 349-360.

Carragher,N.O., Westhoff,M.A., Fincham,V.J., Schaller,M.D., and Frame,M.C. (2003). A novel role for FAK as a protease-targeting adaptor protein: regulation by p42 ERK and Src. Curr. Biol. *13*, 1442-1450.

Casteels,R. and Droogmans,G. (1981). Exchange characteristics of the noradrenaline-sensitive calcium store in vascular smooth muscle cells or rabbit ear artery. J. Physiol *317*, 263-279.

Caterina,M.J., Schumacher,M.A., Tominaga,M., Rosen,T.A., Levine,J.D., and Julius,D. (1997). The capsaicin receptor: a heat-activated ion channel in the pain pathway. Nature *389*, 816-824.

Caterina,M.J., Leffler,A., Malmberg,A.B., Martin,W.J., Trafton,J., Petersen-Zeitz,K.R., Koltzenburg,M., Basbaum,A.I., and Julius,D. (2000). Impaired nociception and pain sensation in mice lacking the capsaicin receptor. Science *288*, 306-313.

Catterall,W.A. (2000). Structure and regulation of voltage-gated Ca2+ channels. Annu. Rev. Cell Dev. Biol. *16*, 521-555.

Chan,W.L., Holstein-Rathlou,N.H., and Yip,K.P. (2001). Integrin mobilizes intracellular Ca(2+) in renal vascular smooth muscle cells. Am. J. Physiol Cell Physiol *280*, C593-C603.

Chevesich,J., Kreuz,A.J., and Montell,C. (1997). Requirement for the PDZ domain protein, INAD, for localization of the TRP store-operated channel to a signaling complex. Neuron *18*, 95-105.

Chrzanowska-Wodnicka,M. and Burridge,K. (1996). Rho-stimulated contractility drives the formation of stress fibers and focal adhesions. J. Cell Biol. *133*, 1403-1415.

Chu,X., Tong,Q., Wozney,J., Zhang,W., Cheung,J.Y., Conrad,K., Mazack,V., Stahl,R., Barber,D.L., and Miller,B.A. (2005). Identification of an N-terminal TRPC2 splice variant which inhibits calcium influx. Cell Calcium *37*, 173-182.

Chuang,H.H., Prescott,E.D., Kong,H., Shields,S., Jordt,S.E., Basbaum,A.I., Chao,M.V., and Julius,D. (2001). Bradykinin and nerve growth factor release the capsaicin receptor from PtdIns(4,5)P2-mediated inhibition. Nature *411*, 957-962.

Chyb,S., Raghu,P., and Hardie,R.C. (1999). Polyunsaturated fatty acids activate the Drosophila light-sensitive channels TRP and TRPL. Nature *397*, 255-259.

Cioffi,D.L., Wu,S., and Stevens,T. (2003). On the endothelial cell I(SOC). Cell Calcium *33*, 323-336.

Clapham,D.E. (1993). Cellular calcium. A mysterious new influx factor? Nature *364*, 763-764.

Clapham,D.E. (1995). Calcium signaling. Cell *80*, 259-268.

Clapham,D.E. (2003). TRP channels as cellular sensors. Nature *426*, 517-524.

Clapham,D.E. and Neer,E.J. (1993). New roles for G-protein beta gamma-dimers in transmembrane signalling. Nature *365*, 403-406.

Corey,D.P., Garcia-Anoveros,J., Holt,J.R., Kwan,K.Y., Lin,S.Y., Vollrath,M.A., Amalfitano,A., Cheung,E.L., Derfler,B.H., Duggan,A., Geleoc,G.S., Gray,P.A., Hoffman,M.P., Rehm,H.L., Tamasauskas,D., and Zhang,D.S. (2004). TRPA1 is a candidate for the mechanosensitive transduction channel of vertebrate hair cells. Nature *432*, 723-730.

Cosens,D.J. and Manning,A. (1969). Abnormal electroretinogram from a Drosophila mutant. Nature *224*, 285-287.

Damjanovich S.; Bene L.; Matko J.; Matyus L.; Krasznai Z.; Szabo G.; Pieri C.; Gaspar R.; Szollosi J. (1999) Two-dimensional receptor patterns in the plasma membrane of cells. A critical evaluation of their identification, origin and information Biophys. Chem. pp.99-108(10)

Davis,M.J., Wu,X., Nurkiewicz,T.R., Kawasaki,J., Gui,P., Hill,M.A., and Wilson,E. (2001). Regulation of ion channels by protein tyrosine phosphorylation. Am. J. Physiol Heart Circ. Physiol *281*, H1835-H1862.

Davis,M.J., Wu,X., Nurkiewicz,T.R., Kawasaki,J., Gui,P., Hill,M.A., and Wilson,E. (2002). Regulation of ion channels by integrins. Cell Biochem. Biophys. *36*, 41-66.

Delmas,P., Wanaverbecq,N., Abogadie,F.C., Mistry,M., and Brown,D.A. (2002). Signaling microdomains define the specificity of receptor-mediated InsP(3) pathways in neurons. Neuron *34*, 209-220.

Digby,J., Harrison,R., Jehanli,A., Lunt,G.G., and Clifford-Rose,F. (1985). Cultured rat spinal cord neurons: interaction with motor neuron disease immunoglobulins. Muscle Nerve *8*, 595-605.

Edlund,M., Lotano,M.A., and Otey,C.A. (2001). Dynamics of alpha-actinin in focal adhesions and stress fibers visualized with alpha-actinin-green fluorescent protein. Cell Motil. Cytoskeleton *48*, 190-200.

Estacion,M., Sinkins,W.G., and Schilling,W.P. (2001). Regulation of Drosophila transient receptor potential-like (TrpL) channels by phospholipase C-dependent mechanisms. J. Physiol *530*, 1-19.

Fasolato,C., Hoth,M., and Penner,R. (1993). A GTP-dependent step in the activation mechanism of capacitative calcium influx. J. Biol. Chem. *268*, 20737-20740.

Fischer,Y., Rose,H., and Kammermeier,H. (1991). Highly insulin-responsive isolated rat heart muscle cells yielded by a modified isolation method. Life Sci. 49, 1679-1688.

Freichel,M., Suh,S.H., Pfeifer,A., Schweig,U., Trost,C., Weissgerber,P., Biel,M., Philipp,S., Freise,D., Droogmans,G., Hofmann,F., Flockerzi,V., and Nilius,B. (2001). Lack of an endothelial store-operated Ca2+ current impairs agonist-dependent vasorelaxation in TRP4-/- mice. Nat. Cell Biol. *3*, 121-127.

Fujimoto,T., Fujimura,K., and Kuramoto,A. (1991). Electrophysiological evidence that glycoprotein IIb-IIIa complex is involved in calcium channel activation on human platelet plasma membrane. J. Biol. Chem. *266*, 16370-16375.

Funayama,M., Goto,K., and Kondo,H. (1996). Cloning and expression localization of cDNA for rat homolog of TRP protein, a possible store-operated calcium (Ca2+) channel. Brain Res. Mol. Brain Res. *43*, 259-266.

Gaburjakova,M., Gaburjakova,J., Reiken,S., Huang,F., Marx,S.O., Rosemblit,N., and Marks,A.R. (2001). FKBP12 binding modulates ryanodine receptor channel gating. J. Biol. Chem. *276*, 16931-16935.

Gamberucci,A., Giurisato,E., Pizzo,P., Tassi,M., Giunti,R., McIntosh,D.P., and Benedetti,A. (2002). Diacylglycerol activates the influx of extracellular cations in T-lymphocytes independently of intracellular calcium-store depletion and possibly involving endogenous TRP6 gene products. Biochem. J. *364*, 245-254.

Garcia,R.L. and Schilling,W.P. (1997). Differential expression of mammalian TRP homologues across tissues and cell lines. Biochem. Biophys. Res. Commun. *239*, 279-283.

Gill,D.L., Waldron,R.T., Rys-Sikora,K.E., Ufret-Vincenty,C.A., Graber,M.N., Favre,C.J., and Alfonso,A. (1996). Calcium pools, calcium entry, and cell growth. Biosci. Rep. *16*, 139-157.

Goeger,D.E., Riley,R.T., Dorner,J.W., and Cole,R.J. (1988). Cyclopiazonic acid inhibition of the Ca2+-transport ATPase in rat skeletal muscle sarcoplasmic reticulum vesicles. Biochem. Pharmacol. *37*, 978-981.

Goel,M., Garcia,R., Estacion,M., and Schilling,W.P. (2001). Regulation of Drosophila TRPL channels by immunophilin FKBP59. J. Biol. Chem. *276*, 38762-38773.

Goel,M., Sinkins,W.G., and Schilling,W.P. (2002). Selective association of TRPC channel subunits in rat brain synaptosomes. J. Biol. Chem. *277*, 48303-48310.

Greka,A., Navarro,B., Oancea,E., Duggan,A., and Clapham,D.E. (2003). TRPC5 is a regulator of hippocampal neurite length and growth cone morphology. Nat. Neurosci. *6*, 837-845.

Guler,A.D., Lee,H., Iida,T., Shimizu,I., Tominaga,M., and Caterina,M. (2002). Heat-evoked activation of the ion channel, TRPV4. J. Neurosci. *22*, 6408-6414.

Gunthorpe,M.J., Benham,C.D., Randall,A., and Davis,J.B. (2002). The diversity in the vanilloid (TRPV) receptor family of ion channels. Trends Pharmacol. Sci. *23*, 183-191.

Halaas,J.L., Gajiwala,K.S., Maffei,M., Cohen,S.L., Chait,B.T., Rabinowitz,D., Lallone,R.L., Burley,S.K., and Friedman,J.M. (1995). Weight-reducing effects of the plasma protein encoded by the obese gene. Science *269*, 543-546.

Hardie,R.C. (2003). Regulation of TRP channels via lipid second messengers. Annu. Rev. Physiol *65*, 735-759.

Hardie,R.C. and Minke,B. (1992). The trp gene is essential for a light-activated Ca2+ channel in Drosophila photoreceptors. Neuron *8*, 643-651.

Hardie,R.C. and Minke,B. (1993). Novel Ca2+ channels underlying transduction in Drosophila photoreceptors: implications for phosphoinositide-mediated Ca2+ mobilization. Trends Neurosci. *16*, 371-376.

Harlow E. and Lane D. Using antibodies a laboratory manual 1999, Cold Spring Harbour Press.

Harteneck,C., Plant,T.D., and Schultz,G. (2000). From worm to man: three subfamilies of TRP channels. Trends Neurosci. *23*, 159-166.

Hassock,S.R., Zhu,M.X., Trost,C., Flockerzi,V., and Authi,K.S. (2002). Expression and role of TRPC proteins in human platelets: evidence that TRPC6 forms the store-independent calcium entry channel. Blood *100*, 2801-2811.

Hersh,B.M., Hartwieg,E., and Horvitz,H.R. (2002). The Caenorhabditis elegans mucolipin-like gene cup-5 is essential for viability and regulates lysosomes in multiple cell types. Proc. Natl. Acad. Sci. U. S. A *99*, 4355-4360.

Hiraoka,M. (2003). A novel action of insulin on cardiac membrane. Circ. Res. *92*, 707-709.

Hochstrate,P. (1989). Lanthanum mimicks the trp photoreceptor mutant of Drosophila in the blowfly Calliphora. J. Comp Physiol [A] *166*, 179-187.

Hofmann,T., Obukhov,A.G., Schaefer,M., Harteneck,C., Gudermann,T., and Schultz,G. (1999). Direct activation of human TRPC6 and TRPC3 channels by diacylglycerol. Nature *397*, 259-263.

Hofmann,T., Schaefer,M., Schultz,G., and Gudermann,T. (2000). Cloning, expression and subcellular localization of two novel splice variants of mouse transient receptor potential channel 2. Biochem. J. *351*, 115-122.

Hofmann,T., Schaefer,M., Schultz,G., and Gudermann,T. (2002). Subunit composition of mammalian transient receptor potential channels in living cells. Proc. Natl. Acad. Sci. U. S. A *99*, 7461-7466.

Hotchin,N.A. and Hall,A. (1995). The assembly of integrin adhesion complexes requires both extracellular matrix and intracellular rho/rac GTPases. J. Cell Biol. *131*, 1857-1865.

Hu,Y., Vaca,L., Zhu,X., Birnbaumer,L., Kunze,D.L., and Schilling,W.P. (1994). Appearance of a novel Ca2+ influx pathway in Sf9 insect cells following expression of the transient receptor potential-like (trpl) protein of Drosophila. Biochem. Biophys. Res. Commun. *201*, 1050-1056.

Huber,A., Sander,P., Gobert,A., Bahner,M., Hermann,R., and Paulsen,R. (1996). The transient receptor potential protein (Trp), a putative store-operated Ca2+ channel essential for phosphoinositide-mediated photoreception, forms a signaling complex with NorpA, InaC and InaD. EMBO J. *15*, 7036-7045.

Huttenlocher,A., Lakonishok,M., Kinder,M., Wu,S., Truong,T., Knudsen,K.A., and Horwitz,A.F. (1998). Integrin and cadherin synergy regulates contact inhibition of migration and motile activity. J. Cell Biol. *141*, 515-526.

Huttenlocher,A., Sandborg,R.R., and Horwitz,A.F. (1995). Adhesion in cell migration. Curr. Opin. Cell Biol. *7*, 697-706.

Ilic,D., Furuta,Y., Kanazawa,S., Takeda,N., Sobue,K., Nakatsuji,N., Nomura,S., Fujimoto,J., Okada,M., and Yamamoto,T. (1995). Reduced cell motility and enhanced focal adhesion contact formation in cells from FAK-deficient mice. Nature *377*, 539-544.

Inoue,R., Okada,T., Onoue,H., Hara,Y., Shimizu,S., Naitoh,S., Ito,Y., and Mori,Y. (2001). The transient receptor potential protein homologue TRP6 is the essential component of vascular alpha(1)-adrenoceptor-activated Ca(2+)-permeable cation channel. Circ. Res. *88*, 325-332.

Irvine,R.F. (1990). 'Quantal' Ca2+ release and the control of Ca2+ entry by inositol phosphates--a possible mechanism. FEBS Lett. *263*, 5-9.

Jacobson,S.L. and Piper,H.M. (1986). Cell cultures of adult cardiomyocytes as models of the myocardium. J. Mol. Cell Cardiol. *18*, 661-678.

Jan,L.Y. and Jan,Y.N. (1992). Tracing the roots of ion channels. Cell *69*, 715-718.

Jordt,S.E. and Julius,D. (2002). Molecular basis for species-specific sensitivity to "hot" chili peppers. Cell *108*, 421-430.

Jungnickel,M.K., Marrero,H., Birnbaumer,L., Lemos,J.R., and Florman,H.M. (2001). Trp2 regulates entry of Ca2+ into mouse sperm triggered by egg ZP3. Nat. Cell Biol. *3*, 499-502.

Katz,B.Z., Zamir,E., Bershadsky,A., Kam,Z., Yamada,K.M., and Geiger,B. (2000). Physical state of the extracellular matrix regulates the structure and molecular composition of cell-matrix adhesions. Mol. Biol. Cell *11*, 1047-1060.

Kim,S.J., Kim,Y.S., Yuan,J.P., Petralia,R.S., Worley,P.F., and Linden,D.J. (2003). Activation of the TRPC1 cation channel by metabotropic glutamate receptor mGluR1. Nature *426*, 285-291.

Kiosses,W.B., Shattil,S.J., Pampori,N., and Schwartz,M.A. (2001). Rac recruits high-affinity integrin alphavbeta3 to lamellipodia in endothelial cell migration. Nat. Cell Biol. *3*, 316-320.

Kiselyov,K., Xu,X., Mozhayeva,G., Kuo,T., Pessah,I., Mignery,G., Zhu,X., Birnbaumer,L., and Muallem,S. (1998). Functional interaction between InsP3 receptors and store-operated Htrp3 channels. Nature *396*, 478-482.

Klinghoffer,R.A., Sachsenmaier,C., Cooper,J.A., and Soriano,P. (1999). Src family kinases are required for integrin but not PDGFR signal transduction. EMBO J. *18*, 2459-2471.

Koshimizu,T.A., Tomic,M., Wong,A.O., Zivadinovic,D., and Stojilkovic,S.S. (2000). Characterization of purinergic receptors and receptor-channels expressed in anterior pituitary cells. Endocrinology *141*, 4091-4099.

Kostin,S., Scholz,D., Shimada,T., Maeno,Y., Mollnau,H., Hein,S., and Schaper,J. (1998). The internal and external protein scaffold of the T-tubular system in cardiomyocytes. Cell Tissue Res. *294*, 449-460.

Kwan,H.Y., Huang,Y., and Yao,X. (2004). Regulation of canonical transient receptor potential isoform 3 (TRPC3) channel by protein kinase G. Proc. Natl. Acad. Sci. U. S. A *101*, 2625-2630.

Lauffenburger,D.A. and Horwitz,A.F. (1996). Cell migration: a physically integrated molecular process. Cell *84*, 359-369.

Laukaitis,C.M., Webb,D.J., Donais,K., and Horwitz,A.F. (2001). Differential dynamics of alpha 5 integrin, paxillin, and alpha-actinin during formation and disassembly of adhesions in migrating cells. J. Cell Biol. *153*, 1427-1440.

Li,H.S. and Montell,C. (2000). TRP and the PDZ protein, INAD, form the core complex required for retention of the signalplex in Drosophila photoreceptor cells. J. Cell Biol. *150*, 1411-1422.

Lievremont,J.P., Bird,G.S., and Putney,J.W., Jr. (2004). Canonical transient receptor potential TRPC7 can function as both a receptor- and store-operated channel in HEK-293 cells. Am. J. Physiol Cell Physiol *287*, C1709-C1716.

Liman,E.R., Corey,D.P., and Dulac,C. (1999). TRP2: a candidate transduction channel for mammalian pheromone sensory signaling. Proc. Natl. Acad. Sci. U. S. A *96*, 5791-5796.

Lin,M.J., Leung,G.P., Zhang,W.M., Yang,X.R., Yip,K.P., Tse,C.M., and Sham,J.S. (2004). Chronic hypoxia-induced upregulation of store-operated and receptor-operated Ca2+ channels in pulmonary arterial smooth muscle cells: a novel mechanism of hypoxic pulmonary hypertension. Circ. Res. *95*, 496-505.

Lin,P., Yao,Y., Hofmeister,R., Tsien,R.Y., and Farquhar,M.G. (1999). Overexpression of CALNUC (nucleobindin) increases agonist and thapsigargin releasable Ca2+ storage in the Golgi. J. Cell Biol. *145*, 279-289.

Lintschinger,B., Balzer-Geldsetzer,M., Baskaran,T., Graier,W.F., Romanin,C., Zhu,M.X., and Groschner,K. (2000). Coassembly of Trp1 and Trp3 proteins generates diacylglycerol- and Ca2+-sensitive cation channels. J. Biol. Chem. *275*, 27799-27805.

Lipp,P., Laine,M., Tovey,S.C., Burrell,K.M., Berridge,M.J., Li,W., and Bootman,M.D. (2000). Functional InsP3 receptors that may modulate excitation-contraction coupling in the heart. Curr. Biol. *10*, 939-942.

Littleton,J.T. and Ganetzky,B. (2000). Ion channels and synaptic organization: analysis of the Drosophila genome. Neuron *26*, 35-43.

Liu,M., Parker,L.L., Wadzinski,B.E., and Shieh,B.H. (2000). Reversible phosphorylation of the signal transduction complex in Drosophila photoreceptors. J. Biol. Chem. *275*, 12194-12199.

Liu X, Bandyopadhyay B, Singh B. B, Groschner K, Ambudkar I. S. (2005). Molecular analysis of a store-operated and OAG sensitive non-selective cation channel: heteromeric assembly of TRPC1-TRPC3. J. Biol. Chem. In Press.

Lockwich,T.P., Liu,X., Singh,B.B., Jadlowiec,J., Weiland,S., and Ambudkar,I.S. (2000). Assembly of Trp1 in a signaling complex associated with caveolin-scaffolding lipid raft domains. J. Biol. Chem. *275*, 11934-11942.

Lucas,P., Ukhanov,K., Leinders-Zufall,T., and Zufall,F. (2003). A diacylglycerol-gated cation channel in vomeronasal neuron dendrites is impaired in TRPC2 mutant mice: mechanism of pheromone transduction. Neuron *40*, 551-561.

Ma,H.T., Venkatachalam,K., Li,H.S., Montell,C., Kurosaki,T., Patterson,R.L., and Gill,D.L. (2001). Assessment of the role of the inositol 1,4,5-trisphosphate

receptor in the activation of transient receptor potential channels and store-operated Ca2+ entry channels. J. Biol. Chem. *276*, 18888-18896.

Mackenzie,L., Bootman,M.D., Laine,M., Berridge,M.J., Thuring,J., Holmes,A., Li,W.H., and Lipp,P. (2002). The role of inositol 1,4,5-trisphosphate receptors in Ca(2+) signalling and the generation of arrhythmias in rat atrial myocytes. J. Physiol *541*, 395-409.

Marks,A.R. (1996). Cellular functions of immunophilins. Physiol Rev. *76*, 631-649.

Maroto,R., Raso,A., Wood,T.G., Kurosky,A., Martinac,B., and Hamill,O.P. (2005). TRPC1 forms the stretch-activated cation channel in vertebrate cells. Nat. Cell Biol. *7*, 179-185.

Matteson,D.R. and Armstrong,C.M. (1986). Properties of two types of calcium channels in clonal pituitary cells. J. Gen. Physiol *87*, 161-182.

McKay,R.R., Szymeczek-Seay,C.L., Lievremont,J.P., Bird,G.S., Zitt,C., Jungling,E., Luckhoff,A., and Putney,J.W., Jr. (2000). Cloning and expression of the human transient receptor potential 4 (TRP4) gene: localization and functional expression of human TRP4 and TRP3. Biochem. J. *351 Pt 3*, 735-746.

McKemy,D.D., Neuhausser,W.M., and Julius,D. (2002). Identification of a cold receptor reveals a general role for TRP channels in thermosensation. Nature *416*, 52-58.

Mery,L., Magnino,F., Schmidt,K., Krause,K.H., and Dufour,J.F. (2001). Alternative splice variants of hTrp4 differentially interact with the C-terminal portion of the inositol 1,4,5-trisphosphate receptors. FEBS Lett. *487*, 377-383.

Mery,L., Strauss,B., Dufour,J.F., Krause,K.H., and Hoth,M. (2002). The PDZ-interacting domain of TRPC4 controls its localization and surface expression in HEK293 cells. J. Cell Sci. *115*, 3497-3508.

Michaely,P. and Bennett,V. (1993). The membrane-binding domain of ankyrin contains four independently folded subdomains, each comprised of six ankyrin repeats. J. Biol. Chem. *268*, 22703-22709.

Mignen,O. and Shuttleworth,T.J. (2000). I(ARC), a novel arachidonate-regulated, noncapacitative Ca(2+) entry channel. J. Biol. Chem. *275*, 9114-9119.

Minke,B. and Cook,B. (2002). TRP channel proteins and signal transduction. Physiol Rev. *82*, 429-472.

Monk,P.D., Carne,A., Liu,S.H., Ford,J.W., Keen,J.N., and Findlay,J.B. (1996). Isolation, cloning, and characterisation of a trp homologue from squid (Loligo forbesi) photoreceptor membranes. J. Neurochem. *67*, 2227-2235.

Montell,C. (1999). Visual transduction in Drosophila. Annu. Rev. Cell Dev. Biol. *15*, 231-268.

Montell,C. (2001). Physiology, phylogeny, and functions of the TRP superfamily of cation channels. Sci. STKE. *2001*, RE1.

Montell,C. and Rubin,G.M. (1989). Molecular characterization of the Drosophila trp locus: a putative integral membrane protein required for phototransduction. Neuron *2*, 1313-1323.

Montero,M., Alonso,M.T., Carnicero,E., Cuchillo-Ibanez,I., Albillos,A., Garcia,A.G., Garcia-Sancho,J., and Alvarez,J. (2000). Chromaffin-cell stimulation triggers fast millimolar mitochondrial Ca2+ transients that modulate secretion. Nat. Cell Biol. *2*, 57-61.

Mori,Y., Wakamori,M., Miyakawa,T., Hermosura,M., Hara,Y., Nishida,M., Hirose,K., Mizushima,A., Kurosaki,M., Mori,E., Gotoh,K., Okada,T., Fleig,A., Penner,R., Iino,M., and Kurosaki,T. (2002). Transient receptor potential 1 regulates capacitative Ca(2+) entry and Ca(2+) release from endoplasmic reticulum in B lymphocytes. J. Exp. Med. *195*, 673-681.

Munsch,T., Freichel,M., Flockerzi,V., and Pape,H.C. (2003). Contribution of transient receptor potential channels to the control of GABA release from dendrites. Proc. Natl. Acad. Sci. U. S. A *100*, 16065-16070.

Nilius,B. (2004). Store-operated Ca2+ entry channels: still elusive! Sci. STKE. *2004*, e36.

Nobes,C.D. and Hall,A. (1995). Rho, rac, and cdc42 GTPases regulate the assembly of multimolecular focal complexes associated with actin stress fibers, lamellipodia, and filopodia. Cell *81*, 53-62.

Norwood,N., Moore,T.M., Dean,D.A., Bhattacharjee,R., Li,M., and Stevens,T. (2000). Store-operated calcium entry and increased endothelial cell permeability. Am. J. Physiol Lung Cell Mol. Physiol *279*, L815-L824.

Nystrom,F.H. and Quon,M.J. (1999). Insulin signalling: metabolic pathways and mechanisms for specificity. Cell Signal. *11*, 563-574.

Okada,T., Inoue,R., Yamazaki,K., Maeda,A., Kurosaki,T., Yamakuni,T., Tanaka,I., Shimizu,S., Ikenaka,K., Imoto,K., and Mori,Y. (1999). Molecular and functional characterization of a novel mouse transient receptor potential protein homologue TRP7. Ca(2+)-permeable cation channel that is constitutively activated and enhanced by stimulation of G protein-coupled receptor. J. Biol. Chem. *274*, 27359-27370.

Okada,T., Shimizu,S., Wakamori,M., Maeda,A., Kurosaki,T., Takada,N., Imoto,K., and Mori,Y. (1998). Molecular cloning and functional characterization

of a novel receptor-activated TRP Ca2+ channel from mouse brain. J. Biol. Chem. *273*, 10279-10287.

Pak,W.L., Grossfield,J., and Arnold,K.S. (1970). Mutants of the visual pathway of Drosophila melanogaster. Nature *227*, 518-520.

Palecek,S.P., Huttenlocher,A., Horwitz,A.F., and Lauffenburger,D.A. (1998). Physical and biochemical regulation of integrin release during rear detachment of migrating cells. J. Cell Sci. *111 (Pt 7)*, 929-940.

Parekh,A.B. and Penner,R. (1997). Store depletion and calcium influx. Physiol Rev. *77*, 901-930.

Perez,C.A., Margolskee,R.F., Kinnamon,S.C., and Ogura,T. (2003). Making sense with TRP channels: store-operated calcium entry and the ion channel Trpm5 in taste receptor cells. Cell Calcium *33*, 541-549.

Peier,A.M., Reeve,A.J., Andersson,D.A., Moqrich,A., Earley,T.J., Hergarden,A.C., Story,G.M., Colley,S., Hogenesch,J.B., McIntyre,P., Bevan,S., and Patapoutian,A. (2002). A heat-sensitive TRP channel expressed in keratinocytes. Science *296*, 2046-2049.

Pelleymounter,M.A., Cullen,M.J., Baker,M.B., Hecht,R., Winters,D., Boone,T., and Collins,F. (1995). Effects of the obese gene product on body weight regulation in ob/ob mice. Science *269*, 540-543.

Percival,A.C. and Slack,J.M. (1999). Analysis of pancreatic development using a cell lineage label. Exp. Cell Res. *247*, 123-132.

Perraud,A.L., Fleig,A., Dunn,C.A., Bagley,L.A., Launay,P., Schmitz,C., Stokes,A.J., Zhu,Q., Bessman,M.J., Penner,R., Kinet,J.P., and Scharenberg,A.M. (2001). ADP-ribose gating of the calcium-permeable LTRPC2 channel revealed by Nudix motif homology. Nature *411*, 595-599.

Petersen,C.C., Berridge,M.J., Borgese,M.F., and Bennett,D.L. (1995). Putative capacitative calcium entry channels: expression of Drosophila trp and evidence for the existence of vertebrate homologues. Biochem. J. *311 (Pt 1)*, 41-44.

Philipp,S. and Flockerzi,V. (1997). Molecular characterization of a novel human PDZ domain protein with homology to INAD from Drosophila melanogaster. FEBS Lett. *413*, 243-248.

Philipp,S., Hambrecht,J., Braslavski,L., Schroth,G., Freichel,M., Murakami,M., Cavalie,A., and Flockerzi,V. (1998). A novel capacitative calcium entry channel expressed in excitable cells. EMBO J. *17*, 4274-4282.

Philipp,S., Trost,C., Warnat,J., Rautmann,J., Himmerkus,N., Schroth,G., Kretz,O., Nastainczyk,W., Cavalie,A., Hoth,M., and Flockerzi,V. (2000). TRP4 (CCE1) protein is part of native calcium release-activated Ca2+-like channels in adrenal cells. J. Biol. Chem. *275*, 23965-23972.

Phillips,A.M., Bull,A., and Kelly,L.E. (1992). Identification of a Drosophila gene encoding a calmodulin-binding protein with homology to the trp phototransduction gene. Neuron *8*, 631-642.

Pinton,P., Pozzan,T., and Rizzuto,R. (1998). The Golgi apparatus is an inositol 1,4,5-trisphosphate-sensitive Ca2+ store, with functional properties distinct from those of the endoplasmic reticulum. EMBO J. *17*, 5298-5308.

Putney,J.W., Jr. (1986). A model for receptor-regulated calcium entry. Cell Calcium *7*, 1-12.

Putney,J.W., Jr. (1997). Type 3 inositol 1,4,5-trisphosphate receptor and capacitative calcium entry. Cell Calcium *21*, 257-261.

Putney,J.W., Jr. (2004). The enigmatic TRPCs: multifunctional cation channels. Trends Cell Biol. *14*, 282-286.

Putney,J.W., Jr. and Bird,G.S. (1993a). The signal for capacitative calcium entry. Cell *75*, 199-201.

Putney,J.W., Jr. and Bird,G.S. (1993b). The signal for capacitative calcium entry. Cell *75*, 199-201.

Putney,J.W., Jr. and McKay,R.R. (1999). Capacitative calcium entry channels. Bioessays *21*, 38-46.

Putney,J.W., Jr. and Ribeiro,C.M. (2000). Signaling pathways between the plasma membrane and endoplasmic reticulum calcium stores. Cell Mol. Life Sci. *57*, 1272-1286.

Qian,F., Huang,P., Ma,L., Kuznetsov,A., Tamarina,N., and Philipson,L.H. (2002). TRP genes: candidates for nonselective cation channels and store-operated channels in insulin-secreting cells. Diabetes *51 Suppl 1*, S183-S189.

Randriamampita,C. and Tsien,R.Y. (1993). Emptying of intracellular Ca2+ stores releases a novel small messenger that stimulates Ca2+ influx. Nature *364*, 809-814.

Riccio,A., Mattei,C., Kelsell,R.E., Medhurst,A.D., Calver,A.R., Randall,A.D., Davis,J.B., Benham,C.D., and Pangalos,M.N. (2002a). Cloning and functional expression of human short TRP7, a candidate protein for store-operated Ca2+ influx. J. Biol. Chem. *277*, 12302-12309.

Riccio,A., Medhurst,A.D., Mattei,C., Kelsell,R.E., Calver,A.R., Randall,A.D., Benham,C.D., and Pangalos,M.N. (2002b). mRNA distribution analysis of human TRPC family in CNS and peripheral tissues. Brain Res. Mol. Brain Res. *109*, 95-104.

Ridley,A.J. and Hall,A. (1992). The small GTP-binding protein rho regulates the assembly of focal adhesions and actin stress fibers in response to growth factors. Cell *70*, 389-399.

Rizzuto,R. (2001). Intracellular Ca(2+) pools in neuronal signalling. Curr. Opin. Neurobiol. *11*, 306-311.

Roitt, I, Brostoff, J, and Male, D. Immunology. Immunological Techniques. [5], 381-395. 1998. Mosby.
Ref Type: Generic

Rosado,J.A., Brownlow,S.L., and Sage,S.O. (2002). Endogenously expressed Trp1 is involved in store-mediated Ca2+ entry by conformational coupling in human platelets. J. Biol. Chem. *277*, 42157-42163.

Rottner,K., Hall,A., and Small,J.V. (1999). Interplay between Rac and Rho in the control of substrate contact dynamics. Curr. Biol. *9*, 640-648.

Rutter,G.A. and Rizzuto,R. (2000). Regulation of mitochondrial metabolism by ER Ca2+ release: an intimate connection. Trends Biochem. Sci. *25*, 215-221.

Sakura,H. and Ashcroft,F.M. (1997). Identification of four trp1 gene variants murine pancreatic beta-cells. Diabetologia *40*, 528-532.

Santillan,G., Baldi,C., Katz,S., Vazquez,G., and Boland,R. (2004). Evidence that TRPC3 is a molecular component of the 1alpha,25(OH)2D3-activated capacitative calcium entry (CCE) in muscle and osteoblast cells. J. Steroid Biochem. Mol. Biol. *89-90*, 291-295.

Saras,J. and Heldin,C.H. (1996). PDZ domains bind carboxy-terminal sequences of target proteins. Trends Biochem. Sci. *21*, 455-458.

Schaefer,M., Plant,T.D., Obukhov,A.G., Hofmann,T., Gudermann,T., and Schultz,G. (2000). Receptor-mediated regulation of the nonselective cation channels TRPC4 and TRPC5. J. Biol. Chem. *275*, 17517-17526.

Scherer,P.E., Lederkremer,G.Z., Williams,S., Fogliano,M., Baldini,G., and Lodish,H.F. (1996). Cab45, a novel (Ca2+)-binding protein localized to the Golgi lumen. J. Cell Biol. *133*, 257-268.

Schoenwaelder,S.M. and Burridge,K. (1999). Bidirectional signaling between the cytoskeleton and integrins. Curr. Opin. Cell Biol. *11*, 274-286.

Schwartz,M.A. (1993). Spreading of human endothelial cells on fibronectin or vitronectin triggers elevation of intracellular free calcium. J. Cell Biol. *120*, 1003-1010.

Schwartz,M.A. and Denninghoff,K. (1994). Alpha v integrins mediate the rise in intracellular calcium in endothelial cells on fibronectin even though they play a minor role in adhesion. J. Biol. Chem. *269*, 11133-11137.

Sedgwick,S.G. and Smerdon,S.J. (1999). The ankyrin repeat: a diversity of interactions on a common structural framework. Trends Biochem. Sci. *24*, 311-316.

Sergeeva,O.A., Korotkova,T.M., Scherer,A., Brown,R.E., and Haas,H.L. (2003). Co-expression of non-selective cation channels of the transient receptor potential canonical family in central aminergic neurones. J. Neurochem. *85*, 1547-1552.

Sharp,W.W., Simpson,D.G., Borg,T.K., Samarel,A.M., and Terracio,L. (1997). Mechanical forces regulate focal adhesion and costamere assembly in cardiac myocytes. Am. J. Physiol *273*, H546-H556.

Shieh,B.H. and Niemeyer,B. (1995). A novel protein encoded by the InaD gene regulates recovery of visual transduction in Drosophila. Neuron *14*, 201-210.

Shieh,B.H. and Zhu,M.Y. (1996). Regulation of the TRP Ca2+ channel by INAD in Drosophila photoreceptors. Neuron *16*, 991-998.

Shuai,J.W. and Jung,P. (2003). Optimal ion channel clustering for intracellular calcium signaling. Proc. Natl. Acad. Sci. U. S. A *100*, 506-510.

Sieg,D.J., Hauck,C.R., and Schlaepfer,D.D. (1999). Required role of focal adhesion kinase (FAK) for integrin-stimulated cell migration. J. Cell Sci. *112 (Pt 16)*, 2677-2691.

Sinkins WG, Estacion M, Schilling WP. (1998). Functional expression of TrpC1: a human homologue of the Drosophila Trp channel. Biochem J *331* (1) 331-339.

Sinkins,W.G., Goel,M., Estacion,M., and Schilling,W.P. (2004). Association of immunophilins with mammalian TRPC channels. J. Biol. Chem. *279*, 34521-34529.

Sjaastad,M.D., Lewis,R.S., and Nelson,W.J. (1996). Mechanisms of integrin-mediated calcium signaling in MDCK cells: regulation of adhesion by IP3- and store-independent calcium influx. Mol. Biol. Cell *7*, 1025-1041.

Smani,T., Zakharov,S.I., Csutora,P., Leno,E., Trepakova,E.S., and Bolotina,V.M. (2004). A novel mechanism for the store-operated calcium influx pathway. Nat. Cell Biol. *6*, 113-120.

Smilenov,L.B., Mikhailov,A., Pelham,R.J., Marcantonio,E.E., and Gundersen,G.G. (1999). Focal adhesion motility revealed in stationary fibroblasts. Science *286*, 1172-1174.

Smith,G.D., Gunthorpe,M.J., Kelsell,R.E., Hayes,P.D., Reilly,P., Facer,P., Wright,J.E., Jerman,J.C., Walhin,J.P., Ooi,L., Egerton,J., Charles,K.J., Smart,D., Randall,A.D., Anand,P., and Davis,J.B. (2002). TRPV3 is a temperature-sensitive vanilloid receptor-like protein. Nature *418*, 186-190.

Somasundaram,B., Norman,J.C., and Mahaut-Smith,M.P. (1995). Primaquine, an inhibitor of vesicular transport, blocks the calcium-release-activated current in rat megakaryocytes. Biochem. J. *309 (Pt 3)*, 725-729.

Spassova,M.A., Soboloff,J., He,L.P., Hewavitharana,T., Xu,W., Venkatachalam,K., van Rossum,D.B., Patterson,R.L., and Gill,D.L. (2004). Calcium entry mediated by SOCs and TRP channels: variations and enigma. Biochim. Biophys. Acta *1742*, 9-20.

Stowers,L., Holy,T.E., Meister,M., Dulac,C., and Koentges,G. (2002). Loss of sex discrimination and male-male aggression in mice deficient for TRP2. Science *295*, 1493-1500.

Strubing,C., Krapivinsky,G., Krapivinsky,L., and Clapham,D.E. (2003). Formation of novel TRPC channels by complex subunit interactions in embryonic brain. J. Biol. Chem. *278*, 39014-39019.

Stuhmer,W., Conti,F., Suzuki,H., Wang,X.D., Noda,M., Yahagi,N., Kubo,H., and Numa,S. (1989). Structural parts involved in activation and inactivation of the sodium channel. Nature *339*, 597-603.

Sun,M., Goldin,E., Stahl,S., Falardeau,J.L., Kennedy,J.C., Acierno,J.S., Jr., Bove,C., Kaneski,C.R., Nagle,J., Bromley,M.C., Colman,M., Schiffmann,R., and Slaugenhaupt,S.A. (2000). Mucolipidosis type IV is caused by mutations in a gene encoding a novel transient receptor potential channel. Hum. Mol. Genet. *9*, 2471-2478.

Suss-Toby,E., Selinger,Z., and Minke,B. (1991). Lanthanum reduces the excitation efficiency in fly photoreceptors. J. Gen. Physiol *98*, 849-868.

Sutton,K.A., Jungnickel,M.K., Wang,Y., Cullen,K., Lambert,S., and Florman,H.M. (2004). Enkurin is a novel calmodulin and TRPC channel binding protein in sperm. Dev. Biol. *274*, 426-435.

Tang,J., Lin,Y., Zhang,Z., Tikunova,S., Birnbaumer,L., and Zhu,M.X. (2001). Identification of common binding sites for calmodulin and inositol 1,4,5-trisphosphate receptors on the carboxyl termini of trp channels. J. Biol. Chem. *276*, 21303-21310.

Tepikin, A. V. Calcium Signalling. Lipp, P., Bootman, M. D., and Collins, T. Photometry, video imaging, confocal and multiphoton approaches in calcium signalling studies. [2], 17-50. 2000. Oxford University Press.
Ref Type: Generic

Tiruppathi,C., Freichel,M., Vogel,S.M., Paria,B.C., Mehta,D., Flockerzi,V., and Malik,A.B. (2002). Impairment of store-operated Ca2+ entry in TRPC4(-/-) mice interferes with increase in lung microvascular permeability. Circ. Res. *91*, 70-76.

Thum,T. and Borlak,J. (2000). Isolation and cultivation of Ca2+ tolerant cardiomyocytes from the adult rat: improvements and applications. Xenobiotica *30*, 1063-1077.

Tracey,W.D., Jr., Wilson,R.I., Laurent,G., and Benzer,S. (2003). painless, a Drosophila gene essential for nociception. Cell *113*, 261-273.

Trebak,M., Bird,G.S., McKay,R.R., and Putney,J.W., Jr. (2002). Comparison of human TRPC3 channels in receptor-activated and store-operated modes. Differential sensitivity to channel blockers suggests fundamental differences in channel composition. J. Biol. Chem. *277*, 21617-21623.

Trebak,M., St,J.B., McKay,R.R., Birnbaumer,L., and Putney,J.W., Jr. (2003). Signaling mechanism for receptor-activated canonical transient receptor potential 3 (TRPC3) channels. J. Biol. Chem. *278*, 16244-16252.

Trebak,M., Vazquez,G., Bird,G.S., and Putney,J.W., Jr. (2003). The TRPC3/6/7 subfamily of cation channels. Cell Calcium *33*, 451-461.

Tsunoda,S., Sierralta,J., Sun,Y., Bodner,R., Suzuki,E., Becker,A., Socolich,M., and Zuker,C.S. (1997). A multivalent PDZ-domain protein assembles signalling complexes in a G-protein-coupled cascade. Nature *388*, 243-249.

Vaca,L., Sinkins,W.G., Hu,Y., Kunze,D.L., and Schilling,W.P. (1994). Activation of recombinant trp by thapsigargin in Sf9 insect cells. Am. J. Physiol *267*, C1501-C1505.

Vannier,B., Peyton,M., Boulay,G., Brown,D., Qin,N., Jiang,M., Zhu,X., and Birnbaumer,L. (1999). Mouse trp2, the homologue of the human trpc2 pseudogene, encodes mTrp2, a store depletion-activated capacitative Ca2+ entry channel. Proc. Natl. Acad. Sci. U. S. A *96*, 2060-2064.

Vazquez,G., Wedel,B.J., Aziz,O., Trebak,M., and Putney,J.W., Jr. (2004). The mammalian TRPC cation channels. Biochim. Biophys. Acta *1742*, 21-36.

Vazquez,G., Wedel,B.J., Trebak,M., St John,B.G., and Putney,J.W., Jr. (2003). Expression level of the canonical transient receptor potential 3 (TRPC3) channel determines its mechanism of activation. J. Biol. Chem. *278*, 21649-21654.

Vazquez,G., Wedel,B.J., Kawasaki,B.T., Bird,G.S., and Putney,J.W., Jr. (2004). Obligatory role of Src kinase in the signaling mechanism for TRPC3 cation channels. J. Biol. Chem. *279*, 40521-40528.

Venkatachalam,K., van Rossum,D.B., Patterson,R.L., Ma,H.T., and Gill,D.L. (2002). The cellular and molecular basis of store-operated calcium entry. Nat. Cell Biol. *4*, E263-E272.

Walker,R.G., Willingham,A.T., and Zuker,C.S. (2000). A Drosophila mechanosensory transduction channel. Science *287*, 2229-2234.

Wang,C., Hu,H.Z., Colton,C.K., Wood,J.D., and Zhu,M.X. (2004). An alternative splicing product of the murine trpv1 gene dominant negatively modulates the activity of TRPV1 channels. J. Biol. Chem. *279*, 37423-37430.

Watson,R.T., Kanzaki,M., and Pessin,J.E. (2004). Regulated membrane trafficking of the insulin-responsive glucose transporter 4 in adipocytes. Endocr. Rev. *25*, 177-204.

Wes,P.D., Chevesich,J., Jeromin,A., Rosenberg,C., Stetten,G., and Montell,C. (1995). TRPC1, a human homolog of a Drosophila store-operated channel. Proc. Natl. Acad. Sci. U. S. A *92*, 9652-9656.

Wissenbach,U., Schroth,G., Philipp,S., and Flockerzi,V. (1998). Structure and mRNA expression of a bovine trp homologue related to mammalian trp2 transcripts. FEBS Lett. *429*, 61-66.

Wong,F., Schaefer,E.L., Roop,B.C., LaMendola,J.N., Johnson-Seaton,D., and Shao,D. (1989). Proper function of the Drosophila trp gene product during pupal development is important for normal visual transduction in the adult. Neuron *3*, 81-94.

Wozniak,M.A., Modzelewska,K., Kwong,L., and Keely,P.J. (2004). Focal adhesion regulation of cell behavior. Biochim. Biophys. Acta *1692*, 103-119.

Wu,X., Babnigg,G., Zagranichnaya,T., and Villereal,M.L. (2002). The role of endogenous human Trp4 in regulating carbachol-induced calcium oscillations in HEK-293 cells. J. Biol. Chem. *277*, 13597-13608.

Wu,X., Zagranichnaya,T.K., Gurda,G.T., Eves,E.M., and Villereal,M.L. (2004). A TRPC1/TRPC3-mediated increase in store-operated calcium entry is required for differentiation of H19-7 hippocampal neuronal cells. J. Biol. Chem. *279*, 43392-43402.

Xu,H., Ramsey,I.S., Kotecha,S.A., Moran,M.M., Chong,J.A., Lawson,D., Ge,P., Lilly,J., Silos-Santiago,I., Xie,Y., DiStefano,P.S., Curtis,R., and Clapham,D.E.

(2002). TRPV3 is a calcium-permeable temperature-sensitive cation channel. Nature *418*, 181-186.

Xu,S.Z. and Beech,D.J. (2001). TrpC1 is a membrane-spanning subunit of store-operated Ca(2+) channels in native vascular smooth muscle cells. Circ. Res. *88*, 84-87.

Xu,X.Z., Chien,F., Butler,A., Salkoff,L., and Montell,C. (2000). TRPgamma, a drosophila TRP-related subunit, forms a regulated cation channel with TRPL. Neuron *26*, 647-657.

Xu,X.Z., Choudhury,A., Li,X., and Montell,C. (1998). Coordination of an array of signaling proteins through homo- and heteromeric interactions between PDZ domains and target proteins. J. Cell Biol. *142*, 545-555.

Xu,X.Z., Li,H.S., Guggino,W.B., and Montell,C. (1997). Coassembly of TRP and TRPL produces a distinct store-operated conductance. Cell *89*, 1155-1164.

Yao,C.J., Lin,C.W., and Lin-Shiau,S.Y. (1999). Roles of thapsigargin-sensitive Ca2+ stores in the survival of developing cultured neurons. J. Neurochem. *73*, 457-465.

Yildirim,E., Dietrich,A., and Birnbaumer,L. (2003). The mouse C-type transient receptor potential 2 (TRPC2) channel: alternative splicing and calmodulin binding to its N terminus. Proc. Natl. Acad. Sci. U. S. A *100*, 2220-2225.

Yildirim,E., Kawasaki,B.T., and Birnbaumer,L. (2005). Molecular cloning of TRPC3a, an N-terminally extended, store-operated variant of the human C3 transient receptor potential channel. Proc. Natl. Acad. Sci. U. S. A.

Yuan J. P, Kiselyov K, Shin D. M, Chen J, Shcheynikov N, Kang S. H, Dehoff M. H, Schwarz M. K, Seeburg P. H, Muallem S, Worley P. F. (2003). Homer binds TRPC family channels and is required for gating of TRPC1 by IP_3 receptors. Cell *114* 777-789.

Zacharias,D.A., Baird,G.S., and Tsien,R.Y. (2000). Recent advances in technology for measuring and manipulating cell signals. Curr. Opin. Neurobiol. *10*, 416-421.

Zaidel-Bar,R., Ballestrem,C., Kam,Z., and Geiger,B. (2003). Early molecular events in the assembly of matrix adhesions at the leading edge of migrating cells. J. Cell Sci. *116*, 4605-4613.

Zamir,E., Katz,B.Z., Aota,S., Yamada,K.M., Geiger,B., and Kam,Z. (1999). Molecular diversity of cell-matrix adhesions. J. Cell Sci. *112 (Pt 11)*, 1655-1669

Zeng,F., Xu,S.Z., Jackson,P.K., McHugh,D., Kumar,B., Fountain,S.J., and Beech,D.J. (2004). Human TRPC5 channel activated by a multiplicity of signals in a single cell. J. Physiol *559*, 739-750.

Zhang,L. and Saffen,D. (2001). Muscarinic acetylcholine receptor regulation of TRP6 Ca2+ channel isoforms. Molecular structures and functional characterization. J. Biol. Chem. *276*, 13331-13339.

Zhang,Y.H. and Hancox,J.C. (2003). A novel, voltage-dependent nonselective cation current activated by insulin in guinea pig isolated ventricular myocytes. Circ. Res. *92*, 765-768.

Zhang,Y., Hoon,M.A., Chandrashekar,J., Mueller,K.L., Cook,B., Wu,D., Zuker,C.S., and Ryba,N.J. (2003). Coding of sweet, bitter, and umami tastes: different receptor cells sharing similar signaling pathways. Cell *112*, 293-301.

Zhu,X., Chu,P.B., Peyton,M., and Birnbaumer,L. (1995). Molecular cloning of a widely expressed human homologue for the Drosophila trp gene. FEBS Lett. *373*, 193-198.

Zhu,X., Jiang,M., Peyton,M., Boulay,G., Hurst,R., Stefani,E., and Birnbaumer,L. (1996). trp, a novel mammalian gene family essential for agonist-activated capacitative Ca2+ entry. Cell *85*, 661-671.

Zitt,C., Halaszovich,C.R., and Luckhoff,A. (2002). The TRP family of cation channels: probing and advancing the concepts on receptor-activated calcium entry. Prog. Neurobiol. *66*, 243-264.

Appendix

A 1 - Over-Expression of hTRPC7

Over-expression of proteins is frequently used to analyse their expression, localisation and function. This is usually carried out by use of an expression vector that will drive the expression of a given protein when introduced into a cell system. Members of our laboratory have made constructs containing full-length *htrpc7*and *htrpc7A*.

A 1.1 - pIRES-EGFP-*htrpc7/7A*

pIRES2-EGFP (Clontech) has been used to make a construct of full-length *htrpc7* and *htrpc7A* (Figure A 1).

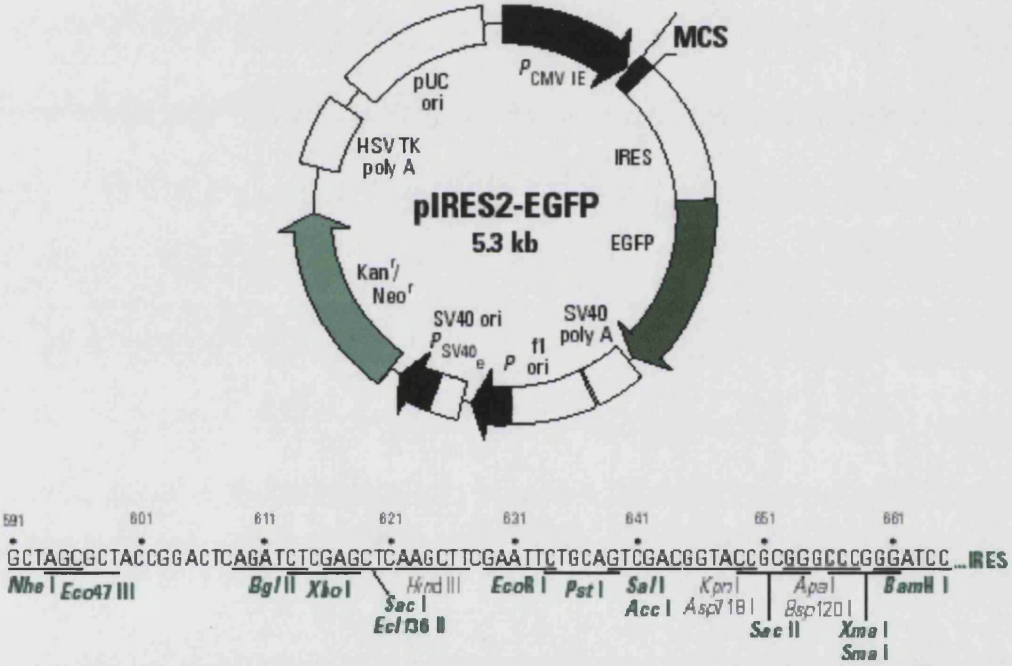

Figure A 1: Map and multiple cloning site (MCS) of the expression vector pIRES2-EGFP (Clontech).

pIRES2-EGFP contains the internal ribosome entry site (IRES; 1, 2) of the encephalomyocarditis virus (ECMV) between the multiple cloning site (MCS) and the enhanced green fluorescent protein (EGFP) coding region. This permits both the gene of interest (cloned into the MCS) and the EGFP gene to be translated from a single bicistronic mRNA (Clontech). *htrpc7* was cloned into pIRES-EGFP between Xho1 and BamH1 in the sense direction (Franklin Unpublished Data). *htrpc7A* was also cloned into

pIRES-EGFP between Xho1 and BamH1 in the sense direction (Chen Unpublished Data).

A 1.2 - pFLAG-*htrpc7*

Full-length *htrpc7* has also been cloned into a pFLAG-CMV expression vector (Sigma; Figure A 1.2); it is cloned between HindIII and KpnI and is tagged with the FLAG sequence at the N-terminus of *htrpc7*. However, there are some PCR induced errors that were incorporated during amplification; G423A, T1058A and C2094T. The only error that causes an amino acid change is T1058A, it leads to the translation of a glutamine instead of a leucine at amino acid 417 on the N-terminal region (Franklin Unpublished Data).

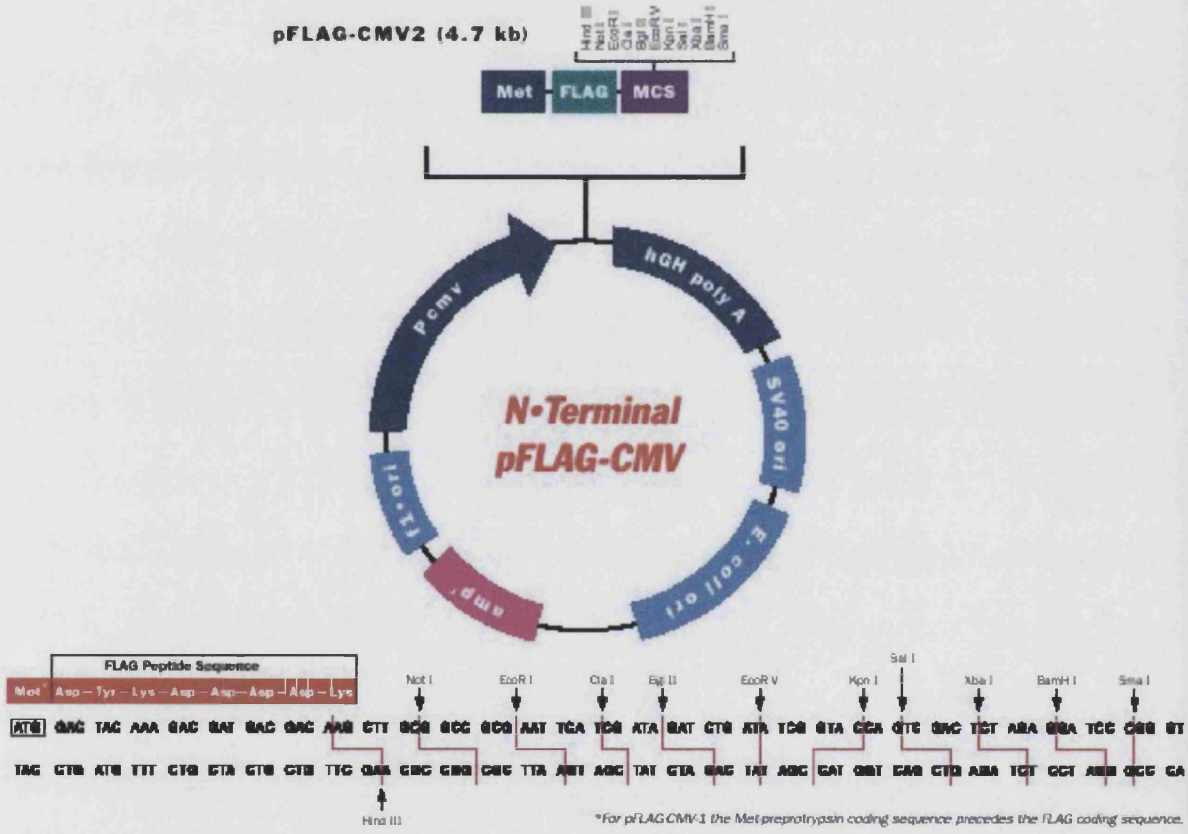

Figure A 1.2: Map and MCS of the expression vector pFLAG (Sigma).

The following pages show alignments of the peptide sequences of all of the TRPCs and the DNA sequence of hTRPC7, for this, highlighted in red is the deleted sequence of hTRPC7A, in blue is hTRPC7B and from the red to the end of the green highlighted area is the deleted part of hTRPC7C.

```
          1                                                                                                                  10
htrp7     .......... .......... .......... .......... .......... .....MLRNS TFKNMQRRHT TLREKGRRQA IRGPAYMFNE KGTSLTPEE
mtrp7     .......... .......... .......... .......... .......... .....MLGSN TFKNMQRRHT TLREKGRRQA IRGPAYMFNE KGTSLTPEE
htrp3     .......... .......... .......... .......... .......... .....MEGSP SL....RRMT VMREKGRRQA VRGPAFMFND RGTSLTAEE
htrp6     MSQSPAFGPR RGISPRGAAG AAARRNESQD YLLMDSELGE DGCPQAPLPC YGYYPCFRGS DNRLAHRRQT VLREKGRRLA NRGPAYMFSD RSTSLSIEE
htrp5     .......... .......... .......... .......... .......... MAQLYYKKVN YSPYRDRIP. .......... .....LQIVR AETELSAEE
htrp4     .......... .......... .......... .......... .......... MAQFYYKRNV NAPYRDRIP. .......... .....LRIVR AESELSPSE
htrp1     .......... .......... .......... .......... .........M MAALYPSTDL SGASSSSLPS SPSSSSPNEV MALKDVREVK EENTL..NE

          101                                                                                                                20
htrp7     RFLDSAEYGN IPVVRKMLEE SKT...LNFN CVDYMGQNAL QLAVGNEHLE VTELLLKKEN LARVGDALLL AISKGYVRIV EAILNHPAFA QGQRLTLSP
mtrp7     RFLDSAEYGN IPVVRKMLEE SKT...LNFN CVDYMGQNAL QLAVGNEHLE VTELLLKKEN LARVGDALLL AISKGYVRIV EAILSHPAFA QGQRLTLSP
htrp3     RFLDAAEYGN IPVVRKMLEE SKT...LNVN CVDYMGQNAL QLAVGNEHLE VTELLLKKEN LARIGDALLL AISKGYVRIV EAILNHPGFA ASKRLTLSP
htrp6     RFLDAAEYGN IPVVRKMLEE CHS...LNVN CVDYMGQNAL QLAVANEHLE ITELLLKKEN LSRIGDALLL AISKGYVRIV EAILSHPAFA EGKRLATSP
htrp5     AFLNAVEKGD YATVKQALQE AEIYYNVNIN CMDPLGRSAL LIAIENENLE IMELLLNHSV Y..VGDALLY AIRKEVVGAV ELLLSYRRPS GEKQVPTLM
htrp4     AYLNAVEKGD YASVKKSLEE AEIYFKININ CIDPLGRTAL LIAIENENLE LIELLLSFNV Y..VGDALLH AIRKEVVGAV ELLLNHKKPS GEKQVPPIL
htrp1     LFLLACDKGD YYMVKKILEE NSS.GDLNIN CVDVLGRNAV TITIENENLD ILQLLLD... Y..GCQKLME RIQ..... .......... .........

          201                                                                                                                30
htrp7     EQELRDDDFY AYDEDGTRFS HDITPIILAA HCQEYEIVHI LLLKGARIER PHDYFCKCNE CTEKQRKDSF SHSRSRMNAY KGLASAAYLS LSSEDPVLT
mtrp7     EQELRDDDFY AYDEDGTRFS HDITPIILAA HCQEYEIVHI LLLKGARIER PHDYFCKCNE CTEKQRKDSF SHSRSRMNAY KGLASAAYLS LSSEDPVLT
htrp3     EQELQDDDFY AYDEDGTRFS PDITPIILAA HCQKYEVVHM LLMKGARIER PHDYFCKCGD CMEKQRHDSF SHSRSRINAY KGLASPAYLS LSSEDPVLT
htrp6     QSELQQDDFY AYDEDGTRSS HDVTPIILAA HCREYEIVHT LLRKGARIER PHDYFCKCND CNQKQKHDSF SHSRSRINAY KGLASPAYLS LSSEDPVMT
htrp5     DTQFSE.... ........FT PDITPIMLAA HTNNYEIIKL LVQKRVTIPR PHQIRCNCVE CVSSSEVDSL RHSRSRLNIY KALASPSLIA LSSEDPILT
htrp4     DKQFSE.... ........FT PDITPIILAA HTNNYEIIKL LVQKGVSVPR PHEVRCNCVE CVSSSDVDSL RHSRSRLNIY KALASPSLIA LSSEDPFLT
htrp1     NPEYST.... .........T MDVAPVILAA HRNNYEILTM LLKQDVSLPK PHAVGCECTL CSAKNKKDSL RHSRFRLDIY RCLASPALIM LTEEDPILR

          301                                                                                                                40
htrp7     LELSNELARL ANIETEFKND YRKLSMQCKD FVVGVLDLCR DTEEVEAILN ..GDVN.... FQVWSDHHRP SLSRIKLAIK YEVKKFVAHP NCQQQLLTM
mtrp7     LELSNELARL ANIETEFKND YRKLSMQCKD FVVGVLDLCR DTEEVEAILN ..GDVN.... LQVWSDHHRP SLSRIKLAIK YEVKKFVAHP NCQQQLLTM
htrp3     LELSNELAKL ANIEKEFKND YRKLSMQCKD FVVGVLDLCR DSEEVEAILN ..GDLESAEP LEV..HRHKA SLSRVKLAIK YEVKKFVAHP NCQQQLLTI
htrp6     LELSNELAVL ANIEKEFKND YKKLSMQCKD FVVGLLDLCR NTEEVEAILN ..GDVETLQ. ...SGDHGRP NLSRLKLAIK YEVKKFVAHP NCQQQLLSI
htrp5     FRLGWELKEL SKVENEFKAE YEELSQQCKL FAKDLLDQAR SSRELEIILN HRD.....DH SEELDPQKYH DLAKLKVAIK YHQKEFVAQP NCQQLLATL
htrp4     FQLSWELQEL SKVENEFKSE YEELSRQCKQ FAKDLLDQTR SSRELEIILN YRD.....DN S.LIEEQSGN DLARLKLAIK YRQKEFVAQP NCQQLLASR
htrp1     FELSADLKEL SLVEVEFRND YEELARQCKM FAKDLLAQAR NSRELEVILN HTSSDEPLDK RGLLEERM.. NLSRLKLAIK YNQKEFVSQS NCQQFLNTV
```


401 S1 50
htrp7 YENLSGLRQQ SIAVKFLAVF GVSIGLPFLA IAYWIAPCSK LGRTLRSPFM KFVAHAVSFT IFLGLLVVNA SDRFEGVKTL PNETFTDYPK QIFRVKTTQ
mtrp7 YENLSGLRQQ SIAVKFLAVF GVSIGLPFLA IAYWIAPCSK LGQTLRSPFM KFVAHAVSFT IFLGLLVVNA SDRFEGVKTL PNETFTDYPK QIFRVKTTQ
htrp3 YENLSGLREQ TIAIKCLVVL VVALGLPFLA IGYWIAPCSR LGKILRSPFM KFVAHAASFI IFLGLLVFNA SDRFEGITTL PNITVTDYPK QIFRVKTTQ
htrp6 YENLSGLRQQ TMAVKFLVAL AVAIGLPFLA LIYWFAPCSK MGKIMRGPFM KFVAHAASFT IFLGLLVMNA ADRFEGTKLL PNETSTDNAK QLFRMKTSC
htrp5 YDGFPGWRRK HWVVKLLTCM TIGFLFPMLS IAYLISPRSN LGLFIKKPFI KFICHTASYL TFLFMLLL.A SQHIVRTD.. ....LHVQGPP
htrp4 YDEFPGWRRR HWAVKMVTCF IIGLLFPVFS VCYLIAPKSP LGLFIRKPFI KFICHTASYL TFLFLLLL.A SQHIDRSD.. ....LNRQGPP
htrp1 FGQMSGYRRK PTCKKIMTVL TVGIFWPVLS LCYLIAPKSQ FGRIIHTPFM KFIIHGASYF TFLLLLNL.Y SLVYNEDK.. ....KNTMGPA
501 S2 S3 60
htrp7 SWTEMLIMKW VLGMIWSECK EIWEEGPREY VLHLWNLLDF GMLSIFVASF TARFMAFLKA TEAQLYVDQH VQDDTLHNVS LPPEVAYFTY ARDKWWPSD
mtrp7 SWTEMLIMKW VLGMIWSECK EIWEEGPREY VLHLWNLLDF GMLSIFVASF TARFMAFLKA SEAQLYVDQY VQDVTLHNVS LPPEVAYFTY ARDKWWPSD
htrp3 TWTEMLIMVW VLGMMWSECK ELWLEGPREY ILQLWNVLDF GMLSIFIAAF TARFLAFLQA TKAQQYVDSY VQESDLSEVT LPPEIQYFTY ARDKWLPSD
htrp6 SWMEMLIISW VIGMIWAECK EIWTQGPKEY LFELWNMLDF GMLAIFPASF IARFMAFWHA SKAQSIIDAN DTLKDLTKVT LGDNVKYYNL ARIKWDPSD
htrp5 TVVEWMILPW VLGFIWGEIK EMWDGGFTEY IHDWWNLMDF AMNSLYLATI SLKIVAYVKY NGSR..... .... PREEWEMWH
htrp4 TIVEWMILPW VLGFIWGEIK QMWDGGLQDY IHDWWNLMDF VMNSLYLATI SLKIVAFVKY SALN..... .... PRESWDMWH
htrp1 ERIDYLLILW IIGMIWSDIK RLWYEGLEDF LEESRNQLSF VMNSLYLATF ALKVVAHNKF HDFA..... .... DRKDWDAFH
601 S4 S5 70
htrp7 QIISEGLYAI AVVLSFSRIA YILPANESFG PLQISLGRTV KDIFKFMVIF IMVFVAFMIG MFNLYSYYRG ....AKYNP AFTTVEESF
mtrp7 QIISEGLYAI AVVLSFSRIA YILPANESFG PLQISLGRTV KDIFKFMVIF IMVFVAFMIG MFNLYSYYRG ....AKYNP AFTTVEESF
htrp3 QIISEGLYAI AVVLSFSRIA YILPANESFG PLQISLGRTV KDIFKFMVLF IMVFFAFMIG MFILYSYYLG ....AKVNA AFTTVEESF
htrp6 QIISEGLYAI AVVLSFSRIA YILPANESFG PLQISLGRTV KDIFKFMVIF IMVFVAFMIG MFNLYSYYIG ....AKQNE AFTTVEESF
htrp5 TLIAEALFAI SNILSSLRLI SLFTANSHLG PLQISLGRML LDILKFLFIY CLVLLAFANG LNQLYFYYET RAIDEPNNCK GIRCEKQ.NN AFSTLFETL
htrp4 TLVAEALFAI ANIFSSLRLI SLFTANSHLG PLQISLGRML LDILKFLFIY CLVLLAFANG LNQLYFYYEE ...TKGLTCK GIRCEKQ.NN AFSTLFETL
htrp1 TLVAEGLFAF ANVLSYLRLF FMYTTSSILG PLQISMGQML QDFGKFLGMF LLVLFSFTIG LTQL..YDKG YTSKEQKDCV GIFCEQQSND TFHSFIGTC
701 PORE S6 80
htrp7 TLFWSIFGLS EVISVV..LK YDHKFIENIG YVLYGVYNVT MVVVLLNMLI AMINNSYQEI EEDADVEWKF ARAKLWLSYF DEGRTLPAPF NLVPSPKSF
mtrp7 TLFWSIFGLS EVISVV..LK YDHKFIENIG YVLYGVYNVT MVVVLLNMLI AMINNSYQEI EEDADVEWKF ARAKLWLSYF DEGRTLPAPF NLVPSPKSF
htrp3 TLFWSIFGLS EVTSVV..LK YDHKFIENIG YVLYGIYNVT MVVVLLNMLI AMINSSYQEI EDDSDVEWKF ARSKLWLSYF DDGKTLPPPF SLVPSPKSF
htrp6 TLFWAIFGLS EVKSVV..IN YNHKFIENIG YVLYGVYNVT MVIVLLNMLI AMINSSFQEI EDDADVEWKF ARAKLWFSYF EEGRTLPVPF NLVPSPKSL
htrp5 SLFWSVFGL. .LNLYVTNVK ARHEFTEFVG ATMFGTYNVI SLVVLLNMLI AMMNNSYQLI ADHADIEWKF ARTKLWMSYF DEGGTLPPPF NIIPSPKSF
htrp4 SLFWSIFGL. .INLYVTNVK AQHEFTEFVG ATMFGTYNVI SLVVLLNMLI AMMNNSYQLI ADHADIEWKF ARTKLWMSYF EEGGTLPTPF NVIPSPKSL
htrp1 ALFWYIFSLA HVAIFVTRFS YGEELQSFVG AVIVGTYNVV VVIVLTKLLV AMLHKSFQLI ANHEDKEWKF ARAKLWLSYF DDKCTLPPPF NIIPSPKTI

```
      801                                                                                                                  90
htrp7 YLIMRIKMCL IKLCKSKAKS CENDLEMGML NSKFKKTRY. .......... .........Q AGMRNSENLT ANNTLSKPTR YQKIMKRLIK RYVLKA.QV
mtrp7 YLIMRIKMCL IELCQSKAKR CENDLEMGML NSKFRKTRY. .......... .........Q AGMRNSENLT ANSTFSKPTR YQKIMKRLIK RYVLKA.QV
htrp3 YFIMRI.... VNFPKCRRRR LQKDIEMGMG NSKSRLNLFT .......... .........Q SNSRVFESHS FNSILNQPTR YQQIMKRLIK RYVLKA.QV
htrp6 YLLLKLKKWI SELFQGHKKG FQEDAEMNKI NEEKKLGILG SHEDLSKLSL DKKQVGHNKQ PSIRSSEDFH LNSFNNPPRQ YQKIMKRLIK RYVLQA.QI
htrp5 YLGNWFNNTF CPKRDPDGRR RRRNLR.... .......... .......... .......... .....SFTER NADSLIQNQH YQEVIRNLVK RYVAAMIRN
htrp4 YLIKWIWTHL CKKK...MRR KPESFG.... .......... .......... .......... .....TIGRR AADNLRRHHQ YQEVMRNLVK RYVAAMIRD
htrp1 YMISSLSKWI CSHTSKGKVK RQNSLK.... .......... .......... .......... ........EW RNLKQKRDEN YQKVMCCLVH RYLTSMRQK

      901                                                                                                                 100
htrp7 RENDEVNEGE LKEIKQDISS LRYELLEEKS QATGELADLI QQLSEKFGKN LNKDHLRVNK GKDI...... .......... .......... .........
mtrp7 RENDEVNEGE LKEIKQDISS LRYELLEEKS QATGELADLI QQLSEKFGKN LNKDHLRVNQ GKDI...... .......... .......... .........
htrp3 KENDEVNEGE LKEIKQDISS LRYELLEDKS QATEELAILI HKLSEKLNPS M....LRCE* .......... .......... .......... .........
htrp6 KESDEVNEGE LKEIKQDISS LRYELLEEKS QNTEDLAELI RELGEKLSME PNQEETNR.. .......... .......... .......... .........
htrp5 KTHEGLTEEN FKELKQDISS FRYEVLDLL. .GNRK....H PRSFSTSSTE LSQRDDNNDG SGGARAKSKS VS.FNLG..C KKKTCHGPPL IRTMPRSSG
htrp4 KTEEGLTEEN FKELKQDISS FRFEVLGLL. .RGSKLSTIQ SANASKESSN SADSDEKSDS EGNSKDKKKN FSLFDLTTLI HPRSAAIASE RHNISNGSA
htrp1 QSTDQATVEN LNELRQDLSK FRNEIRDLLG FRTSKYAMFY PRN*...... .......... .......... .......... .......... .........

      1001                                                                                                                110
htrp7 .......... .......... .......... .......... .......... .......... .......... .......... .......... .........
mtrp7 .......... .......... .......... .......... .......... .......... .......... .......... .......... .........
htrp3 .......... .......... .......... .......... .......... .......... .......... .......... .......... .........
htrp6 .......... .......... .......... .......... .......... .......... .......... .......... .......... .........
htrp5 QGKSKAESSS KRSFMGPSLK KLGLLFSKFN GHMSEPSSEP MYTISDGIVQ QHCMWQDIRY SQMEKGKAEA CSQSEINLSE VELGEVQGAA QSSECPLAC
htrp4 VVQEPPREKQ RKVNFVTDIK NFGLFHRRSK QNAAEQNANQ IFSVSEEVAR QQAAGPLERN IQLE.SRGLA ...SRGDLSI PGLSEQCVLV DHRERNTD.
htrp1 .......... .......... .......... .......... .......... .......... .......... .......... .......... .........

      1101                                                          1161
htrp7 .......... .......... .......... .......... .......... .......... .
mtrp7 .......... .......... .......... .......... .......... .......... .
htrp3 .......... .......... .......... .......... .......... .......... .
htrp6 .......... .......... .......... .......... .......... .......... .
htrp5 SSLHCASSIC SSNSKLLDSS EDV....... ...FETWGEA CDLLMHKWGD GQEEQVTTRL *
htrp4 LGLQVGKRVC PFKSEKVVVE DTVPIIPKEK HAKEEDSSID YDLNLPD.TV THEDYVTTRL *
htrp1 .......... .......... .......... .......... ..........
```

TRPC7 nucleotide alignment

Name: AJ421783 Human (GSK) Name: AJ272034 Human (bath) Name: AF139923 Mouse

```
          1                                                  50
AJ421783  ~~~~~~~~~~ ~~~~~~~~~~ ~~~~~~~~~~ ~~~~~~~~~~ ~~~~~~~~~~~~~~~~~~~~ ~~~~~~~~~~ ~~~~~~~~~~ ~~~~~~~~~~ ~~~~ATGTTG
AJ272034  ~~~~~~~~~~ ~~~~~~~~~~ ~~~~~~~~~~ ~~~~~~~~~~ ~~~~~~~~~~~~~~~~~~~~ ~~~~~~~~~~ ~~~~~~~~~~ ~~~~~~~~~~ ~~~~ATGTTG
AF139923  CCGCCTCGGC CACCCATGGG GAGCCAGATC CCGGAGACTC CGTTCAGGATTCGGGTCATC TAGAGGAGGG ACAAGCCTGC GTATTCTACT CTCGATGTTG

          101                                                150
AJ421783  AGGAACAGCA CCTTCAAAAA CATGCAGCGC CGGCACACAA CGCTGAGGGAGAAGGGCCGT CGCCAGGCCA TCCGGGGTCC CGCCTACATG TTCAACGAGA
AJ272034  AGGAACAGCA CCTTCAAAAA CATGCAGCGC CGGCACACAA CGCTGAGGGAGAAGGGCCGT CGCCAGGCCA TCCGGGGTCC CGCCTACATG TTCAACGAGA
AF139923  GGGAGCAACA CCTTCAAAAA CATGCAGCGC CGGCACACCA CCTTGAGGGAGAAGGGGCGC CGCCAGGCCA TCCGGGGTCC TGCCTACATG TTCAACGAGA

          201                                                250
AJ421783  AGGGCACCAG TCTGACGCCC GAGGAGGAGC GCTTCCTGGA CTCGGCCGAGTATGGCAACA TCCCGGTGGT CCGGAAAATG CTGGAGGAGT CCAAGACCCT
AJ272034  AGGGCACCAG TCTGACGCCC GAGGAGGAGC GCTTCCTGGA CTCGGCTGAGTATGGCAACA TCCCGGTGGT CCGGAAAATG CTGGAGGAGT CCAAGACCCT
AF139923  AGGGCACGAG CCTGACCCCT GAGGAGGAGC GCTTCCTGGA CTCGGCTGAGTATGGCAACA TACCAGTGGT CAGAAAAATG CTGGAGGAAT CCAAGACCCT

          301                                                350
AJ421783  TAACTTCAAC TGTGTGGACT ACATGGGGCA GAACGCTCTG CAGCTGGCTGTGGGCAACGA GCACCTAGAG GTCACGGAGC TGCTGCTGAA GAAGGAGAAC
AJ272034  TAACTTCAAC TGTGTGGACT ACATGGGGCA GAACGCTCTG CAGCTGGCCGTGGGCAACGA GCACCTAGAG GTCACGGAGC TGCTGCTGAA GAAGGAGAAC
AF139923  CAATTTCAAC TGCGTGGACT ACATGGGGCA GAACGCGCTG CAGCTGGCCGTGGGCAACGA GCACTTGGAG GTCACTGAAC TGTTGCTGAA GAAAGAGAAC

          401                                                450
AJ421783  CTGGCACGGG TGGGGGACGC GCTGCCGCTG GCCATCAGCA AGGGCTATGTGCGCATCGTG GAGGCCATCC TCAACCACCC GGCCTTCGCG CAGGGCCAGC
AJ272034  CTGGCACGGG TGGGGGACGC GCTGCTGCTG GCCATCAGCA AGGGCTATGTGCGCATCGTG GAGGCCATCC TCAACCACCC GGCCTTCGCG CAGGGCCAGC
AF139923  TTGGCGCGGG TGGGCGACGC GCTGCTGCTG GCCATCAGCA AGGGCTATGTGCGCATTGTG GAGGCCATCC TCAGCCATCC GGCCTTCGCG CAGGGCCAGC

          501                                                550
AJ421783  GCCTGACGCT CAGCCCGCTG GAACAGGAGC TGCGCGACGA CGACTTCTATGCCTACGACG AGGACGGCAC GCGCTTCTCC CACGACATCA CGCCCATCAT
AJ272034  GCCTGACGCT CAGCCCGCTG GAACAGGAGC TGCGCGACGA CGACTTCTATGCCTACGACG AGGACGGCAC GCGCTTCTCC CACGACATCA CGCCCATCAT
AF139923  GCCTGACGCT CAGCCCGCTG GAGCAGGAGC TGCGGGATGA TGACTTCTATGCCTACGACG AGGATGGCAC GCGCTTCTCC CACGACATCA CACCCATCAT

          601                                                650
AJ421783  CCTGGCGGCG CACTGCCAGG AGTATGAGAT CGTGCACATC CTGCTGCTCAAGGGCGCCCG CATCGAGCGG CCCCACGACT ACTTCTGCAA GTGTAATGAG
AJ272034  CCTGGCGGCG CACTGCCAGG AGTATGAGAT CGTGCACATC CTGCTGCTCAAGGGCGCCCG CATCGAGCGG CCCCACGACT ACTTCTGCAA GTGCAATGAG
AF139923  CCTGGCGGCC CACTGCCAGG AGTATGAGAT TGTGCATATC TTGCTGCTCAAGGGTGCGCG CATTGAGCGG CCCCATGACT ACTTCTGCAA GTGCAATGAG

          701                                                750
AJ421783  TGCACCGAGA AACAGCGGAA AGACTCCTTC AGCCACTCGC GCTCGCGCATGAACGCCTAC AAAGGGCTGG CGAGTGCTGC CTACTTGTCC CTGTCCAGCG
AJ272034  TGCACCGAGA AACAGCGGAA AGACTCCTTC AGCCACTCGC GCTCGCGCATGAACGCCTAC AAAGGACTGG CGAGTGCTGC CTACTTGTCC CTGTCCAGCG
AF139923  TGCACGGAGA AGCAGCGCAA GGACTCCTTC AGTCACTCGC GCTCCCGGATGAATGCCTAC AAAGGACTGG CCAGTGCCGC CTACCTGTCC CTATCCAGTG

          801                                                850
AJ421783  AAGACCCTGT CCTCACCGCC CTGGAGCTCA GCAACGAGTT AGCCAGACTAGCCAACATTG AGACTGAATT TAAGAACGAT TACAGGAAGT TATCTATGCA
AJ272034  AAGACCCTGT CCTCACCGCC CTGGAGCTCA GCAACGAGTT AGCCAGACTAGCCAACATTG AGACTGAATT TAAGAACGAT TACAGGAAGT TATCTATGCA
AF139923  AAGACCCTGT CCTCACTGCG CTGGAGCTAA GCAACGAGTT AGCCCGACTGGCCAACATTG AGACTGAATT TAAGAATGAT TACAGGAAGT TATCTATGCA
```

```
          901                                                 950
AJ421783  ATGCAAAGAT TTTGTAGTGG GCGTGCTGGA CCTGTGCCGA GACACAGAAGAGGTGGAAGC AATTTTAAAC GGTGATGTGA ACTTCCAAGT CTGGTCCGAC
AJ272034  ATGCAAGGAT TTTGTAGTGG GCGTGCTGGA CCTGTGCCGA GACACAGAAGAGGTGGAAGC AATTTTAAAC GGTGATGTGA ACTTCCAAGT CTGGTCCGAC
AF139923  ATGCAAGGAT TTTGTGGTGG GCGTGCTGGA CCTGTGCCGA GACACAGAAGAGGTGGAAGC AATTTTAAAT GGCGATGTGA ACTTGCAAGT CTGGTCCGAC

          1001                                                1050
AJ421783  CACCACCGTC CAAGTCTGAG CCGGATCAAA CTCGCCATTA AGTATGAAGTCAAGAAGTTC GTTGCTCATC CTAACTGTCA GCAGCAATTG CTTACCATGT
AJ272034  CACCACCGTC CAAGTCTGAG CCGGATCAAA CTCGCCATTA AATATGAAGTCAAGAAGTTC GTTGCTCATC CTAACTGTCA GCAGCAATTG CTTACCATGT
AF139923  CACCACCGTC CAAGTCTGAG CCGAATCAAA CTCGCCATTA AGTACGAAGTCAAGAAGTTC GTTGCTCACC CTAACTGTCA GCAGCAATTG CTTACCATGT

          1101                                                1150
AJ421783  GGTATGAAAA TCTCTCAGGC TTACGTCAAC AGTCTATCGC TGTGAAATTCCTGGCTGTCT TTGGAGTCTC CATAGGCCTC CCTTTTCTCG CCATAGCCTA
AJ272034  GGTATGAAAA TCTCTCAGGC TTACGTCAAC AGTCTATCGC TGTGAAATTCCTGGCTGTCT TTGGAGTCTC CATAGGCCTC CCTTTTCTCG CCATAGCCTA
AF139923  GGTATGAAAA TCTCTCAGGC TTACGGCAAC AGTCTATCGC TGTGAAATTCCTGGCTGTCT TTGGAGTCTC CATAGGCCTC CCTTTTCTCG CCATAGCCTA

          1201                                                1250
AJ421783  TTGGATTGCT CCGTGCAGCA AGCTAGGACG AACCCTGAGG AGCCCTTTCATGAAGTTTGT AGCTCATGCA GTTTCTTTTA CAATCTTCTT GGGATTATTA
AJ272034  TTGGATTGCT CCGTGCAGCA AGCTAGGACG AACCCTGAGG AGCCCTTTCATGAAGTTTGT AGCTCATGCA GTTTCTTTTA CAATCTTCTT GGGATTATTA
AF139923  TTGGATTGCT CCGTGCAGCA AGCTAGGACA AACCCTGAGG AGCCCTTTCATGAAGTTTGT GGCCCATGCA GTGTCTTTTA CCATCTTCTT GGGACTGCTA

          1301                                                1350
AJ421783  GTTGTGAATG CATCTGACCG ATTTGAAGGT GTTAAAACCC TGCCAAACGAAACCTTCACA GACTACCCAA AACAAATCTT CAGAGTGAAA ACCACACAGT
AJ272034  GTTGTGAATG CATCTGACCG ATTTGAAGGT GTTAAAACCC TGCCAAACGAAACCTTCACA GACTACCCAA AACAAATCTT CAGAGTGAAA ACCACACAGT
AF139923  GTTGTGAACG CCTCCGACCG GTTTGAGGGC GTTAAGACTC TGCCCAATGAGACCTTCACA GACTACCCCA AACAGATCTT CAGAGTGAAA ACCACACAGT

          1401                                                1450
AJ421783  TCTCCTGGAC AGAAATGCTC ATTATGAAGT GGGTCTTAGG AATGATCTGGTCCGAATGCA AGGAAATCTG GGAGGAGGGG CCACGGGAGT ACGTGCTGCA
AJ272034  TCTCCTGGAC AGAAATGCTC ATTATGAAGT GGGTCTTAGG AATGATTTGGTCCGAATGCA AGGAAATCTG GGAGGAGGGG CCACGGGAGT ACGTGCTGCA
AF139923  TCTCCTGGAC GGAGATGCTC ATCATGAAGT GGGTCTTAGG AATGATCTGGTCCGAATGCA AGGAGATCTG GGAGGAGGGG CCGCGGGAGT ACGTGCTACA

          1501                                                1550
AJ421783  CTTGTGGAAC CTGCTAGATT TCGGGATGCT GTCCATCTTC GTGGCCTCCTTCACAGCACG CTTCATGGCC TTCCTGAAGG CCACGGAGGC ACAGCTGTAC
AJ272034  CTTGTGGAAC CTGCTAGATT TCGGGATGCT GTCCATCTTC GTGGCCTCCTTCACAGCACG CTTCATGGCC TTCCTGAAGG CCACGGAGGC ACAGCTGTAC
AF139923  CTTGTGGAAC CTTCTGGATT TTGGCATGCT GTCCATCTTC GTGGCCTCCTTCACTGCGAG GTTCATGGCT TTCCTCAAGG CCAGCGAGGC CCAGCTGTAC

          1601                                                1650
AJ421783  GTGGACCAGC ACGTGCAGGA CGACACGCTG CACAATGTCT CGCTTCCGCCGGAAGTAGCA TACTTCACCT ACGCCAGGGA CAAGTGGTGG CCTTCAGACC
AJ272034  GTGGACCAGC ACGTGCAGGA CGACACGCTG CACAATGTCT CGCTTCCGCCGGAAGTGGCA TACTTCACCT ACGCCAGGGA CAAGTGGTGG CCTTCAGACC
AF139923  GTGGACCAGT ACGTGCAGGA TGTAACGCTG CACAACGTCT CACTTCCACCGGAAGTGGCC TACTTCACCT ACGCCAGGGA TAAGTGGTGG CCTTCAGACC

          1701                                                1750
AJ421783  CTCAGATCAT ATCGGAAGGG CTCTACGCGA TAGCCGTCGT GCTGAGCTTCTCTCGCATTG CATACATTCT GCCAGCCAAC GAGAGTTTTG GGCCCCTGCA
AJ272034  CTCAGATCAT ATCGGAAGGG CTCTACGCGA TAGCCGTCGT GCTGAGCTTCTCTCGCATTG CATACATTCT GCCAGCCAAC GAGAGTTTTG GGCCCCTGCA
AF139923  CCCAGATCAT CTCGGAAGGG CTGTACGCCA TTGCGGTTGT CCTCAGCTTCTCCCGGATCG CCTACATCCT GCCAGCCAAT GAGAGCTTCG GACCTTTGCA
```

```
        1801                                                1850
AJ421783  GATCTCGCTA GGGAGAACTG TGAAAGATAT CTTCAAGTTC ATGGTCATTTTCATCATGGT ATTTGTGGCC TTCATGATTG GGATGTTCAA CCTGTACTCT
AJ272034  GATCTCGCTA GGGAGAACTG TGAAAGATAT CTTCAAGTTC ATGGTCATTTTCATCATGGT ATTTGTGGCC TTCATGATTG GGATGTTCAA CCTGTACTCT
AF139923  GATCTCCCTG GGAAGAACTG TGAAAGACAT CTTCAAGTTC ATGGTCATTTTTATCATGGT ATTTGTGGCC TTTATGATCG GAATGTTCAA CCTGTACTCC

        1901                                                1950
AJ421783  TACTACCGAG GTGCCAAATA CAACCCAGCG TTTACAACGG TTGAAGAAAGTTTTAAAACT TTGTTTTGGT CCATATTCGG CTTATCTGAA GTAATCTCAG
AJ272034  TACTACCGAG GTGCCAAATA CAACCCAGCG TTTACAACGG TTGAAGAAAGTTTTAAAACT TTGTTTTGGT CCATATTCGG CTTATCTGAA GTAATCTCAG
AF139923  TACTACCGAG GTGCAAAGTA CAACCCAGCG TTTACCACAG TTGAAGAAAGCTTTAAAACC TTGTTTTGGT CCATATTTGG CTTGTCTGAG GTCATCTCGG

        2001                                                2050
AJ421783  TGGTGCTGAA ATACGACCAC AAATTCATCG AGAACATTGG CTACGTTCTCTACGGCGTTT ATAACGTCAC CATGGTGGTA GTGTTGCTCA ACATGCTAAT
AJ272034  TGGTGCTGAA ATACGACCAC AAATTCATCG AGAACATTGG CTACGTTCTCTACGGCGTTT ATAACGTCAC CATGGTGGTA GTGTTGCTCA ACATGCTAAT
AF139923  TGGTGCTGAA ATACGACCAC AAGTTCATCG AGAATATTGG CTACGTGCTGTATGGGGTTT ATAATGTCAC CATGGTGGTT GTACTACTCA ACATGCTGAT

        2101                                                2150
AJ421783  AGCCATGATA AACAACTCCT ATCAGGAAAT TGAGGAGGAT GCAGATGTGGAATGGAAGTT CGCCCGAGCA AAACTCTGGC TGTCTTACTT TGATGAAGGA
AJ272034  AGCCATGATA AACAACTCCT ATCAGGAAAT TGAGGAGGAT GCAGATGTGGAATGGAAGTT CGCCCGAGCA AAACTCTGGC TGTCTTACTT TGATGAAGGA
AF139923  AGCCATGATC AACAACTCCT ATCAGGAAAT CGAGGAAGAC GCGGACGTGGAGTGGAAATT TGCTCGAGCG AAGCTCTGGC TTTCTTACTT TGATGAAGGA

        2201                                                2250
AJ421783  AGAACTCTAC CTGCTCCTTT TAATCTAGTG CCAAGTCCTA AATCATTTTATTATCTCATA ATGAGAATCA AGATGTGCCT CATAAAACTC TGCAAATCTA
AJ272034  AGAACTCTAC CTGCTCCTTT TAATCTAGTG CCAAGTCCTA AATCATTTTATTATCTCATA ATGAGAATCA AGATGTGCCT CATAAAACTC TGCAAATCTA
AF139923  AGAACTCTCC CTGCTCCCTT TAACCTGGTG CCGAGCCCTA AATCCTTTTATTATCTCATA ATGAGAATCA AGATGTGCCT CATAGAGCTC TGCCAATCTA

        2301                                                2350
AJ421783  AGGCCAAAAG CTGTGAAAAT GACCTTGAAA TGGGCATGCT GAATTCCAAATTCAAGAAGA CTCGCTACCA GGCTGGCATG AGGAATTCTG AAAATCTGAC
AJ272034  AGGCCAAAAG CTGTGAAAAT GACCTTGAAA TGGGCATGCT GAATTCCAAATTCAAGAAGA CTCGCTACCA GGCTGGCATG AGGAATTCTG AAAATCTGAC
AF139923  AGGCCAAACG CTGTGAAAAC GACCTGGAAA TGGGCATGCT GAACTCCAAGTTCAGGAAGA CTCGCTACCA GGCTGGCATG AGGAATTCTG AAAACCTGAC

        2401                                                2450
AJ421783  AGCAAATAAC ACTTTGAGCA AGCCCACCAG ATACCAGAAA ATCATGAAACGGCTCATAAA AAGATACGTC CTGAAAGCCC AGGTGGACAG AGAAAATGAC
AJ272034  AGCAAATAAC ACTTTGAGCA AGCCCACCAG ATACCAGAAA ATCATGAAACGGCTCATAAA AAGATACGTC CTGAAAGCCC AGGTGGACAG AGAAAATGAC
AF139923  AGCCAATAGC ACCTTCAGCA AGCCCACCAG ATACCAGAAG ATCATGAAGCGGCTCATAAA GAGATACGTG CTGAAGGCCC AGGTGGACAG AGAGAACGAT

        2501                                                2550
AJ421783  GAAGTCAATG AAGGCGAGCT GAAGGAAATC AAGCAAGATA TCTCCAGCCTGCGCTATGAG CTTCTTGAGG AAAAATCTCA AGCTACAGGT GAGCTGGCAG
AJ272034  GAAGTCAATG AAGGCGAGCT GAAGGAAATC AAGCAAGATA TCTCCAGCCTGCGCTATGAG CTTCTTGAGG AAAAATCTCA AGCTACTGGT GAGCTGGCAG
AF139923  GAAGTCAATG AAGGTGAACT CAAGGAGATC AAACAAGACA TCTCAAGCCTTCGCTATGAG CTCCTGGAGG AGAAGTCTCA GGCTACAGGA GAGCTGGCAG

        2601                                                2650
AJ421783  ACCTGATTCA ACAACTCAGC GAGAAGTTTG GAAAGAACTT AAACAAAGACCACCTGAGGG TGAACAAGGG CAAAGACATT TAG
AJ272034  ACCTGATTCA ACAACTCAGC GAGAAGTTTG GAAAGAACTT AAACAAAGACCACCTGAGGG TGAACAAGGG CAAAGACATT TAG
AF139923  ACCTGATTCA GCAGCTCAGC GAGAAGTTTG GGAAGAATCT GAACAAAGACCACCTGCGGG TGAACCAGGG CAAGGACATT TAG
```